Processing and Analysis of Transient Pressure from Permanent Down-hole Gauges

Fei Wang

Submitted for the
Degree of Doctor of Philosophy
Institute of Petroleum Engineering
Heriot-Watt University
June 2010

Abstract

With the permanent down-hole gauge (PDG) widely installed in oilfields around the world in recent years, a continuous stream of transient pressure data in real time are available, which motivates a new round of research interests in further developing pressure transient analysis techniques.

PDG data is recorded under the unconstrained circumstances, so that it cannot avoid effects due to noise, rate fluctuation and interference from other wells. These effects make the measured pressure trends declining or rising and then obscure or distort the traditional flow behavior, which makes the following analysis difficult.

In this thesis, the problems encountered in analysis of PDG transient pressure are investigated. A new algorithm, multi-well deconvolution, and corresponding computer codes are developed. The algorithm is based on linear recursion with added non-linear least squares optimization to deal with the noise problem in time domain. With this developed algorithm, the inter-well interference effect can be extracted and the variable-rate superposition effect can be solved at the same time. New deconvolution-based rate transient analysis and pressure transient analysis methods are both proposed in this thesis. Numerical well testing synthetic studies are performed to demonstrate these procedures. The results prove that the new method works well in homogeneous reservoirs with two wells flowing at single phase, multiple rates.

To my family.

Acknowledgements

I would like to express my sincere thanks to my supervisor Dr. Shiyi Zheng who has provided me with the opportunity to work on this PhD at the Institute of Petroleum Engineering of Heriot-Watt University. His guidance and encouragement throughout my research time are wealth of my lifetime.

I would also like to thank Conoco-Philips, BG group and Wintershall Holding AG for their technical support. Schlumberger and Edinburgh Petroleum Services (EPS) Ltd. are gratefully thanked for providing with the simulation and well testing analysis software.

I am thankful to the academics, research staff, secretaries, librarian and those who helped during the course of this study in the Institute of Petroleum Engineering at Heriot-Watt University.

Finally, special thanks would like to be given to the PRIME project group members and all my friends in UK during the course of this study. Their advice, company, and help are gratefully appreciated.

Table of Contents

List of Figures

List of Tables

Nomenclature

A : Drainage area, ft^2

B_o : Oil formation volume factor, rb/STB

c_t : Total compressibility, psi^{-1}

c_f : Rock compressibility, psi^{-1}

C : Wellbore or tool storage coefficient, rb/psi

C_A : Shape factor

D : Non-Darcy Flow Coefficient, $(MSCF/D)^{-1}$

D_i : Initial decline rate coefficient, h^{-1}

g : Reservoir impulse response, psia/ (STB/d)/h

k : Permeability, md

H : Formation thickness, ft

m : Slope of semi-log straight line

P_{bub} : The bubble point pressure, psi

P_c : Capillary pressure, dimensionless

P_i : Initial pressure, psi

R_{inv} : Investigation radius, ft

R : Reservoir radius, ft

R_s : Gas-oil ratio, fraction

r_w : Wellbore radius, ft

r_e : External boundary radius, ft

S_g : Gas saturation, fraction

S_w : Water saturation, fraction

s : Skin factor, dimensionless

t : Time, hours

τ : Time, hours (integration variable)

V_p : Pore volume

λ: Regularization parameter

μ: Fluid viscosity, cp

ϕ : Porosity, fraction

N_i : Cumulative oil production, stb

N_{pi} : Cumulative oil production to a reservoir shut-in pressure of 0, stb

p_u : Unit rate drawdown pressure, psi/stb/day

Δp : Drawdown pressure drop, psia/day

L : Inter-well distance, ft

h : Primary pressure derivative of p_{u11}

S : Van Everdingen and Hurst skin factor

γ : Exponential of Euler constant (~1.78)

p_o : Initial pressure, psia

p_{ur} : Unit rate drawdown pressure, psia/stb/day

p_{cq} : Constant rate pressure, psia

p_{wf} : Bottom hole flowing pressure, psia

p_{uii} : Pressure response at well i due to the unit-rate production of well i , psia/stb/day

p_{uij} : Pressure response at well i due to the unit-rate production of well j , psia/stb/day

q_i : Flow rate, stb/day

q_o : Initial surface flow rate at t=0

q_{up} : Unit pressure flow rate, stb/day /psia

q_{cp} : Constant pressure flow rate, stb/day

Subscripts

i : initial

cq : constant-rate

w : wellbore

m : measured

u : unit

ur : unit-rate

up : unit-pressure

Name

BHP: Bottom-hole Pressure

BU: Buildup test

DD: Drawdown test

PDG: Permanent Down-hole Gauges

PBU: Pressure Buildup

PDD: Pressure Drawdown

PPD: Primary Pressure Derivative

OOIP: Original Oil In Place

ROIP: Recovery Oil In Place

EUR: Estimate Ultimate Recovery

FVF: Formation Volume Factor

Chapter 1
Introduction

1.1 Background

Permanent down-hole gauge (PDG) is a pressure and temperature real time monitoring systems installed at the bottom hole near the reservoir. The main objective is to help the reservoir management and the production by continuously measuring pressure and temperature in the reservoir. It has been widely installed in the oilfield around the world in recent years.

Transient pressure from permanent down-hole gauges are characterized by long term and large volume. Usually the whole sequence of PDG pressure comprises hundreds of pressure drawdown (PDD) and pressure build-up (PBU) flow periods. So it has the potential to provide more information about a reservoir than those from relatively short test duration. However, the current pressure transient analysis (PTA) techniques are mainly based on the analysis of individual flow periods in isolation, namely PDD or PBU period in the test. Therefore, it becomes a challenge to analyze PDG transient pressure with the existing PTA techniques.

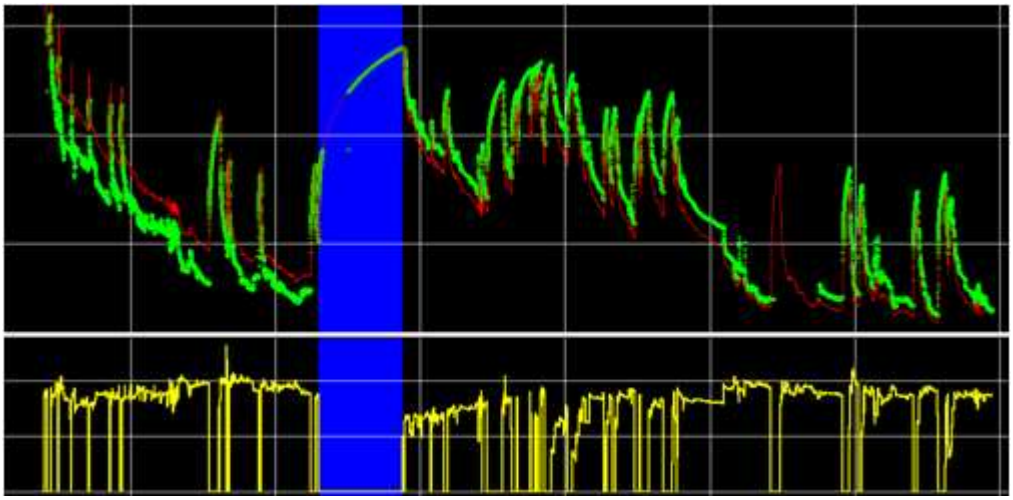

Figure 1. 1 PDG transient pressure data

Moreover, there are several issues related to this kind of long-term PDG data, such as the data are inherently noisy because they are obtained under uncontrolled conditions.

Besides, the measured long-term pressures, which combined test and production data, are both achieved under the variable conditions. In practice it is impossible to keep a constant flow condition for obtaining transient rate or transient pressure, so the practical dataset is either variable-rate transient pressure or variable-pressure transient rate. While current theoretical methods for rate transient analysis (RTA) and pressure transient analysis (PTA) in well testing are based on constant rate or pressure solutions, which means before the transient analysis, the transient data (pressure or rate) need to be normalized to that due to either a constant-rate or constant-pressure form.

In addition to the noise problem and variable-rate superposition effect, multi-well interference effect is another common issue for transient pressure from PDG in practice. Interference effect between wells makes the measured pressure trends declining or rising and then obscures or distorts the traditional flow behaviour, which makes the following analysis difficult.

All the stated issues above, i.e. long-term, noise problem, variable-rate superposition and multi-well interference effects in PDG transient pressure data make the straightforward interpretation unavailable due to the limitation of the current PTA and RTA theory. Therefore, this thesis attempts to understand the problems in processing

and analyzing PDG transient pressure data and to develop a more practical method to solve them.

1.2 Main Conflict in Analysis of PDG Transient Pressure

The main conflict in analysis of PDG transient pressure lies in the pre-analysis processing of the inherent issues in PDG data. In this section of the thesis, a general review of PDG data and relevant processing and analysis techniques is provided. Details of the problems which cause the conflict will be discussed in review of following literatures.

The review starts with the characteristics of PDG data, and then goes through the relevant methods to solve the mentioned data issues. Pressure and rate transient analysis methods for processing transient pressure data are presented in detail. Deconvolution techniques and recent advances in deconvolution application are reviewed. Finally, the main problems in processing and analysis of PDG transient pressure are outlined.

1.2.1 Review of PDG and PDG Data

Permanent down-hole gauges (PDG) are metering devices installed down-hole to monitor the well and reservoir conditions in real time. Technology has evolved over more than 40 years since the first installation (Chorneyko, D.M., *et al*., 2006[75]). Installation of these gauges has been an increasingly common industry practice in worldwide because of the improved reliability and the value of information that the gauges provide.

PDG components include gauges, housing, cable, connections, and acquisition systems. Permanent monitoring systems measure and record well performance and reservoir behavior from sensors, which are placed downhole during the completion. These measurements give engineers information essential to dynamically manage hydrocarbon assets, allowing them to optimize production techniques, diagnose problems, refine field development and adjust reservoir models. Sensors are placed downhole with the completion string close to the heart of the reservoir. Modern communications provide direct access to sensor measurements from anywhere in the world. Reservoir and well behaviors may now be monitored easily in real time, 24 hours a day, day after day,

throughout the lifetime of the reservoir. Engineers can catch performance daily, examine responses to changes in production or secondary recovery processes and also have a record of events to help diagnose problems and monitors in a power plant's control room. (Athichanagorn, Suwat, *et al*, 1999[63]; Frota, H.M. and Destro, W., 2006[72])

Data from permanent down-hole gauges can be examined and collected almost as soon as they are acquired at the down-hole of the well. A wide range of application of permanent downhole gauge data has been reported in the oil and gas industry (Ouyang, L.B. and Kikani, J., 2002[81]; McCracken, M. and Chorneyko, D., 2006[76]; Tibold, M.P., *et al*., 2000[78]; Queipo, N.V., *et al*., 2002[79]; Gringarten, A.C., *et al*., 2003[80]). These applications include: reduce ambiguity and uncertainties in the interpretation; detect the changes in reservoir properties; monitor skin, permeability, pressure drawdown over time; monitor hydraulic fracturing operations; monitor pump inlet and outlet pressures for pumping wells; evaluate the performance of well completion, simulation or workover; identify reservoir connectivity; evaluate operational efficiency; reduce the flowback time of new wells; and assist reservoir simulation and history matching.

In practice, there are issues associated with the data that these gauges collect. Vast amounts of data are being gathered continuously at intervals down to one second over several years. This data contains more information about the reservoir parameters changing during short and long time intervals than data from traditional pressure transient tests which last for relatively small durations. In this situation, more information will be hidden in this long-term PDG pressure record than just a collection of drawdowns and buildups, which makes the interpretation of PDG data a new challenge.

The advent of the permanent down-hole gauge motivates a new round of research interest in pressure transient analysis (PTA), also known as well test interpretation. Specifically, multi-rate pressure transient analysis techniques are improved. Because of the pressure data from permanent down-hole gauges are composited with hundreds of drawdown and buildup.

However, current pressure transient analysis techniques, i.e. PBU analysis and PDD analysis, have drawbacks, such as it gives a limited reservoir volume, reveals limited

reservoir information and sometimes provides an incorrect diagnosis of the reservoir model (Du, K.F., 2007[70]).

Besides the characteristic of long term and large volume, there are several issues related to this kind of PDG pressure data, such as the data are inherently noisy because they are obtained under uncontrolled conditions. In processing the noise issue, it has motivated several studies in data processing, noise reduction and new interpretation methodologies for the PDG data (Ouyang, L.B. and Sawiris, Ramzy, 2003[77]). Athichanagorn et al. (1999[73]) proposed a wavelet based data processing and interpretation procedure. This procedure was presented as a seven-step methodology that tackled the different issues relating to the data acquired from permanent down-hole gauges.

Moreover, it involves two key effects in the transient pressure data from permanent down-hole gauges, namely, multi-rate superposition and multi-well interference effects. These issues have motivated several studies in data processing, noise reduction and new interpretation methodologies for the permanent down-hole gauge data.

Since 20th century, almost all of giant fields in the world reached their maturity still having considerable amount of oil left behind to be recovered. Increasing demand for energy and the consequent high oil prices made small size fields, which were abandoned due to uneconomic operational conditions, renewedly attractive to oil companies. Because of these reasons, mature field development is increasingly becoming an attractive but challenging subject (Babadagli, T., 2005[10]; Ormerod, L., *et al*., 2006[9]; Claverie, M., *et al*., 2006[13]).

The key issue in mature field development is the estimation of remaining reserves focusing on determination of the amount and location of the residual oil after primary and secondary recovery using field, log, and core data. After valuing the remaining oil, the right technique, such as tertiary recovery, infills, horizontals, and optimal placement of new wells to recover it, will be chosen. (Chedid, R. and Colmenares, F.,2002[1]; Carr, Brian, *et al*., 2000[2]; Mahroos, F.A., 2005[3]; Li, X.G., *et al*., 2005[4]; Naguib, M.A., *et al*., 2005[6])

Numerous mature field well tests have shown that in a multi-well reservoir system, the bottom hole pressure measured in one well is affected by the production from other

operating wells. This phenomenon is so-called inter-well interference effect, which potentially leads to misinterpret well test data. (Leaver, J.D., *et al*., 1988[90]; Onur, M., *et al*., 1991[91]; Hallford, D.L., *et al*., 1995[93]; Marhaendrajana, T., *et al*., 2003[95]; Bischoff, R. and. Bejaoui, R., 2005[8]) Such effect becomes dominant in high-permeability reservoirs, as well as in some intermediate- permeability or low-permeability reservoirs with short inter-well distance.

In processing multi-well interference effect, traditional methodology is from multiple well tests (Kama, M. M., 1983[82]; Economies, M.J., and Ogbe, D.O., 1985[89]). The pressure response is measured in an observation well some distance away from the active well, which may be a producing or an injection well. Through the analysis of the observation well, average reservoir properties in the area separating the wells are determined. However, a drawback of multiple well tests is that it requires one or more potentially productive wells to be shut-in (Dominique Bourdet., 2002[83]).

Many different techniques have been published to analyze transient pressure data affected by this multi-well interference effect. The first attempt to provide a generalized approach for the analysis of well test data from multi-well reservoir systems was presented by Onur, et al. (1988[84], 1989[85]). Onur, et al. assumed that all wells start producing at the same time and that the producing time is long enough for pseudo-steady state flow to occur. It was also observed that for short producing times, the inter-well interference behavior does not affect the semi-log straight line, i.e. pressure buildup data follow the Horner semi-log straight line. The application of this method is limited as it assumes that all of the wells under the production at the same time and that the pseudo-steady state flow condition is achieved prior to shut-in.

Marhaendrajana, et al. (1997[87], 1999[88]) developed a new solution for the analysis and interpretation for wells that exhibit the well interference effect, in which production time as well as the symmetry of the multi-well configuration were taken into account. Their method also considered the case where the focus well does not need to begin production at the same time as the offset wells. Numerous cases of pressure buildup tests were observed that the pressure actually declines at later times during the test, indicating communication with the surrounding wells that are still on production. Their approach employs a straight-line graphical analysis of data on a Cartesian plot, where this yields a direct estimation of permeability. And “corrected” data functions were

generated using their well interference model to use type curve and semi-log analysis. The application of their method is limited as it can just for analyzing pressure buildup data from a well in a multi-well reservoir system.

As mentioned before, multi-well interference effect is very common in PDG pressure data in oilfield practice (Britt, L.K., *et al*., 1991[92]; Erwin, M.D., *et al*., 2002[94]). It makes the measured pressure trends declining or rising and then obscures or distorts the traditional flow behavior, which makes the following analysis difficult, i.e. the construction of the incorrect semi-log straight line or the incorrect radial flow regime on a pressure derivative log-log plot.

For multi-rate superposition effect, which is inevitable in PDG pressure, there have been several classical rate normalization methods. The purpose is to make sure normalized data, namely rate-normalized pressure, fit the traditional pressure transient theory. Methods published in the literature, on this subject area include various types of superposition and normalization methods (Palacio, J. C. and Blasingame, T.A., 1993[29]; Agarwal et al., 1999[23]).

Deconvolution is one of these rate normalization methods because it can transfer the variable rate pressure data into an equivalent pressure response due to the constant rate profile. This equivalent constant rate pressure response can be used for reservoir model identification. Deconvolution technique has been applied to long-term PDG data in recent years. Schroeter et al. (2001[64], 2002[48]), presented a deconvolution technique by considering deconvolution as a nonlinear total least squares problem. Levitan et al. (2004[65]) also produced a more practical deconvolution algorithm by utilizing an unconstrained, nonlinear weighted least-squares objective function involving the sum of three mismatch terms for pressure, rate and curvature. Pimonov et al. (2009[69]) presented a pressure-pressure deconvolution algorithm, through which the flow rate is eliminated from the convolution formulation, so it can be used for analyzing multipoint pressure transient data such as interference test and MDT test.

All the stated above, current methods of both pressure transient analysis and rate transient analysis have respective drawbacks and limitations. While the issues, i.e. long-term, noise problem, variable-rate superposition and multi-well interference effects in transient pressure data from permanent down-hole gauges make the straightforward

interpretation unavailable. This is my original intention to develop the multi-well deconvolution algorithm and deconvolution-based transient analysis technique to deal with the problems in PDG transient pressure.

1.2.2 Review of Pressure and Rate Transient Analysis Techniques

Pressure Transient Analysis (PTA) Technique

Flow in a reservoir is often characterized as being one of two types, namely transient or boundary-dominated. Transient flow takes place during the early life of a well, when the reservoir boundaries have not been felt, and the reservoir is said to be infinite-acting. During this period, the size of the reservoir has no effect on the well performance, and from analysis of pressure or production, nothing can be deduced about the reservoir size (in theory, the size of the reservoir does have an effect even at very early times, but in reality, this effect is so small as to be negligible- and not quantifiable with any kind of confidence). Transient flow forms the basis of a domain of reservoir engineering called pressure transient analysis (PTA), also known as well test interpretation (Lee, W.J., and Spivey, J.P., 1998[99]).

The field of well testing relies heavily on equations of flow for a well flowing at constant rate. Initially, the flow regime is transient, but eventually when all the reservoir boundaries have been felt, the well will flow at steady state (if a constant pressure boundary exists) or at pseudo-steady state (if all the boundaries are no-flow boundaries). During pseudo-steady state, the pressure throughout the reservoir declines at the same rate, and the reservoir acts like a tank (hence the alternative name, tank-type behavior). The concept of pseudo-steady state is applicable to a situation where the well is flowing at a constant flow state.

Since the beginning of the 1980’s, the technical advances in hardware, data acquisition and interpretation techniques have significantly increased the scope and capabilities of transient well test analysis. These advancements have been reviewed by Horne (1990[97]): (1) pressure derivative analysis method, (2) the common availability of computer software/packages for rapid graphical presentation, (3) the use of non-linear regression (automated type curve matching), (4) the availability of higher precision, high frequency data (pressure and flow rate), and (5) the development of new interpretation models such as those for multiphase flow, multi-layered, radial composite and compartmentalised reservoirs.

In this past decade, well testing has been transformed from a level mainly interested in determining a well's productivity to a sophisticated discipline capable of characterising the reservoir geometry, boundary and heterogeneity (Weiland, J., 2008[102]; Nnadi. M. and Onyekonwu.M., 2004[104]; Freddy, H.E.,2004[105]; Kamal, M.M., *et al*., 2005[101]; Jackson, R.R. and Banerjee.R.,2000[100]; Landa, J.L., *et al*., 2000[103]; Zakirov, S.N., *et al*., 2006[106]).

Transient analysis is based on the assumption that the production rate during the test has been constant. In practise, well test analysis is the interpretation of the pressure response of the reservoir to a given change in the rate, from zero to a constant value for a drawdown, or from a constant value to zero for a build up (Perrine, R.L., 1956[96]).

The analysis of recorded pressure as a function of time is termed transient analysis. The procedure of pressure change in the formation caused by production, namely drawdown, or well shut-in after production, namely build-up, can be modelled by a second order partial differential equation:

$$\frac{\partial}{\partial x}\left(\rho\frac{k_x}{\mu}\frac{\partial p}{\partial x}\right)+\frac{\partial}{\partial y}\left(\rho\frac{k_y}{\mu}\frac{\partial p}{\partial y}\right)+\frac{\partial}{\partial z}\left(\rho\frac{k_z}{\mu}\frac{\partial p}{\partial z}\right)=\phi\mu C_t\frac{\partial p}{\partial t} \tag{1.1}$$

With properly defined assumptions for the application to the slightly compressible, single phase fluid flow in the porous media, the equation can be linearised and reduced to a new form, which has been defined as the diffusivity equation:

$$\frac{\partial^2 P}{\partial X^2}\eta_x+\frac{\partial^2 P}{\partial Y^2}\eta_y+\frac{\partial^2 P}{\partial Z^2}\eta_z=\frac{\partial p}{\partial t} \tag{1.2}$$

Where:

$$\eta_j=\frac{k_j}{\phi\mu C_t}\quad,\quad j=x,y,z \tag{1.3}$$

are called the hydraulic diffusivities. For radial flow, the corresponding equation is:

$$\frac{1}{r}\frac{\partial}{\partial r}\left(r\frac{\partial P}{\partial r}\right)=\frac{1}{\eta}\frac{\partial P}{\partial t} \tag{1.4}$$

For well testing, the first attempt to solve this equation was made by Van Everdingen and Hurst by applying the Laplace transformation. The principle solution for transient analysis is the constant rate solution, i.e. a line source solution (compared to the reservoir geometry, the well was approximated as a line with zero radius) which describes the pressure drop in the well bore due to constant rate production. With one initial and two boundary conditions specified, and the following assumptions:

- Homogeneous and isotropic porous medium of uniform thickness;
- Pressure independent rock and fluid properties;
- Small pressure gradients;
- Radial flow;
- Applicability of Darcy's law;
- Negligible gravity forces, in an infinite acting reservoir.

This solution in field units has been given by Matthews and Russell:

$$P(t,r) = P_i - \frac{170.6qB\mu}{kh}\left[-\mathrm{E}i\left(\frac{-\phi\mu C_t r^2}{0.001056kt}\right)\right] \tag{1.5}$$

The mathematical function, $\mathrm{E}i(-x)$, is the exponential integral and is defined by:

$$\mathrm{E}i(-x) = -\int_x^{\infty}\frac{e^{-u}du}{u} = \left[\ln x - \frac{x}{1!} + \frac{x^2}{2(2!)} - \frac{x^3}{3(3!)}.....\right] \tag{1.6}$$

For x <0.01, this term can be further simplified as:

$$\mathrm{E}i(-x) = \ln(x) + 0.5772 \tag{1.7}$$

Where the number 0.5772 is Euler's constant and the constants in Equation (1.5) are due to application of field units.

For well test analysis, since the pressure is measured at the well bore, it is usually found that the condition x<0.01 is satisfied even for small values of testing time, t. Therefore, the Equation (1.5) can be re-written as:

$$P(r_w,t) = P_{wf} = P_i - \frac{170.6qB\mu}{kh}\left[-\ln\left(\frac{\phi\mu C_t r_w^{\ 2}}{0.001056kt}\right) - 0.5772\right] \tag{1.8}$$

This is the basic equation for transient well test analysis (constant rate drawdown).

The analytical solution to the diffusivity equation for a uniform pressure initial condition and a constant flow rate inner boundary condition has led to an expression for the dynamic wellbore pressure behavior of a model reservoir having homogeneous formation permeability and instantaneous skin effect. The objective of a well test is to measure the dynamic response of an actual reservoir under these same conditions and determine unknown reservoir parameters. The two most important such parameters are the permeability thickness product, kh, and the skin factor, s. The productivity of a well can only be predicted if these quantities are known.

The problem of well testing is essentially one of parameter estimation in which the unknown properties are adjusted until the theoretical solution or ideal model matches the measured system behavior. In linear systems this can often be achieved directly without a search process.

Often the first significant transient event at an oil well is the initial production period that results in a pressure drawdown at the formation face. Provided the production rate can be controlled at a constant value, the physical situation corresponds to the model conditions and thus it seems logical to investigate what can be learned about the well and the reservoir from pressure drawdown data.

The drawdown test is run by producing the well at a constant flow rate while continuously recording down-hole pressure. While most reservoir information obtained from a drawdown test can also be obtained from a pressure build-up test, there is an economic advantage of drawdown testing since the well is produced during the test. The main technical advantage of drawdown testing is the possibility of estimating reservoir volume. The main disadvantage is the difficulty of maintaining a constant production rate and the fact that the skin factor may change due to the well cleaning up.

The down-hole pressure at an active well producing at a constant rate in an infinite-acting reservoir is given by:

$$p_{wf} = p_i - \frac{q_s B\mu}{2\pi kh} \cdot \frac{1}{2}\left[\ln \frac{kt}{\phi\mu C_t r_w^2} + 0.80908 + 2S \right] \tag{1.9}$$

i.e.

$$p_{wf} = p_i - \frac{q_s B\mu}{2\pi kh} \cdot \frac{1}{2}\left[\ln t + \ln \frac{k}{\phi\mu C_t r_w^2} + 0.80908 + 2S \right] \tag{1.10}$$

if the reservoir is at p_i initially and t is the time from the start of production.

Theoretically a plot of measured flowing down-hole pressure versus the natural logarithm of flowing time, i.e. semi-log plot, should be a straight line of slope m and intercept $p_{t=1}$. Hence the analysis of drawdown data consists of making a plot of p_{wf} against $\ln t$ giving:

$$p_{wf} = m \ln t + p_{t=1} \tag{1.11}$$

From equation (1.11) the slope is given by:

$$m = -\frac{q_s B\mu}{4\pi kh} \tag{1.12}$$

and the intercept corresponding to $\ln t$ equals to 0 by:

$$p_{t=1} = p_i + m\left[\ln \frac{k}{\phi\mu C_t r_w^2} + 0.80908 + 2S \right] \tag{1.13}$$

Once the slope of the straight line portion of the semi-log plot, m , has been determined the permeability thickness product, kh , can be calculated from equation(1.12). This presumes that the oil production rate, q_s , has been measured in the test and the oil formation volume factor, B , and viscosity, μ , are known from laboratory PVT studies. If the formation thickness, h , is known from log evaluation, the formation permeability, k , can be obtained. Equation (1.13) may be rearranged as an explicit expression for the skin factor, i.e.

$$S = \frac{1}{2}\left[\frac{p_{t=1} - p_i}{m} - \ln \frac{k}{\phi\mu C_t r_w^2} - 0.80908 \right] \tag{1.14}$$

Hence if the initial reservoir pressure, p_i , the porosity, ϕ , the total compressibility, C_t , and the wellbore radius, r_w , are known the skin factor can be calculated from the slope and intercept of the plot using equation (1.14).

The preceding equations can be used with either of the sets of consistent units. However, within the oil industry, there is still a preference for using field units and the working

equations are easily transformed to accommodate this. The field unit's version of equation (1.10) is:

$$p_{wf} = p_i - \frac{887.217 q_s B\mu}{2\pi kh}\left[\ln\frac{0.0002637kt}{\phi\mu C_t r_w^2} + 0.80908 + 2S\right] \tag{1.15}$$

or on rearranging:

$$p_{wf} = p_i - \frac{70.6 q_s B\mu}{kh}\left[\ln t + \ln\frac{k}{\phi\mu C_t r_w^2} - 7.43173 + 2S\right] \tag{1.16}$$

Hence, in field units, a plot of p_{wf} versus $\ln t$ gives a straight line of slope, m, and intercept, $p_{t=1}$, where:

$$m = -\frac{70.6 q_s B\mu}{kh} \tag{1.17}$$

and

$$p_{t=1} = p_i + m\left[\ln\frac{k}{\phi\mu C_t r_w^2} - 7.43173 + 2S\right] \tag{1.18}$$

Which on solving for the skin factor, S, becomes:

$$S = \frac{1}{2}\left[\frac{p_{t=1} - p_i}{m} - \ln\frac{k}{\phi\mu C_t r_w^2} + 7.43173\right] \tag{1.19}$$

If the drawdown test is long enough, the down-hole flowing pressure will eventually derivate from the semi-log straight line and make the transition from infinite-acting to semi-steady state behavior.

Although pressure drawdown tests give considerable information about the reservoir, the well testing interpretation is an inverse problem, which is a process of resolving the unknown system by items of the known input signal (such as flow rate changes) and output signal (such as reservoir pressure changes). It is well known that there is no unique resolution for this kind of inverse problems, so one of main tasks is to determine the reservoir model before interpretation.

Rate Transient Analysis (RTA) Technique

Rate transient analysis (RTA), also known as production data analysis, has advanced significantly over the past years (Mohaghegh, S.D., *et al.*, 2005[39]; Gaskari, R., *et al*., 2006[40])

The first systematic approach to analyzing oil and gas production rate data was presented by Arps in the 1950's. Arps decline equation is based on empirical relationships of rate vs. time for oil wells. It covers three decline types: exponential, hyperbolic and harmonic, which is based on different decline exponent (Slider, H. C., 1968[17]; Huffman, C.H. and Thompson, R.S., 1994[36]).

Arps decline curve analysis is a graphical procedure used for analyzing declining production rates and forecasting future performance of oil and gas wells. A curve fit of past production performance is done using certain standard curves. This curve fit is then extrapolated to predict potential future performance. Decline curve analysis is a basic tool for estimating recoverable reserves. Conventional or basic decline curve analysis can be used only when production history is long enough that a trend can be identified.

This rate analysis is not grounded in fundamental theory but is based on empirical observations of production decline. There are theoretical equivalents to these decline curves (for example, it can be demonstrated that under certain circumstances, such as constant well backpressure, equations of fluid flow through porous media under "boundary-dominated flow" conditions are equivalent to "exponential" decline).

It is implicitly assumed, when using decline curve analysis, the factors causing the historical decline continue unchanged during the forecast period. These factors include both reservoir conditions and operating conditions. Some of the reservoir factors that affect the decline rate include: pressure depletion, number of producing wells, drive mechanism, reservoir characteristics, saturation changes, and relative permeability. Operating conditions that influence the decline rate are: separator pressure, tubing size, choke setting, workovers, compression, operating hours, and artificial lift. As long as these conditions do not change, the trend in decline can be analyzed and extrapolated to forecast future well performance. If these conditions are altered, for example through a well workover, then the decline rate determined pre-workover will not be applicable to

the post-workover period (Jericho L.P. , *et al*., 2004[42]; Kabir, C.S. and Izgec, B., 2006[43]).

When analyzing rate decline, two sets of curves are normally used. The flow rate is plotted against either time or cumulative production (Li, K. and Horne, R.N., 2005[45]). Time is the most convenient independent variable because extrapolation of rate-time graphs can be directly used for production forecasting and economic evaluations. However, plots of rate vs. cumulative production have their own advantages. Not only do they provide a direct estimate of the ultimate recovery at a specified economic limit, but will also yield a more rigorous interpretation in situations where the production is influenced by intermittent operations.

The following steps are taken for exponential decline analysis, and for predicting future flow rates and recoverable reserves:

1. Plot flow rate vs. time on a semi-log plot (y-axis is logarithmic) and flow rate vs. cumulative production on a Cartesian (arithmetic coordinate) scale.

2. Allowing for the fact that the early time data may not be linear, fit a straight line through the linear portion of the data, and determine the decline rate "D" from the slope (-D/2.303) of the semi-log plot, or directly from the slope (D) of the rate-cumulative production plot.

3. Extrapolate to q = qE to obtain the recoverable hydrocarbons.

4. Extrapolate to any specified time or abandonment rate to obtain a rate forecast and the cumulative recoverable hydrocarbons to that point in time.

A testament to the success of Arps style decline analysis is its continued popularity today. One of the most attractive features of the Arps methodology is its simplicity. Because it is an empirical method, it requires no knowledge of reservoir or well parameters. The application of the method involves using an empirical curve match to predict the future performance of the well. Thus, it can be applied to production through any type of reservoir drive mechanism. In fact, a practical set of guidelines has been assembled through extensive field analysis, which suggests what curves belong with which type of reservoir (Gentry, R. W., 1972[21]).

One of the restrictions of Arps decline analysis is its inability to disassociate the production forecast from operating constraints. In other words, the ultimate recoverable reserves, predicted by the Arps decline must inherently assume that historical operating conditions remain constant in the future. Another drawback of Arps is its limited applicability in the transient (or infinite acting) flow regime. In fact, Arps decline analysis is often misused for transient dominated production data, such as hydraulically fractured tight gas wells. Under such conditions, an analysis technique capable only of predicting ultimate recovery (such as Arps) has very limited application. Instead, other methods that use transient solutions should be used.

Although Arps equation is strictly applicable for pseudo-steady state conditions, it has been often misused for oil and gas wells whose flow regimes are still in a transient state.

Fetkovich, M.J. et al. (1985[31], 1987[27], and 1996[30]) extended the concept of using type curves (previously reserved for welltest analysis) to the analysis of production data. The Fetkovich methodology uses the same Arps depletion stems to analyze boundary dominated flow, and constant pressure type curves (originally developed by Van Everdingen and Hurst) for transient production. The most valuable feature of type curves lies not in the analysis, but in the diagnostics. For example, the type curve match can show whether or not production data is still in transient or has become boundary dominated (something that Arps decline analysis does not do). Like Arps, the Fetkovich method calculates expected ultimate recovery, but is constrained to existing operating conditions. The transient portion of the Fetkovich type curves assumes constant bottomhole flowing pressure. Thus, for discontinuities in production data (such as extended shut-in or placing a well on compression) a segmented approach must be taken. Furthermore, if the well is rate restricted, such an approach will not work.

Fetkovich Liquid System Decline Curves were published (1980[24]) for analyzing oil wells producing at a constant pressure. He combined early time, analytical transient solutions with Arps equations for the later time, pseudo steady-state solutions. Although the value of the b ranges from 0 to 1, curves for b> 1 are often misused to match transient data. These liquid system curves are not recommended for gas wells when the amount of pressure drawdown is moderate to large. Alternately, these curves (b=0 and

b= 1) may be used for gas wells if gas well data are converted to an equivalent liquid system data.

Carter Gas System Type Curves were developed (1985[25]) to fill the gap which left with the method of Fetkovich decline curves. Carter used a variable λ reflecting the magnitude of pressure drawdown in gas wells. His λ = 1, 0 curves corresponds to b = 0 on the Fetkovich liquid decline curves and represents a liquid system curve with an exponential decline. Curves with λ = 0.75 and 0.55 are used for gas wells with an increasing magnitude of pressure drawdown. Obviously, Carter type curves are better suited to estimate reserves for gas wells.

Palacio & Blasingame Type Curves were presented (1993[29]) which provide a major advancement in the area of analyzing oil or gas well performance data using type curves. This paper is an excellent culmination of their work and the work of other investigators whose goals were to convert gas well production data into equivalent constant rate liquid data. They also established a clear relationship among the previously discussed decline curves. Palacio-Blasingame type curves provide a useful tool to estimate gas in place (GIP), reservoir permeability and skin. However, the transient period are strictly valid only for radial flow and thus may not be suitable for analyzing gas wells with relatively long vertical hydraulic fractures of infinite or finite conductivity. It is also difficult to pick up a clear transition between the transient and the PSS flow periods from these and the other previously discussed decline curves. Palacio-Blasingame utilizes derivative methods to help with the type curve matching process but this result in multiple curves even for the radial flow system.

Agarwal-Gardner Rate-Time Type curves were presented (1998[18]) which represent advancement over previous work because a clearer distinction can be made between transient and boundary dominated flow periods. The new curves also contain derivative functions, similar to those used in the pressure transient literature to aid in the matching process. These production decline curves are, to our knowledge, the first to be published in this format specifically for hydraulically fractured wells of both infinite and finite conductivity. Finally, these new curves have been extended to utilize cumulative production data in addition to commonly used rate decline data.

Normalized Pressure Integral (NIP) Type curves use normalized pressure instead of

normalized rate. Analysis is the inverse of Agarwal-Gardner Rate-Time Type curves (Rietman, N.D., 1995[33]).

There are also modern analytical methods that do not use type curves. One such method is called the Flowing Material Balance (Doublet, L.E., *et al.*, 1994[22]). This is a new production data analysis method, based on a modified version of the Agarwal-Gardner Rate-Cumulative type curves. The method is similar to a conventional material balance analysis, but requires no shut-in pressure data (except initial reservoir pressure). Instead, it uses the concepts of pressure normalized rate and material balance (pseudo) time to create a simple linear plot, which extrapolates to fluids-in-place.

Like all analytical methods, modern decline analysis makes certain simplifying assumptions about the reservoir and production data. Most of the methods mentioned assume single phase, volumetric reservoirs. However, some non-volumetric effects, such as water-drive and interference among multiple wells can be handled effectively, using influence functions (e.g. Blasingame type curves have a multiple-well feature that can accommodate and account for interference effects) (Blasingame, T .A. and Lee, W J.,1986[26]; Blasingame, T.A., *et al.*, 1989[19]; Blasingame, T.A., *et al.*, 1991[28]; Blasingame, T.A. and Rushing, J.A., 2005[20]) The assumption of single-phase production in the reservoir is, in most cases, also considered valid; especially for gas wells (gas compressibility dominates the material balance). The primary impact of multi-phase production in gas wells is in the wellbore, where special care must be taken to ensure that the pressure loss from surface to bottomhole conditions is estimated correctly.

Modern methods, such as those of Blasingame and Agarwal-Gardner are similar to Fetkovich, in that they use type curves for production data analysis. However, the primary difference is that the modern methods incorporate the flowing pressure data along with production rates and they use analytical solutions to calculate hydrocarbons-in-place. Thus, expected recoverable reserves can be quantified independently of production constraints. The traditional techniques are not capable of quantifying hydrocarbons-in-place, except by using an empirical recovery factor.

Two features of modern decline analysis that improve upon the traditional techniques are:

- Normalizing of rates using flowing pressure drop: plotting a normalized rate (q/ p) enables the effects of back pressure changes to be accommodated in the reservoir analysis.
- Handling the changing compressibility of gas with pressure: using pseudo-time as the time function enables the gas material balance to be handled rigorously as the reservoir pressure decreases with time.

In summary, rate transient analysis techniques have advanced significantly over the past few years. There are many different methods available currently. However, for practice, each current method of production data analyses has its own strengths and limitations. There is no single production data analysis method is capable of handling all types of data and reservoir types and there is no one clear method that always yields the most reliable answer (Jalali, J., *et al*., 2006[41]). Hence, a reliable method which is maximally suitable for various reservoir and wells with more accurate and frequent data is required.

With the real-time monitoring of the production system, a wide range of rate analysis should be carried out to manage the reservoir performance, e.g. production optimization, facilities design, production forecasting, and allocation and loss management, etc. Production rate analysis should be more valid as a reservoir characterization tool, with the advent of continuous measurement (surface and downhole pressure measurements, continuous surface rate and pressure measurements, etc).

1.2.3 Review of Deconvolution Technique

Deconvolution technique has been developed for over forty years and has received much attention recently as it has made an important challenge on traditional well test (pressure transient analysis) and production data analysis (rate transient analysis). It is not a new interpretation method, but a new tool to process pressure and rate data in order to obtain more interpretable data for well test and production analysis. Deconvolution provides the equivalent constant–rate pressure response or constant-pressure rate response of the well / reservoir system affected by variable rates/ pressures. With the implementation of permanent downhole pressure and flow-rate

measurement systems, the importance of deconvolution has increased because it is now possible to process the well test/production data simultaneously and obtain the underlying well/reservoir model.

Theoretical Background of Deconvolution Techniques

Hypothesis: $h(t)$ is a linear response of a system, the output is $y(t)$ and input is $x(t)$.

So $y(t)$ can be written as a convolution integral as follows:

$$y(t) = \int_{-\infty}^{\infty} h(t-\tau)x(\tau)d\tau \tag{1.20}$$

With given output $y(t)$ and input $x(t)$ to recover the system response $h(t)$ is so-called Deconvolution.

The single-well problem of deconvolution is given by Duhaml's integral or principle superposition, which as a function of time; the pressure drop is the convolution product of rate and reservoir response:

$$\Delta p(t) = p_i - p(t) = \int_0^t q(\tau)g(t-\tau)d\tau \tag{1.21}$$

Where, $q(t)$ and $p(t)$ are the measured flow rate and pressure at any place in the wellbore including wellhead, and p_i is the initial pressure. In equation (1.21), g is referred to as the impulse response of the system.

Thus, estimating the reservoir response essential amounts to inverting this convolution integral and is therefore an instance of a widely encountered mathematical problem called deconvolution.

Pressure-rate deconvolution

In pressure-rate deconvolution, the unit constant-rate pressure response of the reservoir can be reconstructed based on the following convolution integral:

$$\Delta p(t) = p_i - p(t) = \int_0^t q(\tau)\frac{dp_u(t-\tau)}{dt}d\tau \tag{1.22}$$

Where, $q(t)$ and $p(t)$ are the measured flow rate and bottom-hole pressure. p_i is the initial pressure and p_u is the unit-rate pressure response.

Rate-pressure deconvolution

In rate-pressure deconvolution, the unit constant-pressure rate response of the reservoir can be reconstructed based on the following convolution integral:

$$q(t) = \int_0^t q_{up}(t-\tau)\frac{d\Delta p(\tau)}{dt}d\tau \tag{1.23}$$

Where, q_{up} represents the rate response of the system if the well was produced at a unit constant-pressure condition.

Classification of Deconvolution Methods

All the existing deconvolution methods can be broadly classified into two groups: spectral methods and time domain methods. Spectral methods are based on the convolution theorem of spectral analysis. They apply spectral transform like the Laplace and Fourier transform to get the convolution product (Kuchuk, F.J. and Ayestaran, L., 1985[61]; Roumboutsos, A. and Stewart, G., 1988[62]; Bourgeois M.J. and Horne R.N., 1993[58]; Cheng, Y.M., *et al*., 2003[60]; Ilk, D. *et al*., 2005[52]; Iseger, P.D., 2006[66]; Al-Ajmi, N., *et al*., 2008[68]).Time domain methods discretize the convolution integral using interpolation scheme and proceed to solve the linear system. In order to reduce solution oscillation, a set of smoothing constraints have been imposed on the solution. Time domain methods including the linear solution (Jargon J.R. and van Pollen, H.K., 1965[54]; Thompson L.G., Reynolds A.C.,1986[56]), constrained total least squares (Kuchuk F.J. *et al*., 1990[55]; Baygun B. *et al*., 1997[57]), nonlinear total least squares(von Schroeter, T., *et al*., 2004[49]; Levitan, M.M., 2005[50]; Kuchuk, F.J., *et al*., 2005[47])and etc have been proposed.

The simplest algorithm for deconvolution known in numerical mathematics is the linear recursion method. This algorithm performs polynomial division in iterative scheme and is not stable for the rate data error larger than 1%, since after the discretization of Duhamel's integral, the linear equations of the reservoir system get ill-conditioned coefficient matrices, accumulating errors and providing big oscillations in the solution.

In order to deal with the instability problem in deconvolution, Thompson (1986[56]), Kuchuk et al (1985[61]) firstly made the system linear equations overdetermined through reducing the number of parameters in the solution and secondly seek solutions through minimizing a measure of the error signal.

Minimization problem still was subjected to instability since many local minima can exist for minimization function. The number of constraints was applied by Kuchuk (1990[55]). And other upgrades to the solution space, namely positiveness of the solution signal, its derivative and concaveness, the extent of autocorrelation for solution and energy constraint, during deconvolution in time space make the constrained Total-Least-Square methods robust enough, up to the rate error 2%, to be further developed for successful transformation of pressure-rate data into the constant-rate pressure response.

Recently, two important deconvolution algorithms (Von Schroeter et al., 2004[49]; Levitan, 2005[50]) have been published in the literature. Von Schroeter et al. first presented a time-domain method for deconvolution that have been shown to work when a reasonable level of noise is present in both pressure and rate data. There are three novel ideas about their algorithm. Firstly, in order to remove the sign constraints the reservoir response function must be satisfied with, equation (1.22) is solved not for unit-rate pressure response p_{ur}, but for the logarithmic derivative $\ln\left[dp_{ur}(t)/d\ln(t)\right]$ directly. Secondly, a regularization based on the curvature of the derivative is imposed to achieve some degree of smoothness of the solution. Finally, error in both pressure and rate data is allowed by considering a total least-square formulation in their algorithm. Von Schroeter et al.'s method can get stable deconvolution result even under the condition of 10 percents of flow-rate measurement errors.

However the assumption of this algorithm about the first node in solution as that corresponding to the unit-slope wellbore storage pressure vs. time behavior. The latter is needed to start solving the system of non-linear equations and also to recover the pressure response from its logarithmic derivative for which the above equations are initially solved. Based on the work of Von Schroeter et al., Levitan presented some practical considerations and made some improvement on the algorithm. Levitan's algorithm avoids this assumption by another less critical about the smallness of the first point time in the solution albeit does not prohibit for this point pressure to be negative. Both Levitan's and von Schroeter et al. algorithms allow for simultaneous initial and rate correction when deconvolving.

Assumptions and Limitations of Deconvolution

The basic assumption of all deconvolution techniques is the consistency of measured pressure and rate data with the linear Duhamel's model, which is based on the principle of superposition. The linearity of the system suggests only one well creating pressure perturbation to initially equalized region and static character of the parameters of reservoir and well. It sets some limitations that, for example, we cannot apply deconvolution if there is some interference from other wells nearby. Also we cannot apply deconvolution if there is aquifer or gas cap influence. Another requirement for linearity of the system is the single-phase flow, which means that the down-hole pressure for deconvolution must be higher than the reservoir bubble point pressure in oil reservoir. Moreover, the initial uniformity of pressure, within the whole investigated part of reservoir and the well rate from all the production by this well, all the way from initial equilibrium state must be satisfied.

However, deconvolution requires the solution of an ill-conditioned problem, meaning that small changes in input (measured pressure and rate data) can lead to large changes in the output (deconvolved) result. For the cause of ill-conditioned problem, the results of linear solution are very unstable and the flow-rate measurement errors have much influence on the deconvolution methods. Therefore, it needs to develop robust deconvolution algorithms which are error-tolerant. In the recent several stable algorithms(Cinar M., *et al*., 2006[59]) were built that are capable of resolving the problem stated at pressure error up to 1% and rate error less than 10% that is crucial fact for development of deconvolution methods and its broad application.

The Application of Deconvolution Techniques in Well Test Analysis

Over the past forty years, pressure-rate deconvolution techniques have been applied to well test pressure and rate data to obtain the constant-rate behaviour of the reservoir system. The primary objective of applying pressure-rate deconvolution is to transform the pressure data response from a variable-rate test or production sequence into an equivalent pressure profile that would have been obtained if the well were produced at a constant rate for the entire duration of the production history.

If such an objective can be achieved with some success then the deconvolved response will remove the constraints of conventional analysis techniques that have been built around idea of applying a special time transformation (based on the logarithmic

multi-rate superposition time) to the test pressure data so that the pressure behaviour observed during individual flow periods would be similar in some way to constant-rate system response. As is well known, the superposition-time transform does not completely remove all effects of pervious rate variations and often complicates test analysis due to residual superposition effects, which can distort the regular pressure trends. Due to these reasons, pressure-rate deconvolution problem has attracted considerable interest over the past many years.

Because deconvolution operation highly depends on the consistency of measured pressure and rate data with the linear Duhamel's model, it is important to make rate measurement regularly. Apart from the rate precision, the linearity of the system, which was built on the principle of superposition, suggests only one well creating pressure perturbation to initially equalized region and static character of the parameters of reservoir and well. It sets some limitations that, for example, deconvolution cannot be applied if there is some interference from other wells nearby. Also deconvolution cannot be applied if there is aquifer or gas cap influence. Another requirement for linearity of the system is the single-phase flow, which means that the down-hole pressure for deconvolution must be higher than the reservoir bubble point pressure in oil reservoir. Moreover, the initial uniformity of pressure, within the whole investigated part of reservoir and the well rate from all the production by this well, all the way from initial equilibrium state must be satisfied.

Recently, robust pressure-rate deconvolution algorithms (Hollaender, F., *et al*., 2001[64]; Levitan, M.M., *et al*., 2006[51]; Ilk, D., *et al*., 2006[53]) have emerged, which motivate the development of new methods for analyzing well test data.

The Application of Deconvolution Techniques in Production Analysis

With the advent of continuous measurement (surface and downhole pressure measurements, continuous surface rate and pressure measurements, etc.), production analysis for reservoir characterization has become very popular in recent years (Anderson, D.M., *et al*., 2006[38]).

Analysis of the long-time flowrate data has been traditionally done using Arps decline curves (1950s[15]) to predict future production. In early 1980s, Fetkovich combined the empirical decline curves from Arps with the constant-pressure analytical solution for

transient production analysis and brought a much more rigorous foundation to decline-curve analysis. Fetkovich has also incorporated backpressure variations into the analysis. However, the effect of wellbore-pressure variations, including backpressure, that can mask the decline characteristics of curves.

Conventional (constant-pressure) decline curves are needed to determine decline types. Therefore, wellbore or surface-pressure variations during the decline analysis should be minimized at least for diagnostic purposes. A large number of papers on decline-type curves have been published for a variety of reservoir types, based on the constant-pressure production mode.

Various types of superposition and normalization methods, which aim at converting variable-pressure liquid solution to the corresponding constant-pressure solution, have been published in the literatures (Palacio, J. C. and Blasingame, T.A., 1993[29]; Agarwal et al., 1999[23]). As is well known, rate-normalized or pressure-normalized solutions are only approximate for variable rate/pressure histories and may not work if rate and pressure variations are not monotonic.

While, deconvolution can be a way to solve the pressure variations and avoids the transformation problem mentioned above in the meantime. As rate-pressure deconvolution directly provides the unit-rate pressure vs. real time based on constant downhole pressure production.

Recently, deconvolution-based method has been proposed in decline-curve analysis by Kuchuk (Kuchuk, F.J., *et al*., 2005[47]). Unneland, T., et al. (2005[37]) presented a procedure for applying continuous downhole pressure and rate measurements in decline curve analysis. The convolution of a constant pressure model extends classic decline-curve methods to the cases of wells operated at varying pressures, and allows reservoir description and well performance monitoring to be performed without shutting the well down for data acquisition.

1.2.4 Problems in Processing and Analyzing PDG Transient Pressure

The whole record sequence of the PDG pressure usually comprise several cycles of pressure drawdown (PDD) and pressure build-up (PBU) flow periods. The duration of

each PBU or PDD period is relatively short and the pseudo-steady state is not established in the area of investigation given such short production times.

Therefore, analysis of individual flow periods in isolation, i.e. PBU analysis or PDD analysis, gives a limited reservoir volume, reveals limited reservoir information and sometimes provides an incorrect diagnosis of the reservoir model.

To address this issue it need to develop a new method for the analysis of PDG pressure data from a well in multi-well reservoirs where both buildup and drawdown data can be taken into account even with short test times.

As reviewed before, deconvolution technique can solve multi-rate superposition problem in single-well reservoir system. It has become a useful addition to the suite of techniques used in well test analysis. However, the existing deconvolution algorithm is applicable only for the case when there is just one active well in the reservoir. It cannot be used for pressure transient analysis when there are several active wells operating in the field and the bottom hole pressure measured in one well is affected by the production from other wells operating in the same reservoir.

In order to apply deconvolution technique into multi-well interference analysis, a new deconvolution algorithm has to be developed. This new multi-well deconvolution algorithm will be possible to remove not only the rate variation effect of the well itself but also the pressure interference with other wells in the same reservoir. Then it will be able to reconstruct the true characteristic well pressure responses to unit-rate production of each producing well in the reservoir. These responses will reflect the reservoir/well properties and will be used for recovering these properties by the techniques of pressure transient analysis.

1.3 Motivation and Objective

It has been noted that the current RTA and PTA methods are not satisfied with PDG transient pressure data. A pre-analysis data processing is required so that the long-term, noise, variable-rate superposition and multi-well interference effects in PDG transient

pressure can be solved and traditional analysis methods can be fully utilized. It is the demand that motivated the work in the thesis.

The main objective of the thesis is to develop an algorithm for processing PDG transient pressure with noise, variable-rate superposition and multi-well interference effect. After the processing, the pressure/rate variations can be solved and the inter-well interference can be extracted. The entire history of PDG transient pressure can be analyzed. Thereby additional reservoir diagnostics and more distant reservoir features, such as reservoir boundaries can be obtained.

To achieve this objective, I have performed the following work:

- Developed a deconvolution algorithm for processing single-well PDG transient pressure with variable-rate superposition effect
- Developed a deconvolution algorithm for processing PDG transient pressure with multi-well interference effect
- Developed a deconvolution-based diagnostic tool, i.e. Primary Pressure Derivative diagnostic, for multi-well interference effect
- Proposed a deconvolution-based RTA method and a deconvolution-based PTA method.
- Proposed a double-checked practice method for analysis of transient pressure integrated with the transient rate analysis.

1.4 The Outline of the Thesis

This thesis includes seven chapters. The outline is as follows:

This Chapter has introduced the background of PDG development and main issues in PDG transient pressure data. Current methods for processing and analyzing transient pressure and rate data are reviewed and the main conflicts are discussed. As a result, the development of a new method for processing and analyzing PDG transient pressure will be the focus of this thesis. The remaining chapters are used to provide more details and

the development and application of the new method.

In Chapter2, the analytical pressure diffusion theory for single-well reservoir system is presented to describe the variable rate transient flowing conditions. A new time-domain deconvolution algorithm is then developed to deal with the flow rate variations and noise problem in single-well PDG data. Deconvolution-based transient pressure analysis theory and procedure are then derived in detail. Finally synthetic cases and numerical well testing are studied. Results are presented to prove the validity of the developed single-well pressure-rate deconvolution algorithm and corresponding deconvolution-based pressure transient analysis.

In Chapter3, the analytical theory of single-well rate transient analysis is presented. A new rate-pressure deconvolution algorithm in time-domain is then developed for the rate normalization. Then, deconvolution-based rate transient analysis theory is derived in detail. Finally synthetic cases are studied and results are presented to prove the validity of the developed single-well rate-pressure deconvolution algorithm and corresponding deconvolution-based rate transient analysis. A double-checked practice method for analysis of transient pressure integrated with the transient rate analysis is also proposed.

In Chapter4, the analytical pressure diffusion theory and derivation for two-well reservoir system is presented to describe the different transient flowing conditions**.** A new two-well deconvolution algorithm is then developed to extract the interference and normalize the variable flowing rate. Deconvolution-based self pressure analysis method is derived in detail. Finally numerical well testing synthetic studies are performed to demonstrate the procedures of processing and analysis.

In Chapter5, the analytical inter-well interference theory and derivation for two-well reservoir system is presented. The computing procedure of the developed two-well deconvolution is outlined. This algorithm is based on linear recursion with added non-linear least squares optimization procedure. Deconvolution-based interference analysis method is then derived in detail. Finally numerical well testing synthetic studies are performed to demonstrate these procedures of processing and analysis.

In Chapter6, single-well deconvolution has been applied to oil-gas reservoir system, interference diagnostics and reservoir boundary identification. Current single-well algorithm has been modified for this application. Multi-well deconvolution has been applied for interference extraction and analysis. Several synthetic cases are investigated and the results demonstrate the performance of the developed deconvolution algorithm on synthetic multi-well test data as well as multi-phase test data.

Summary and conclusions are given in Chapter7. An overview of achievements is outlined and the guideline for future research work is suggested.

Chapter 2
Deconvolution-based Pressure Transient Analysis of Single-Well PDG Data

2.1 Introduction

Traditionally well testing is completed by analyzing transient pressure due to constant production rate to derive reservoir properties such as skin, permeability and outer boundary conditions. This constant rate transient pressure, which is due to fixed flowing rate, is obtained from the measurement gauge in the well bore during the well test period.

However, in the oil industry practice, the constant flowing condition is hard to maintain, so the transient pressure data obtained will result from variable flowing rate history. And this is particularly true in the case, when transient pressure data is from a PDG over a relatively long period of production time. Therefore, the well testing interpretation methods cannot be applied directly before having the specified conditions met the criteria. A mathematical algorithm called deconvolution can solve this problem.

Deconvolution technique is capable of transferring the transient pressure, due to variable or step rate history, into an equivalent constant rate transient pressure. Once

having this task completed, the traditional well test analysis methods can be used for reservoir system identification and parameter estimation.

This chapter presents study results based on synthetic cases and numerical well testing. A new time-domain deconvolution algorithm and corresponding computer codes were developed for the study. It was proved that the new deconvolution algorithm works well in the case with single phase oil, but breaks down when dealing with cases having multi-phase flow and well interference effects in the data. These aspects will be addressed in the following chapters.

The organization of this chapter is as follows. The analytical pressure diffusion theory for single-well reservoir system is presented to describe the variable rate transient flowing conditions**.** A new time-domain deconvolution algorithm is then developed to deal with the flow rate variations. Then, deconvolution-based transient pressure analysis theory and procedure are derived in detail. Finally synthetic cases, which were based on the same numerical model, are studied and results are presented to prove the validity of the developed deconvolution algorithm and corresponding deconvolution-based analysis.

2.2 Analytical Theory of Single-Well Pressure Transient Analysis

2.2.1 Description of Single-Well Pressure Diffusion

Flow in a reservoir is often characterized as being one of two types, namely transient or boundary-dominated.

Transient flow takes place during the early life of a well, when the reservoir boundaries have not been felt, and the reservoir is said to be infinite-acting. During this period, the size of the reservoir has no effect on the well performance, and from analysis of pressure or production, nothing can be deduced about the reservoir size. Transient flow forms the basis of a domain of reservoir engineering called Pressure Transient Analysis (PTA), also known as well test interpretation.

The field of well testing relies heavily on equations of flow for a well flowing at constant rate. Initially, the flow regime is transient, but eventually when all the reservoir boundaries have been felt, the well will flow at steady state (if a constant pressure boundary exists) or at pseudo-steady state (if all the boundaries are no-flow boundaries). During pseudo-steady state, the pressure throughout the reservoir declines at the same rate, and the reservoir acts like a tank. The concept of pseudo-steady state is applicable to a situation where the well is flowing at a constant flow state.

In infinite reservoirs, if there is a single well, which is producing as shown in **Figure 2.1**, the pressure distribution of this well can be described as infinite acting reservoir behavior.

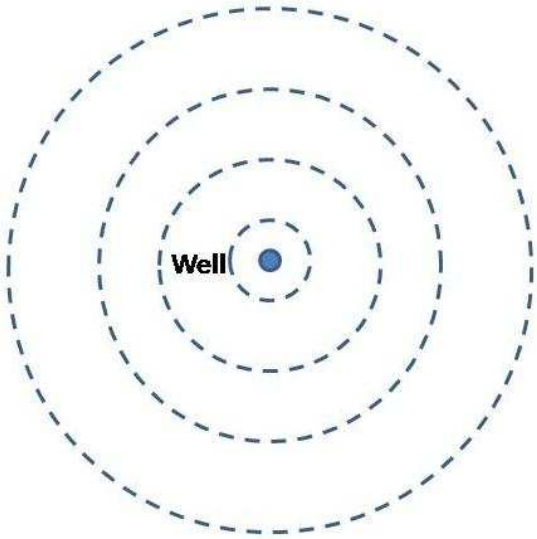

Figure 2. 1 Pressure distribution of one well (Well 1) in an infinite reservoir

In closed reservoirs, if there a single well, which is producing as shown in **Figure 2.2**, the pressure distribution of this well can be described as follows:

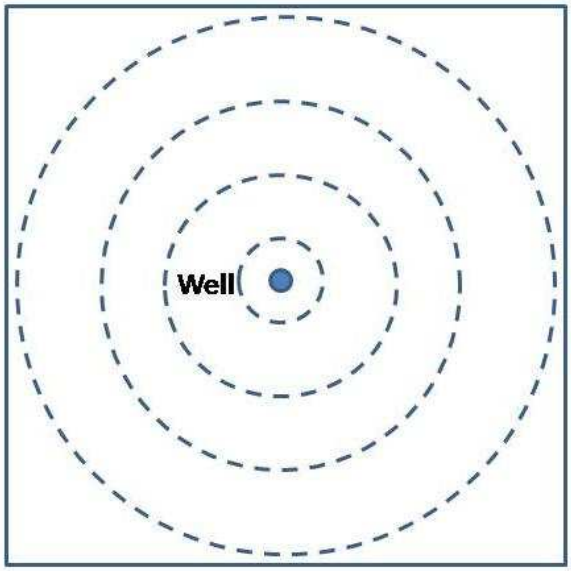

Figure 2. 2 Pressure distribution of one well (Well 1) in a closed reservoir

The pressure distribution of the two wells can be described as follows:

Firstly, the pressure transient is not reached the boundary. Well 1 shows the infinite acting reservoir behavior. Then the pressure transient has reached the boundary, the boundary influence is seen on Well 1. When the influence of the closed boundary reaches the Well 1, it changes to the pseudo-steady state flow behavior.

2.2.2 Theory and Derivation for Single-Well Pressure Diffusion

In a closed reservoir with single phase fluid, single well producing, two flow regimes will be encountered for the well. (Storage is not taken into account in this study), namely: 1st flow state (radial flow) and 2nd flow state (pseudo-steady). The pressure distribution function and its derivation in each flow regime are shown below:

Transient Flow:

The pressure distribution in the infinite reservoir is a function of the time and the distance to the producing well (space). It can be expressed with the Exponential Integral function:

$$\Delta p(t,r) = -0.5\frac{141.2qB\mu}{kh}\mathrm{E}i\left[\frac{-\phi\mu C_t r^2}{0.001056kt}\right] \tag{2.1}$$

For small x value, $Ei(-x) = -\ln(\gamma x)$, the Exponential Integral can be approximated by a log function (with $\gamma = 1.78$, Euler's constant). Therefore:

$$\Delta p(t,r) = \frac{162.6qB\mu}{kh}\left[\log\frac{0.000264kt}{\phi\mu C_t r_w^{\ 2}} + 0.809\right] \tag{2.2}$$

The primary pressure derivative here can be written as

$$PPD' = d\Delta p / dt = cons\tan t / t \tag{2.3}$$

The logarithmic derivative can be expressed as $d\Delta p / d\ln t = t \times d\Delta p / dt$ (2.4)

Pseudo Steady State Flow (closed reservoir):

In closed reservoirs, when all boundaries have been reached, the flow regime changes to pseudo steady state. The shape of the pressure profile becomes linear with time, and it simply declines as the reservoir is being depleted. During the pseudo steady state flow regime, the bottom-hole flowing pressure is a linear function of the elapsed time.

$$\Delta p = 0.234\frac{qB}{\phi c_t hA}t + 162.6\frac{qB\mu}{kh}\left[\log\frac{A}{r_w^{\ 2}} - \log(C_A) + 0.351 + 0.87S\right] \tag{2.5}$$

Primary Pressure Derivative:

$$d\Delta p / dt = \Delta p' = d(p_i - p_{wf}) / dt = 0.234\frac{qB}{\phi c_t hA} \tag{2.6}$$

Logarithmic Derivative:

$$d\Delta p / d\ln t = t\Delta p' = t \times d\Delta p / dt = 0.234\frac{qB}{\phi c_t hA}t \tag{2.7}$$

So the primary derivative of the pressure response versus time on log-log plot will be a zero slope line, while the corresponding logarithmic derivative on log-log scale should be a constant value.

2.3 Single-Well Pressure-Rate Deconvolution

2.3.1 Single-Well Pressure-Rate Deconvolution Theory

In single-well reservoir system, the equation of deconvolution is given by Duhaml's integral or principle of superposition, which is a function of time, where the pressure

drop across the reservoir is the convolution product of rate and reservoir response as shown in Eq.1 below.

$$\Delta p(t) = p_i - p(t) = \int_0^t q(\tau) g(t-\tau) d\tau \tag{2.8}$$

Where, $q(t)$ and $p(t)$ are the measured flow rate and pressure at any place in the well-bore up to the wellhead, and p_i is the initial reservoir pressure. In this equation, g is referred to as the impulse response of the reservoir system.

Therefore, in order to estimate the reservoir system response, the inversion of this convolution integral and this mathematical problem is so-called deconvolution.

Pressure-rate Deconvolution Problem

In pressure-rate deconvolution, the unit constant-rate transient pressure response of the reservoir system can be reconstructed based on the following convolution integral:

$$\Delta p(t) = p_i - p(t) = \int_0^t q(\tau) \frac{dp_{ur}(t-\tau)}{dt} d\tau \tag{2.9}$$

Where, $q(t)$ and $p(t)$ are the measured flow rate and bottomhole pressure. p_i is the initial reservoir pressure and p_{ur} is the unit-rate pressure drop (subscript *ur* stands for unit rate).

2.3.2 New Single-Well Pressure-Rate Deconvolution Algorithm

The pressure-rate convolution integral can be expressed as:

$$\Delta p(t) = p_i - p_{wf}(t) = \int_0^t q(\tau) h(t-\tau) d\tau \tag{2.10}$$

Where, $p_{wf}(t)$ is the down-hole pressure and $h(t)$ represents the system response function of the reservoir. It equals to primary derivative of unit-rate pressure drop of the well, which can be written as:

$$h(t) = dp_{ur}(t)/dt \tag{2.11}$$

The discrete convolution function can be written as:

$$\Delta p(n) = \sum_{k=0}^{N-1} q(k)h(n-k) \tag{2.12}$$

$q(n), n = 1,2,..., N$

$\Delta p(n), n = 1,2,..., N$

The linear recursion algorithm can be expressed as follows:

$$h(1) = \Delta p(1) / q(1) \quad (n = 1) \tag{2.13}$$

$$h(n) = \frac{\Delta p(n) - q(n)h(1) - q(n-1)h(2) - q(n-2)h(3) - ... - q(2)h(n-1)}{q(1)} \ (n = 2,3,..., N) \tag{2.14}$$

With cumulative trapezoidal integral, unit-rate pressure drop can be written as：

$$p_{ur}(1) = h(1) \quad (n = 1) \tag{2.15}$$

$$p_{ur}(n) = \frac{h(n) + h(n-1)}{2} + \frac{h(n-1) + h(n-2)}{2} + ... + \frac{h(2) + h(1)}{2} + h(1) \quad (n = 2,3,..., N) \tag{2.16}$$

The above-mentioned linear recursion deconvolution algorithm cannot give a stable solution due to the error accumulation at late time. So I add nonlinear least square (NLS) functions to the algorithm. With the added NLS optimization procedure, the developed deconvolution algorithm can give more accurate results.

The nonlinear least square algorithm includes following steps:

Step 1: Input data (p_{wf} , q)

Step 2: 1st Subtraction (calculate Δp)

$$\Delta p(t) = p_i - p_{wf}(t) \tag{2.17}$$

Step 3: 1st Deconvolution (calculate h)

$$F(X) = \min_X \frac{1}{2} \left\| conv(q, h\ ) - \Delta p \right\|_2^2 = \frac{1}{2} \sum_{i=1}^{n} (conv(q_i, h\ _i) - \Delta p_i)^2 \tag{2.18}$$

Step 4: 1st Summation (calculate p_u)

$$p_{ur}(1) = h(1) \quad (n = 1)$$

$$p_{ur}(n) = \frac{h(n) + h(n-1)}{2} + \frac{h(n-1) + h(n-2)}{2} + \ldots + \frac{h(2) + h(1)}{2} + h(1)$$

$$(n = 2,3,\ldots, N)$$

2.4 Deconvolution-based Pressure Transient Analysis

2.4.1 Analytical Solutions of Deconvolution-based Transient Pressure

1st Flow State (Radial Flow):

The pressure distribution in the infinite reservoir is a function of the time and the distance to the producing well. It can be expressed with the exponential integral function:

$$\Delta p(t,r) = 0.5\frac{141.2qB\mu}{kh}\mathrm{Ei}\left[\frac{\phi\mu C_t r^2}{0.001056kt}\right] \tag{2.19}$$

The pressure distribution of Well 1 can be written as follows:

$$\Delta p(t) = \frac{141.2qB\mu}{kh}\left\{-\frac{1}{2}\mathrm{Ei}\left[\frac{-\phi\mu C_t r_w^{\ 2}}{0.001056kt)}\right]\right\} \quad (r = r_w) \tag{2.20}$$

Here, r_w is a very small value. For small x, $Ei(-x) = -\ln(\gamma x)$, the exponential integral can be approximated by a log(with $\gamma = 1.78$, Euler's constant):

$$\Delta p\ (t) = \frac{162.6qB\mu}{kh}\left[\log\frac{0.000264kt}{\phi\mu C_t r_w^{\ 2}} + 0.809\right] \tag{2.21}$$

$$\Delta p = cons\tan t \times \log t + cons\tan t \tag{2.22}$$

$$PPD = d\Delta p / dt = cons\tan t / t \tag{2.23}$$

$$\log(PPD) = -\log t + cons\tan t \tag{2.24}$$

So in this state, the slope of *PPD* versus time on log-log plot is -1, shown in **Figure 2.3**.

2nd Flow State (Pseudo-steady):

In closed reservoirs, when all boundaries have been reached, the flow regime changes to pseudo steady state. When all boundaries have been reached, the shape of the pressure profile becomes constant with time, and it simply drops as the reservoir is being depleted. During the pseudo steady state regime, the bottom-hole flowing pressure is a linear function of the elapsed time as below:

$$\Delta p\ (t) = 0.234\frac{qB}{\phi c_t hA}t + 162.6\frac{qB\mu}{kh}\left[\log\frac{A}{r_w^{\ 2}} - \log(C_A) + 0.351 + 0.87S\right] \tag{2.25}$$

$$\Delta p\ = cons\tan t \times t + cons\tan t \tag{2.26}$$

$$PPD = d\Delta p / dt = cons\tan t \tag{2.27}$$

$$\log(PPD) = cons\tan t \tag{2.28}$$

So in this state, the slope of *PPD* versus time on log-log plot is zero, shown in **Figure 2.3**.

.

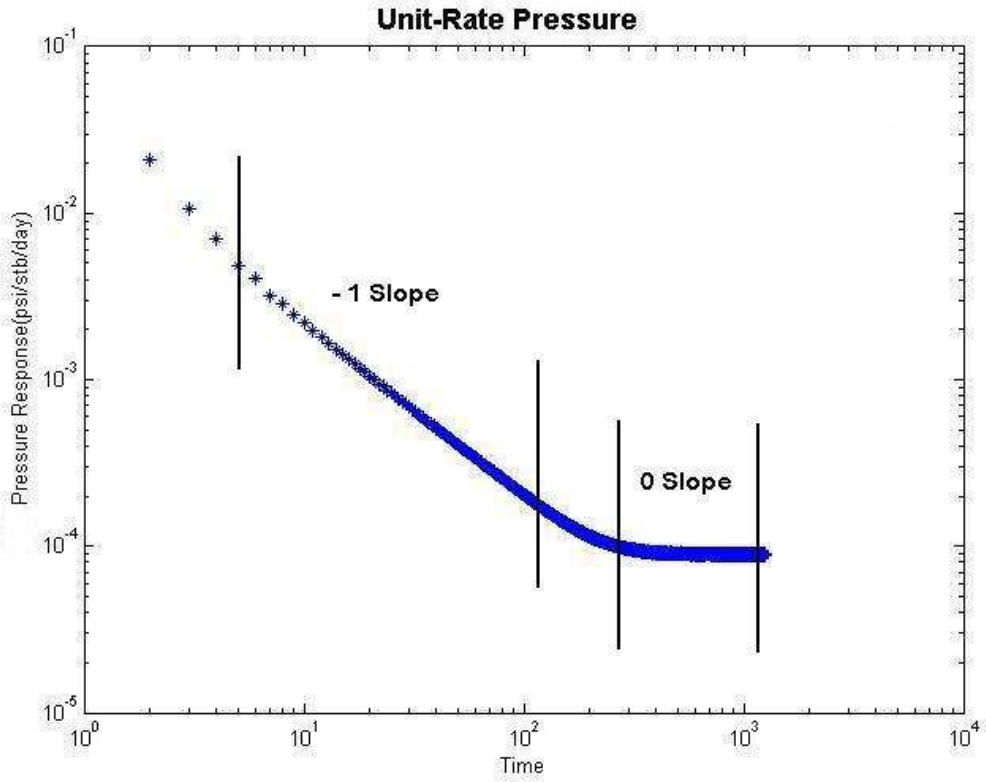

Figure 2. 3 Primary derivative of the unit-rate pressure drop on log-log plot

2.4.2 Deconvolution Product and Corresponding Physical Expressions

The developed single-well pressure-rate deconvolution algorithm is based on homogeneous reservoirs. And the deconvolution products is h , shown in **Figure 2.3**.

In **Figure 2.3**, h shows a -1 slope curve followed by a zero slope line. And this profile looks consistent with that from analytical solutions discussed above.

That is because h is the primary derivative of p_{ur}, while p_{ur} is the unit-rate Δp. So the profile of h is consistent with the pressure derivative PPD .

So the single-well deconvolution product is consistent with the unit-rate pressure response from theoretical analytical solutions. This agreement validates the developed single-well pressure-rate deconvolution algorithm.

2.4.3 Workflow of Deconvolution-based Pressure Transient Analysis

The workflow, which shows procedures of applying deconvolution method for transient pressure analysis is as follows:

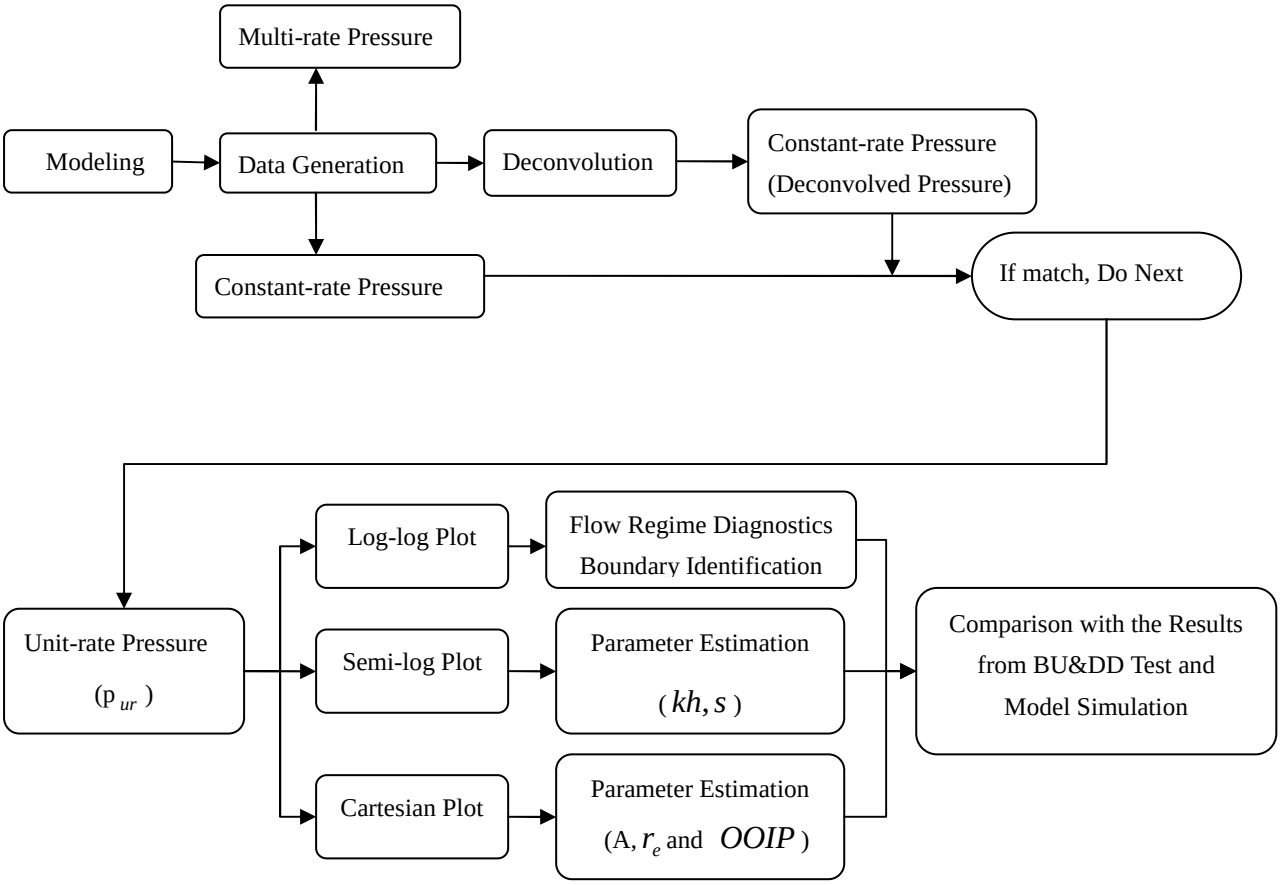

Figure 2. 4 Workflow of Deconvolotion-based Pressure Transient Analysis

2.5 Synthetic Case Studies

In order to validate the developed deconvolution algorithm, several sets of synthetic pressure and rate data are produced. These numerical experiments are particularly useful because the exact result from the deconvolution algorithm produce is known.

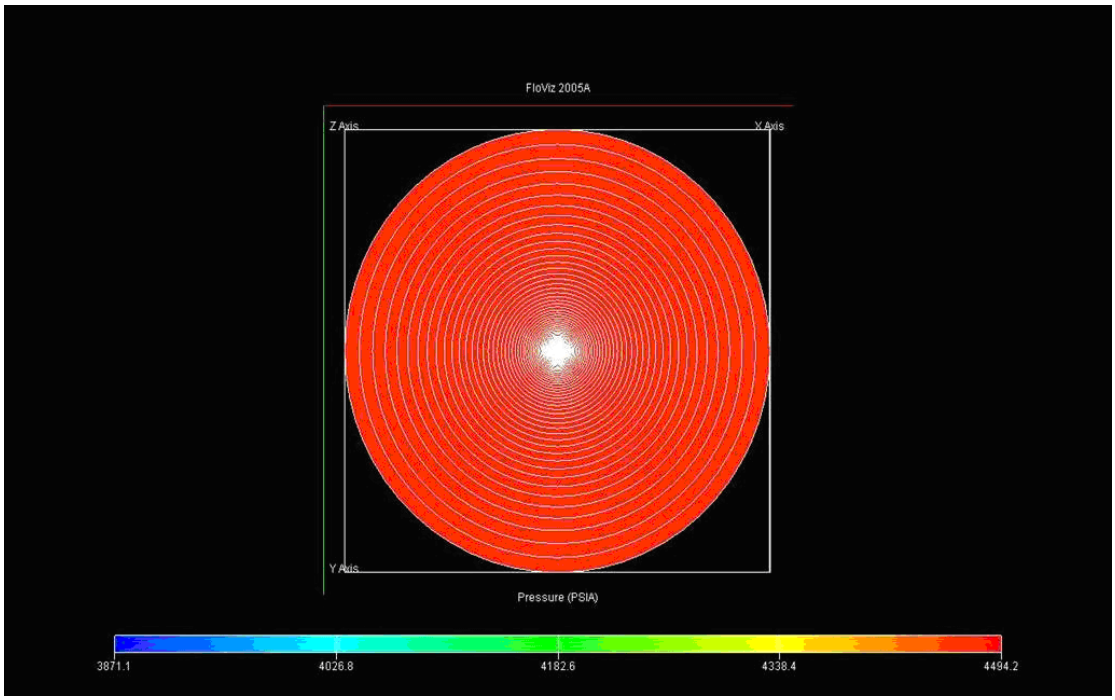

Figure 2. 5 Reservoir Model for Synthetic Case 1-5

The reservoir model, as shown in **Figure 2.5** used for case 1-2 is a fully penetrating single vertical well, located in a uniform formation, bounded on all sides by no-flow boundaries. Other parameters are listed in **Table2.1**. Results from these cases are interpreted below.

Initial reservoir pressure, p_i	= 4500 psia
Porosity, ϕ	= 0.3
Permeability, k	= 50 mD
Thickness, h	= 20 ft
Oil formation volume factor, B_o	= 1.22rb/STB
Viscosity, μ	= 0.9 cp
Total compressibility, c_t	=1.02e-5 1/psia

Well radius, r_w	= 0.3 ft
Reservoir radius, R	= 4000 ft

Table 2. 1 Reservoir and Fluid Properties for Synthetic Cases 1-2

Case 1

This case is designed to test the performance of the pressure-rate deconvolution algorithm. **Figure 2.6** shows the simulated production history, which includes two short buildups and three drawdown periods. Pressure-rate deconvolution has been implemented for the whole test period. The result is shown in **Figure 2.7**, which is the unit-rate pressure response as a result of deconvolution. **Figure 2.8** shows a match of the equivalent constant-rate-pressure response reconstructed from the deconvolution algorithm with the simulated constant-rate transient pressure. They are almost identical.

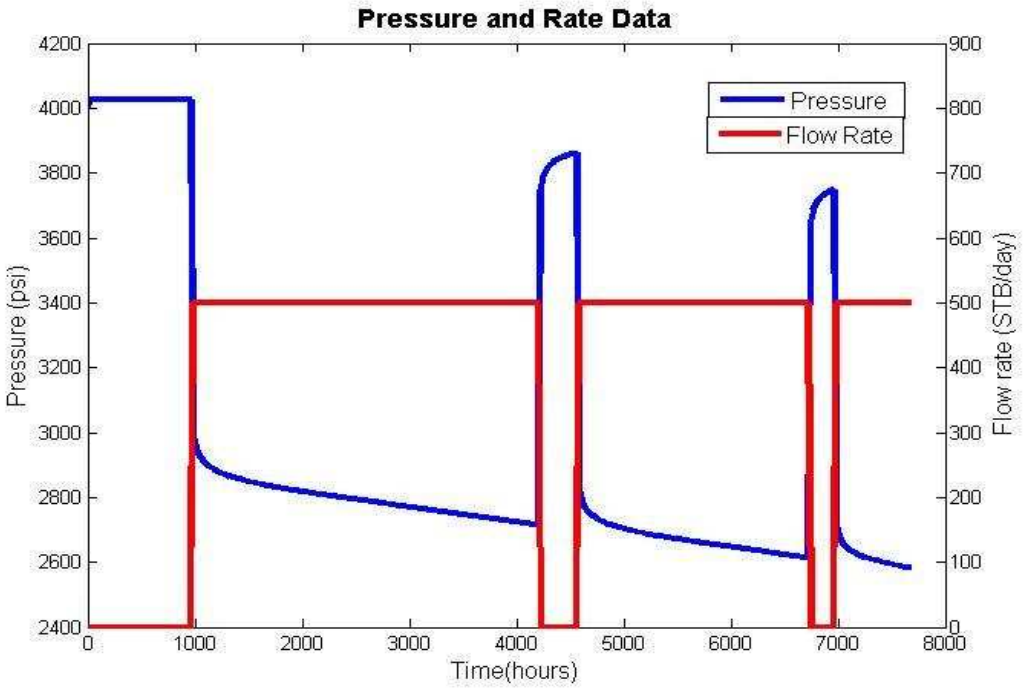

Figure 2. 6 Simulated production history, which includes three pressure draw downs and two short build ups. The red line is flowing rate and the blue line is the corresponding pressure response.

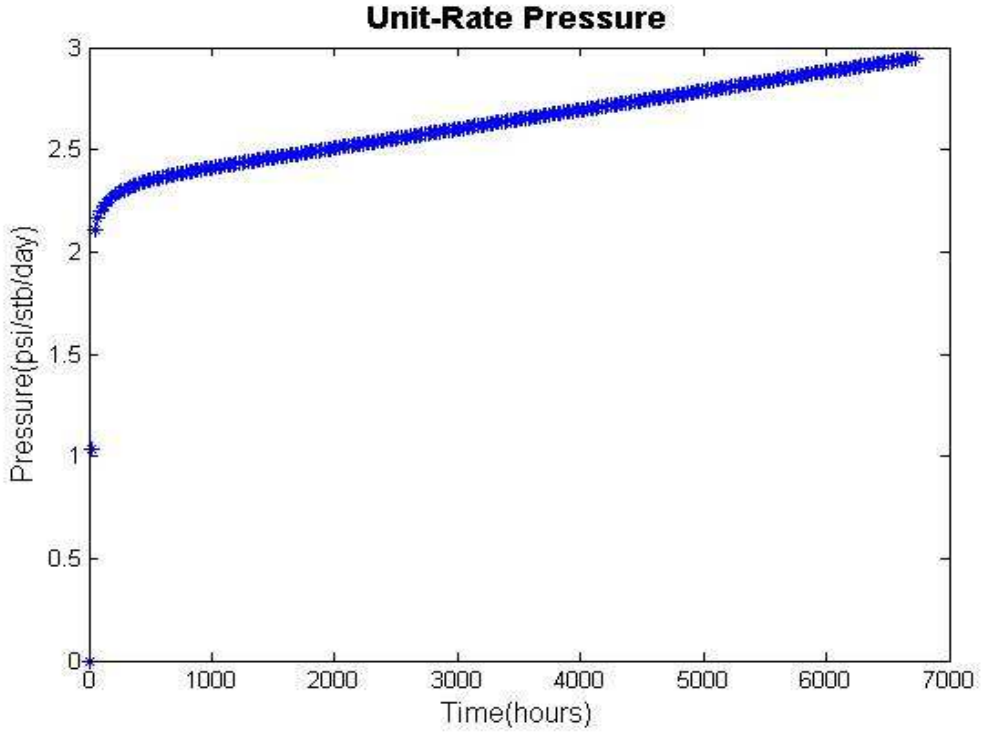

Figure 2. 7 The pressure-rate deconvolution result of the whole testing history in Cartesian plot, where the horizontal axis shows the elapsed time, while the vertical axis shows the unit-rate pressure response.

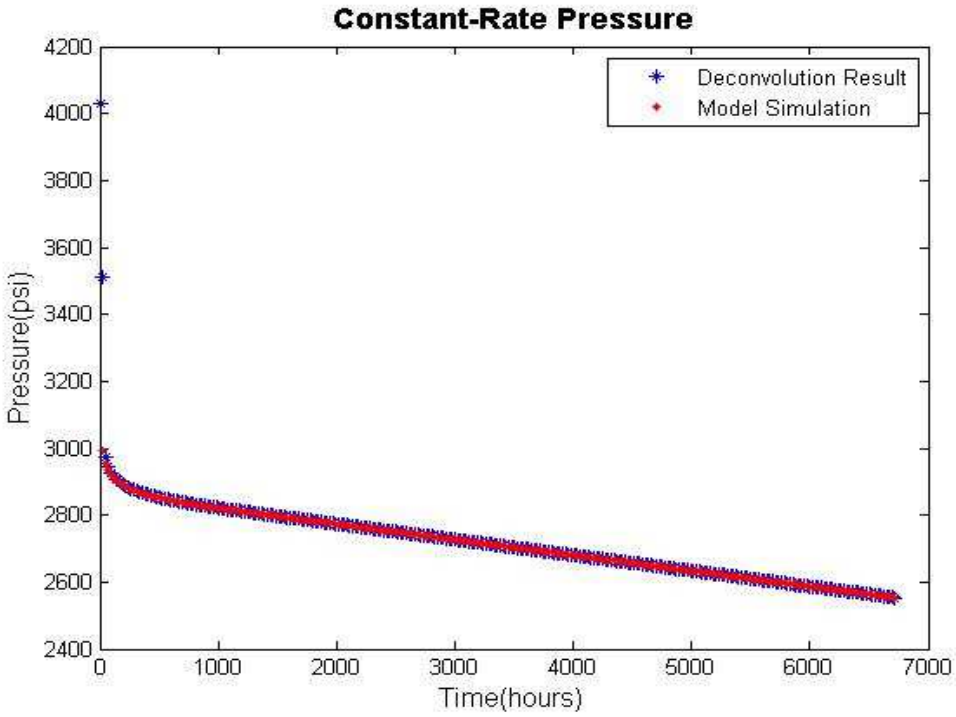

Figure 2. 8 The comparison of constant-rate pressure response between the deconvolution result (step rate) and simulated case (constant flowing rate). The blue

line is the deconvolved pressure, while the red line is that from simulation under the constant flowing rate condition.

Once the unit-rate pressure response is generated from the pressure-rate deconvolution, one can investigate such response to identify the reservoir model and its parameters. **Figure 2.9** shows the diagnostic comparison of the deconvolution results for the whole flowing history with the longest drawdown (the first one) period and simulated production history, in which the transient pressure and their derivatives for the first pressure drawdown period (3240hrs); constant-rate drawdown pressure from deconvolution and the simulated pressure response under the equivalent constant-rate condition are all in good agreement. This indicates that the behaviour of deconvolved data can represent the true reservoir response under the constant flowing conditions. **Figure 2.10** shows the comparison of deconvolution results of the whole flow history with the longest drawdown period and simulated production history on semi-log plot and **Figure 2.11** shows the comparison above all in Cartesian plot. All the plots show the good match.

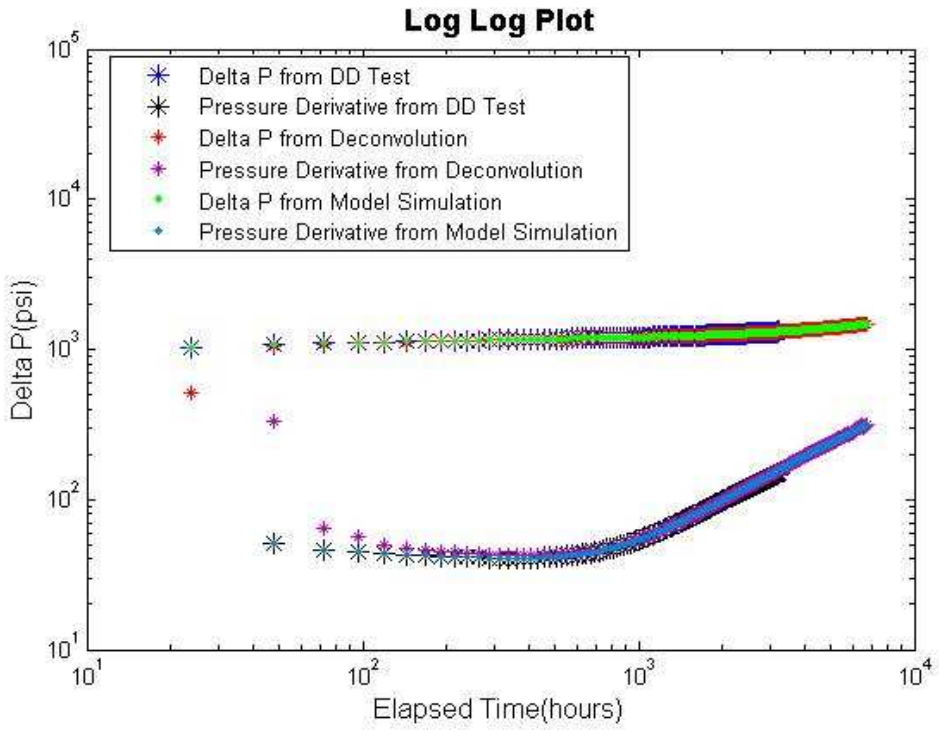

Figure 2. 9 The comparison of pressure and pressure derivatives between drawdown, deconvolution and simulation results on log-log diagnostic plot. Two short blue and

black lines show the longest pressure drawdown period, which takes 3240 hours, while other four longer lines represent the deconvolution and simulation results for the whole testing history.

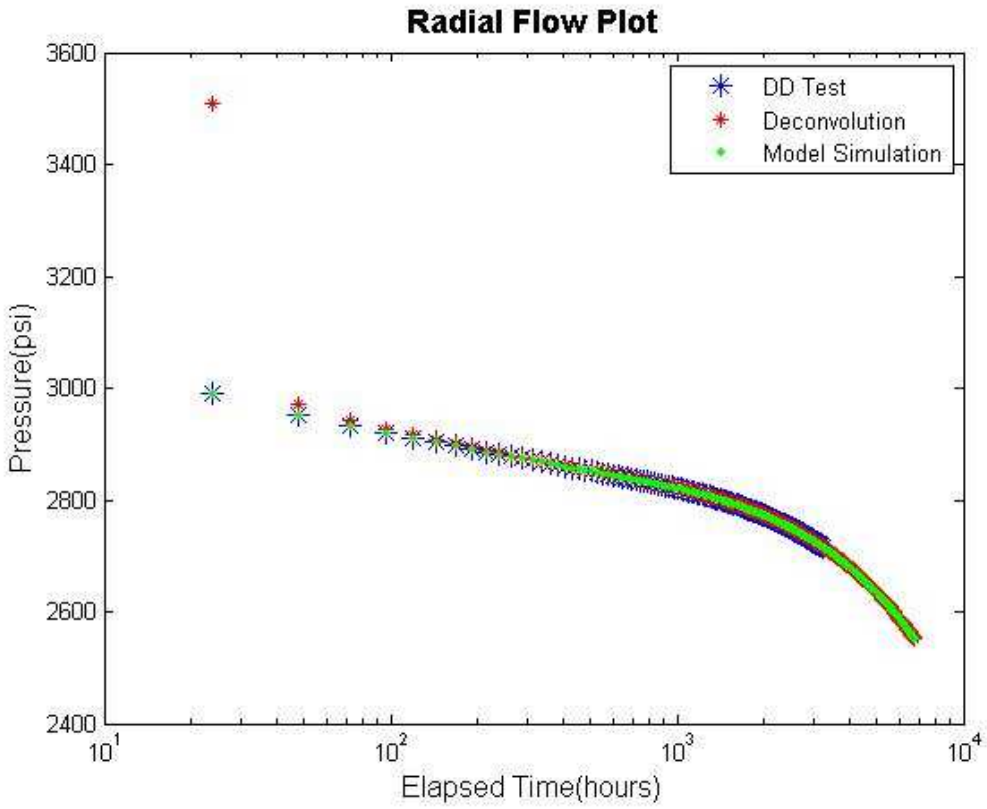

Figure 2. 10 Comparison of drawdown test, deconvolution and simulation results on semi-log plot

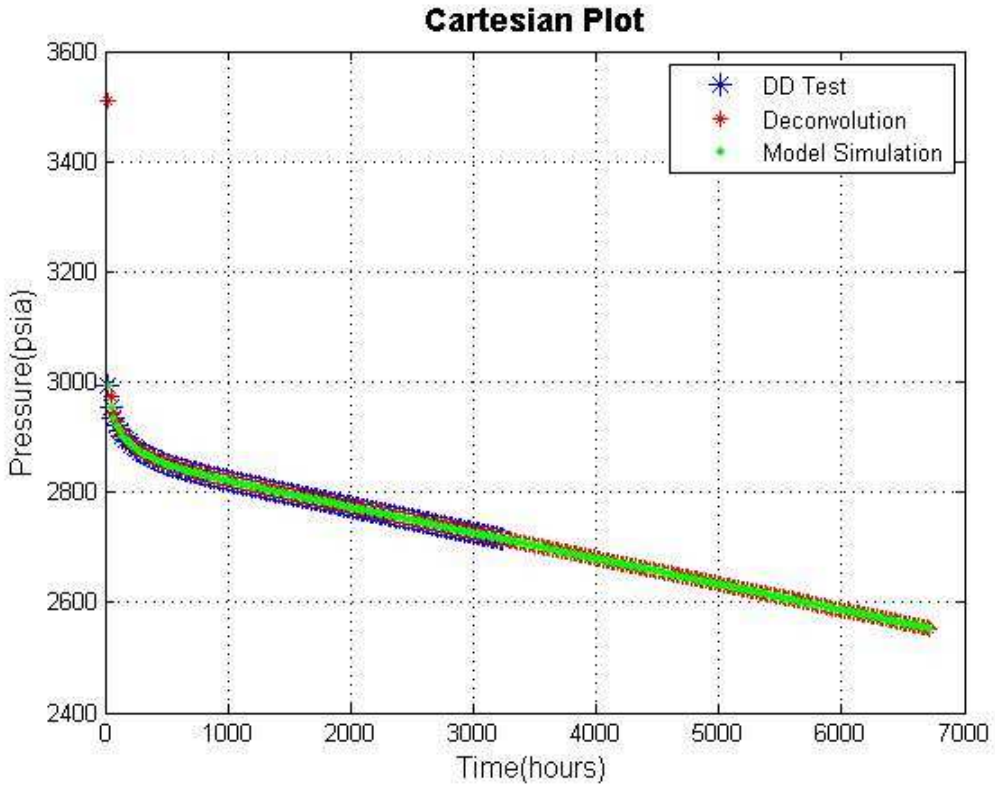

Figure 2. 11 Comparison of drawdown test, deconvolution and simulation results on Cartesian plot

Thereafter the traditional well-test analysis method can be used to calculate the reservoir parameters. Results in this case have shown in **Table 2.2**. It shows that the results from drawdown, deconvolution and simulated cases are almost the same.

	DD Test	Deconvolution	Calculation	True Model	Relative Error
k(md)	47.6338	46.2274	47.6338	50	3.0136%
S	5.5288	5.1049	5.5288	5	7.6671%
A(acre)	1144.0005	1146.3837	1147.8431	1148.9977	1.2714%
R (ft)	3982.7415	3986.8877	3989.4248	4000	0.6359%
OOIP (STB)	4.3650e7	4.3741e7	4.3797e7	4.4e7	0.1279%

Table 2. 2 Comparison of the parameters estimated by drawdown test, deconvolution and calculation from the true model parameters

Case 2

As well known, both pressure and rate data are subjected to be uncertain in practice. This gives rise to error in the final solution. This case is designed to test the performance of the deconvolution algorithms in dealing with noise and error from the measurements.

Drawdown pressure data was simulated with added noise. In the same time, noise was also added to the corresponding flowing rate. **Figure 2.12** shows the simulated flow-rate and transient pressure history. Pressure-rate deconvolution and rate-pressure deconvolution are implemented on the whole set of data using the developed algorithms respectively. Nonlinear Total Least-Square (NTLS) method was used in processing the deconvolution results, i.e. unit-pressure rate from rate-pressure deconvolution and unit-rate pressure from pressure-rate deconvolution. These are shown in **Figure 2.13**. The black line is deconvolved unit-rate pressure with noise, while the red line is deconvolved unit-rate pressure without noise. The good match indicates the good performance of the modified deconvolution algorithm on dealing with noisy data.

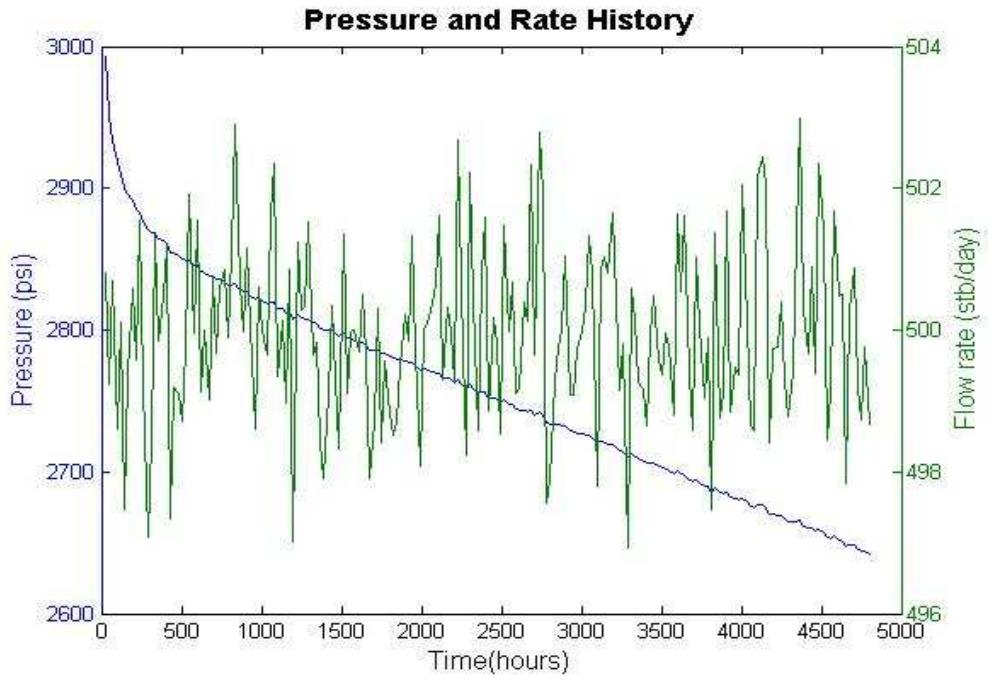

Figure 2. 12 One set of simulated data with added random noise. The green line is

flowing rate, while the blue line is corresponding pressure response. Both rate and pressure is with the added noise.

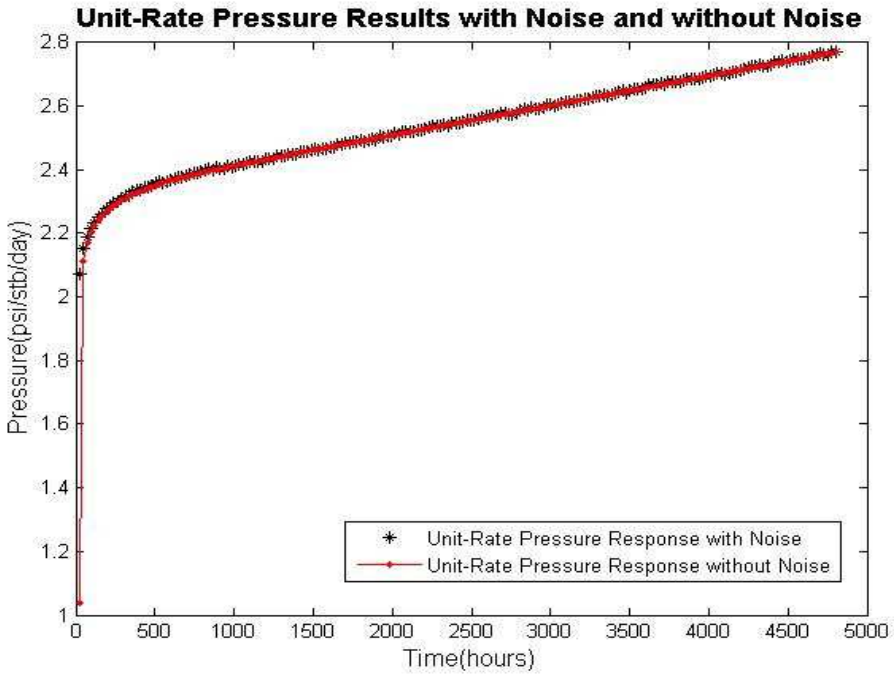

Figure 2. 13 This figure shows the comparison of deconvolved pressure without noise from original algorithm and that with noise from modified algorithm. The black line is deconvolved unit-rate pressure with noise, while the red line is deconvolved unit-rate pressure without noise.

The deconvolution results, i.e. unit-pressure rate, constant-pressure rate which are from rate-pressure deconvolution and unit-rate pressure, constant-rate pressure which are from pressure-rate deconvolution, all shown in following figures.

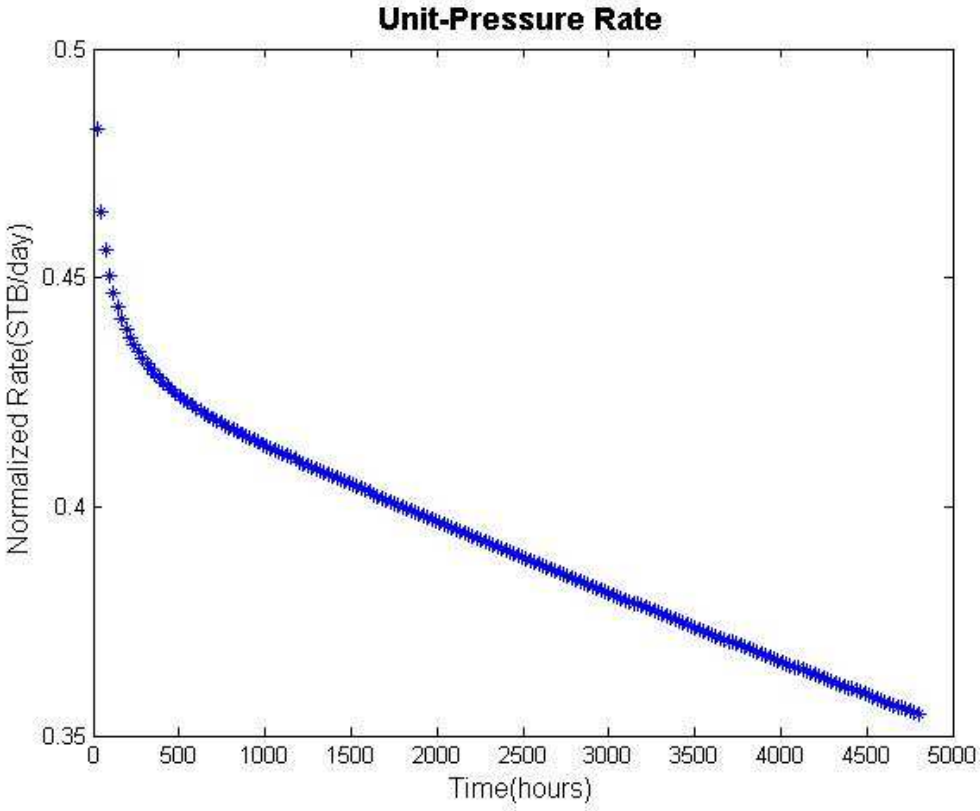

Figure 2. 14 Deconvolved unit-pressure rate decline response

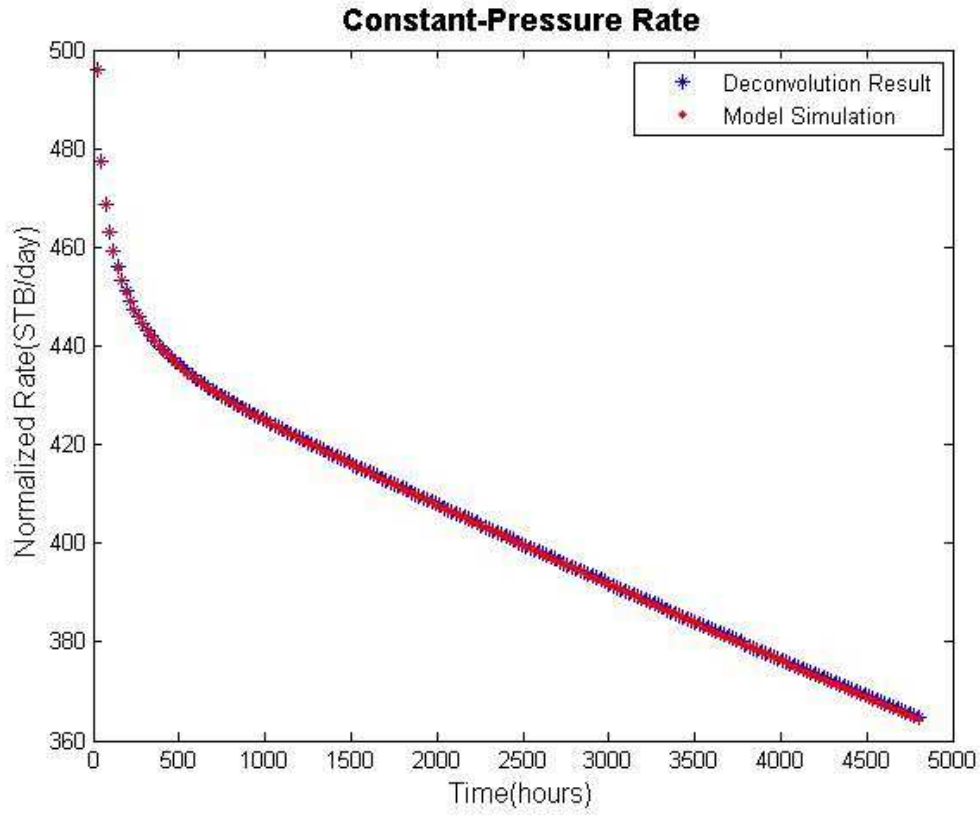

Figure 2. 15 Deconvolved constant-pressure rate decline response

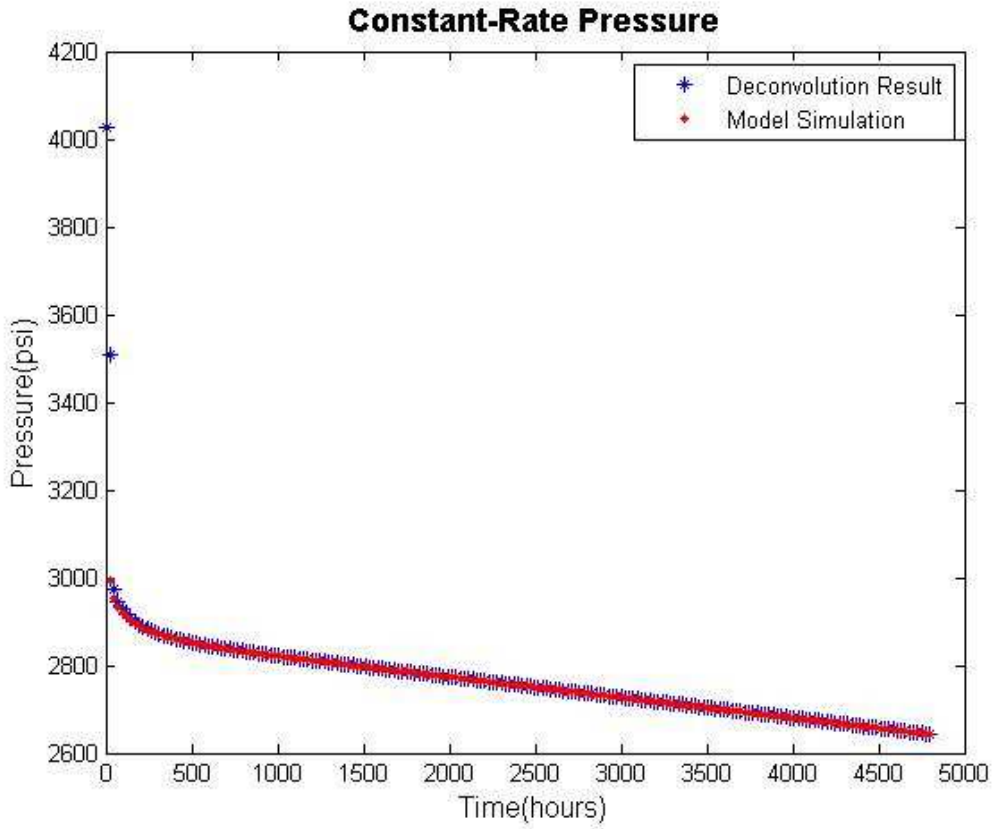

Figure 2. 16 Deconvolved constant-rate pressure response

Case3

The deconvolution algorithms described above are ideally suited for the analysis of the data from a single active well in the reservoir. However, in practical situation, there usually have several active wells operating in the same field and the bottom-hole flowing pressure measured in the well during a test is affected by production from other wells. The transient data obtained from the gauge have so called interference effect.

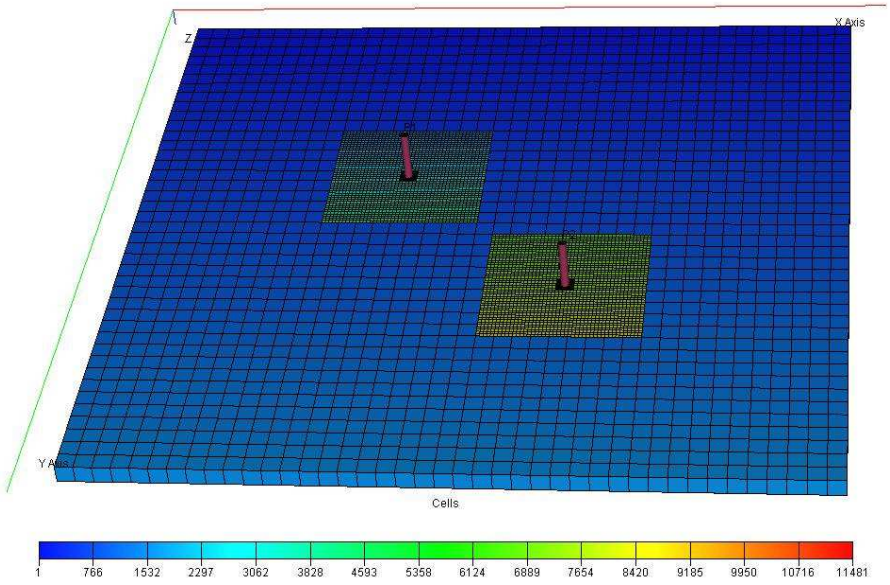

Figure 2. 17 Two-well Reservoir Model

In order to test the capability of the developed algorithms in handling data with interference effect, one synthetic case from a two-well model is constructed and simulated. This reservoir model with two wells is shown in **Figure 2.17**. Fully penetrating two vertical wells, located in the homogeneous formation, bounded on all sides by no-flow boundaries. The distance between the two wells is 2260ft. Other associated parameters are listed in **Table 2.3**.

Initial reservoir pressure, p_i	= 3000 psia
Porosity, ϕ	= 0.3
Permeability, k	= 50 mD
Thickness, h	= 100 ft
Oil formation volume factor, B_o	= 1.2rb/STB
Viscosity, μ	= 1.2 cp

Total compressibility, c_t	=6e-6 1/psia
Well radius, r_w	= 0.3 ft
Reservoir radius, R	= 4100 ft

Table 2. 3 Reservoir and Fluid Properties for Synthetic Case 3

The Well 1 is put on production first and then the Well 2 starts to produce around 840 hours later. Several pressure buildups are performed in each of the wells. The total time period of the data is 4800 hours. **Figure 2.18** shows the pressure and flow rate history of the two wells.

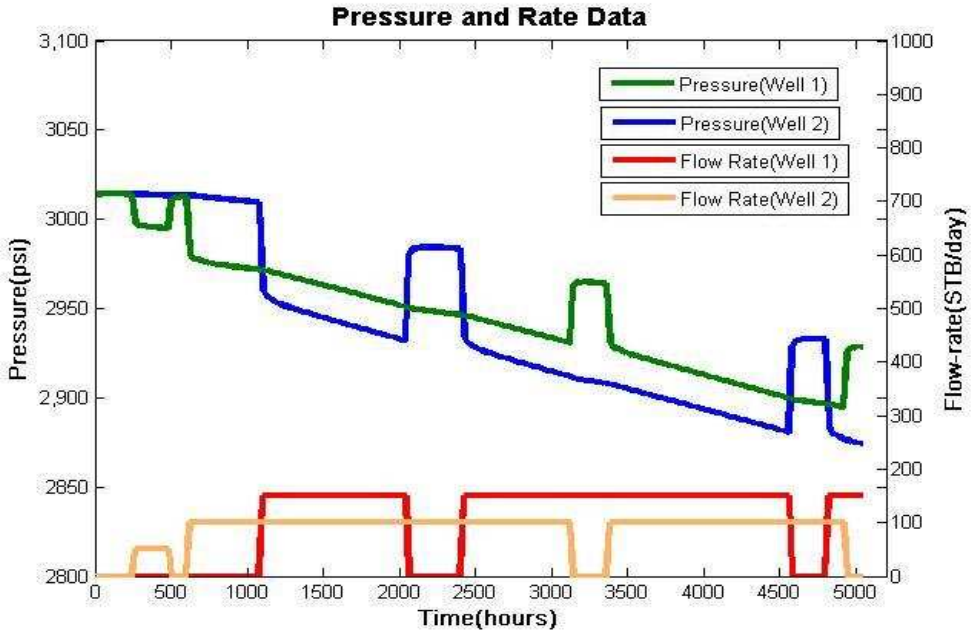

Figure 2. 18 Simulated two-well testing history, which includes several pressure draw downs and buildups. The green line and blue line present the pressure and flow rate for well 1. The red line and yellow line are for well 2, production started 840 hours later following the well 1 production.

Figure 2.19 shows the pressure and flow rate history of Well 1.Deconvolution is implemented on the whole period of the test data from Well 1 and the results presented as the unit-rate pressure is shown in **Figure 2.20**. The developed deconvolution algorithms totally failed in this case.

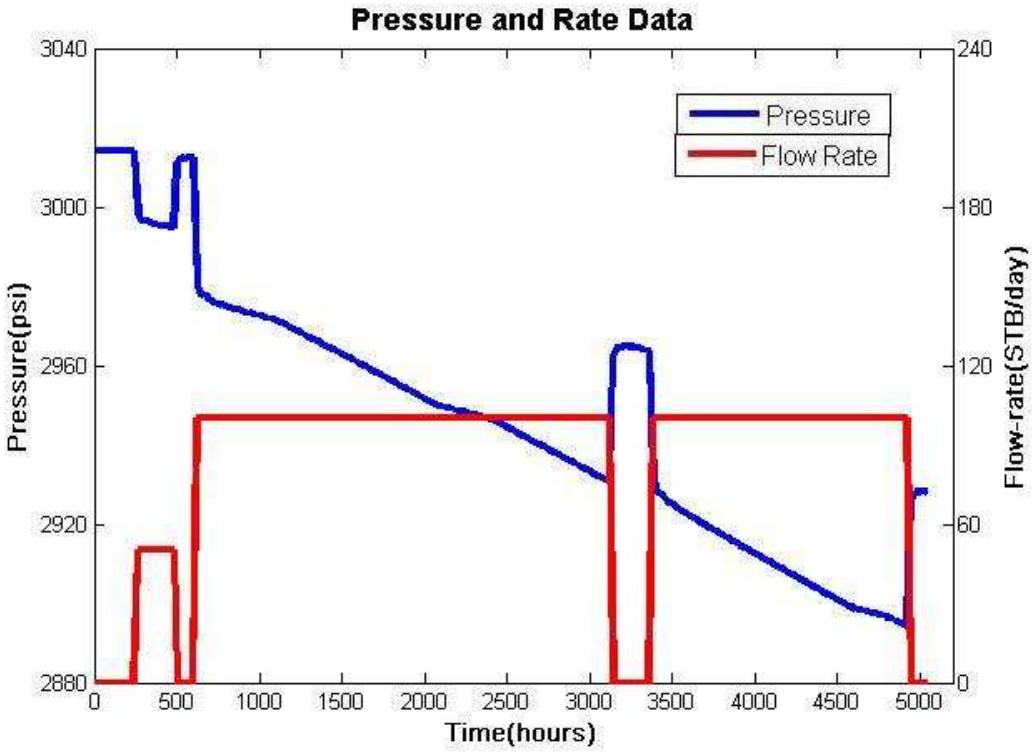

Figure 2. 19 Simulated production rate and pressure history of Well 1

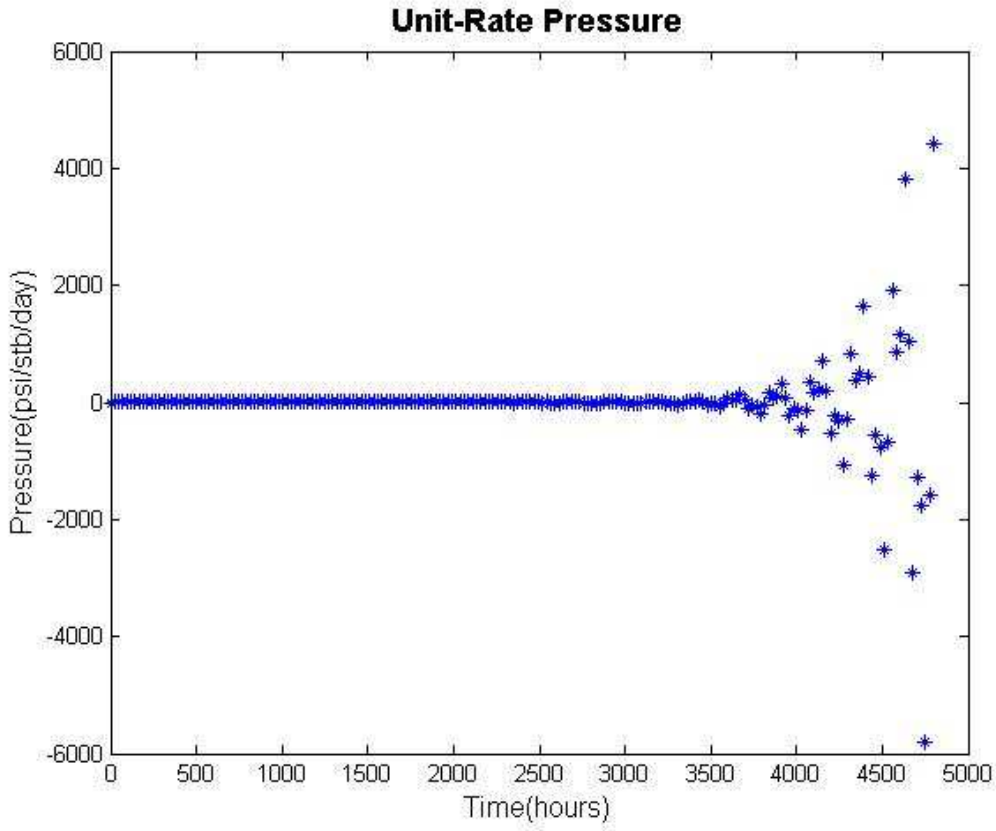

Figure 2. 20 The deconvolved unit-rate pressure response of Well1. Before about 3700 hours, the deconvolved pressure values of vertical axis are totally zero and after that the calculated values show a scatter, which means that the deconvolution algorithm

failed.

The same procedures were repeated for well 2, as shown in **Figure 2.21**. The deconvolution result is shown in **Figure 2.22**, which is also proved the failure of the developed deconvolution algorithms due to interference.

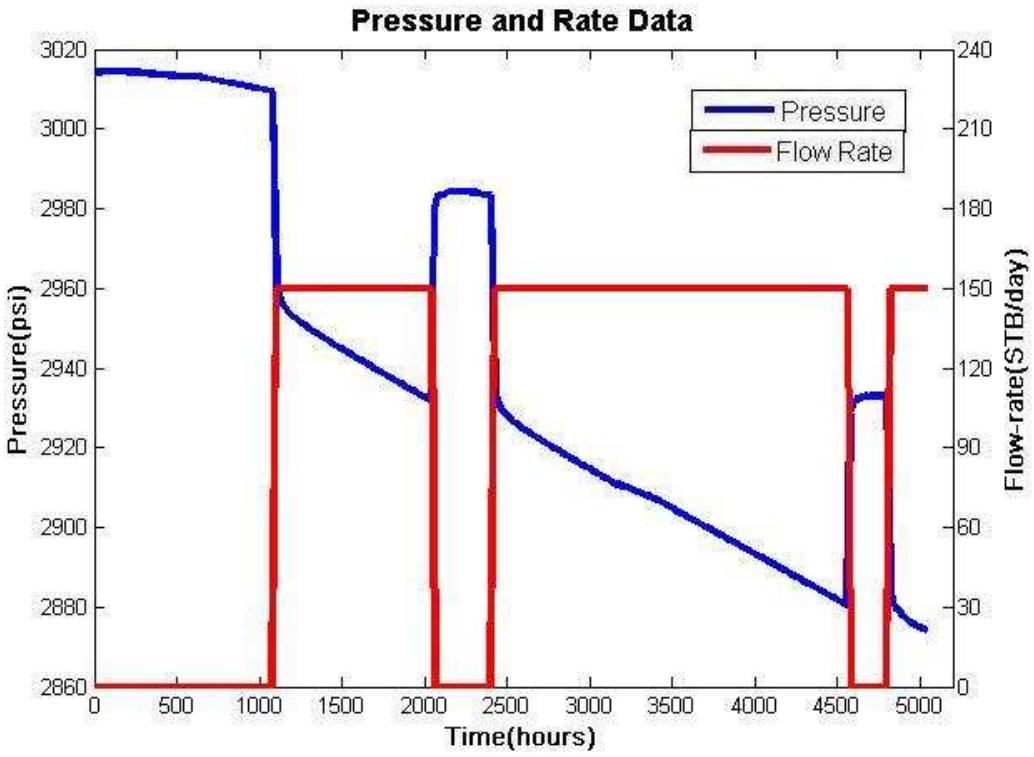

Figure 2. 21 Simulated production rate and pressure history of Well 2

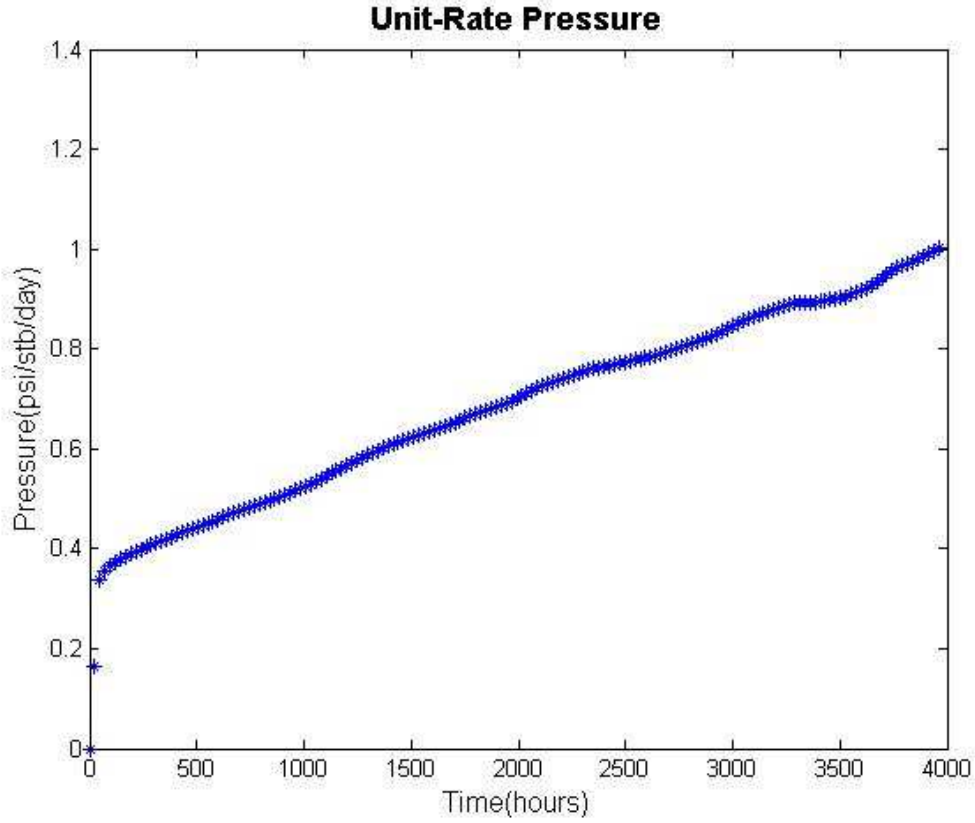

Figure 2. 22 The deconvolved unit-rate pressure response of Well 2. The resulted curve is not continuous due to the interference effect from Well 1. But it seems better that the result of Well 1 because the interference effect on well 2 is much less than that on Well 1 due to later production.

New algorithm need to be developed in deconvolving pressure and rate data affected by production from another well operating in the same reservoir. This is the ongoing research currently. The result will be reported in the near future.

Field case studies

Since deconvolution algorithm strictly relies on the assumption that the convolution integral of the reservoir system is linear, i.e. the superposition principle has to be satisfied. So the flow has to be single phase. However, the bottom-hole pressure of the well cannot always be kept higher than the reservoir bubble point pressure. Multi-phase flow cannot be avoided. Once multi-phase flow is developed in the well, the condition specified for deconvolution will fail to work. In the following, two field

cases believed with multi-phase flow are used to investigate this problem and further test the developed deconvolution algorithm.

Case 4

About one month transient pressure with two-phase flow from the permanent down hole gauge in a North Sea field is shown in **Figure 2.23.** The flow rate is recovered from wavelet transform algorithm developed parallel to the current research.

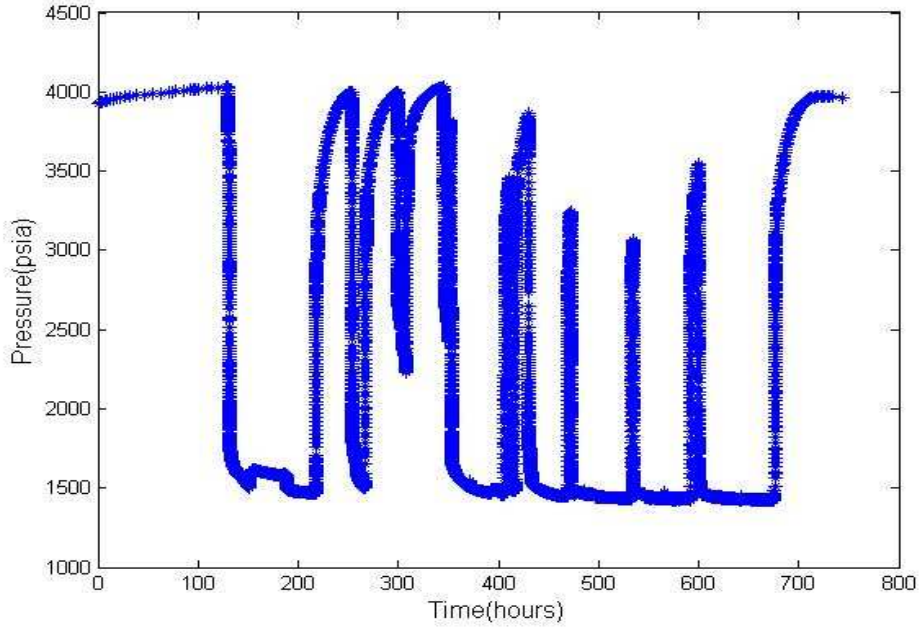

Figure 2. 23 This figure shows one month Permanent Downhole Gauge (PDG) data set (about 30,000 data points) from an oilfield in the North Sea in Cartesian plot, where the horizontal axis shows the elapsed time, while the vertical axis shows the recorded pressure. A series of transient pressure draw downs and build ups are shown as continuous changes due to flowing rate changing or well shut-in.

The pressure-rate deconvolution and rate-pressure deconvolution are implemented on this data set. The deconvolution results are shown in **Figure 2.24** and **Figure 2.25** respectively. Apparently, the developed deconvolution algorithms failed again in handling this situation.

There is also a need to further develop new algorithm capable dealing with multi-phase flow deconvolution problem. This is not available currently in the industry.

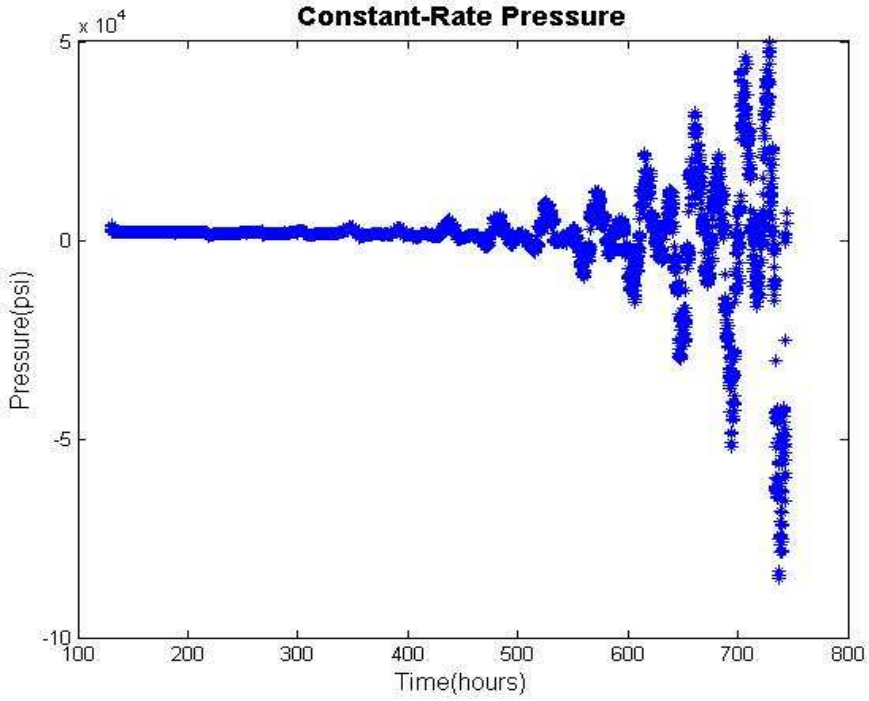

Figure 2. 24 The result using pressure-rate deconvolution algorithm on two phase flow data. The calculated values show a wide scatter, which proved that the deconvolution algorithms failed in this case.

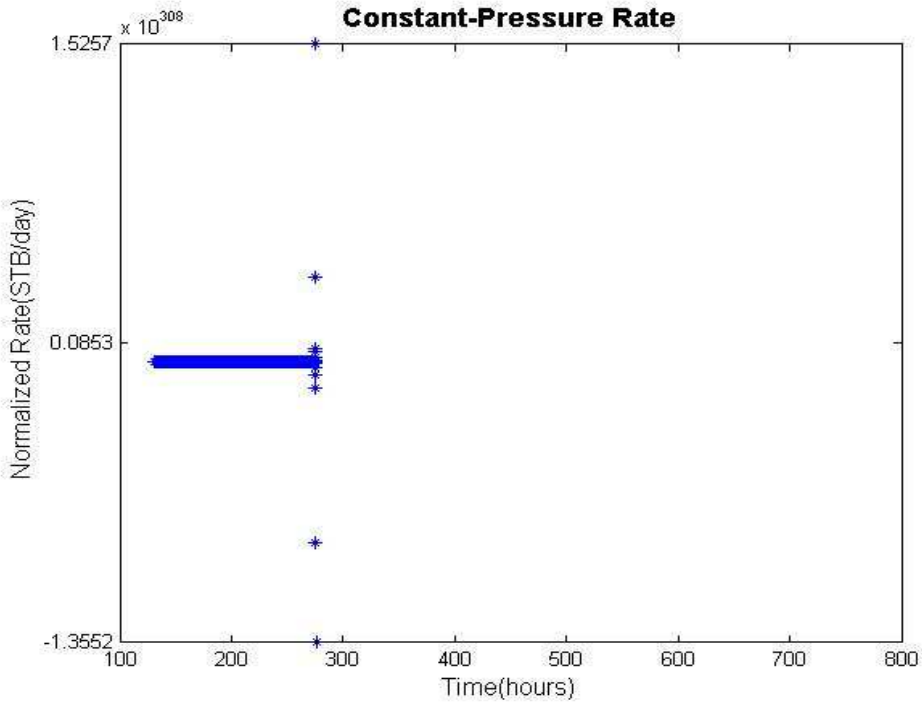

Figure 2. 25 The result using rate-pressure deconvolution algorithm on two phase flow data. The order of magnitude of deconvolved rate values is significantly big, which failed the deconvolution algorithm developed.

Case 5

Figure 2.26 shows a 30-hour flow period of two phases, oil and water. I do pressure-rate deconvolution on this set of data. The result, shown in **Figure 2.27,** presents wrong.

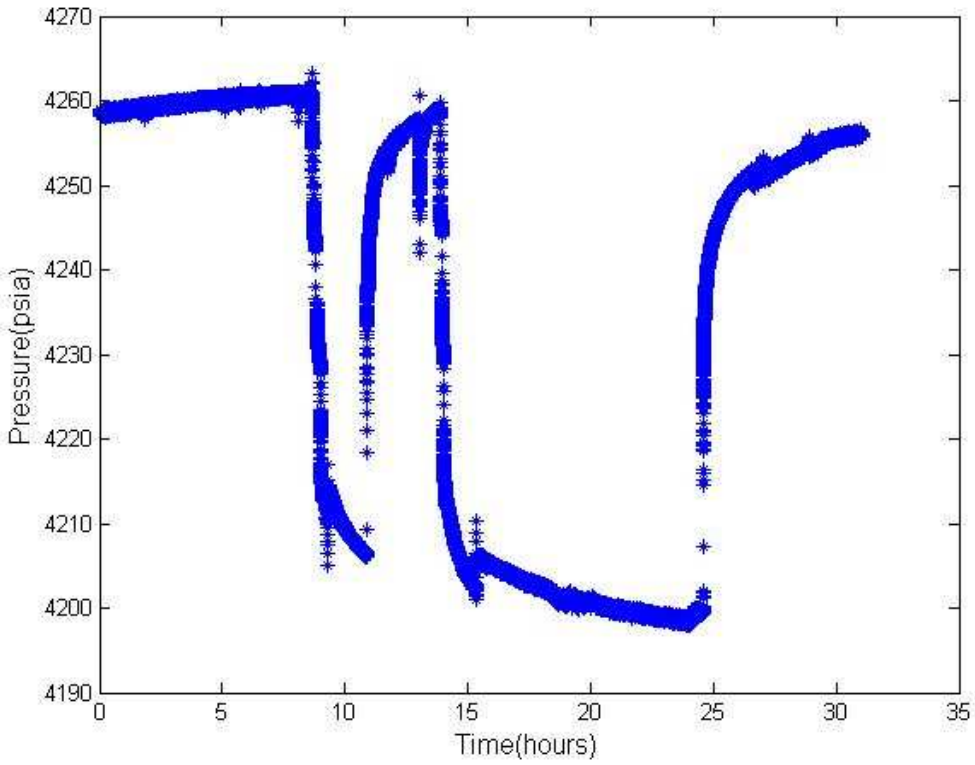

Figure 2. 26 Production rate and pressure history

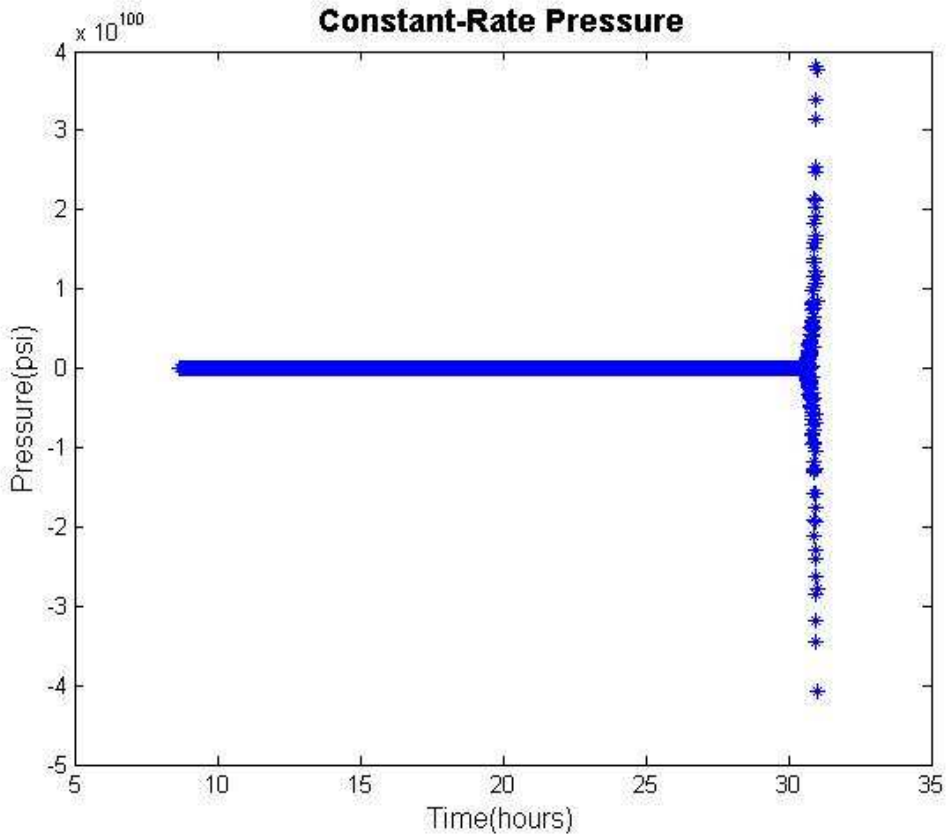

Figure 2. 27 Deconvolved constant-rate pressure response

2.6 Chapter Conclusions

According to this study, several conclusions can be derived, as follows:

A new pressure-rate deconvolution algorithm is developed to deal with the flow rate variations and noise problem in single-well PDG data. The constant-rate pressure response of a single-well reservoir system was calculated using the developed pressure-rate algorithm.

Theoretical derivation of the pressure-rate deconvolution product has been finished, which proved that the deconvolution product consistent with that from traditional pressure transient theory.

Analytical and simulation cases have been produced for comparison. The results from analytical, simulation and deconvolution solutions agree with each other, which prove that the developed single-well pressure-rate deconvolution algorithm works well.

Deconvolution-based transient pressure analysis theory and corresponding workflow are proposed in detail. This deconvolution-based analysis procedure has improved the traditional well testing methods.

Numerical well testing synthetic studies have been performed to demonstrate the procedure of this deconvolution-based transient pressure analysis. The results proved that this deconvolution-based analysis method worked well in homogeneous reservoirs with one well flowing at single phase, multiple rates. And this new method improved the traditional pressure transient analysis technique.

The problems of multi-phase and multi-well interference were addressed with field case studies. Single-well deconvolution algorithm in this chapter failed in handling these situations. New algorithm is required and results addressing interference and multi-phase problems will be presented in the following chapters.

Chapter 3
Deconvolution-based Rate Transient Analysis of Single-Well PDG Data

3.1 Introduction

Decline-cure analysis is a method to match the observed production rates of individual well, group wells or reservoirs for reserve estimation and production forecast. Traditional decline curve analysis such as exponential; hyperbolic or harmonic methods, were presented by Arps in the 1950s. In early 1980s, Fetkovich combined the empirical decline curves from Arps with the constant-pressure analytical solution for transient production analysis. This set decline-curve analysis on a more rigorous foundation. Therefore Arps decline curve parameters can be related to reservoir parameters due to constant down-hole flowing pressure.

However, in reality, due to the condition constraints or changes in operating procedures, the down-hole flowing pressure is seldom kept constant over long periods of time. So the method cannot be applied directly. Various types of superposition and normalization methods (Palacio, J. C. and Blasingame, T.A., 1993[29]; Agarwal et al., 1999[23]) have been published in the literature.

Since deconvolution can transfer the variable-rate pressure data into an equivalent pressure response due to the constant rate, it can be used as a rate normalization method. Therefore, this deconvolved rate, equivalent constant-pressure rate as normalized data then fit the decline-curve analysis theory and can be used to provide information on the reservoir properties, hydrocarbon in place and estimated ultimate recovery (EUR).

This chapter presents study results using synthetic cases to investigate the potential of deconvolution technique in rate transient analysis. A new rate-pressure deconvolution algorithm and corresponding computer codes are developed for this study. A deconvolution-based analysis method is proposed in detail.

The organization of this chapter is as follows. Firstly, the analytical theory of single-well rate transient analysis is presented. A new time-domain deconvolution algorithm is then developed for the rate normalization. Then, deconvolution-based transient analysis theory and procedure are derived in detail. Finally synthetic cases, which were based on the same numerical model, are studied. A double-checked practice method for analysis of transient pressure integrated with the transient rate analysis is proposed here. And results are presented to prove that the new deconvolution algorithm works well in single phase oil reservoir system and corresponding deconvolution-based analysis methods look very promising.

3.2 Analytical Theory of Single-Well Rate Transient Analysis

3.2.1 Theory and Derivation of Arps Decline Curves

Decline curve analysis technique has been developed over the past decades through interpreting rate transient data in controlled environments. It is derived from empirical observations of the production performance of oil and gas wells. Three types of decline have been observed historically: exponential, hyperbolic, and harmonic, as shown in **Figure 3.1**.

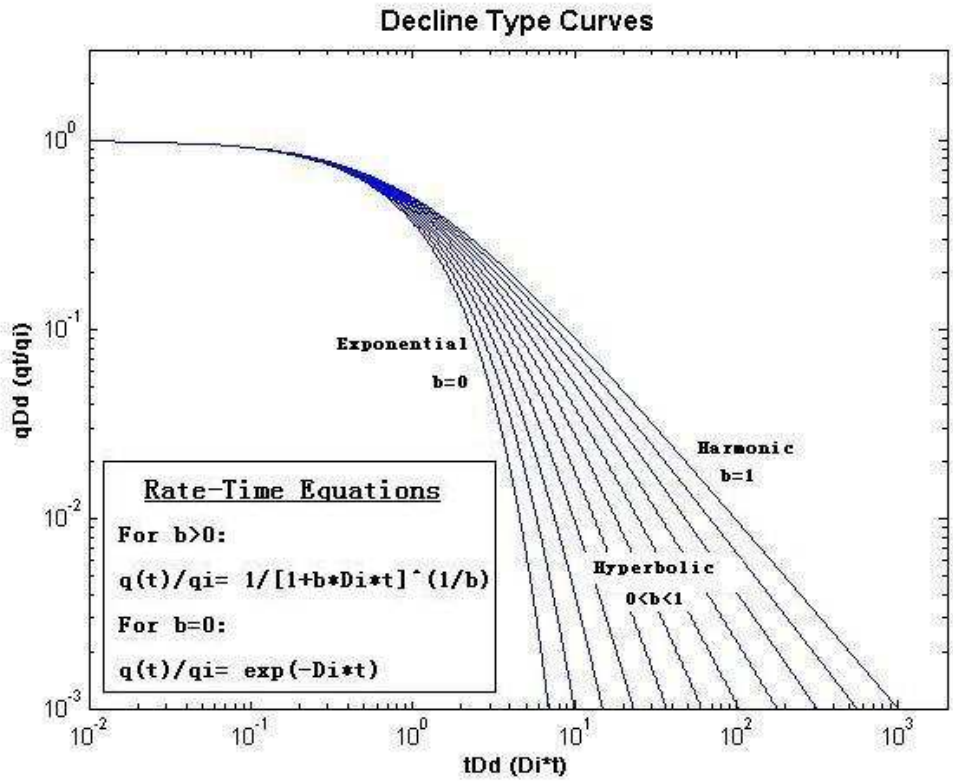

Figure 3. 1 Type curves for Arps empirical rate-time decline equations, unit solution ($D_i = 1$)

The most general form of decline equation is shown below:

$$q(t) = \frac{q_i}{\left(1 + bD_{it}\right)^{\frac{1}{b}}} \tag{3.1}$$

In this equation, when b equals 0 and 1 represents exponential and harmonic decline, respectively. During PSS for liquid system, the exponential decline is a characteristic of constant pressure production whereas the harmonic decline is due to constant rate production. Any other value of b represents a hyperbolic decline.

The definition of the instantaneous or current decline rate (D) is as follows:

$$D = -\frac{\Delta q / q}{\Delta t} \tag{3.2}$$

D is the fractional change in rate per unit time, frequently expressed in "% per year". The decline rate D is not constant, so it must be associated with a specified rate, hence

D_i at flow rate q_i. b is the decline exponent. The values of b have been derived for different reservoir drive or recovery mechanisms.

Exponential decline occurs when the decline rate "D", is constant and the decline exponent "b" is 0, which can be expressed as follows:

$$D = K * q^0 = -\frac{dq/dt}{q} \tag{3.3}$$

Integrating the above formulation: $\int_0^t D dt = -\int_{q_i}^{q} \frac{dq}{q}$ (3.4)

, which yields:

$$-Dt = \ln q/q_i \tag{3.5}$$

So the rate-time equation can be given by: $q = q_i * e^{-Dt}$ (3.6)

The cumulative rate $Q = \int_0^t q * dt = \int_0^t q_i * e^{-Dt} * dt$ (3.7)

Integrating the formulation above can yield:

$$Q = \frac{q_i - q_i * e^{-Dt}}{D} \tag{3.8}$$

Substitute from Rate-time equation above to find:

$$Q = \frac{q_i - q}{D} \tag{3.9}$$

this is Rate–Cumulative function.

If D varies, the decline is considered to be either hyperbolic or harmonic, in which case, an exponent "b" is incorporated into the equation of the decline curve, to account for the changing decline rate.

Hyperbolic decline occurs when the decline is proportional to a fractional power of the production rate 0 < b< 1, which can be expressed as follows:

$$D = K * q^b = -\frac{dq/dt}{q} \tag{3.10}$$

for initial conditions $K = \frac{D_i}{q^b}$ (3.11)

Integrating the above formulation $\int_0^t \frac{D_i}{q_i^b} * dt = -\int_{q_i}^{q} \frac{dq}{q^{b+1}}$ (3.12)

, which yields:

$$\frac{bD_i t}{q_i^b} = q^{-b} - q_i^{-b} \tag{3.13}$$

So the rate-time equation can be given by: $q = q_i(1+bD_i t)^{\frac{-1}{b}}$ (3.14)

The cumulative rate $Q = \int_0^t q * dt = \int_0^t q_i(1+bD_i t)^{\frac{-1}{b}} * dt$ (3.15)

Integrating the formulation above can yield:

$$Q = \frac{q_i}{(1-b)D_i}\left[(1+bD_i t)^{\frac{b-1}{b}} - 1\right] \tag{3.16}$$

Substitute from Rate-time equation:

$$(1+bD_i t) = (\frac{q_i}{q})^b \tag{3.17}$$

to find the Rate–Cumulative function:

$$Q = \frac{q_i^b}{(1-b)D_i}(q_i^{1-b} - q^{1-b}) \tag{3.18}$$

, where Di is the decline rate at flow rate qi, and b varies from 0 to 1.

Harmonic Decline occurs when the decline is proportional to production rate (b = 1), which can be expressed as follows:

$$D = K * q^1 = -\frac{dq/dt}{q} \tag{3.19}$$

for initial conditions $K = \frac{D_i}{q_i}$ (3.20)

Integrating the above formulation $\int_0^t \frac{D_i}{q_i} * dt = -\int_{q_i}^{q} \frac{dq}{q^2}$ (3.21)

, which yields:

$$\frac{D_i t}{q_i} = \frac{1}{q_i} - \frac{1}{q_t} \tag{3.22}$$

So the rate-time equation can be given by: $q = q_i(1 + D_i t)^{-1}$ (3.23)

The cumulative rate $Q = \int_0^t q * dt = \int_0^t q_i(1 + bD_i t)^{-1} dt$ (3.24)

Integrating the formulation above can yield:

$$Q = \frac{q_i}{D_i}\left[\ln(1 + D_i t)\right] \tag{3.25}$$

Substitute from the Rate-time equation above to find:

$$Q = \frac{q_i}{D_i} \ln \frac{q_i}{q} \tag{3.26}$$

this is Rate–Cumulative function.

Decline curve analysis is usually conducted graphically, and in order to help in the interpretation, the equations are plotted in various combinations of "rate", "log-rate", "time," and "cumulative production". The intent is to use the combination that will result in a straight line, which then becomes easy to extrapolate for forecasting purposes. The decline equations can also be used to forecast recoverable reserves at specified abandonment rates.

3.2.2 Reserve Estimation and Production Forecast

Using the following, we can calculate the expected ultimate recovery for a variety of situations.

Exponential: $EUR = Q_f + \frac{q_f - q_{ab}}{D}$ (3.27)

$$q_f = q_i e^{-Dt_f} \tag{3.28}$$

where;

q_i : initial rate. This is the starting rate of the period preceding the forecast

q_{ab} : abandonment rate

q_f : rate at the beginning of the forecast period

Q_i : cumulative production at the start of the forecast

D : decline rate

Note: The ‘f’ subscript denotes conditions at the beginning of the forecast period.

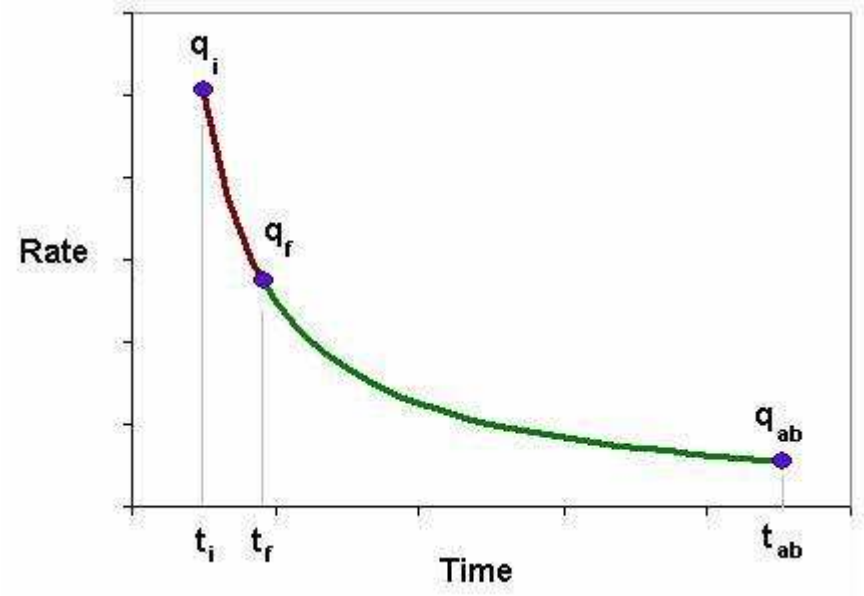

Figure 3. 2 Schematic diagram of the rate decline curve

Hyperbolic: $$EUR = Q_f + \frac{q_f}{(1-b)D_f}\left[q_i^{1-b}(1+bD_i t_f)^{1-1/b} - q_{ab}^{1-b}\right] \tag{3.29}$$

Harmonic: $$EUR = Q_f + \frac{q_f}{D_f}\ln(\frac{q_f}{q_{ab}}) \tag{3.30}$$

With knowledge of the EUR, we can estimate fluid-in-place and drainage area:

$$N = \frac{EUR}{c_t(P_i - P_{wf})} \quad (\text{MBbls}) \tag{3.31}$$

$$A = \frac{NB_0}{\Phi h S_0(43560)} \quad (\text{acres}) \tag{3.32}$$

3.3 Single-Well Rate-Pressure Deconvolution

3.3.1 Single-Well Rate-Pressure Deconvolution Theory

In single-well rate-pressure deconvolution, the unit constant-pressure transient rate response of the reservoir system can be reconstructed based on the following convolution integral:

$$q(t) = \int_0^t q_{up}(t-\tau)\frac{d\Delta p(\tau)}{d\tau}dt \tag{3.33}$$

Where, q_{up} represents the transient rate response of the reservoir system if the well

was produced at a unit constant-pressure condition (subscript up stands for unit pressure).

3.3.2 New Single-Well Rate-Pressure Deconvolution Algorithm

In the rate-pressure convolution integral equation (3.33), the down-hole pressure drop here can be expressed as:

$$\Delta p(t) = p_i - p_{wf}(t) \tag{3.34}$$

Given that $h' = d\Delta p / dt$ (3.35)

So function (3.33) can be rewritten as:

$$q(t) = \int_0^t q_{up}(t-\tau)h'(\tau)d\tau \tag{3.36}$$

The discrete convolution function can be written as:

$$q(n) = \sum_{k=0}^{N-1} q_{up}(k)h'(n-k) \tag{3.37}$$

$q(n), n = 1,2,..., N$

$h'(n), n = 1,2,..., N$

The linear recursion algorithm can be expressed as follows:

$$q_{up}(1) = q(1)/h'(1) \quad (n=1) \tag{3.38}$$

$$q_{up}(n) = \frac{q(n) - q_{up}(n)h'(1) - q_{up}(n-1)h'(2) - q_{up}(n-2)h'(3) - ... - q_{up}(2)h'(n-1)}{h'(1)}$$

$$(n = 2,3,..., N) \tag{3.39}$$

The above-mentioned linear recursion deconvolution algorithm cannot give a stable solution due to the error accumulation at late time. So I add nonlinear least square (NLS) functions to the algorithm. With the added NLS optimization procedure, the developed deconvolution algorithm can give more accurate results.

The nonlinear least square algorithm includes following steps:

Step 1: Input data (p_{wf} , q)

Step 2: 1st Subtraction (calculate Δp)

$$\Delta p(t) = p_i - p_{wf}(t)$$

Step 3: 1st Derivation (calculate $d\Delta p / dt$)

$$h' = d\Delta p / dt$$

Step 4: 1st Deconvolution (calculate q_{up})

$$F(X) = \min_X \frac{1}{2} \left\| conv(q_{up}, h') - q \right\|_2^2 = \frac{1}{2} \sum_{i=1}^{n} (conv(q_{upi}, h'_i) - q_i)^2$$

3.4 Deconvolution-based Rate Transient Analysis

3.4.1 Analytical Solutions of Deconvolotion-based Transient Pressure

My developed single-well rate-pressure deconvolution algorithm is based on homogeneous reservoirs. And the deconvolution product, q_{up}, is the rate response per unit pressure drop.

Since the decline curve analysis is based on empirical observations of production rate decline, and not on theoretical derivations, attempts to explain the observed behaviour, using the theory of flow in porous media, lead to the fact that these empirically observed declines are related to "boundary dominated flow". When a well is placed on production, there will be transient flow initially. Eventually, all the reservoir boundaries will be felt, and it is only after this time, that decline curve analysis becomes applicable, and the value of "b" lies in the range of 0 to 1, depending on the reservoir boundary conditions and the recovery mechanism.

For homogeneous single-layer systems with single-phase liquid (highly undersaturated oil wells), the value of b is zero, exponential (Fetkovich).

And it can be shown that, theoretically, when a well is producing at constant backpressure, exponential decline is equivalent to "boundary dominated flow", which fits the deconvolution solutions, as follows:

$$q_{up}(t) = q_i * e^{-Dt} / \Delta p(t) \tag{3.40}$$

It can be shown mathematically, that an exponential decline will also result in a straight line when plotted as Flow Rate vs. Cumulative Production.

Under ideal conditions, plots of log-rate vs. time, and rate vs. cumulative production should both result in straight lines from which the decline rate can be determined.

For exponential decline, D is constant. Equation (3.1) can rewrite as follows:

$$\ln(q / q_i) = -Dt \tag{3.41}$$

or,

$$\log(q / q_i) = -\frac{Dt}{2.303} \tag{3.42}$$

which illustrates that a plot of log-rate vs. time will yield a straight line of slope D/2.303. Cumulative Production is obtained by integrating the rate-time relationship. It can be shown that the flow rate is related to the cumulative production, Q, by:

$$q = q_i - DQ \tag{3.43}$$

which shows that a plot of rate vs. Cumulative Production will be a straight line of slope D. Extrapolation of this straight line to any specified abandonment rate (including zero) gives the recoverable reserves.

Cumulative production between time t_1 and t_2 can be obtained from

$$Q = \frac{q_1 - q_2}{D} \tag{3.44}$$

or, in terms of time;

The following equation can be used for either oil or gas, provided the units are as specified below.

$$D = \frac{\ln(q_1 / q_2)}{\Delta t} \tag{3.45}$$

When forecasting remaining reserves, one can extrapolate the decline curve to intercept with the economic rate. To calculate the ROIP one can use either rate-time or rate-cumulative.

3.4.2 Workflow of Deconvolution-based Rate Transient Analysis

The workflow, which shows procedures of applying deconvolution method for transient rate analysis is as follows:

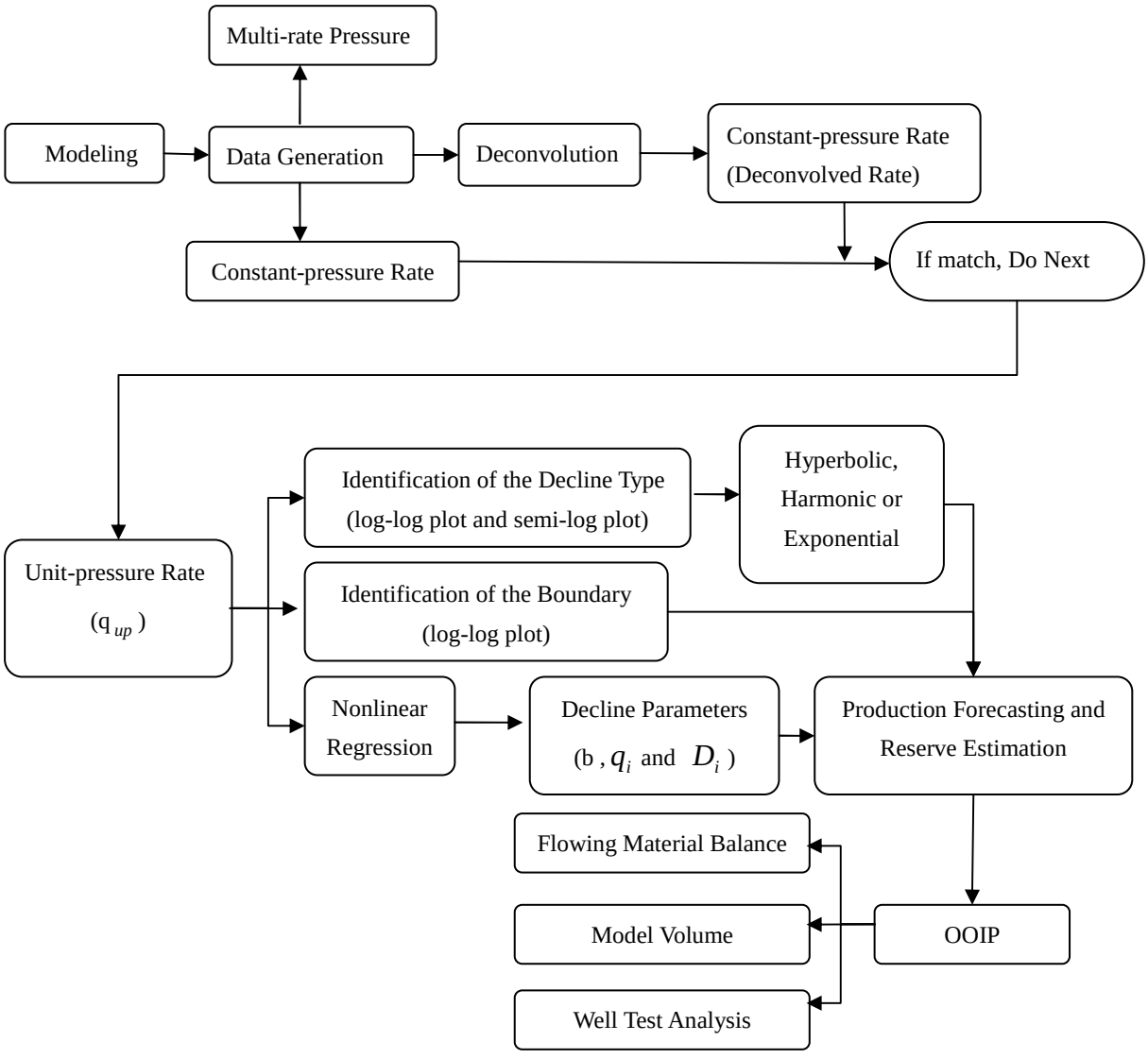

Figure 3. 3 Workflow of Deconvolotion-based Rate Transient Analysis

3.5 Field Example

This example serves to illustrate a rudimental conduct of this methodology for production forecasting. In this example, the Arps decline analysis will be used to predict the expected ultimate recovery (EUR), and the method of flowing material balance will be used to obtain the original-oil-in-place (OOIP).Then the estimated results will be confirmed using model history match. The well / reservoir parameters of this field example are listed in **Table 3.1**.

Initial pressure, p_i	163.5 bar (2370.8 psia)
Formation thickness , H	20 m
Porosity, ϕ	0.20
Water saturation, S_w	0.31
Permeability, k	300 md
Viscosity, μ	1.1 cp

Table 3. 1 The well / reservoir parameters of the field example

This single well produces monophasic oil from a small structure that is not connected to any aquifer pressure support. Its geological models have shown in **Figure 3.4** and **Figure 3.5**, which present the oil saturation profile and pressure change respectively from the beginning to the recorded production period. It is apparent that the well production has affected the total reservoir system. So it can be confirmed that this well produces under the boundary-dominated flow condition.

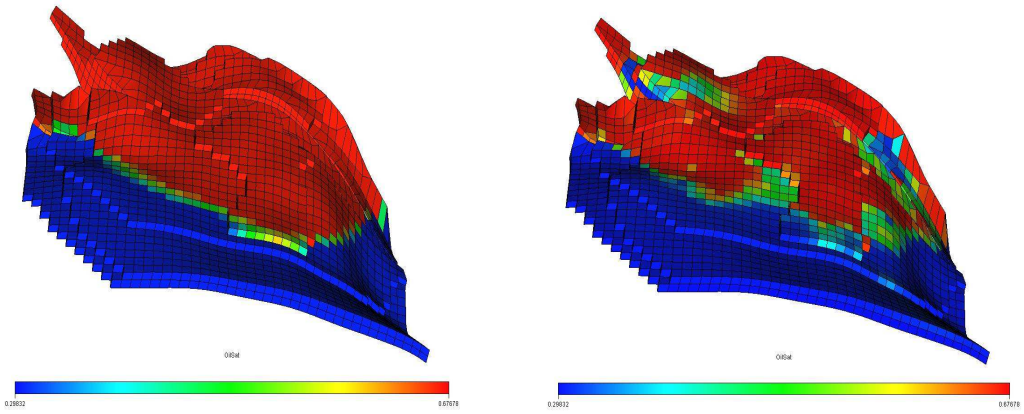

Figure 3. 4 Oil Saturation Profile for Field Example

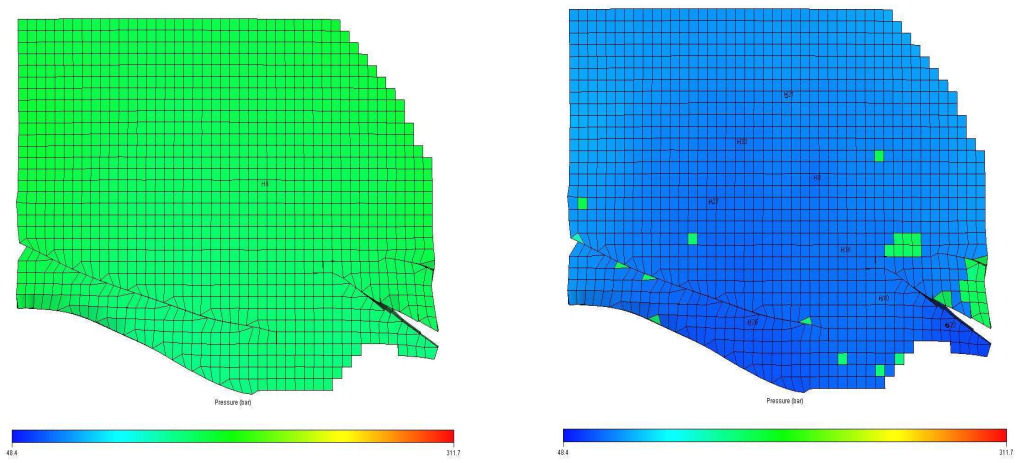

Figure 3. 5 Pressure Change for Field Example

The production data from this well, namely flow rate and downhole pressure versus time is shown in **Figure 3.6**.

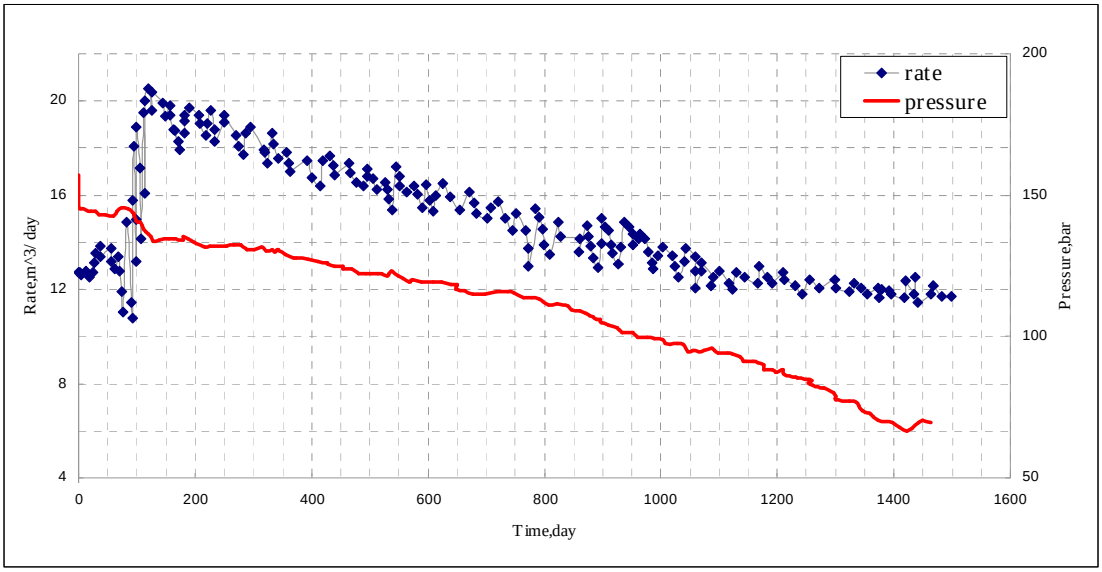

Figure 3. 6 Raw Data for Field Example

Figure 3.7 shows the result of nonlinear regression on production data versus time. The decline parameters obtained from this regression curve, namely, initial flow rate (q_i), initial decline rate (D_i) and decline exponent (b), will be used to confirm the decline type and forecast expected ultimate recovery (EUR) in the following sections.

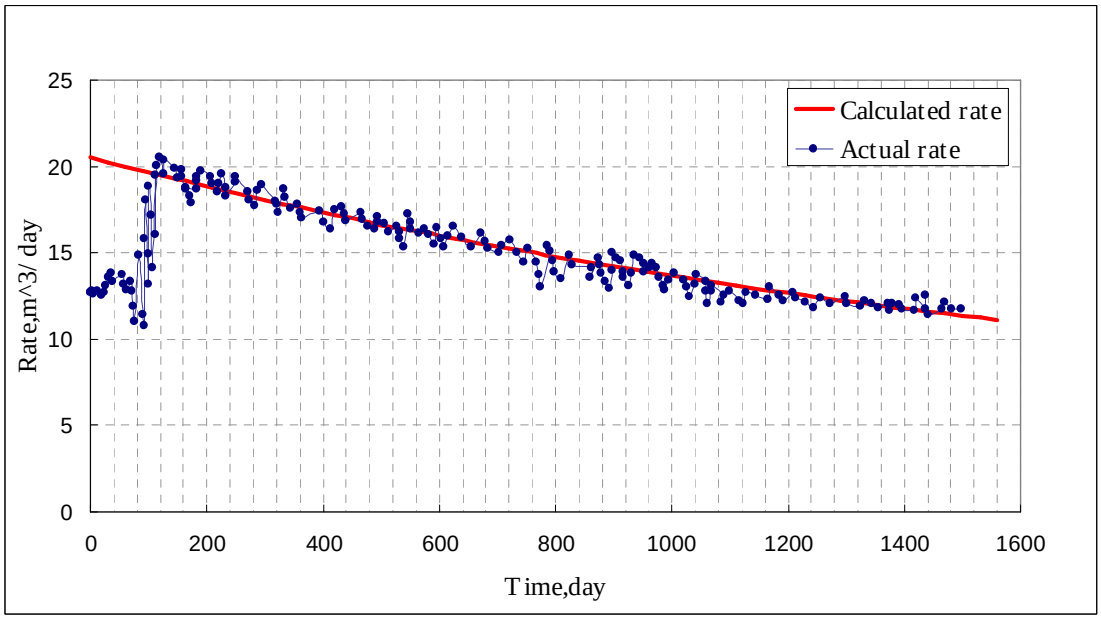

Figure 3. 7 Nonlinear Regression Result for Field Example

Figure 3.8 and **Figure 3.9** shows the cartesian analysis plots. **Figure 3.8** is a graph of rate versus time, which shows two models of decline analysis (exponential analysis and hyperbolic analysis).As illustrated here, hyperbolic decline predicts a slower decline rate than exponential. As a result, it is sometimes used to calculate the "probable reserves", while exponential decline is used to obtain minimum "proved reserves". **Figure 3.9** is a rate versus cumulative production plot. The exponential analysis, in this case indicates an *EUR* of approximately $50000\,m^3$, which the value obtained from hyperbolic analysis is about $69000\,m^3$. **Figure 3.10** is a flowing material balance plot. The OOIP estimated using this method is approximately $67000\,m^3$.

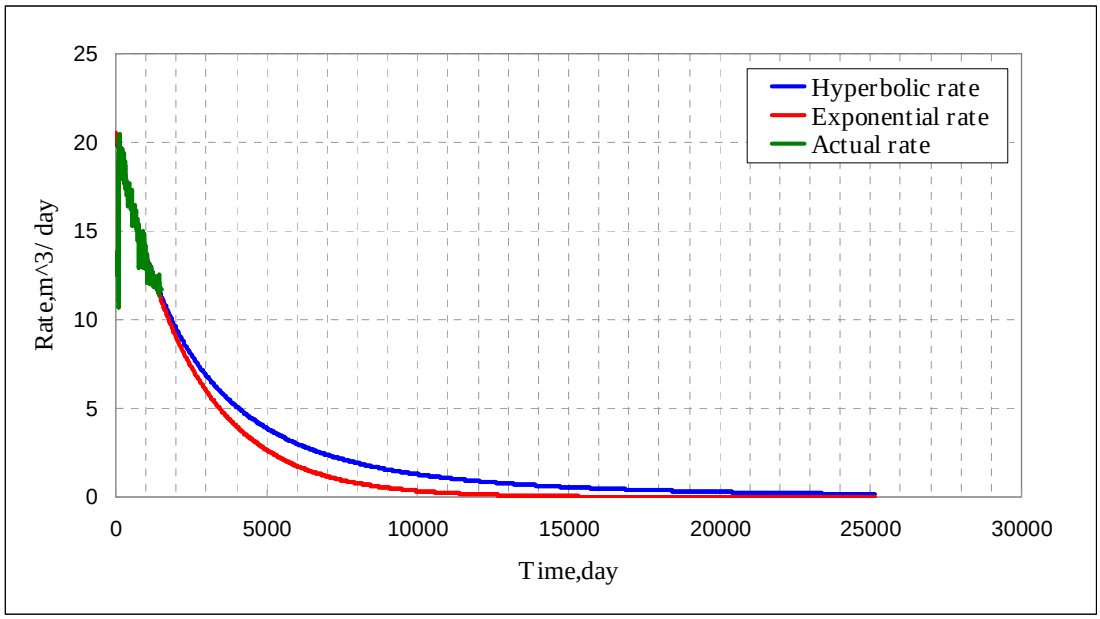

Figure 3. 8 Rate vs. Time Analysis for Field Example

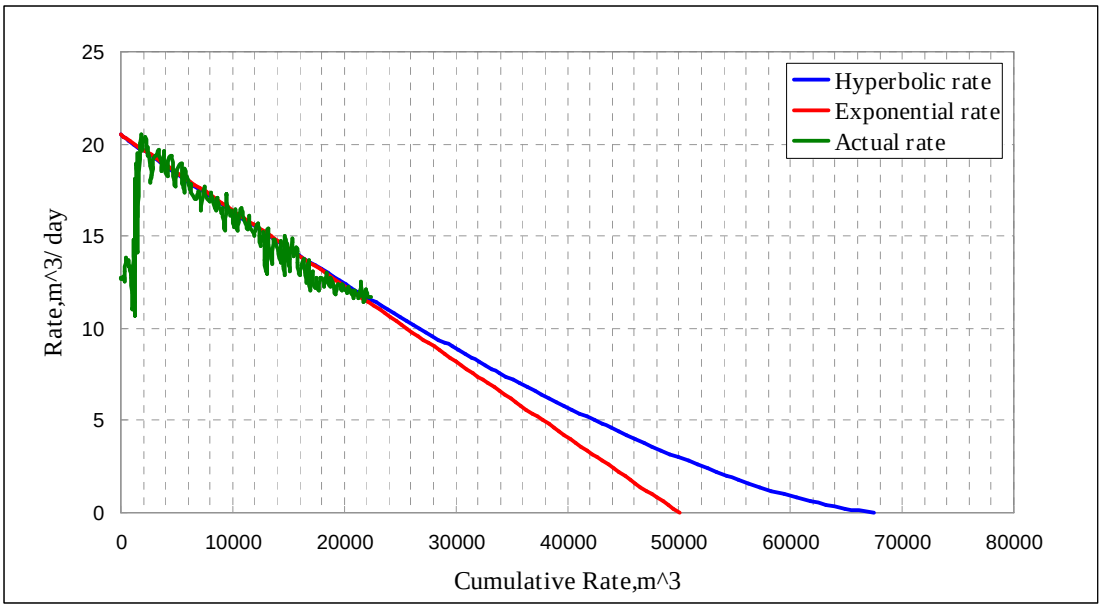

Figure 3. 9 Rate vs. Cumulative Rate Analysis for Field Example

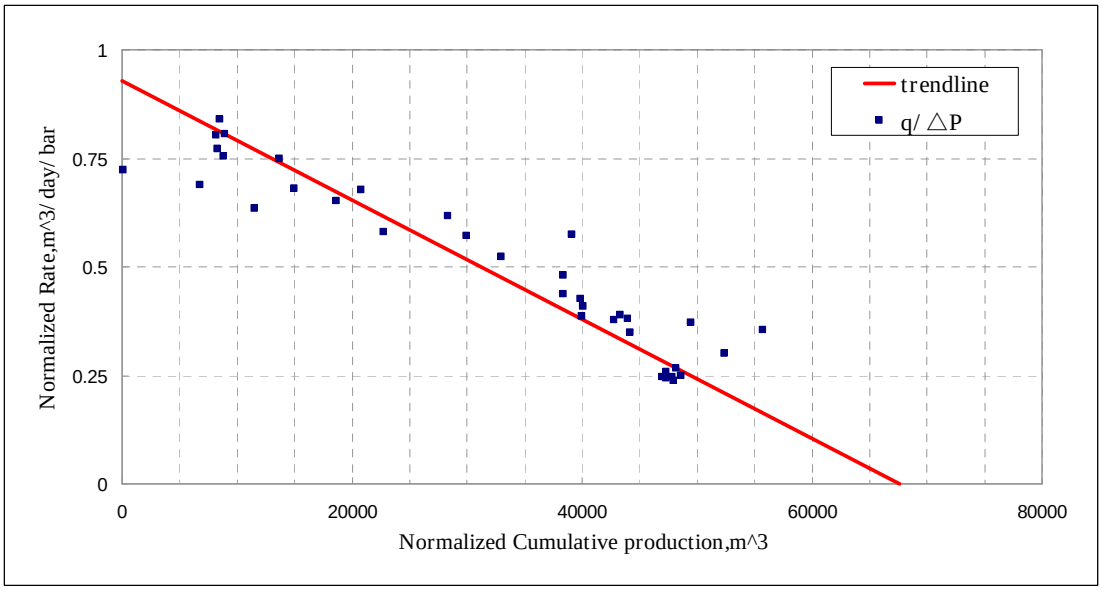

Figure 3. 10 Flowing Material Balance Analysis for Field Example

Here, the discrepancy clearly suggests that one of the analyses must be wrong. The value of OOIP should be higher than that of the EUR. That is because at some point in period of production decline, the hyperbolic decline will be converted into an exponential decline. Extrapolation of hyperbolic declines over long periods of time frequently results in unrealistically high reserves, without considering the conversion of decline exponent. In this respect, a modified hyperbolic decline model, which starts

as a hyperbolic decline curve and transitions into an exponential decline curve at a specified decline rate, D, value, should be used. And the value of EUR should be between 50000 m^3 and 67000 m^3, depending on specified final decline rate.

Again, the model history matching, shown in **Figure 3.11**, confirms the estimated OOIP using the flowing material balance.

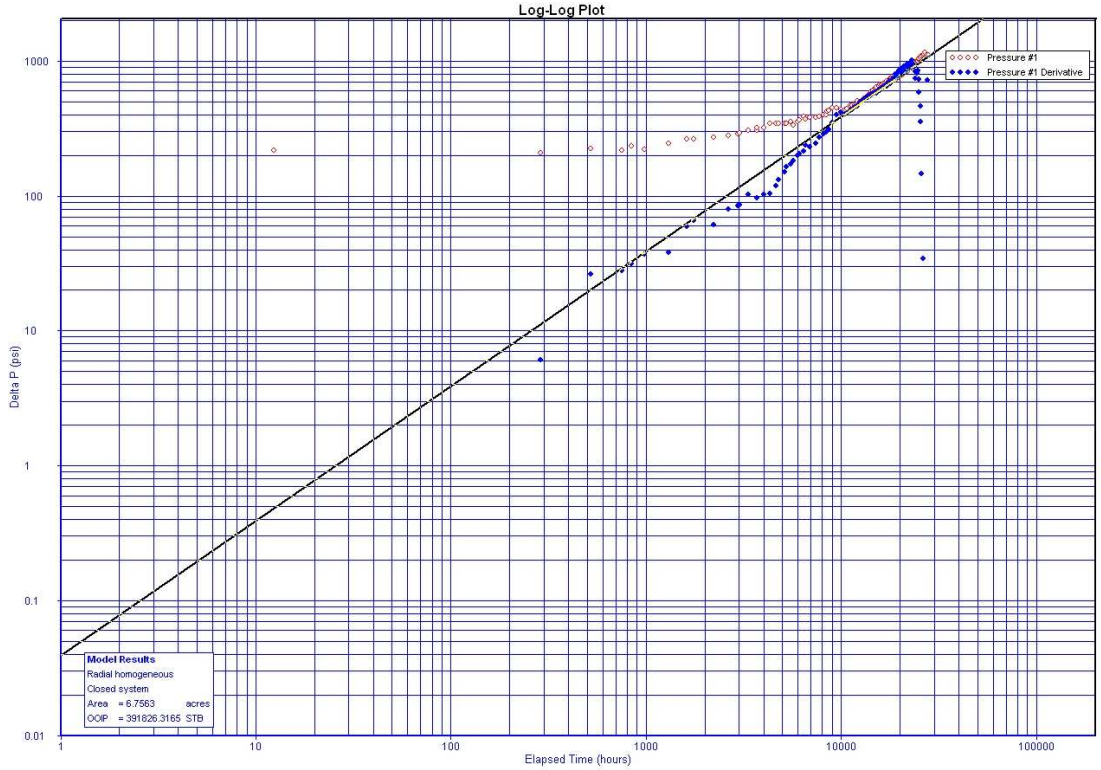

Figure 3. 11 Analytical Model History Match for Field Example

3.6 Synthetic Case Studies

In order to validate the existing deconvolution algorithm, several sets of synthetic pressure and rate data are produced. These numerical experiments are particularly useful because the exact result from the deconvolution algorithm must produce is known.

The well/reservoir model used for case 1-3 is a fully penetrating single vertical well, located in a uniform formation, bounded on all sides by no-flow boundaries, shown in

Figure 3.12. Other parameters are listed in **Table 3.2**. Results from these cases are interpreted below.

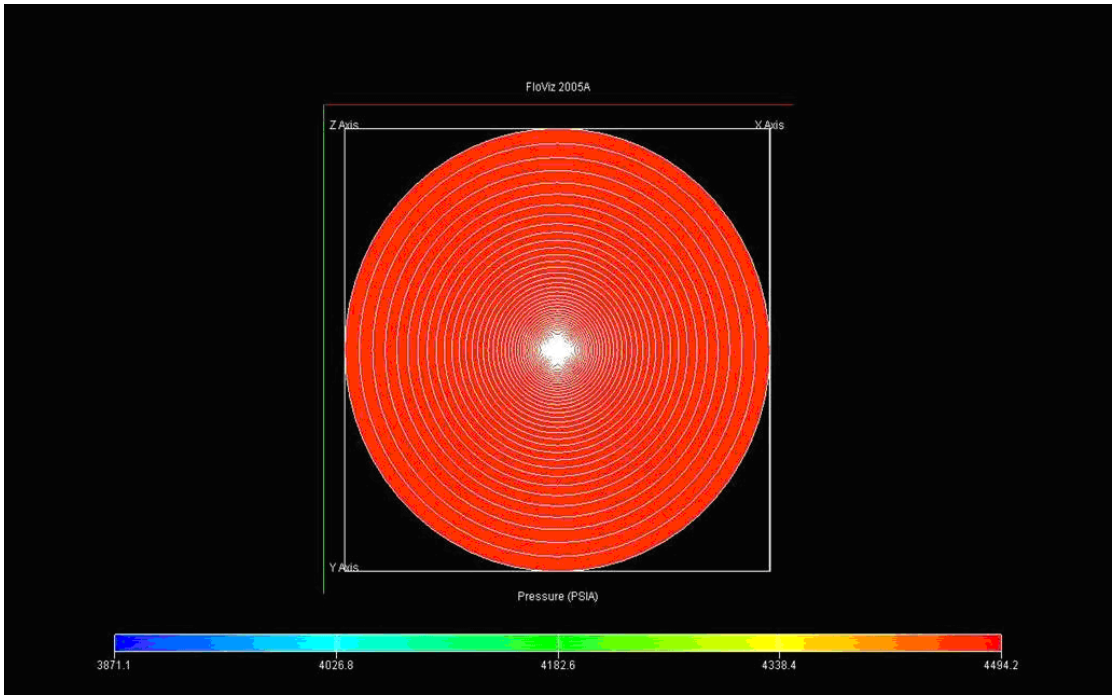

Figure 3. 12 Reservoir Model for Synthetic Case 1-3

Initial reservoir pressure, p_i	= 4500 psia
Porosity, ϕ	= 0.3
Permeability, k	= 50 mD
Thickness, h	= 20 ft
Oil formation volume factor, B_o	= 1.22rb/STB
Viscosity, μ	= 0.9 cp
Total compressibility, c_t	=1.02e-5 1/psia
Well radius, r_w	= 0.3 ft
Reservoir radius, R	= 4000 ft

Table 3. 2 Reservoir and Fluid Properties for Synthetic Cases 1-3

Case 1

This case is designed to test the performance of the rate-pressure deconvolution algorithm. **Figure 3.13** shows the simulated production-rate history and corresponding pressure response. The blue line in **Figure 3.14** shows the rate-pressure deconvolution result, which is the unit-pressure-rate response. **Figure 3.15** shows the match of the constant-pressure-rate response reconstructed from deconvolution with the simulated constant-pressure transient rate.

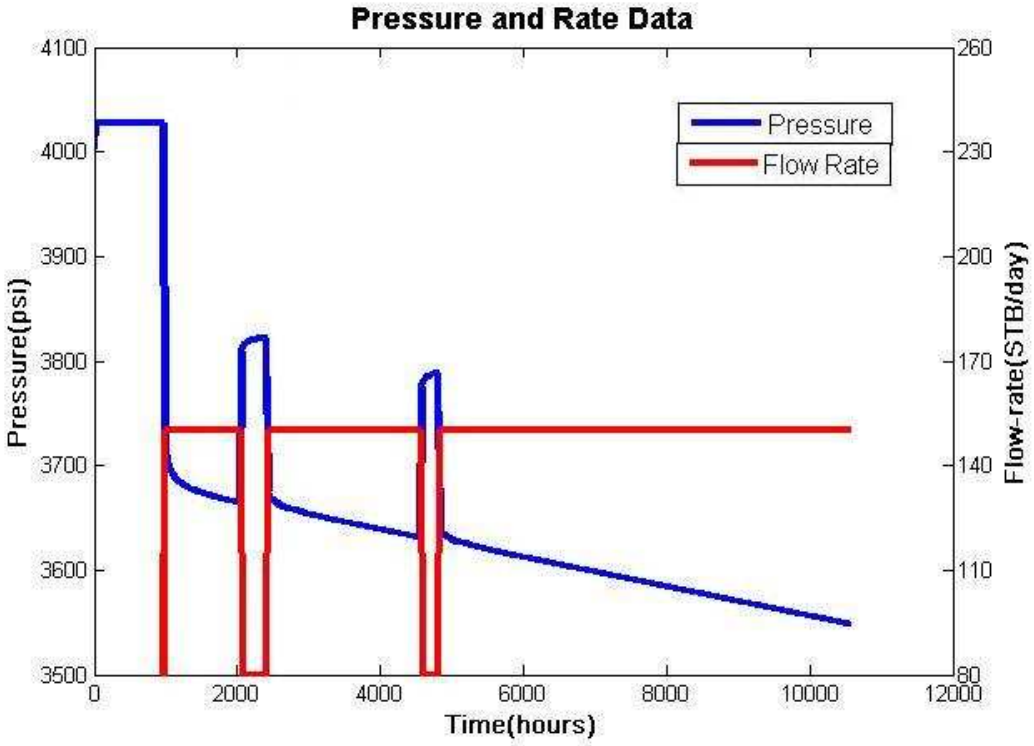

Figure 3. 13 This figure shows a simulated test history, which includes three pressure draw downs and two short build ups. The red line is flowing rate and the blue line is the corresponding pressure response.

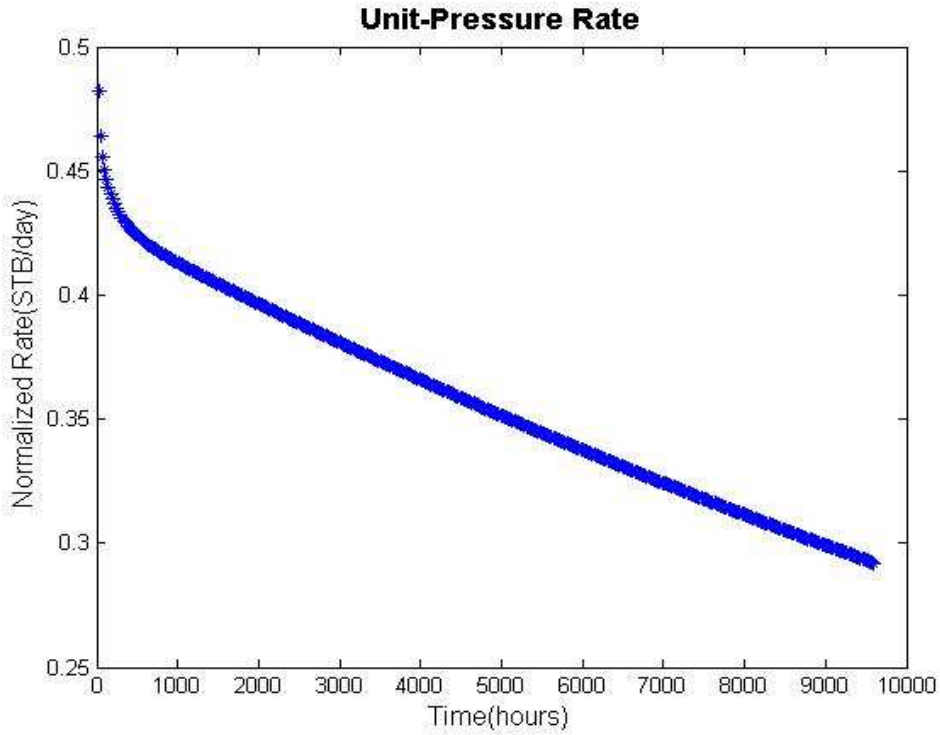

Figure 3. 14 This figure shows the rate-pressure deconvolution result of the whole testing history in Cartesian plot, where the horizontal axis shows the elapsed time, while the vertical axis shows the unit- pressure rate response.

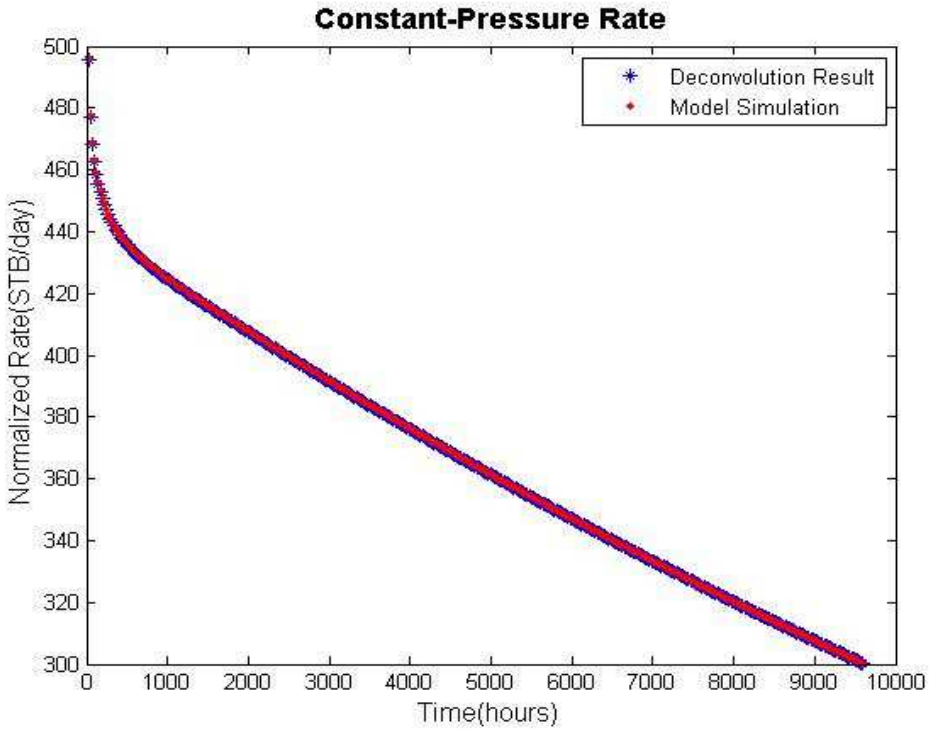

Figure 3. 15 This figure shows the comparison of constant- pressure rate response between the deconvolution result and simulated case. The blue line is deconvolved

transient rate, while the red line is from model simulation under the constant flowing pressure condition.

Since the unit-pressure rate response is generated from the rate-pressure deconvolution, traditional decline-curve methods based on analytical solutions can be used to estimate reservoir recoverable reserves and to do production forecast. **Figure 3.16** shows the trend of production decline curve (unit-pressure rate from deconvolution) plotted on the log-log plot, which does not exhibit a straight line. This is different from the outcomes of traditional Hyperbolic or Harmonic decline models. Therefore as shown in **Figure 3.17**, the deconvolved rate data are plotted on the semi-log plot, on which the late-time response exhibits a well-defined straight line.

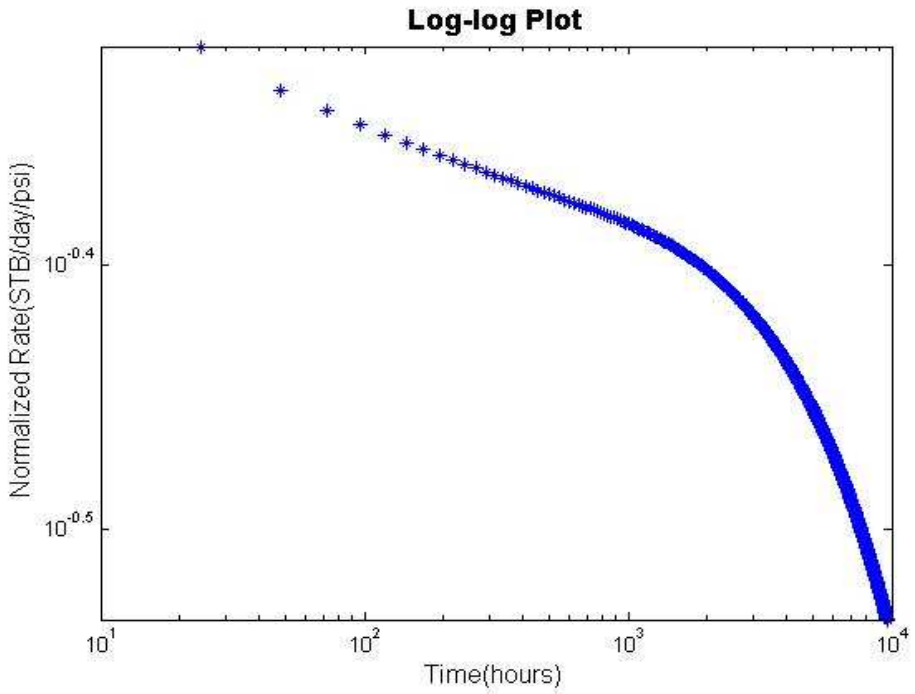

Figure 3. 16 This figure shows the deconvolved unit-pressure rate response on log- log plot. Apparently, the decline type of this data is different from the traditional Hyperbolic or Harmonic types, as it does not exhibit a straight line on this log-log plot.

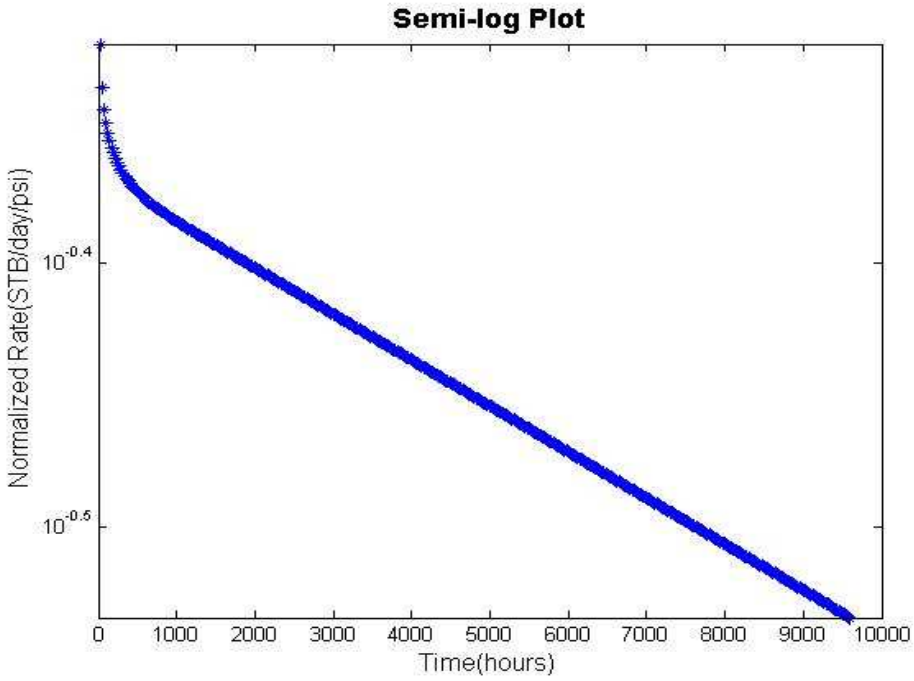

Figure 3. 17 This figure shows the deconvolved unit-pressure rate response on semi-log plot. The late-time (after 800 hours) response exhibits a well-defined straight line, which fits a classic Exponential decline curve.

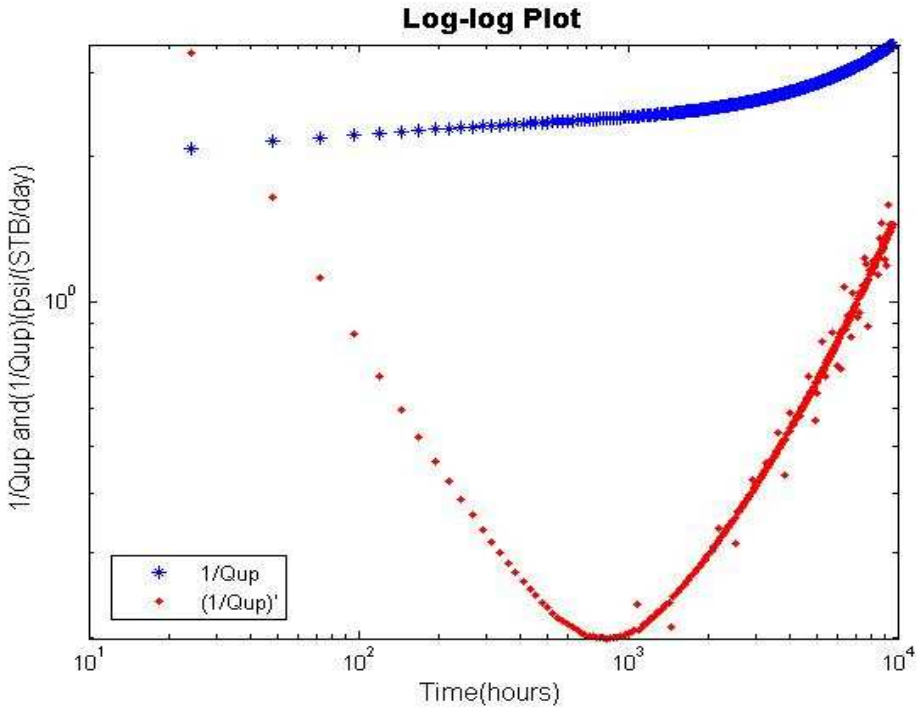

Figure 3. 18 This figure shows the deconvolved transient rate and associated derivatives on log- log plot. The blue line is the reciprocal value of unit-pressure rate, while the red line is associated derivatives. Clearly the flow was dominated by the

boundary effect at about 800 hours as shown above.

This is a classic Exponential decline trend (from about 800 hours). The decline curve parameters shown in **Figure 3.19** were estimated by non-linear regression for times greater than 800 hours, as the log-log diagnostic plot of unit-pressure rate responses (**Figure 3.18**) clearly determines that it has reached pseudo-steady state at 800 hours.

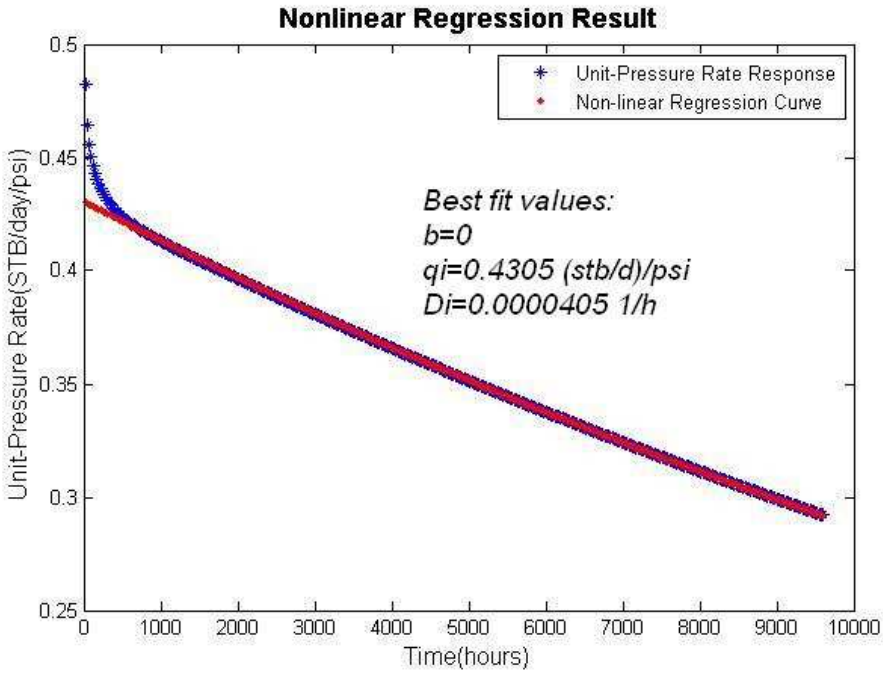

Figure 3. 19 This figure shows the non-linear regression of deconvolved unit-pressure rate response. The blue line is the original deconvolved rate, while the red line is the nonlinear regression curve from 800 hours. The best fit values are derived from regression curve fitting.

Finally, traditional Arp's decline curve model and the decline curve parameters, b, D_i and q_i, are obtained by non-linear fitting for production forecast. **Figure 3.20** and **Figure 3.21** shows production forecasting and estimated ultimate recovery (EUR) under the different pressure conditions. **Figure 3.22** shows production forecasting of this well under the different pressure conditions.

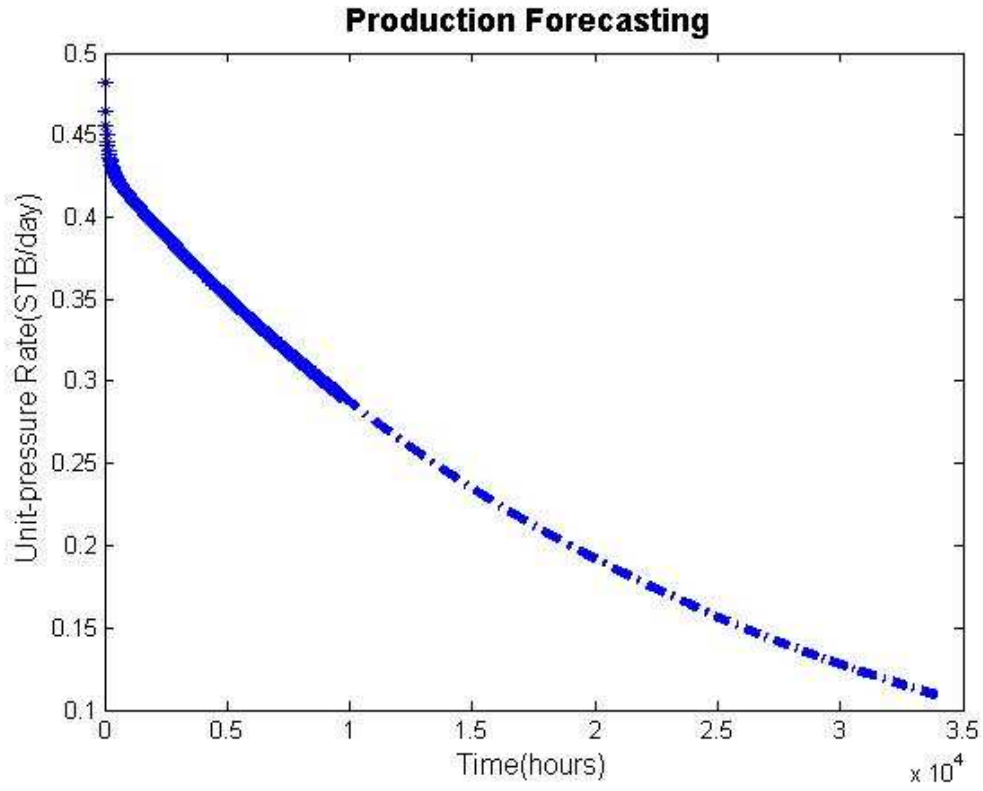

Figure 3. 20 Production forecasting-Unit-pressure rate vs. Time

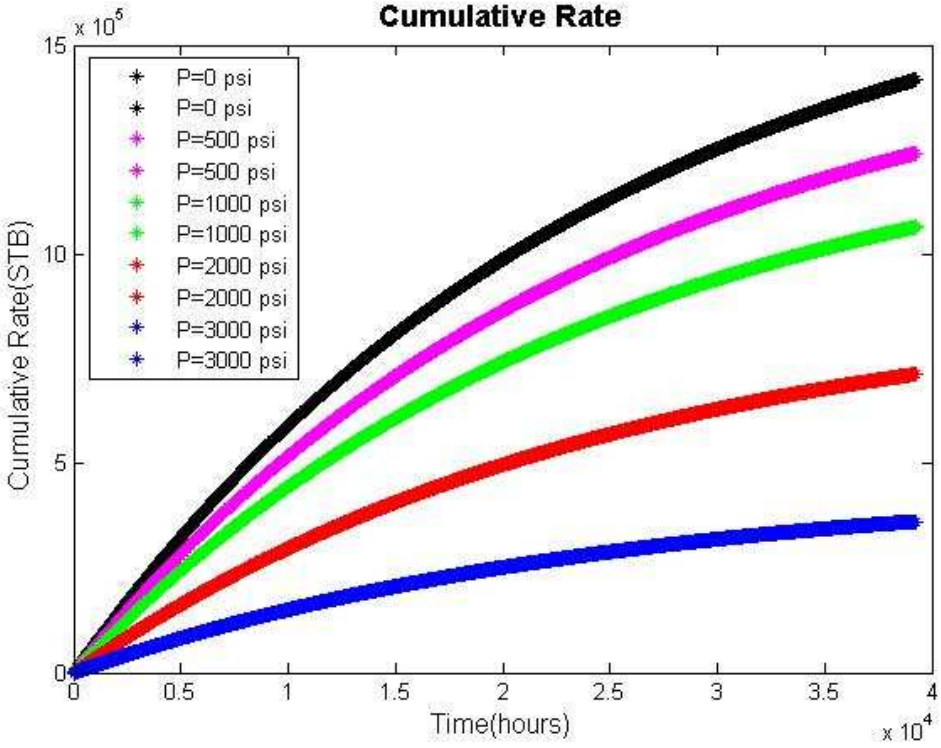

Figure 3. 21 Production forecasting-Cumulative rate vs. Time

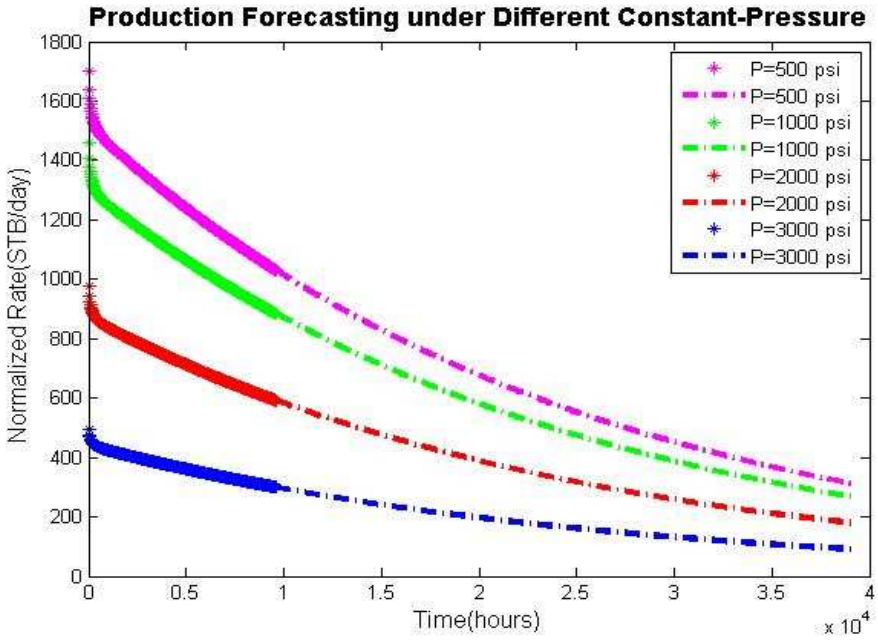

Figure 3. 22 This figure shows production forecasting, where the horizontal axis shows the production time, while the vertical axis shows the production rate. The solid line presents existing production, while the dotted line presents the future production. Different colors show well production under different pressure conditions.

This synthetic case described above confirmed the good performance of the developed rate-pressure deconvolution algorithm.

Case2

Following the same procedure in case1, a set of multi-step rate data with added noise is generated by simulation. Noise was also added to the corresponding pressure response. Nonlinear Total Least- Square (NTLS) method was used in processing the deconvolution results. The original pressure and rate history together is shown in **Figure 3.23** and the deconvolution result after the NTLS solved is shown in **Figure 3.24**.

The blue line in **Figure 3.25** shows the rate-pressure deconvolution result, which is the unit-pressure-rate response. **Figure 3.26** shows the match of the constant-pressure-rate response reconstructed from deconvolution with the simulated constant-pressure transient rate.

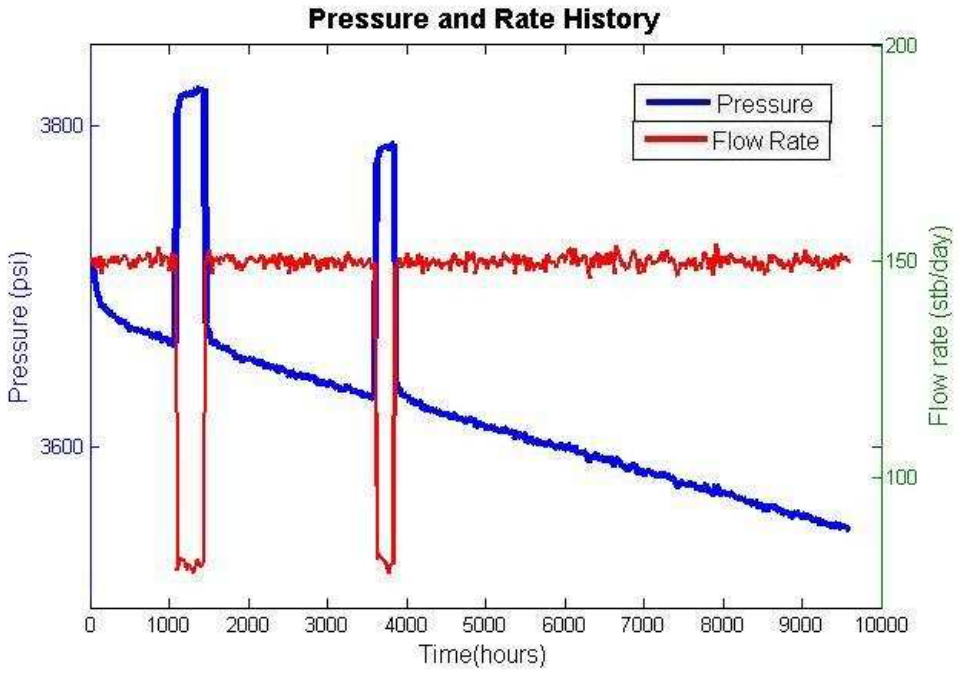

Figure 3. 23 This figure shows a set of simulated multi-step rate data with three pressure draw downs. The red line is the flowing rate, while the blue line is the corresponding pressure response. Both rate and pressure data is with the added noise.

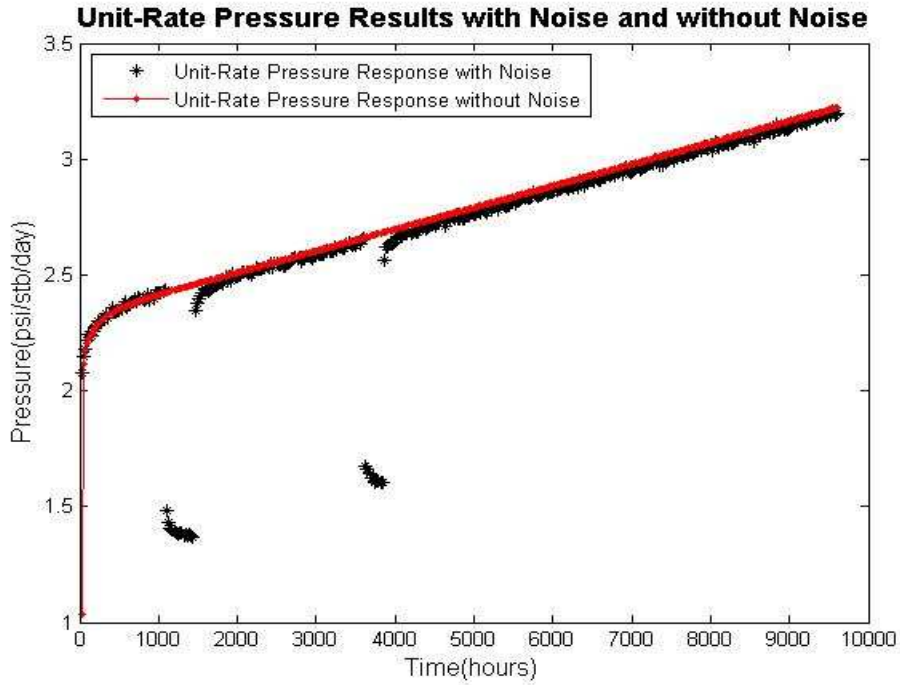

Figure 3. 24 This figure shows the comparison of deconvolved pressure without noise from original algorithm and that with noise from modified algorithm. The black line is the deconvolved unit-rate pressure with noise, while the red line is the deconvolved

unit-rate pressure without noise.

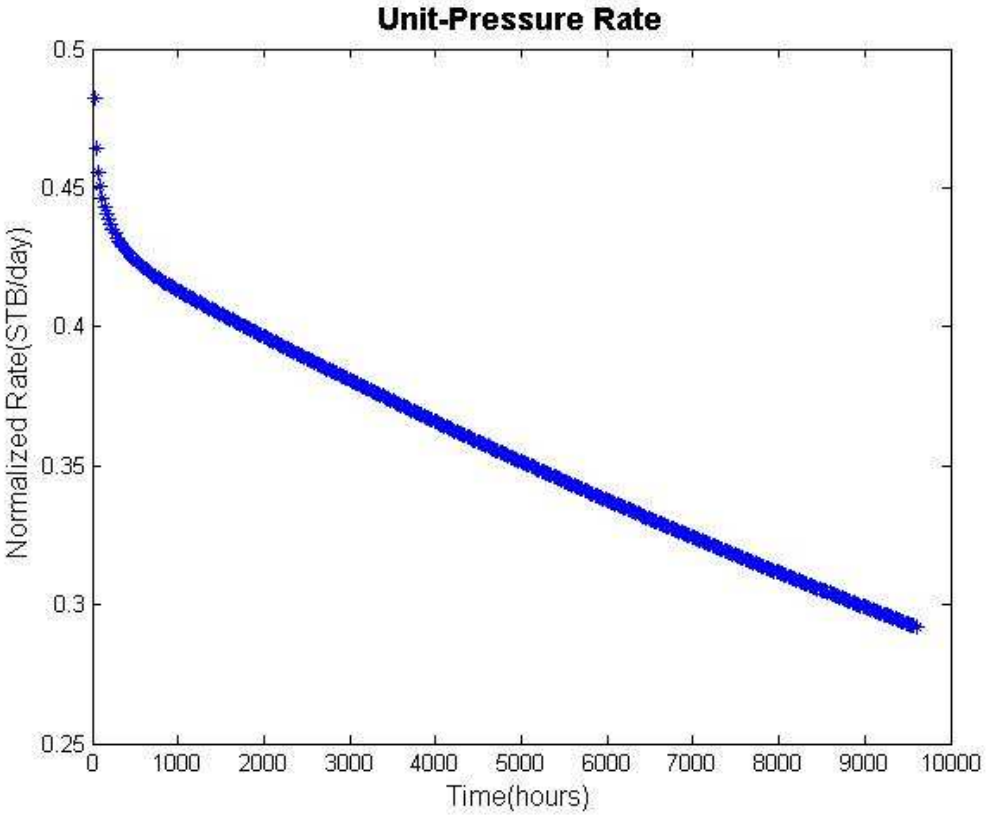

Figure 3. 25 Deconvolved unit-pressure rate decline response

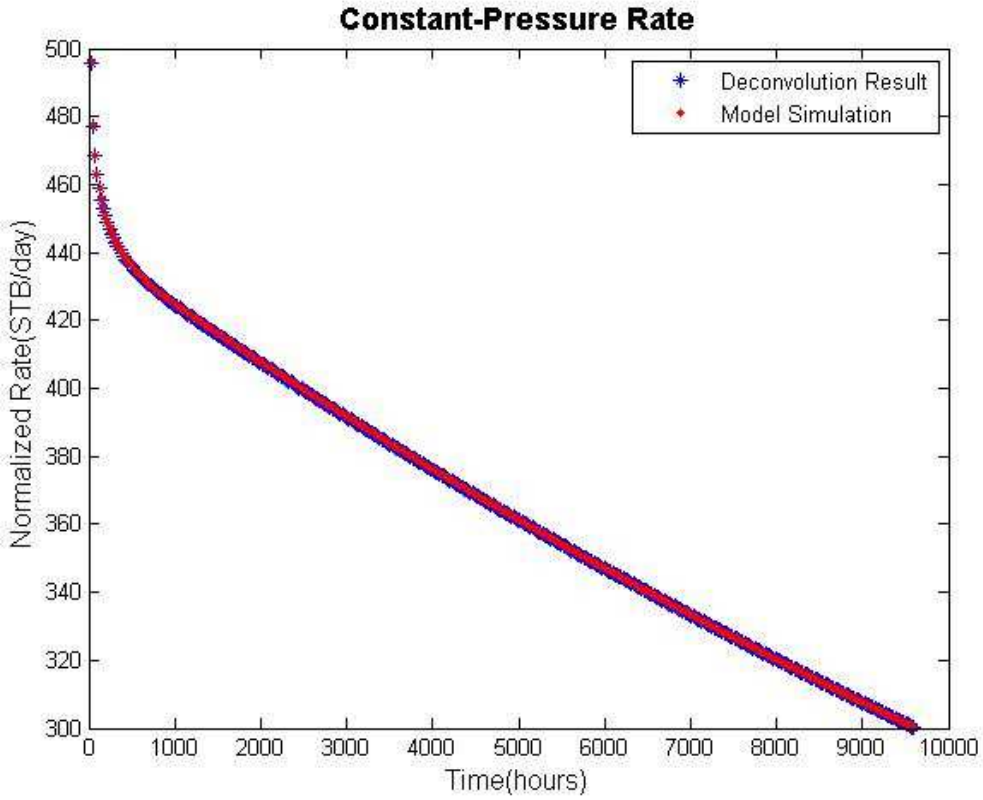

Figure 3. 26 Deconvolved constant-pressure rate decline response

From the synthetic case described above, the applicability of the developed deconvolution algorithm on handling noisy data was tested. It appeared to be working well with synthetic data.

Case 3

This case is designed for evaluating performance of deconvolution in traditional well testing and decline-curve analysis. **Figure 3.27** shows the simulated step rate production history and corresponding pressure response. The total time period of the data is 235 days.

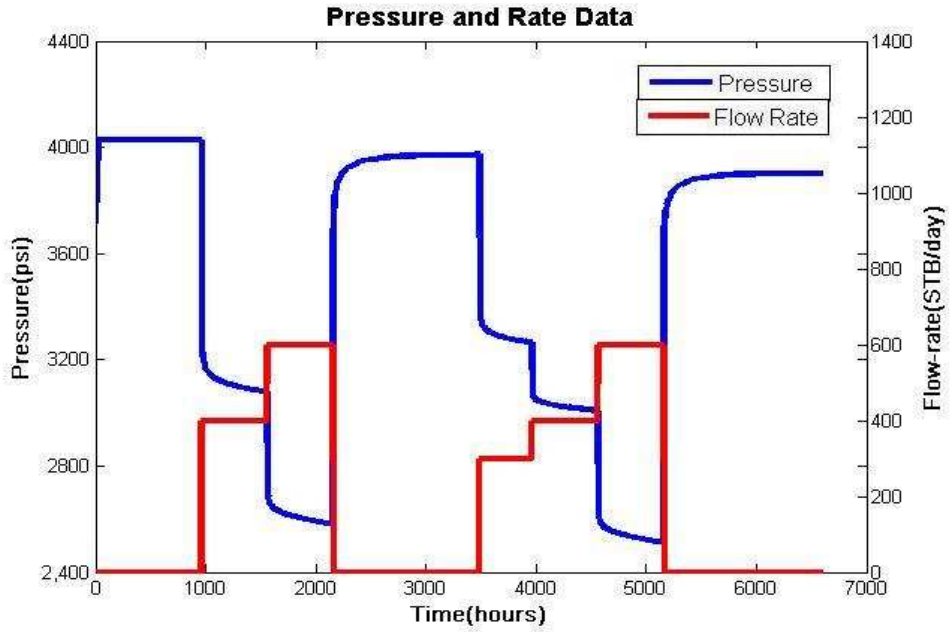

Figure 3. 27 This figure shows a simulated testing history, which includes several draw downs and build ups. The red line is flowing rate and the blue line is the corresponding pressure response.

Firstly, pressure-rate deconvolution is implemented on this test history using the developed algorithms. **Figure 3.28** shows the pressure-rate deconvolution result, which is the unit-rate-pressure response. Then, another 235-day constant flowing rate simulation was carried out. The comparison of the constant-rate-pressure response reconstructed from deconvolution with the simulated constant-rate drawdown-pressure behavior is shown in **Figure 3.29**. The pressure match quality is good.

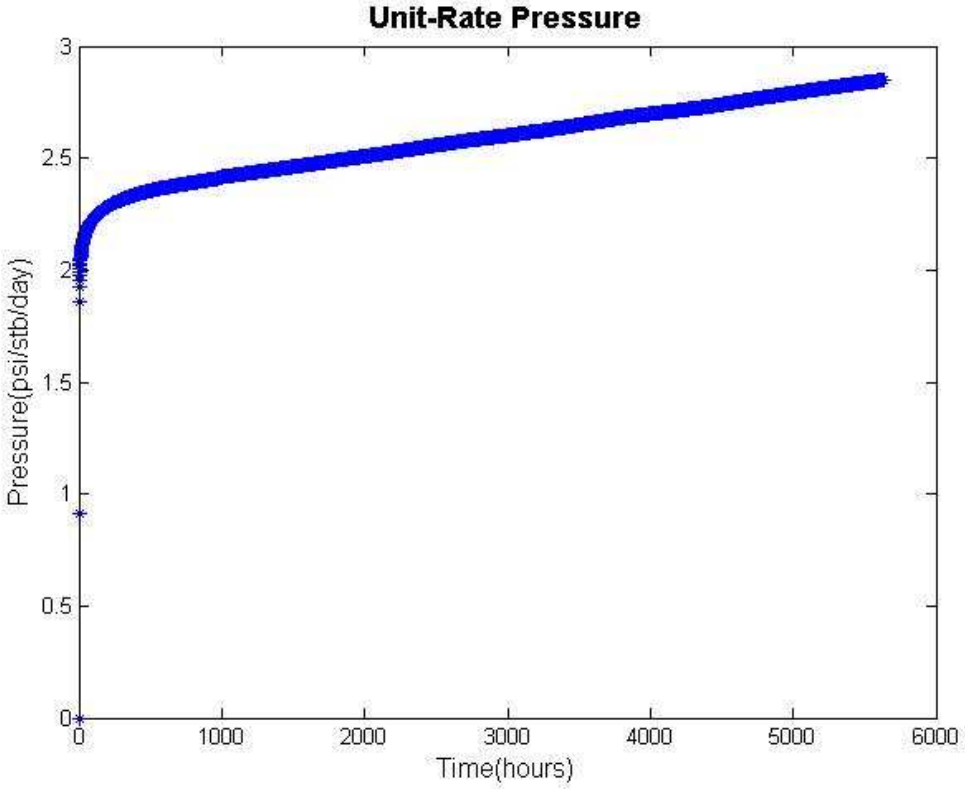

Figure 3. 28 Deconvolved unit-rate pressure response

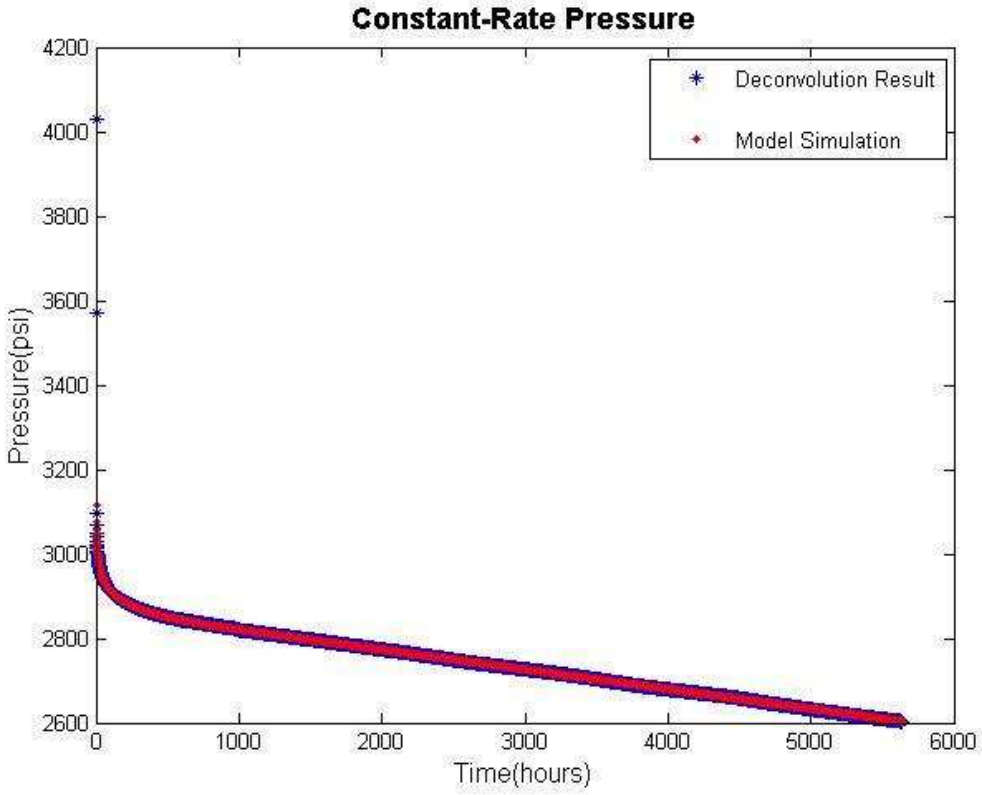

Figure 3. 29 Deconvolved constant-rate pressure response

The comparison between the deconvolved results for the step rate flow simulation and the constant flowing rate simulation along with the longest build up period (the last one) was made and the results is shown in **Figure 3.30**.

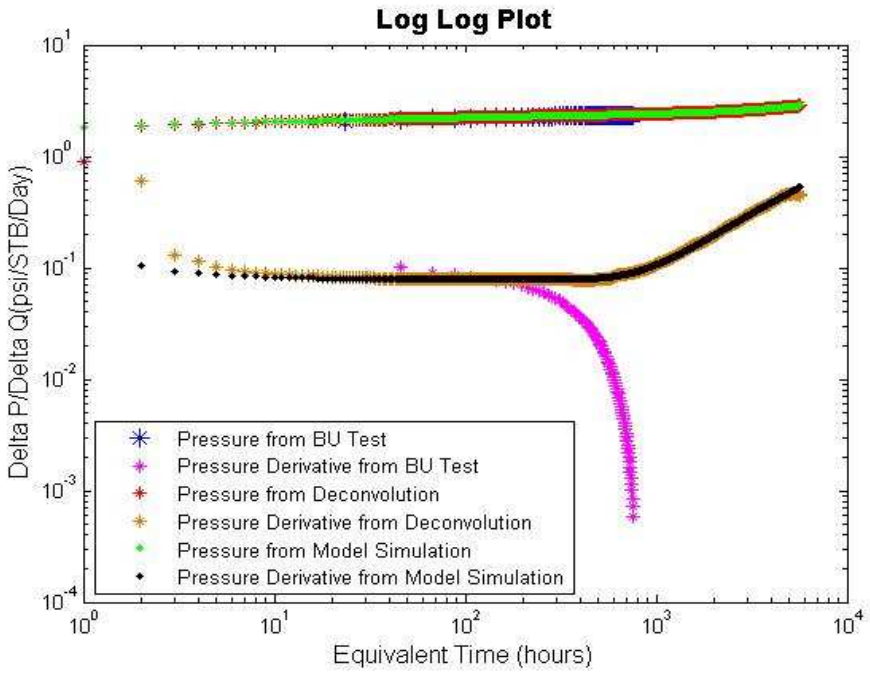

Figure 3. 30 This figure shows the comparison of pressure draw-down and associated derivatives between Longest buildup, deconvolution of step rate test across the full period and constant rate flow simulation results on log-log diagnostic plot. Two short blue and pink lines shows the pressure buildup period, which takes 1440 hours, while other four longer lines present the deconvolution and simulation results for the whole testing history. Both the pressure and associated derivatives are in good agreement.

The results are in good agreement, which indicates that the behaviour of deconvolved data can represent the true reservoir response under the constant flowing conditions. **Figure 3.31** shows the comparison of above three on semi-log plot.

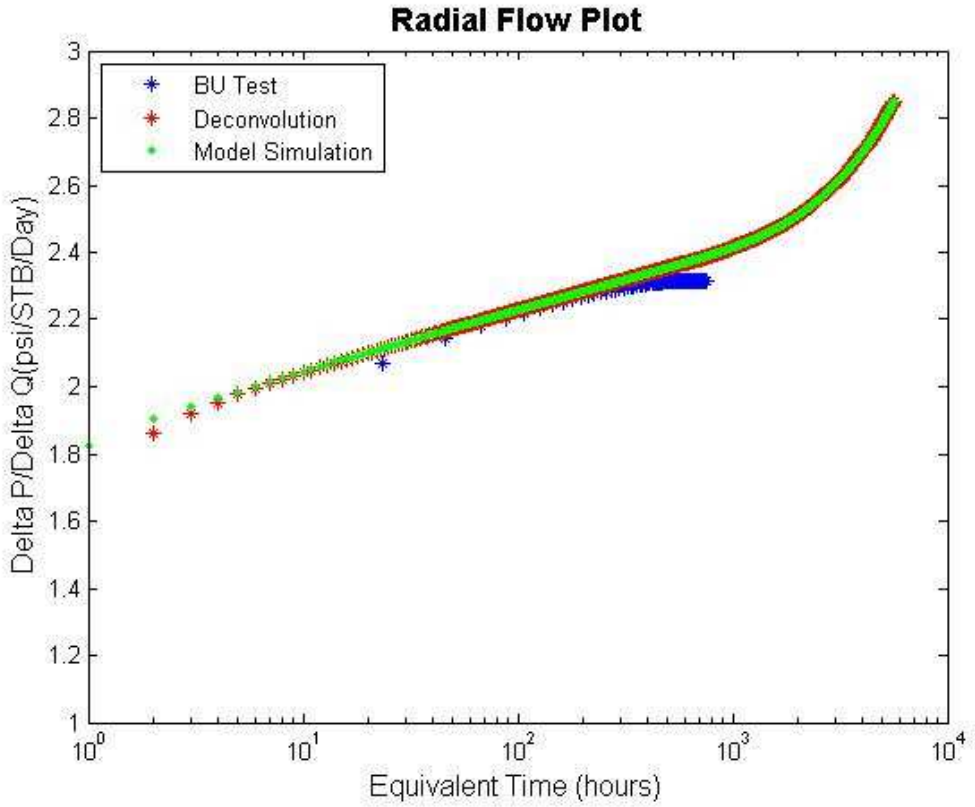

Figure 3. 31 Comparison between buildup test, deconvolution and simulation results on semi-log plot

Thereafter, the rate-pressure deconvolution is implemented on this test history using the developed algorithm. The blue line in **Figure 3.32** shows the rate-pressure deconvolution result, which is the unit-pressure-rate response. Then I match the constant-pressure-rate response reconstructed from deconvolution with the simulated constant-pressure transient rate. **Figure 3.33** shows the rate match quality, which is still good.

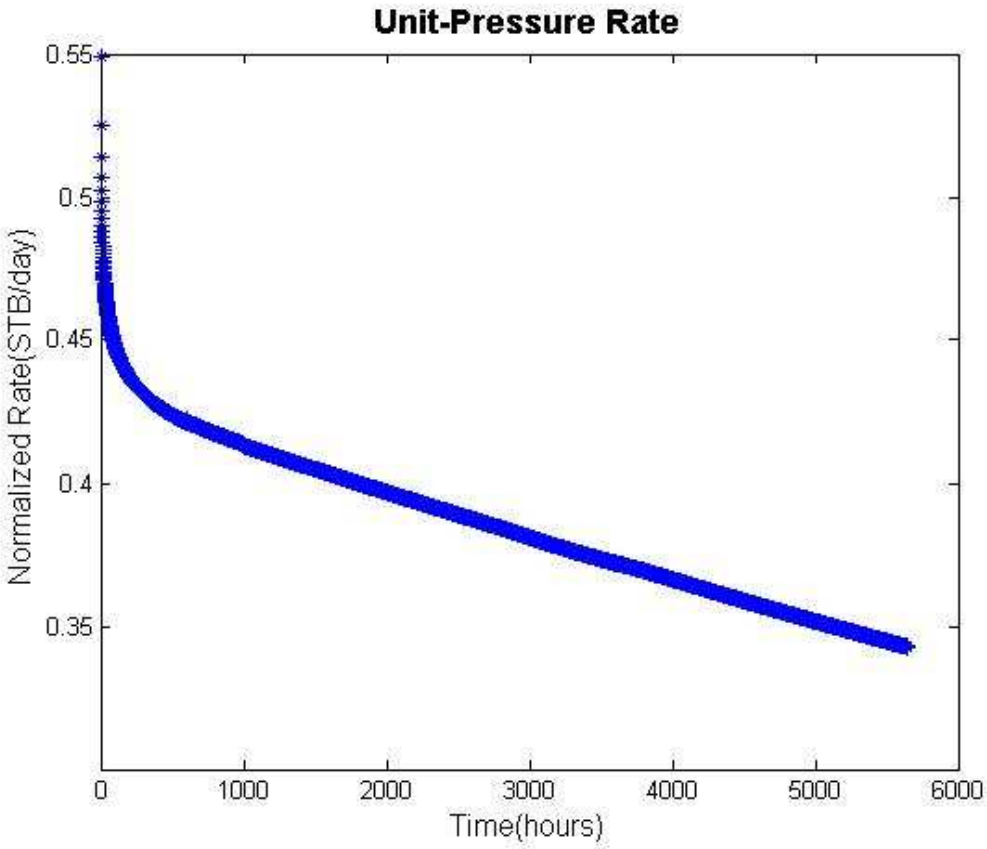

Figure 3. 32 Deconvolved unit-pressure rate decline response

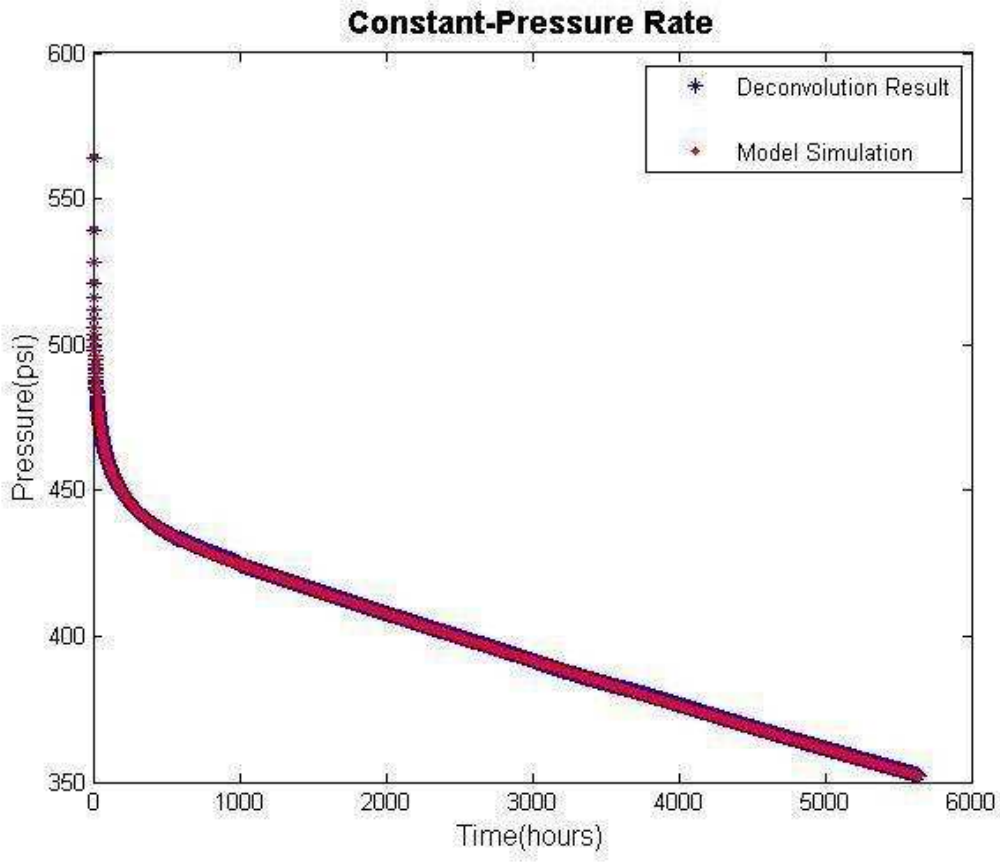

Figure 3. 33 Deconvolved constant-pressure rate decline response

From the log-log diagnostic plot of deconvolved unit-pressure rate response shown in **Figure 3.34**, it is obvious that pseudo-steady state flowing condition was reached at a time of about 800 hours. This is consistent with the result from diagnostic plot of deconvolved unit-rate pressure response shown in **Figure 3.30**.

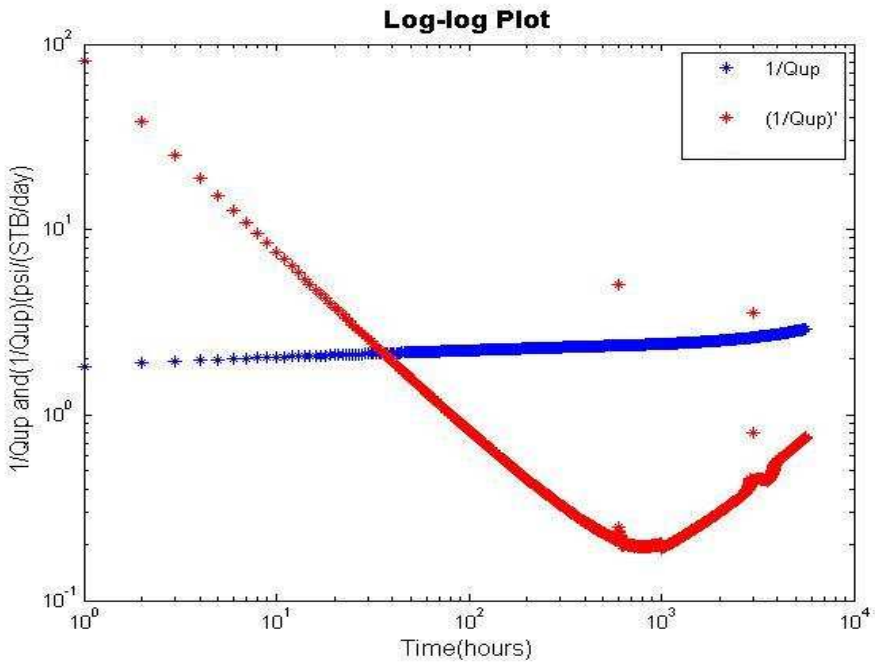

Figure 3. 34 This figure shows the deconvolved transient rate and its derivatives on the log-log plot. The blue line is the reciprocal value of unit-pressure rate, while the red line is associated derivatives.

The reservoir parameters estimated from the longest buildup, simulation, deconvolution-based decline-curve analysis and deconvolution-based pressure-transient analysis are shown together in **Table 3.3**. This reveals that the deconvolution results are consistent with those from the traditional well testing analysis and decline-curve analysis. The results derived from different approaches can support each other in practical case.

	BU Test	Deconvolution -based Pressure-Transient Analysis	Calculation	True Model	Deconvolution -based Decline-curve Analysis
k(md)	49.6204	49.2178	49.4395	50	33.6378
S	6.0902	6.0075	6.0684	6	*
A(acre)	*	1141.4976	1147.8722	1148.9977	1136.9725
R (ft)	*	3978.3821	3989.4751	4000	3971.4956
OOIP(STB)	*	4.3555e7	4.3798e7	4.4e7	4.3379e7

Table 3. 3 Comparison of the parameters estimated by buildup test, deconvolution and calculation from the true model parameters

3.7 Chapter Conclusions

According to this study, several conclusions can be derived, as follows:

A new rate-pressure deconvolution algorithm in time-domain is developed to deal with the flowing pressure variations and noise problem in single-well PDG data. The constant-pressure rate response of a single-well reservoir system was calculated using the developed rate-pressure algorithm.

Theoretical derivation of the rate-pressure deconvolution product has been finished, which proved that the deconvolution product consistent with that from traditional rate transient theory.

Analytical and simulation cases have been produced for comparison. The results from analytical, simulation and deconvolution solutions agree with each other, which prove that the developed single-well rate-pressure deconvolution algorithm works well.

Deconvolution-based transient rate analysis theory and corresponding workflow are proposed in detail. This deconvolution-based analysis procedure has improved the

traditional decline-curve methods.

Numerical synthetic studies have been performed to demonstrate the procedure of this deconvolution-based transient rate analysis. The results proved that this deconvolution-based analysis method worked well in homogeneous reservoirs with one well flowing at single phase, multiple rates. And this new method improved the traditional rate transient analysis technique.

A double-checked practice method for analysis of transient pressure integrated with the transient rate analysis is proposed.

Chapter 4
Deconvolution-based Self Response Analysis of Multi-Well PDG Transient Pressure Data

4.1 Introduction

Interference effect between wells is very common in transient pressure data from PDG. As soon as the recorded pressure interfered by the pressure disturbance from other wells nearby, the PDG pressure becomes the product of two components, i.e. self response due to the well production and interference response from neighboring wells.

This interfered pressure data recorded by the PDG usually combines with noise information and multi-rate superposition effect, which cannot be analyzed by traditional well testing principles.

This chapter presents a newly developed multi-well deconvolution algorithm specially designed for processing and analyzing long-term transient pressure with interference from neighboring wells in the same reservoir. This developed algorithm is based on linear recursion with added non-linear least squares optimization to solve the multi-well deconvolution problem in time domain. With this developed algorithm,

multi-rate superposition effect can also be solved at the same time.

The procedure is firstly to extract the interference effect from the total pressure response. Thereafter, the analysis of the remaining self pressure response can be made using the available traditional well testing methods.

The organization of this chapter is as follows. The analytical pressure diffusion theory and derivation for two-well reservoir system is presented to describe the different transient flowing conditions**.** A new two-well deconvolution algorithm is then developed to extract the interference and normalize the variable flowing rate. Then, deconvolution-based self pressure response analysis method and procedure are derived in detail. Finally numerical well testing synthetic studies are performed to demonstrate these procedures.

The results prove that the new method work well in homogeneous reservoirs with two wells flowing at single phase, multiple rates.

4.2 Analytical Theory of Two-Well Pressure Transient Analysis

4.2.1 Description of Two-Well Pressure Diffusion

In infinite reservoirs, if there are two wells, i.e. Well 1 and Well 2 in an infinite reservoir. Well 2 is some distance away from Well 1. Well 1 is a producing well and Well 2 is for observation as shown in **Figure 4.1**.

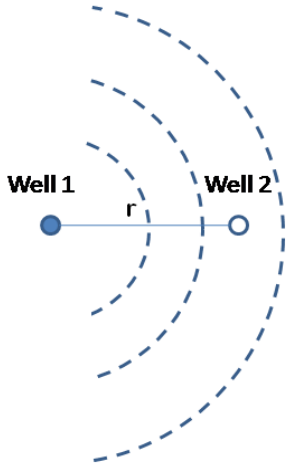

Figure 4. 1 Pressure distribution from Well 1 to Well 2 in an infinite reservoir

The pressure distribution of the two wells can be described as follows:

1. The interference has not reached the observation well. Well 1 show the infinite acting reservoir behavior, while well 2 is at initial pressure.

2. The interference has reached well 2. The behavior of Well1 and Well 2 shows the infinite reservoir response.

In closed reservoirs, if there are two wells, i.e. Well 1 and Well 2 in a closed reservoir. Well2 is some distance away from Well 1. Well 1 is a producing well and Well 2 is for observation as shown in **Figure 4.2**.

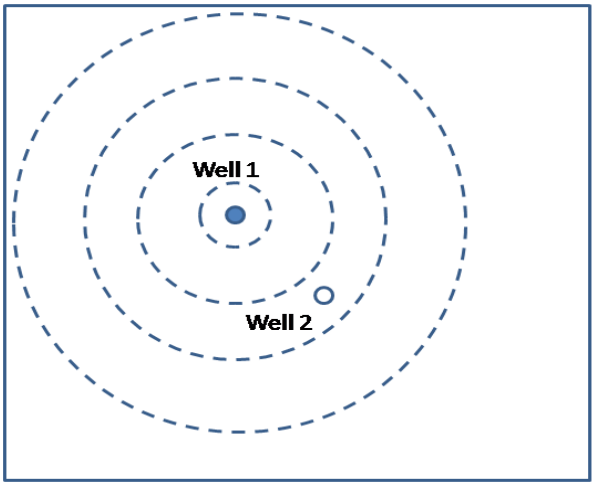

Figure 4. 2 Pressure distribution from Well 1 to Well 2 in a closed reservoir

The pressure distribution of the two wells can be described as follows:

1. The interference has not reached the observation well. Well 1 shows the infinite acting reservoir behavior, Well 2 is at initial pressure.

2. The interference has reached Well 2 but not the boundary. The behavior of Well1 and Well 2 shows the infinite reservoir response.

3. The boundary influence is seen on Well 1 but not Well 2, which is still in an infinite acting regime.

4. The influence of the closed boundary reaches the Well 2. Well 1 and Well 2 change to the pseudo-steady state flow behavior.

4.2.2 Theory and Derivation for Two-Well Pressure Diffusion

Transient Flow:

The pressure distribution in the infinite reservoir is a function of the time and the distance to the producing well (space). It can be expressed with the Exponential Integral function:

$$\Delta p(t,r) = -0.5\frac{141.2qB\mu}{kh}\mathrm{E}i\left[\frac{-\phi\mu C_t r^2}{0.001056kt}\right] \tag{4.1}$$

And this function can be simplified as a constant value multiplying an exponential integral

$$\Delta p = cons\tan t \times Ei(1/t) \tag{4.2}$$

The Primary Pressure Derivative (PPD) can be expressed as $PPD = d\Delta p / dt$ (4.3)

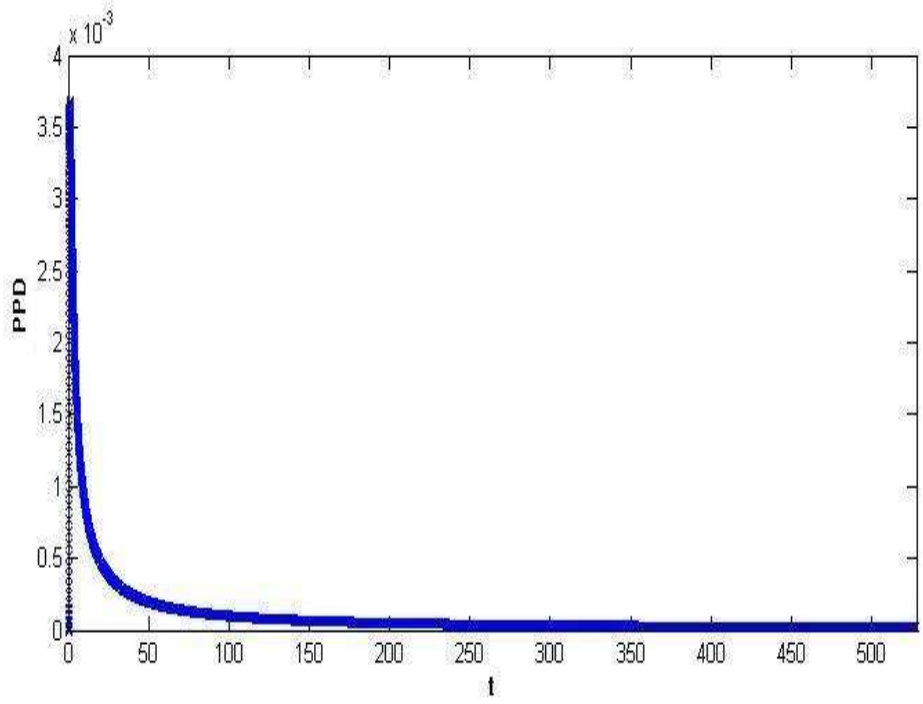

Figure 4. 3 *PPD* of the *Ei* function versus t on Cartesian plot

Figure 4.3 shows the profile of PPD of the exponential integral function above versus time on Cartesian plot. The slope of PPD increases with time at first and then followed by decreasing. **Figure 4.4** shows the profile of the PPD versus time on log-log plot, which has the characteristics of a "hump".

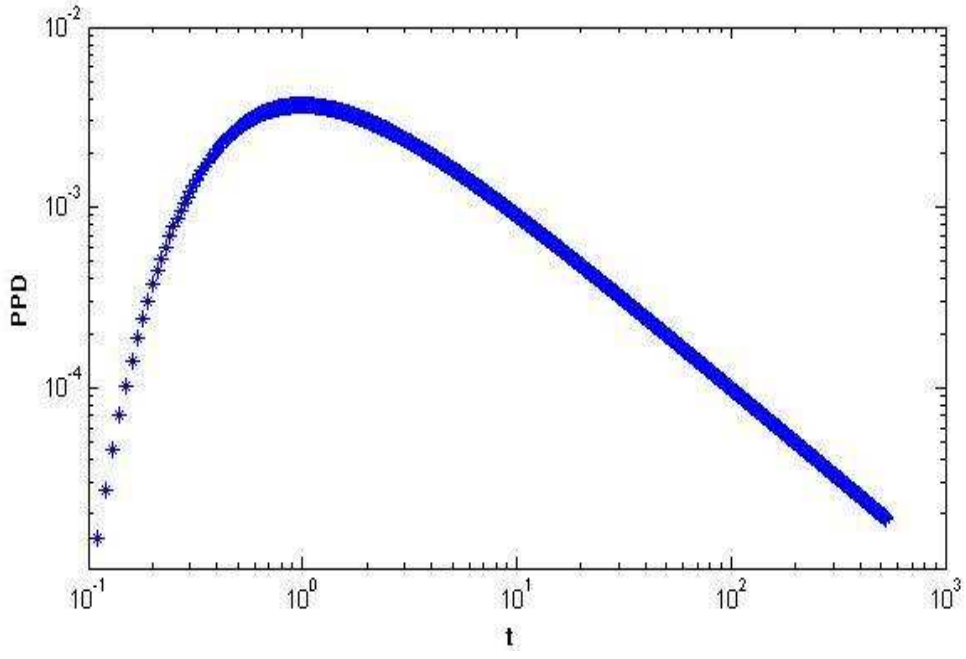

Figure 4. 4 *PPD* of the *Ei* function versus t on log-log plot

For small x value, $Ei(-x) = -\ln(\gamma x)$, the Exponential Integral can be approximated by a log function (with $\gamma = 1.78$, Euler's constant). Therefore:

$$\Delta p(t,r) = \frac{162.6qB\mu}{kh}\left[\log\frac{0.000264kt}{\phi\mu C_t r_w{}^2} + 0.809\right] \tag{4.4}$$

$$\Delta p = cons\tan t \times \log t + cons\tan t \tag{4.5}$$

The primary pressure derivative here can be written as

$$PPD' = d\Delta p / dt = cons\tan t / t \tag{4.6}$$

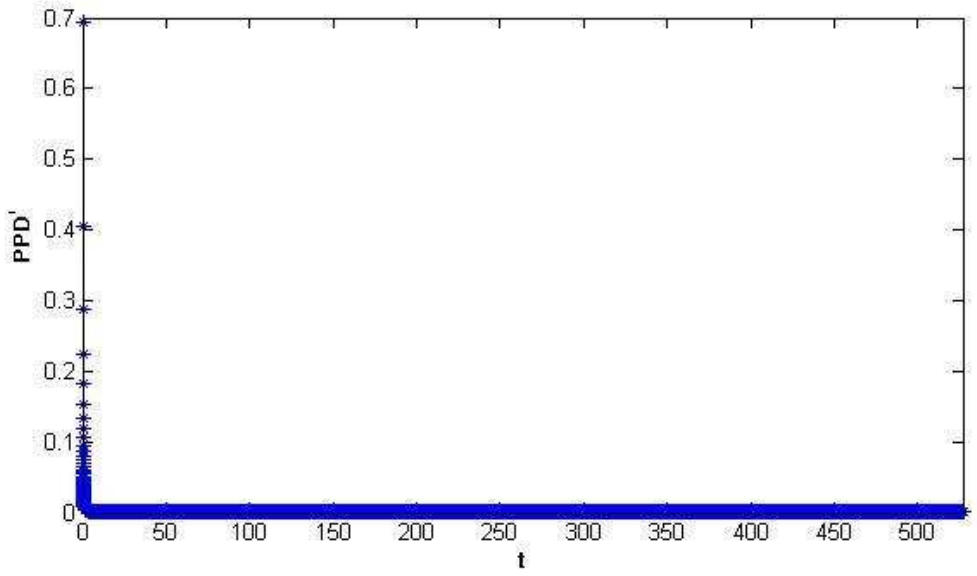

Figure 4. 5 PPD' of the log function versus t on Cartesian plot

Figure 4.5 shows the profile of PPD' of this log function versus time on Cartesian plot. The slope of this PPD monotonously decreases with time.

The logarithm of this PPD is obtained as $\log(PPD') = -\log t + cons\tan t$ (4.7)

So the slope of PPD versus time on log-log plot is -1, as shown in **Figure 4.6**.

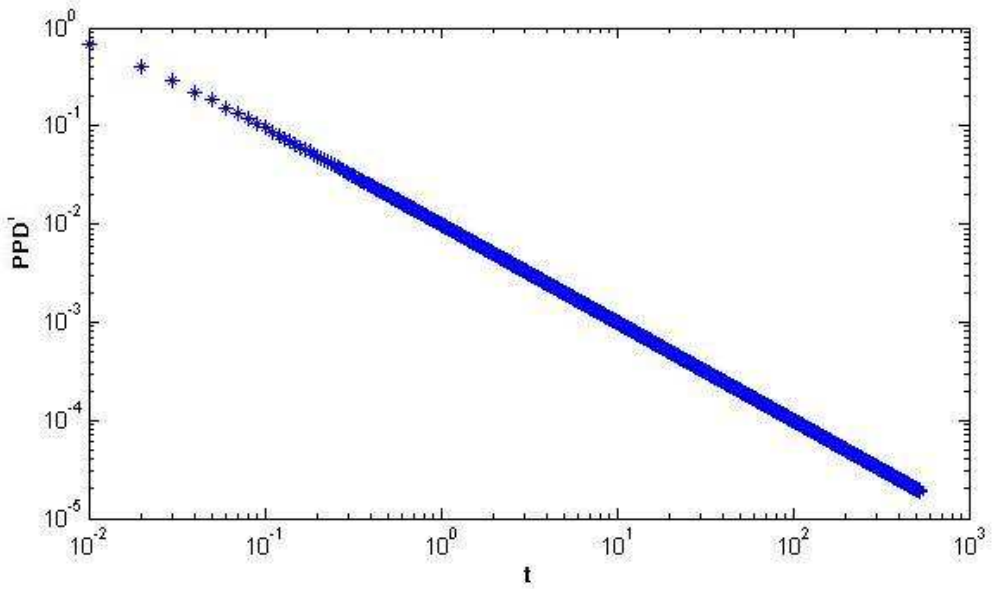

Figure 4. 6 PPD' of the log function versus t on log-log plot

In the above two cases, Ei function and log function represent interference pressure response and self pressure response, respectively. **Figure 4.4** represents the primary pressure derivative of interference pressure response, while **Figure 4.6** represents the primary pressure derivative of self pressure response.

The logarithmic derivative can be expressed as $d\Delta p / d\ln t = t \times d\Delta p / dt$ (4.8)

Figure 4.7 shows the comparison of the self pressure drop with its corresponding logarithmic derivative and primary derivative, while **Figure 4.8** shows the comparison of interference pressure drop with its corresponding logarithmic derivative and primary derivative.

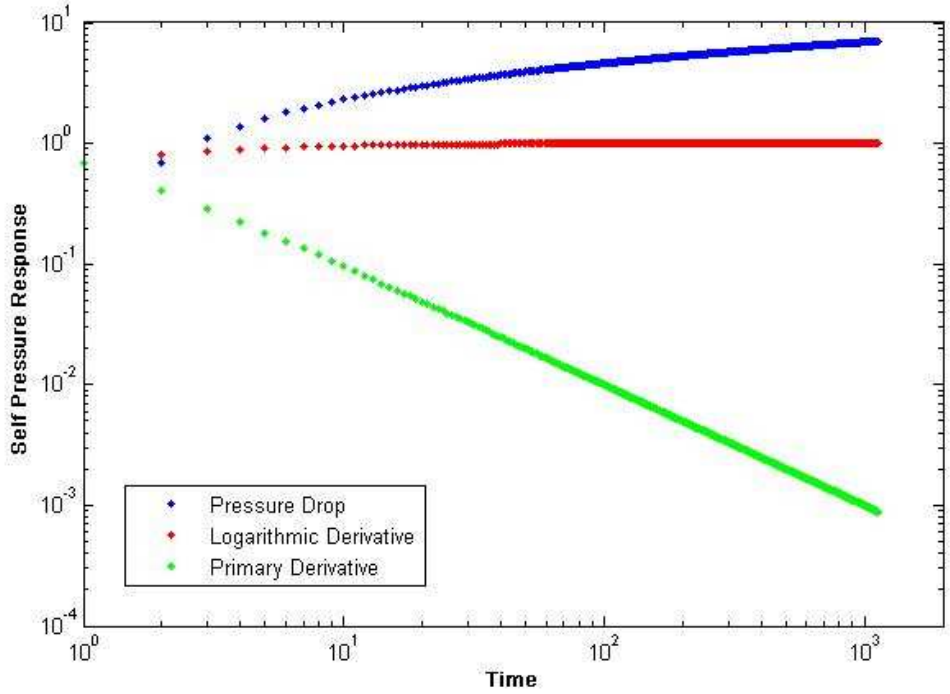

Figure 4. 7 Comparison of self pressure drop with its corresponding logarithmic derivative and primary derivative on log-log plot

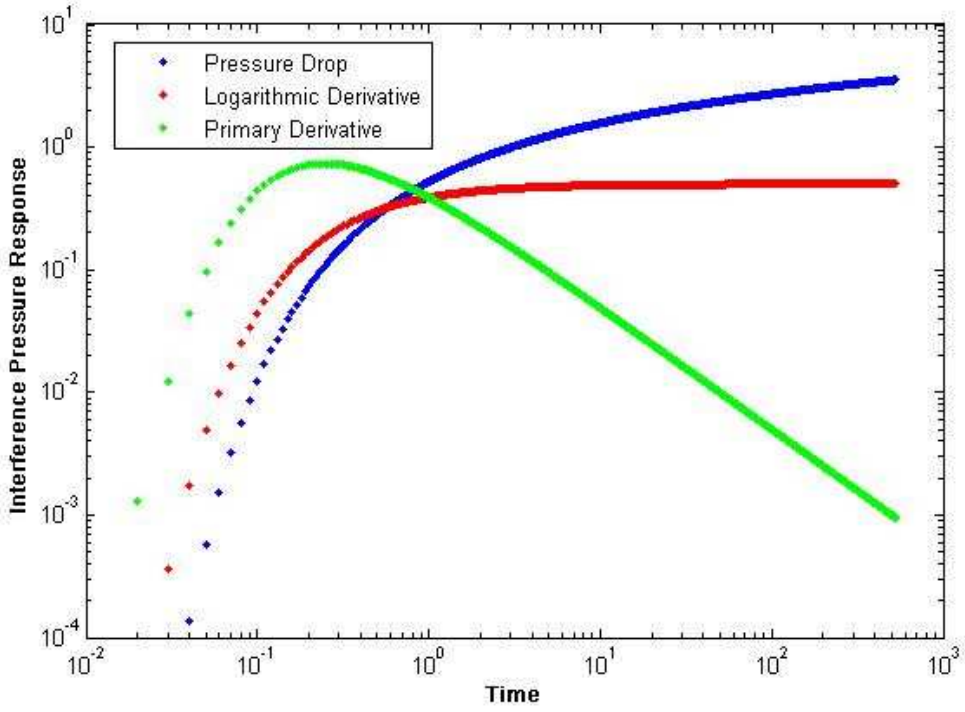

Figure 4. 8 Comparison of interference pressure drop with its corresponding logarithmic derivative and primary derivative on log-log plot

The two type curves above exhibit three important characteristics:

1. The two curves, pressure drop and its logarithmic derivative intersect each other. At the start of the response, the amplitude of the derivative curve is higher than the pressure drop, but later the two curves intersect and the derivative stabilizes on a constant value line while the pressure drop continues to increase.

2. The start of the semi-log straight line is later. The radial flow behavior is characterized by the derivative stabilization, which exhibits a zero slope for logarithmic derivative or a -1 slope for primary derivative.

3. For the primary derivative of the interference response curve, there is an obvious "hump". The point corresponding to the top of the "hump" represents the time delay of pressure diffusion from one well to the other. While for the self pressure response curve, there is no time delay period. It starts with a -1 slope on primary derivative curve.

Pseudo Steady State Flow (closed reservoir):

In closed reservoirs, when all boundaries have been reached, the flow regime changes to pseudo steady state. The shape of the pressure profile becomes linear with time, and it simply declines as the reservoir is being depleted. During the pseudo steady state flow regime, the bottom-hole flowing pressure is a linear function of the elapsed time.

$$\Delta p = 0.234\frac{qB}{\phi c_t hA}t + 162.6\frac{qB\mu}{kh}\left[\log\frac{A}{r_w{}^2} - \log(C_A) + 0.351 + 0.87S\right] \tag{4.9}$$

Primary Pressure Derivative:

$$d\Delta p/dt = \Delta p' = d(p_i - p_{wf})/dt = 0.234\frac{qB}{\phi c_t hA} \tag{4.10}$$

Logarithmic Derivative:

$$d\Delta p/d\ln t = t\Delta p' = t \times d\Delta p/dt = 0.234\frac{qB}{\phi c_t hA}t \tag{4.11}$$

So the primary derivative of the pressure response verse time on log-log plot will be a

zero slope line, while the corresponding logarithmic derivative on log-log scale should be a constant value.

4.3 Multi-Well Pressure-Rate Deconvolution

4.3.1 Multi-Well Pressure-Rate Deconvolution Theory

Mathematical Theory: Convolution and Deconvolution

Hypothesis: $h(t)$ is a linear response of a system, the output is $y(t)$ and input is $x(t)$.

So $y(t)$ can be written as a convolution integral as follows:

$$y(t) = \int_{-\infty}^{\infty} h(t-\tau)x(\tau)d\tau \tag{4.12}$$

With given output $y(t)$ and input $x(t)$ to recover the system response $h(t)$ is so-called Deconvolution.

Once the convolution integral is applied to single-well problem, it turns to be Duhamel principle:

$$\Delta p(t) = p_i - p_{wf}(t) = \int_0^t q(\tau)h(t-\tau)d\tau \tag{4.13}$$

Here $h(t)$ represents the system response function of the reservoir. It equals to primary derivative of unit-rate pressure drop of the well:

$$h(t) = dp_u(t)/dt \tag{4.14}$$

Assuming that there are n active wells in a reservoir and these wells are in good connectivity with each other. Once the convolution integral is applied to multi-well problem, the down-hole pressure of one well can be expressed as follows:

$$p_1(t) = p_i - \int_0^t q_1(t-\tau)\frac{dp_{u11}(\tau)}{dt}d\tau \qquad (n=1)$$

$$p_1(t) = p_i - \int_0^t q_1(t-\tau)\frac{dp_{u11}(\tau)}{dt}d\tau - \int_0^t q_2(t-\tau)\frac{dp_{u12}(\tau)}{dt}d\tau \qquad (n=2)$$

$$p_1(t) = p_i - \int_0^t q_1(t-\tau)\frac{dp_{u11}(\tau)}{dt}d\tau - \int_0^t q_2(t-\tau)\frac{dp_{u12}(\tau)}{dt}d\tau - \int_0^t q_3(t-\tau)\frac{dp_{u13}(\tau)}{dt}d\tau \qquad (n=3)$$

. .

. .

. .

$$p_1(t) = p_i - \int_0^t q_1(t-\tau)\frac{dp_{u11}(\tau)}{dt}d\tau - \int_0^t q_2(t-\tau)\frac{dp_{u12}(\tau)}{dt}d\tau - \int_0^t q_3(t-\tau)\frac{dp_{u13}(\tau)}{dt}d\tau - \ldots - \int_0^t q_n(t-\tau)\frac{dp_{u1n}(\tau)}{dt}d\tau \qquad (n=N)$$

(4.15)

When using $x = 1,2,\ldots,n$ to denote each of these wells. The total bottom-hole pressure drop of well x can be given by the function below:

$$p_x(t) = p_i - \int_0^t q_x(t-\tau)\frac{dp_{uxx}(\tau)}{dt}d\tau - \sum_{y=1}^{n}\int_0^t q_y(t-\tau)\frac{dp_{uxy}(\tau)}{dt}d\tau$$

$$(x \in n, y \in n, x \neq y) \qquad (4.16)$$

It means that the down-hole pressure drop measured in one well benefits not only from its self-production but also from the production of other active wells in the same reservoir. And the relationship follows superposition principle.

In the multi-well convolution function above, p_{uxx} represents the pressure response at the down-hole of well x due to the production itself, while p_{uxy} represents the interference response, namely the pressure response at the down-hole of well x due to

the unit-rate production of well y ($y \in n$). Obviously, the calculation of this multi-well deconvolution problem (when $n \geq 3$) will be a complicated work.

If $n = 2$, it becomes a two-well problem. And the down-hole pressure of each well can be expressed below:

$$p_1(t) = p_i - \int_0^t q_1(t-\tau)\frac{dp_{u11}(\tau)}{dt}d\tau - \int_0^t q_2(t-\tau)\frac{dp_{u12}(\tau)}{dt}d\tau \tag{4.17}$$

$$p_2(t) = p_i - \int_0^t q_2(t-\tau)\frac{dp_{u22}(\tau)}{dt}d\tau - \int_0^t q_1(t-\tau)\frac{dp_{u21}(\tau)}{dt}d\tau \tag{4.18}$$

In which, p_{u12} represents the interference pressure response from Well 2 to Well 1, p_{u11} represents the self pressure response of Well 1 and p_{u22} represents the self pressure response of Well 2.

In homogeneous reservoirs, p_{u11} equals to p_{u22}, assuming that p_{u12} equals to p_{21}, and we use h_{11} and h_{12} to replace the primary derivatives of p_{u11} and p_{u12}. So function (4.17) and (4.18) can be re-written as:

$$p_1(t) = p_i - \int_0^t q_1(t-\tau)h_{11}(\tau)d\tau - \int_0^t q_2(t-\tau)h_{12}(\tau)d\tau \tag{4.19}$$

$$p_2(t) = p_i - \int_0^t q_1(t-\tau)h_{12}(\tau)d\tau - \int_0^t q_2(t-\tau)h_{11}(\tau)d\tau \tag{4.20}$$

4.3.2 New Two-Well Pressure-Rate Deconvolution Algorithm

If there are two active wells in a reservoir system and the two wells are in good connection with each other. The convolution integral of each well based on superposition principle can be written as below:

$$p_1(t) = p_i - \int_0^t q_1(t-\tau)h_{11}(\tau)d\tau - \int_0^t q_2(t-\tau)h_{12}(\tau)d\tau \tag{4.21}$$

$$p_2(t) = p_i - \int_0^t q_1(t-\tau)h_{21}(\tau)d\tau - \int_0^t q_2(t-\tau)h_{22}(\tau)d\tau \tag{4.22}$$

Where, h_{11} and h_{22} are referred to the self impulse response of two wells. h_{12} and

h_{21} are the interference impulse response from one well to another, respectively.

In homogeneous reservoirs, the self impulse response of each well is equal (i.e. $h_{11} = h_{22}$). And it is assumed that the interference impulse response between two wells is equal (i.e. $h_{12} = h_{21}$). So equation (4.22) and equation (4.23) can be written as:

$$p_1(t) = p_i - \int_0^t q_1(t-\tau)h_{11}(\tau)d\tau - \int_0^t q_2(t-\tau)h_{12}(\tau)d\tau \quad (4.23)$$

$$p_2(t) = p_i - \int_0^t q_1(t-\tau)h_{12}(\tau)d\tau - \int_0^t q_2(t-\tau)h_{11}(\tau)d\tau \quad (4.24)$$

Where, the impulse response is the primary derivative of the unit-rate drawdown response, which can be expressed as follows:

$$h_{11}(t) = \frac{dp_{u11}(t)}{dt}; \quad (4.25)$$

$$h_{12}(t) = \frac{dp_{u12}(t)}{dt}; \quad (4.26)$$

Where, p_{u11} is the pressure response at Well 1 due to the unit-rate production of Well 1, while p_{u12} is the pressure response at Well 1 due to the unit-rate production of Well 2.

The target of this two-well deconvolution is to calculate the algorithm impulse response functions (i.e. h_{11} and h_{12}). And the detailed algorithm is as follows:

Taking subtraction of equation (4.24) and equation (4.25) gives

$$p_2(t) - p_1(t) = \int_0^t [q_1(t-\tau) - q_2(t-\tau)][h_{11}(\tau) - h_{12}(\tau)]d\tau \quad (4.27)$$

With given that

$$\Delta p(t) = p_2(t) - p_1(t), \quad (4.28)$$

$$\Delta q(t) = q_1(t) - q_2(t), \quad (4.29)$$

and

$$\Delta h(t) = h_{11}(t) - h_{12}(t) \quad (4.30)$$

So equation (4.28) can be written as:

$$\Delta p(t) = \int_0^t \Delta q(t-\tau)\Delta h(\tau)d\tau\,, \tag{4.31}$$

Which can be written as a discrete format as below

$$conv(\Delta q, \Delta h) = \sum_{k=0}^{N-1} \Delta q(k)\Delta h(n-k) \tag{4.32}$$

Where, n denotes the time point and the total number is N, namely, $\Delta q(n), n = 1,2,..., N$ and $\Delta h(n), n = 1,2,..., N$.

The objective function of the non-linear least-squares is given by

$$F(x) = \min_x \frac{1}{2}\left\| conv(\Delta q, \Delta h) - \Delta p \right\|_2^2 = \frac{1}{2}\sum_{i=1}^{N} (conv(\Delta q, \Delta h_i) - \Delta p_i)^2 \tag{4.33}$$

Where, Δp_i is the calculated pressure at time point i in equation (4.28), while Δh_i is the proposed solution of this objective function at the time point i (there are totally N time points). Through the nonlinear optimization to ensure that the calculated Δp match the convolution component $conv(\Delta q, \Delta h)$ in equation (4.32) in order to give a best fit value of Δh.

Replacing h_{12} with Δh, so equation (4.23) can be written as:

$$p_0 - p_1(t) + \int_0^t q_2(t-\tau)\Delta h(\tau)d\tau = \int_0^t [q_1(t-\tau) + q_2(t-\tau)]h_{11}(\tau)d\tau \tag{4.34}$$

With given that

$$\Psi p(t) = p_i - p_1(t) + \int_0^t q_2(t-\tau)\Delta h(\tau)d\tau \tag{4.35}$$

and

$$\Psi q(t) = q_1(t) + q_2(t) \tag{4.36}$$

So equation (4.34) can be written as:

$$\Psi p(t) = \int_0^t \Psi q(t-\tau)h_{11}(\tau)d\tau\,, \tag{4.37}$$

Which can be written as a discrete format as below

$$conv(\Psi q, h_{11}) = \sum_{k=0}^{n-1} \Psi q(k)h_{11}(n-k) \tag{4.38}$$

Where $\Psi q(n), n = 1,2,..., N$; and $h_{11}(n), n = 1,2,..., N$.

The final objective function of the non-linear least-squares is given by

$$F(X) = \min_X \frac{1}{2} \left\| conv(\Psi q, h_{11}) - \Psi p \right\|_2^2 = \frac{1}{2} \sum_{i=1}^{N} (conv(\Psi q, h_{11i}) - \Psi p_i)^2 \quad (4.39)$$

Where, Ψp_i is the calculated pressure at time point i in equation (4.35), while h_{11_i} is the proposed solution of this final objective function at the time point i (there are totally N time points). Through the nonlinear optimization to ensure that the calculated Ψp match the convolution component $conv(\Psi q, h_{11})$ in equation (4.38) to give a best fit value of h_{11} .

Then, the system response function $h_{12}(t)$ can be obtained by a subtraction as below

$$h_{12}(1) = h_{11}(1) - \Delta h(1) \quad (n = 1) \quad (4.40)$$

and

$$h_{12}(n) = h_{11}(n) - \Delta h(n) \ (n = 2,3,..., N) \quad (4.41)$$

Using nonlinear least-squares method to solve the two-well deconvolution problem has been introduced by Levitan, M. M. (2006[67]). However, all stated above is from the new developed nonlinear least-squares deconvolution algorithm, which is different from that from Levitan due to the deconvolution products. After twice recursive convolution procedures and twice non-linear optimization procedures, the new nonlinear least-squares deconvolution algorithm can give the primary pressure derivatives of both self pressure response and interference pressure response, i.e. h_{11} and h_{12} .

4.4 Deconvolution-based Self Pressure Analysis

4.4.1 Analytical Solutions of Deconvolotion-based Self Pressure Response

In a closed reservoir with single phase fluid, where Well 1 produces and Well 2 is shut-in to get interference, several flow regimes will be encountered for each well.(Storage is not taken into account in this study.)

For the producing Well 1, two flow regimes can be encountered, namely: 1st flow state (radial flow) and 2nd flow state (pseudo-steady). The pressure distribution function and its derivation in each flow regime are shown below:

1st Flow State (Radial Flow):

The pressure distribution in the infinite reservoir is a function of the time and the distance to the producing well. It can be expressed with the exponential integral function:

$$\Delta p(t,r) = 0.5\frac{141.2qB\mu}{kh}\mathrm{E}i\left[\frac{\phi\mu C_t r^2}{0.001056kt}\right] \tag{4.42}$$

The pressure distribution of Well 1 can be written as follows:

$$\Delta p_{11}(t) = \frac{141.2qB\mu}{kh}\left\{-\frac{1}{2}\mathrm{E}i\left[\frac{-\phi\mu C_t r_w^{\ 2}}{0.001056kt)}\right]\right\} \quad (r = r_w) \tag{4.43}$$

Here, r_w is a very small value. For small x, $Ei(-x) = -\ln(\gamma x)$, the exponential integral can be approximated by a log(with $\gamma = 1.78$, Euler's constant):

$$\Delta p_{11}(t) = \frac{162.6qB\mu}{kh}\left[\log\frac{0.000264kt}{\phi\mu C_t r_w^{\ 2}} + 0.809\right] \tag{4.44}$$

$$\Delta p_{11} = cons\tan t \times \log t + cons\tan t \tag{4.45}$$

$$PPD_{11} = d\Delta p / dt = cons\tan t / t \tag{4.46}$$

$$\log(PPD_{11}) = -\log t + cons\tan t \tag{4.47}$$

So in this state, the slope of *PPD* versus time on log-log plot is -1, shown in **Figure 4.9**.

2nd Flow State (Pseudo-steady):

In closed reservoirs, when all boundaries have been reached, the flow regime changes to pseudo steady state. When all boundaries have been reached, the shape of the pressure profile becomes constant with time, and it simply drops as the reservoir is being depleted. During the pseudo steady state regime, the bottom-hole flowing pressure is a linear function of the elapsed time as below:

$$\Delta p_{11}(t) = 0.234\frac{qB}{\phi c_t hA}t + 162.6\frac{qB\mu}{kh}\left[\log\frac{A}{r_w{}^2} - \log(C_A) + 0.351 + 0.87S\right] \quad (4.48)$$

$$\Delta p_{11} = cons\tan t \times t + cons\tan t \quad (4.49)$$

$$PPD_{11} = d\Delta p / dt = cons\tan t \quad (4.50)$$

$$\log(PPD_{11}) = cons\tan t \quad (4.51)$$

So in this state, the slope of *PPD* versus time on log-log plot is zero, shown in **Figure 4.9**.

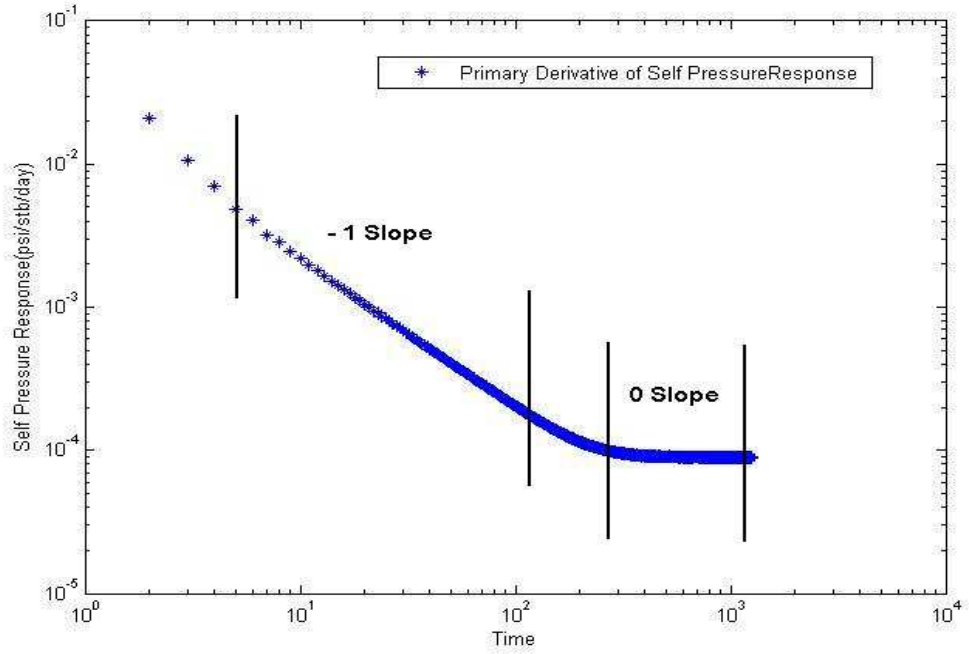

Figure 4. 9 Primary derivative of self pressure response on log-log plot

For the observation Well 2, three response regimes can be encountered, namely: 1st response state (transient hump), 2nd response state (radial flow) and 3rd response state (pseudo-steady). The pressure distribution function and its derivation in each flow regime are shown below:

1st Response State:

The pressure distribution in the infinite reservoir is a function of the time and the distance to the producing well. It can be expressed with the exponential integral function:

$$\Delta p(t,r) = 0.5\frac{141.2qB\mu}{kh}\mathrm{Ei}\left[\frac{\phi\mu C_t r^2}{0.001056kt}\right] \tag{4.52}$$

The interference distribution recorded in Well 2 can be written as follows:

$$\Delta p_{12} = 0.5\frac{141.2qB\mu}{kh}\mathrm{Ei}\left[\frac{\phi\mu C_t L^2}{0.001056kt}\right](r = L) \tag{4.53}$$

$$\Delta p_{12} = cons\tan t \times Ei(1/t) \tag{4.54}$$

$$PPD_{12} = d\Delta p_{12}/dt = Ei(1/t)/t \tag{4.55}$$

So in this state, the profile of *PPD* versus time on log-log plot, as shown in **Figure 4.10** increases with time at first and then begins to decrease. The whole period is neither monotonic nor static, which looks like a "Hump".

2nd Response State (Radial Flow):

For small x, $Ei(-x) = -\ln(\gamma x)$, the exponential integral can be approximated by a log(with $\gamma = 1.78$, Euler's constant). So when the pressure interference reached Well 2, the down-hole pressure drop of Well 2 can be written as below:

$$\Delta p_{12} = \frac{162.6qB\mu}{kh}\left[\log\frac{0.000264kt}{\phi\mu C_t r_w^{\ 2}} + 0.809\right] \tag{4.56}$$

$$\Delta p_{12} = cons\tan t \times \log t + cons\tan t \tag{4.57}$$

$$PPD_{12} = d\Delta p_{12}/dt = cons\tan t/t \tag{4.58}$$

$$\log(PPD_{12}) = -\log t + cons\tan t \tag{4.59}$$

So in this state, the slope of *PPD* versus time on log-log plot is -1, as shown in **Figure 4.10**.

3rd Response State (Pseudo-steady):

During the pseudo steady state regime, the bottom-hole pressure drop is a linear function of the elapsed time as below:

$$\Delta p_{12} = 0.234\frac{qB}{\phi c_t hA}t + 162.6\frac{qB\mu}{kh}\left[\log\frac{A}{r_w^{\ 2}} - \log(C_A) + 0.351 + 0.87S\right] \tag{4.60}$$

$$\Delta p_{12} = cons\tan t \times t + cons\tan t \tag{4.61}$$

$$PPD_{12} = d\Delta p / dt = cons\tan t \tag{4.62}$$

$$\log(PPD_{12}) = cons\tan t \tag{4.63}$$

So in this state, the slope of *PPD* versus time on log-log plot is zero, as shown in **Figure 4.10**.

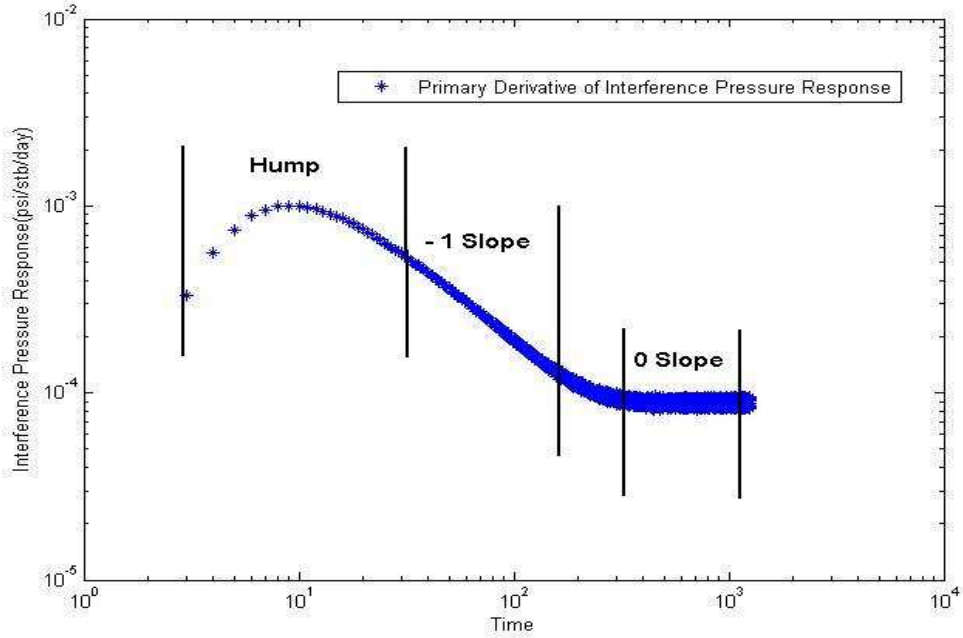

Figure 4. 10 Primary derivative of interference pressure response on log-log plot

4.4.2 Deconvolution Products and Corresponding Physical Expressions

Our developed two-well deconvolution algorithm is based on homogeneous reservoirs. And the deconvolution products are h_{11} and h_{12}. Here is a set of deconvolution results from a homogeneous closed reservoir with two active wells. The deconvolution products are obtained and their profiles are shown below.

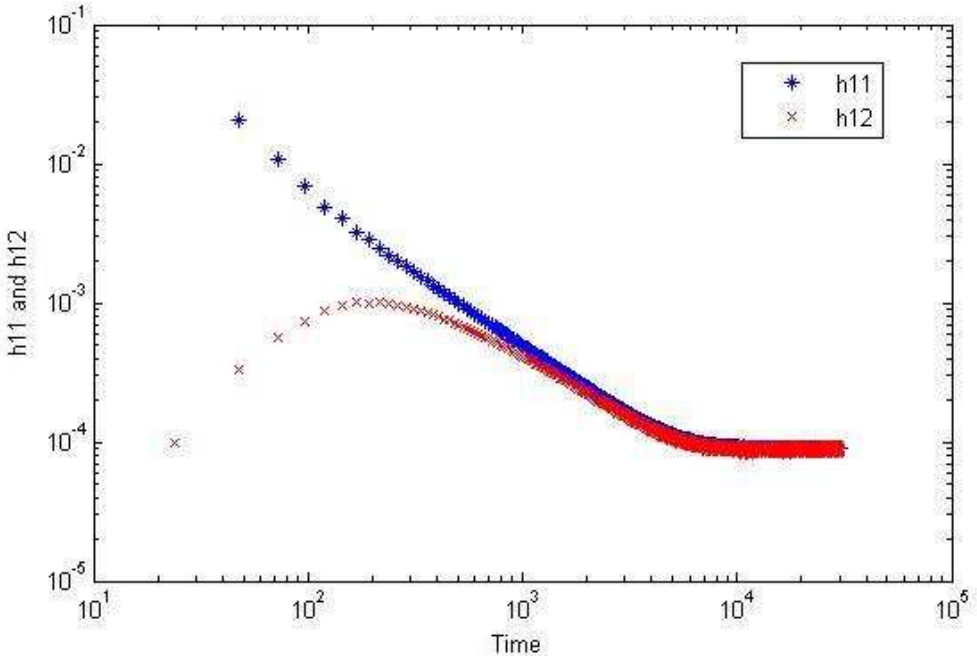

Figure 4. 11 Deconvolution products (h_{11} and h_{12}) on log-log plot

In **Figure 4.11**, h_{11} shows a -1 slope curve followed by a zero slope line. h_{12} shows a "hump" followed by a -1 slope curve and then a zero slope line. The zero-slope lines from h_{11} and h_{12} will overlap at last.

Generally, h_{11} shows two flow periods: -1 slope period and 0 slope period, While h_{12} shows three flow periods: hump period, -1 slope period and 0 slope period. All these profiles look consistent with those from analytical solutions discussed above.

That is because h_{11} is the primary derivative of p_{u11}, while p_{u11} is the unit-rate Δp_{11}. So the profile of h_{11} is consistent with interference pressure derivative PPD_{12}. While, h_{12} is the primary derivative of p_{u12}, while p_{u12} is the unit-rate Δp_{11}.So the profile of h_{12} is consistent with interference pressure derivative PPD_{12}.

So the two deconvolutin products are consistent with the self response and interference response from theoretical analytical solutions. This agreement validates our developed

two-well deconvolution algorithm.

4.5 Synthetic Case Study

Synthetic Model

For the multi-well interference study, a two-well synthetic model, shown in **Figure 4.12**, is produced. This reservoir model is a fully penetrating model with two vertical wells, located in a uniform formation, bounded on all sides by no-flow boundaries. The distance between two wells is 2121ft. Other parameters are listed in **Table 4.1**.

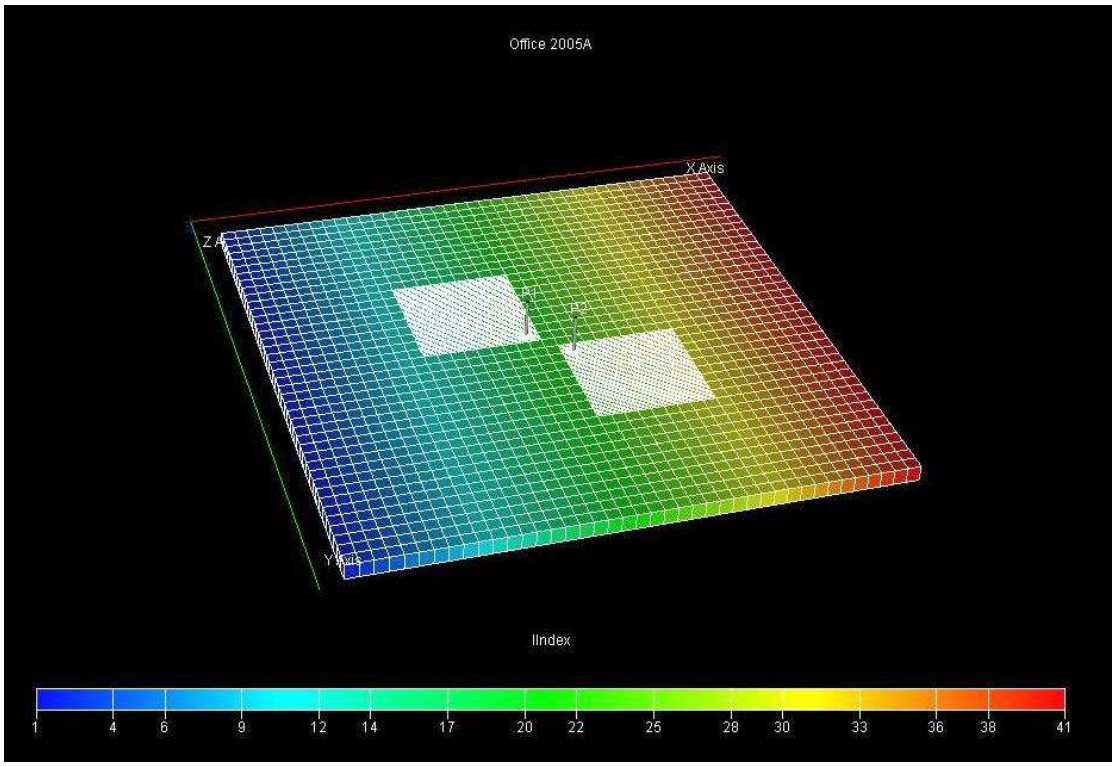

Figure 4. 12 Reservoir Model

Initial pressure, p_i	= 3014.2psia
Porosity, ϕ	= 0.3
Permeability, k	= 50 mD
Thickness, H	= 100 ft
Oil formation volume factor, B_o	= 1.2rb/STB
Viscosity, μ	= 1.2 cp
Total compressibility, c_t	$=6e^{-6}$ 1/psia
Well radius, r_w	= 0.3 ft
Reservoir length, R	= 20500 ft
Reservoir width, R	= 20500 ft

Table 4. 1 Reservoir and fluid properties for the developed model

Simulation Case

With the model, one synthetic case is produced, in which only Well 1 produce with a constant flow rate. During the flowing period of Well 1, Well 2 keeps shut-in for observation of the interference from Well 1 to Well 2. The total time period is about 5000 hours. **Figure 4.13** shows the simulated pressure and flowing rate history of two wells.

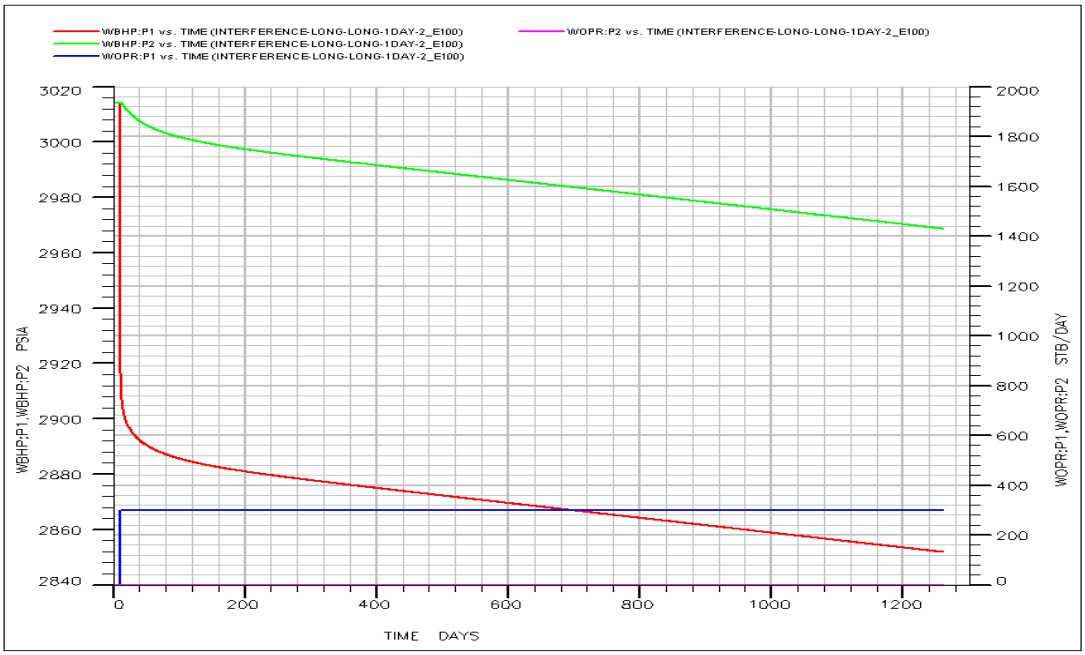

Figure 4. 13 Pressure and flow rate history for simulation case, in which Well 1 produces at a constant rate and Well 2 keeps shut in. The total time period is about 5000 hours.

The pressure drop at the bottom-hole of Well 2 reflects the interference effect due to the production of Well 1. The interference response under the unit-rate condition can be calculated with the following function:

$p_{u12} = (p_i - p_{wf\,2}) / q_1$ where, q_1 is a constant value(300 stb/day);

And the primary pressure derivative of the interference response can be calculated as below: $h_{12} = dp_{u12} / dt$

In this case, p_i is a given model parameter. $p_{wf\,2}$ and q_1 are from simulation results. So the simulated interference pressure response p_{u12} and its primary derivative h_{12} can be obtained.

Deconvolution Case

This synthetic case is designed for extracting the interference pressure response p_{u12} and its primary derivative h_{12} from self pressure response of the well with multi-well deconvolution. In this case, Well 1 and Well 2 are put on production at the

same time, including three short buildups and three drawdown periods for Well 1, and two short buildups and three drawdown periods for Well 2. **Figure 4.14** shows the simulated production history of two wells.

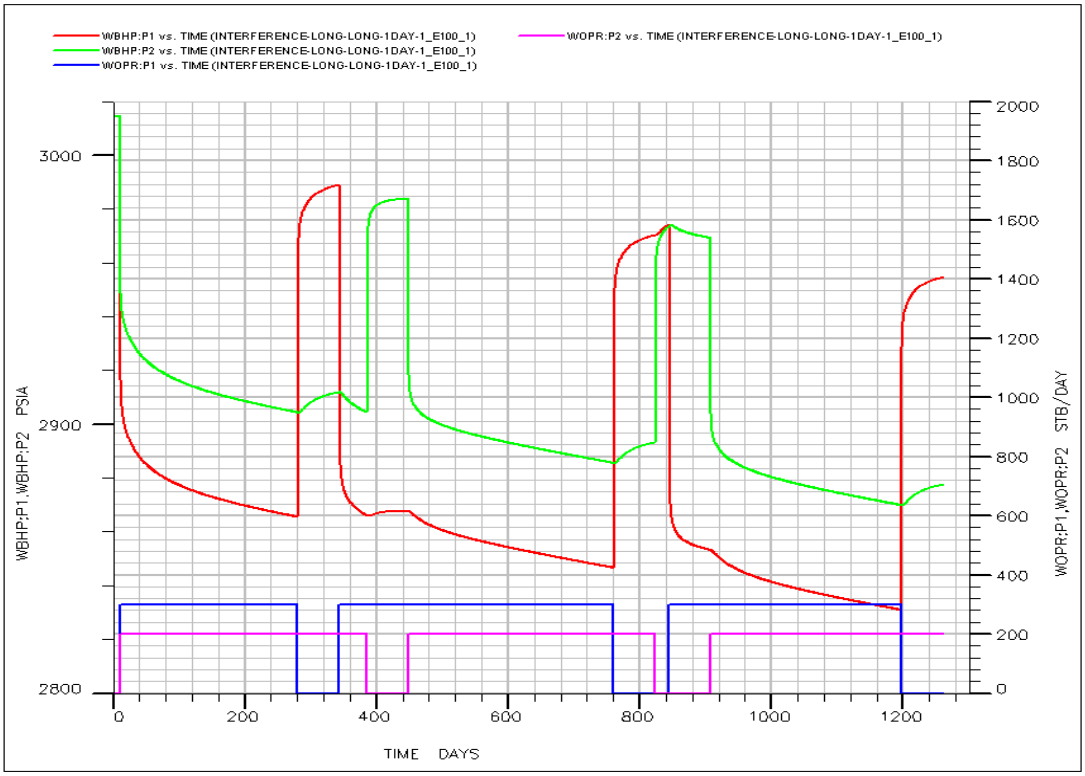

Figure 4. 14 Simulated pressure and flow rate history for two-well transient pressure analysis, in which Well 1 and Well 2 are put on production at the same time, including three short buildups and three drawdown periods for Well 1, and two short buildups and three drawdown periods for Well 2.

Multi-well deconvolution algorithm is implemented on the pressure and rate data of two wells. The interference pressure response p_{u12} from Well 1 to Well 2 is extracted with our developed algorithm. Besides, the self pressure response p_{u11} of Well 1 can be obtained simultaneously.

Analytical Case

For comparison, analytical solution of the interference pressure response p_{u12} and its primary derivative h_{12} is obtained in this case. Given that, the flowing rate of Well 1 is

300 stb/day, so the down-hole pressure drop of Well 2 due to the production of Well 1 can be written as:

$$\Delta p_2 = p_i - \frac{141.2 q_1 B\mu}{kh}\left\{-\frac{1}{2}\mathrm{E}i\left[\frac{-\phi\mu c_t r^2}{0.001056\,kt)}\right]\right\}$$

The interference response under the unit-rate production can be calculated with the following function: $p_{u12} = \Delta p_2 / q_1$ (q_1 here is a constant value);

And the primary pressure derivative of the interference response can be calculated as below: $h_{12} = dp_{u12} / dt$

In this case, all the reservoir parameters are same with the model input. So the analytical interference pressure response p_{u12} and its primary derivative h_{12} can be obtained.

Model Validation

Primary pressure derivatives of the interference response h_{12} from model simulation and analytical solution are put on linear plot and log-log plot together. The good match, shown in **Figure 4.15** and **Figure 4.16**, validates the synthetic model.

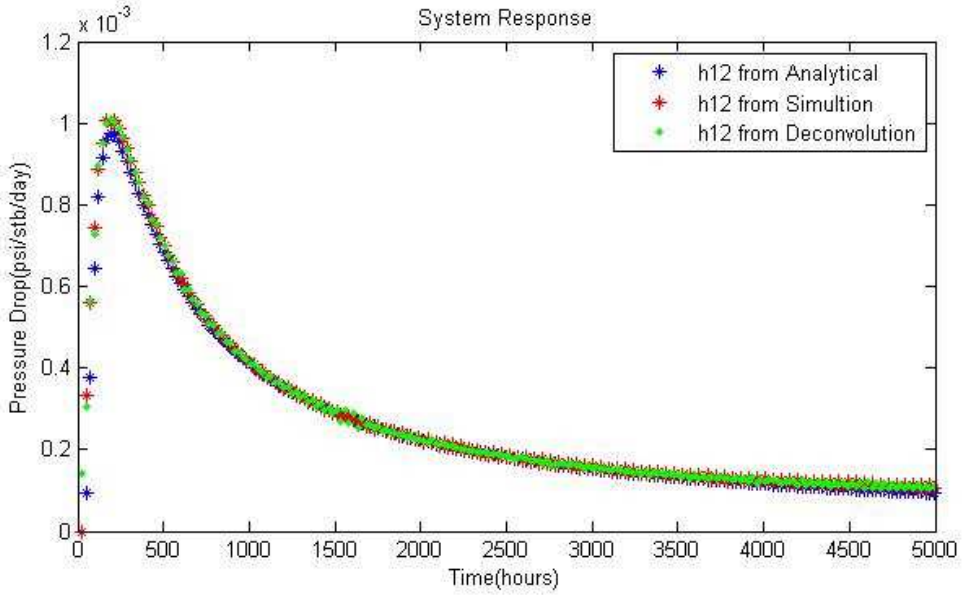

Figure 4. 15 Comparison of primary pressure derivative from analytical solution, simulation and deconvolution results on linear plot. The good match validates the synthetic model and proves that the developed multi-well deconvolution algorithm

works well.

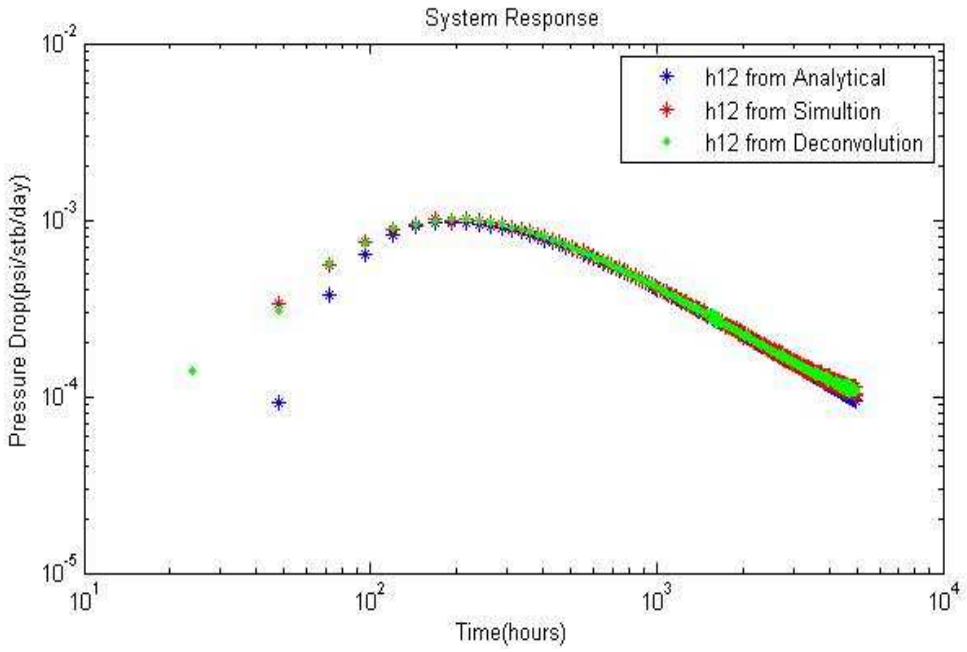

Figure 4. 16 Comparison of primary pressure derivative from analytical solution, simulation and deconvolution results on log-log plot. The good match validates the synthetic model and proves that the developed multi-well deconvolution algorithm works well.

Algorithm Validation

Primary pressure derivative of the interference response h_{12} from deconvolution is compared with those from model simulation and analytical solution on linear plot and log-log plot together. The good match, shown in **Figure 4.15** and **Figure 4.16**, proves that the developed multi-well deconvolution algorithm works well on transient pressure data with interference.

Multi-well Transient Pressure Analysis

This synthetic case is designed for self response and interference response analysis after multi-well deconvolution processing. In this case, Well 1 and Well 1 are put on production at the same time, including three short buildups and three drawdown periods for Well 1, and two short buildups and three drawdown periods for Well 2. **Figure 4.17** shows the simulated production history of two wells.

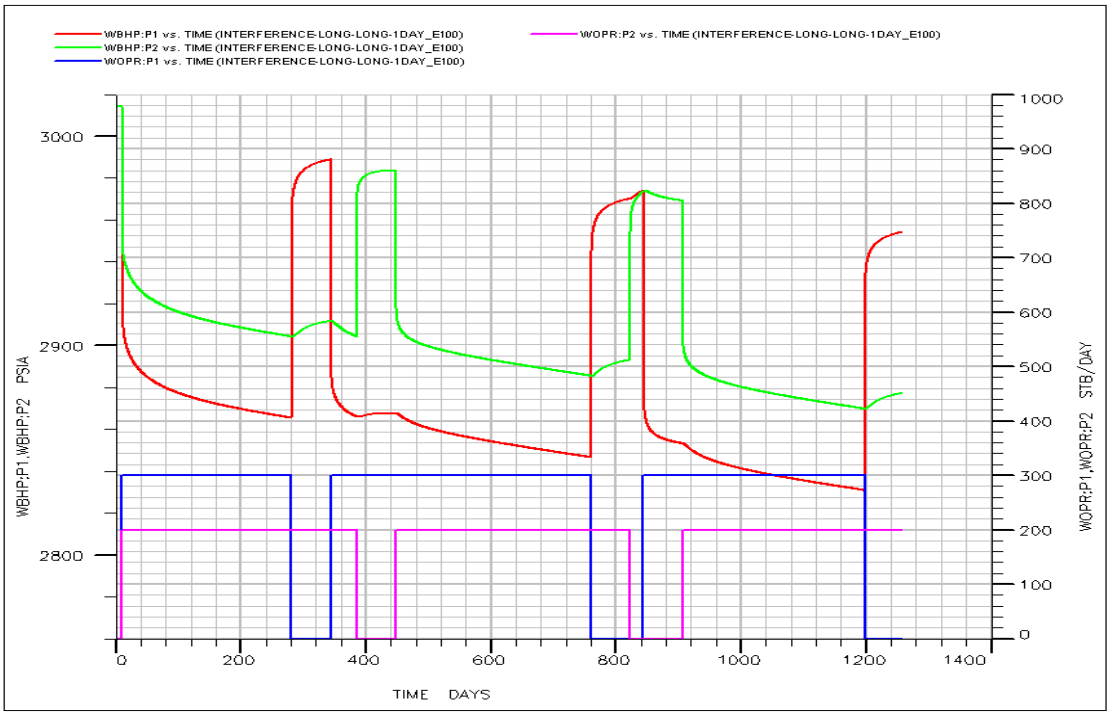

Figure 4. 17 Simulated pressure and flow rate history for two-well transient pressure analysis, in which Well 1 and Well 2 are put on production at the same time, including three short buildups and three drawdown periods for Well 1, and two short buildups and three drawdown periods for Well 2.

Multi-well deconvolution algorithm is implemented on the pressure and rate data of two wells. The interference pressure response p_{u12} from Well 1 to Well 2 is extracted from the self pressure response p_{u11} of Well 1.

Their primary derivatives (h_{11} and h_{12}) are put on linear plot for comparison, shown in **Figure 4.18**. On log-log scale, they are shown in **Figure 4.19**. The good match of those derivatives from simulation results and deconvolution results proves that the developed multi-well deconvolution algorithm works well on this long-term transient pressure data with interference.

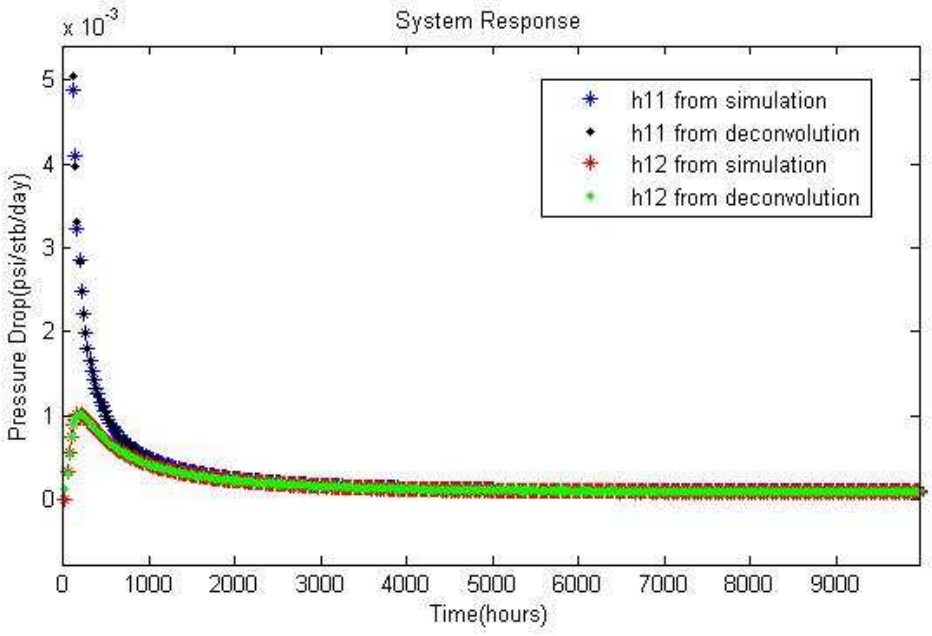

Figure 4. 18 shows the comparison of primary pressure derivative from self response and interference response on linear plot.

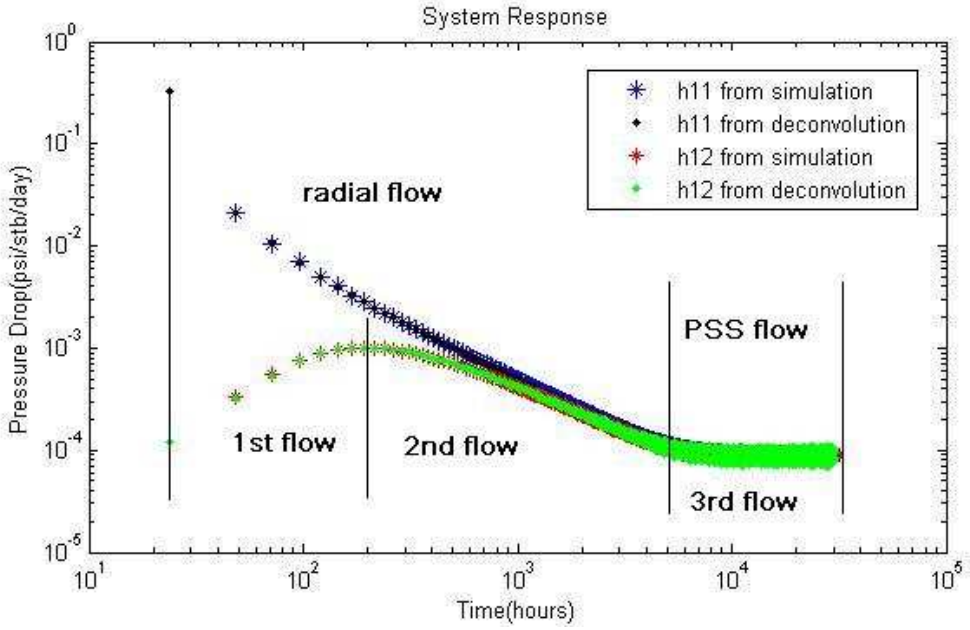

Figure 4. 19 shows the comparison of primary pressure derivative from self response and interference response on log-log plot.

In **Figure 4.19**, it can clearly define the flow regimes of the pressure distribution. For the pressure of Well 1 itself, there are two flow regimes, namely radial flow and pseudo-steady state, shown minus one slope and zero slope on log-log scale. For interference pressure from Well 1 to Well 2, there are three flow regimes. The first

regime, shown inconstant slope on log-log scale, reflects the interference distribution period between two wells. Once the interference from Well 1 reaches Well 2, it turns to distribute as a radial flow behavior until it reaches the reservoir boundary.

Pressure Transient Analysis

After the multi-well deconvolution processing, the extracted interference pressure response (p_{u12}) and the remaining self pressure response (p_{u11}) can be used for transient analysis.

For self pressure response analysis, its logarithmic derivative ($dp/d\ln t$) and primary derivative (dp/dt) are put on log-log scale together, as shown in **Figure 4.20**. Obviously, the flow regimes defined by two derivatives agree with each other with corresponding constant slopes.

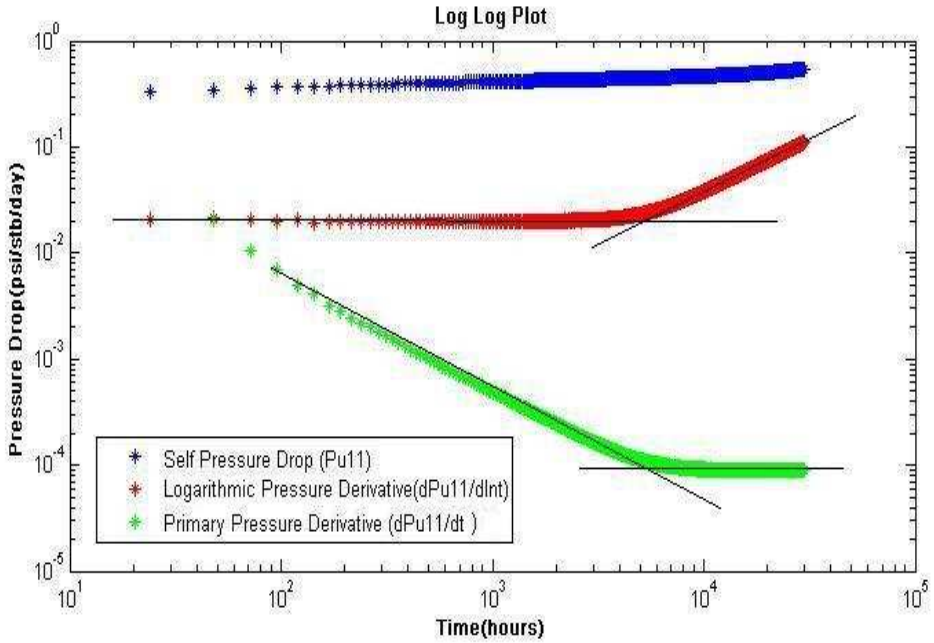

Figure 4. 20 shows the comparison of primary derivative and logarithmic derivative of self pressure response on log-log plot. The flow regimes defined by two derivatives agree with each other with corresponding constant slopes.

For interference response analysis, its logarithmic derivative and primary derivative are put on log-log scale together as well, as shown in **Figure 4.21**. Zero slope period of semi-log derivative agrees with the minus one slope of primary derivative on log-log, both reflecting radial flow behavior. Unit slope period of semi-log derivative agrees with the zero slope of primary derivative on log-log, both reflecting pseudo-steady state behavior.

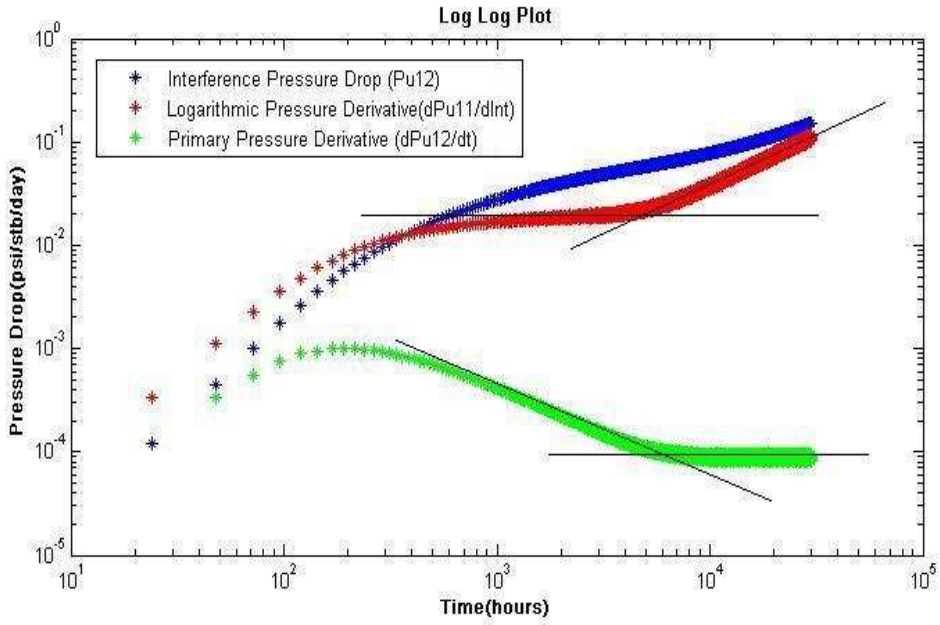

Figure 4. 21 shows the comparison of primary derivative and logarithmic derivative of interference pressure response on log-log plot. Zero slope period of semi-log derivative agrees with the minus one slope of primary derivative, both reflecting radial flow behavior. Unit slope period of semi-log derivative agrees with the zero slope of primary derivative, both reflecting pseudo-steady state behavior.

All the agreements above prove that the primary pressure derivatives from multi-well deconvolution can be used for diagnostic and analysis. The flow regimes diagnosed by primary pressure derivative are consistent with those from traditional logarithmic derivative diagnostic.

4. 6 Chapter Conclusions

According to this study, several conclusions can be derived, as follows:

A new multi-well deconvolution algorithm has been developed for analyzing long-term PDG transient pressure with interference and multi-rate superposition effects. With added nonlinear least-squares optimization, this algorithm can solve noisy data problem and improve the precision in calculation.

The self pressure response (p_{u11}) of a well in multi-well reservoir systems was extracted using the developed deconvolution algorithm.

Theoretical derivation of the two-well deconvolution products has been finished, which proved that the primary pressure derivative (h_{11}) as one of the two-well deconvolution products, consistent with that from traditional logarithmic derivative method, which can be used for reservoir diagnostics.

Analytical and simulation cases have been produced for comparison. The results from analytical, simulation and deconvolution solutions agree with each other, which prove that the developed two-well deconvolution algorithm works well.

Deconvolution-based self pressure analysis theory is proposed in detail. This deconvolution-based analysis procedure has improved the traditional well testing methods.

Numerical well testing synthetic studies have been performed to demonstrate the procedure of this deconvolution-based self pressure response analysis. The results proved that this deconvolution-based analysis method worked well in homogeneous reservoirs with two well flowing at single phase, multiple rates. And this new method improved the traditional pressure transient analysis technique.

Chapter 5
Deconvolution-based Interference Analysis of Multi-Well PDG Transient Pressure Data

5.1 Introduction

Numerous field well tests show that in a multi-well reservoir system the bottom hole pressure measured in one well is affected by the production from other operating wells. This phenomenon is so-called “well interference” effect.

Traditional method for analyzing inter-well interference effect is from multiple well tests (Kama, M. M., 1983[82]). The pressure response is measured in an observation well some distance away from the active well, which may be a producing or an injection well. Through the analysis of the observation well, average reservoir properties in the area separating the wells are determined. However, a drawback of multiple well tests is that it requires one or more potentially productive wells to be shut-in.

Since inter-well interference effect is very common in PDG pressure data in which no shut-in test condition is satisfied. It requires a new approach to pre-process this interfered PDG data by extracting the interference effect from the total pressure response. Thereafter, the extracted interference can be analyzed with the multiple well

test theory.

This chapter presents a newly developed multi-well deconvolution algorithm for processing and analyzing long-term transient pressure with interference from other wells in the same reservoir. This developed algorithm is based on linear recursion with added non-linear least squares optimization procedure.

In this chapter, the analytical inter-well interference theory and derivation for two-well reservoir system is presented. A new two-well deconvolution algorithm is then developed to extract the interference and normalize the variable flowing rate. Then, deconvolution-based interference analysis method and procedure are derived in detail. Finally numerical well testing synthetic studies are performed to demonstrate these procedures.

The results prove that the new method work well in homogeneous reservoirs with two wells flowing at single phase, multiple rates.

5.2 Analytical Theory of Interference Pressure Analysis

In processing multi-well interference effect, traditional methodology is from multiple well tests. Multiple-well tests are used to establish communication between wells and determine the inter-well reservoir properties. With multiple well tests, the pressure response is measured in an observation well some distance away from the active well, which may be a producing or injection well. Through the analysis of the observation well, average reservoir properties in the area separating the wells are determined. When several observation wells are located in different directions, any permeability anisotropy can also be evaluated.

In the case of homogeneous reservoir, the log-log pressure type-curve of **Figure 5.1**, presented by Theis in 1935, is used. This type-curve, called the exponential integral solution, express the dimensionless pressure p_D versus the dimensionless

time-distance group t_D / r_D^2 on a unique response curve. In the case of heterogeneous systems, the log-log analysis of the response provides a diagnosis of the reservoir behavior, and defines the choice of the appropriate interference model.

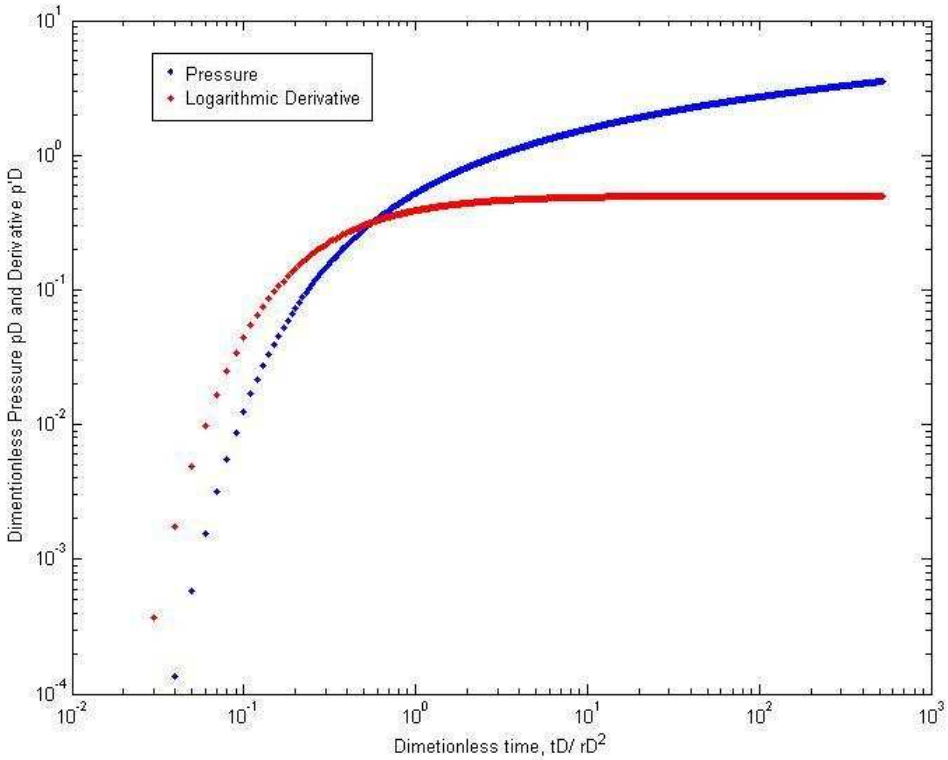

Figure 5. 1 The Theis solution (exponential integral). Log-log scales, pressure and derivative versus t_D / r_D^2

The exponential integral solution of the line-source flow model for pressure, p, at any location, r, and time, t, can be written as:

$$p = p_i - \frac{141.2qB\mu}{kh}\left\{-\frac{1}{2}\mathrm{E}i\left[\frac{-\phi\mu c_t r^2}{(4)(0.0002637kt)}\right]\right\} \tag{5.1}$$

Use of the following definitions of dimensionless variables,

$$t_D = \frac{0.0002637kt}{\phi\mu c_t r_w^2} \tag{5.2}$$

$$p_D = \frac{kh(p_i - p)}{141.2qB\mu} \tag{5.3}$$

And

$$r_{Dw} = \frac{r}{r_w} \tag{5.4}$$

Enables the exponential integral solution to be written as

$$p_D = -\frac{1}{2}\mathrm{E}i\left(-\frac{r_{Dw}^2}{4t_D}\right) \tag{5.5}$$

Once the match point is obtained, the reservoir properties can be determined from the following equations.

$$\frac{kh}{\mu} = 141.2qB\frac{(p_D)_M}{\Delta p_M} \tag{5.6}$$

And

$$\phi c_t h = \frac{0.0002637}{r_{bw}^2}\frac{kh}{\mu}\frac{t_M}{(t_D/r_{Dw}^2)_M} \tag{5.7}$$

The interference type curve of **Figure 5.1**exhibits two characteristics:

1, The two curves intersect. At the start of the response, the amplitude of the derivative curve is higher than the pressure change but, later the two curves intersect and the derivative stabilizes on the 0.5 line while the pressure continues to increase.

2, The start of the semi-log straight line is late. The semi-log radial flow behavior, characterized by the derivative stabilization, starts at approximately $t_D / r_D^2 = 5$.

Figure 5.2 compares on a linear scale the response of a producing well to the response of an observation well some distance away. The flow sequence is a 200hours drawdown followed by a 300 hours build-up period. The two wells have the same wellbore storage and skin damage. And the reservoir is homogeneous and infinite.

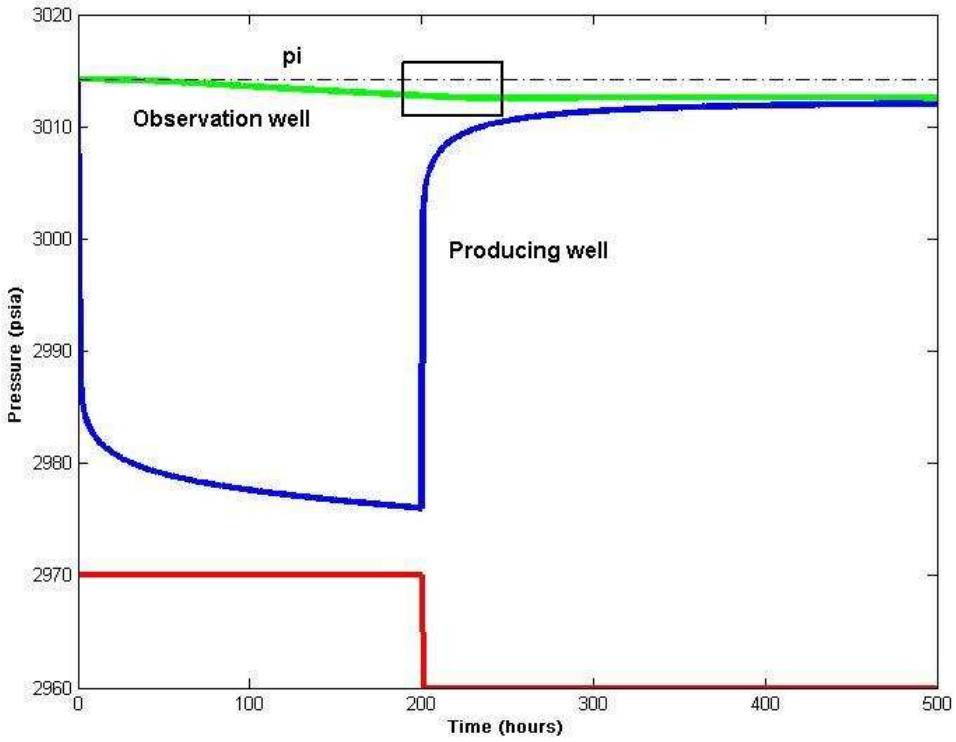

Figure 5. 2 Response of a producing and an observation wells. Linear scale, p versus t

At the start of the flow period, the pressure drop is instantaneous at the active well but at the observation well, the drawdown response is only established very slowly. At the end of 200hrs of production, the pressure change is 40psi at the producer and less than 5 psi at the observation well. At shut-in time, the pressure at the active well increases immediately but not at the observation well. As shown on the expanded scale of **Figure 5.3**, the pressure continues to fall for several hours, until the influence of the shut-in has travelled the distance separating the two wells. Then it starts to turn upwards.

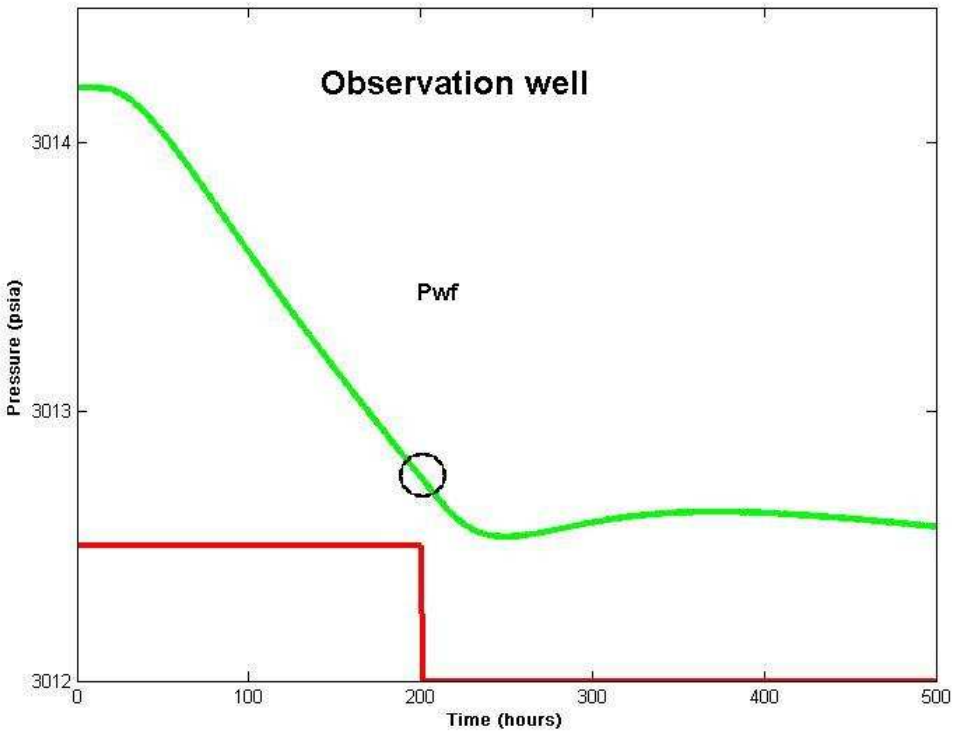

Figure 5. 3 The observation well pressure is presented on enlarged scale at time of shut-in.

Figure 5.4 is the log-log pressure and derivative plot of the two build-up responses. For each well, the pressure difference $\Delta p = p_{ws} - p_{wf}$ is calculated with respect to the flowing pressure p_{wf} defined at the time of shut-in, $\Delta t = 200hr$.

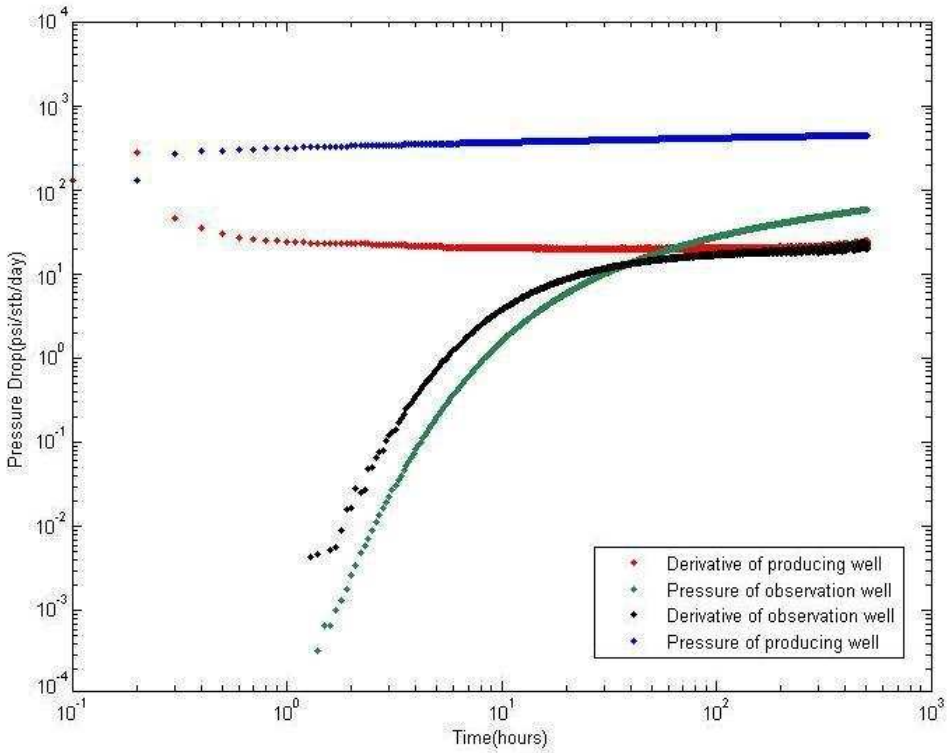

Figure 5. 4 Build-up response of the producing and observation wells on log-log plot

It illustrates that the analysis of interference pressure response is more difficult than for producing wells:

1, at the observation well, the build-up response starts to be identified after 1 or 2 hours, the intersection of the pressure and derivative curves is seen at $\Delta t = 30$ hours when $\Delta p = 10$ psi and the 300 hour long build-up period covers less than three log-cycles on the log-log plot. The semi-log approximation is reached only at the end of the 300 hours shut-in.

2, in the producer, the build-up response curve extends over more than four log-cycles, and the semi-log approximation is reached after 5 hours of shut-in.

5.3 New Mathematical Algorithm for Two-Well Deconvolution

A new algorithm is developed to solve the two-well deconvolution problem. The developed deconvolution algorithm can yield primary derivatives of both self pressure response and interference pressure response at the same time. And the procedure of the developed algorithm is shown step by step as follows:

Step 1: Input data ($p_1\ p_2\ q_1\ q_2$)

Step 2:1st Subtraction (calculate Δp , Δq)

$$\Delta p(t) = p_2(t) - p_1(t) \tag{5.8}$$

$$\Delta q(t) = q_1(t) - q_2(t) \tag{5.9}$$

Step 3:1st Convolution (calculate $conv.(\Delta q, \Delta h)$)

$$conv(\Delta q, \Delta h) = \Delta q(1)\Delta h(n) + \Delta q(2)\Delta h(n-1) + ... + \Delta q(n)\Delta h(1) \tag{5.10}$$

Step 4:1st Deconvolution (calculate Δh)

$$F(x) = \min_x \frac{1}{2}\left\| conv(\Delta q, \Delta h) - \Delta p \right\|_2^2 = \frac{1}{2}\sum_{i=1}^{n} (conv(\Delta q, \Delta h_i) - \Delta p_i)^2 \tag{5.11}$$

Step 5: 2nd Convolution (calculate $conv.(q_{2,} \Delta h)$)

$$conv.(q_2, \Delta h) = q_2(1)\Delta h(n) + q_2(2)\Delta h(n-1) + ... + q_2(n)\Delta h(1) \tag{5.12}$$

Step 6: 2nd Subtraction (calculate Ψp , Ψq)

$$\Psi p(t) = p_i - p_1(t) + conv.(q_2, \Delta h) \tag{5.13}$$

$$\Psi q(t) = q_1(t) + q_2(t) \tag{5.14}$$

Step 7: 3rd Convolution (calculate $conv.(\Psi q, h_{11})$)

$$conv.(\Psi q, h_{11}) = \Psi q(1)h_{11}(n) + \Psi q(2)h_{11}(n-1) + ... + \Psi q(n)h_{11}(1) \tag{5.15}$$

Step 8: 2nd Deconvolution (calculate h_{11})

$$F(X) = \min_X \frac{1}{2}\left\| conv(\Psi q, h_{11}) - \Psi p \right\|_2^2 = \frac{1}{2}\sum_{i=1}^{n} (conv(\Psi q, h_{11i}) - \Psi p_i)^2 \tag{5.16}$$

Step 9: 3rd Subtraction (calculate h_{12})

$$h_{12}(1) = h_{11}(1) - \Delta h(1) \quad (n = 1)$$

$$h_{12}(n) = h_{11}(n) - \Delta h(n) \ (n = 2,3,..., N) \tag{5.17}$$

Once the primary pressure derivatives (h_{11} and h_{12}) are calculated, the unit-rate pressure response of both self and interference (p_{u11} and p_{u12}) can be calculated with the

cumulative trapezoidal integral as below:

$$p_{u11}(1) = h_{11}(1) \quad (n = 1)$$

$$p_{u11}(n) = \frac{h_{11}(n) + h_{11}(n-1)}{2} + \frac{h_{11}(n-1) + h_{11}(n-2)}{2} + \ldots + \frac{h_{11}(2) + h_{11}(1)}{2} + h_{11}(1)$$

$$(n = 2,3,\ldots,N) \tag{5.18}$$

And

$$p_{u12}(1) = h_{12}(1) \quad (n = 1)$$

$$p_{u12}(n) = \frac{h_{12}(n) + h_{12}(n-1)}{2} + \frac{h_{12}(n-1) + h_{12}(n-2)}{2} + \ldots + \frac{h_{12}(2) + h_{12}(1)}{2} + h_{12}(1)$$

$$(n = 2,3,\ldots,N) \tag{5.19}$$

5.4 Deconvolution-based Interference Pressure Analysis

5.4.1 Analytical Solutions of Deconvolution-based Interference Response

The radius of investigation

The pressure distribution in the reservoir is a function of the time and the distance to the producing well. It can be expressed with the exponential integral function:

$$\Delta p(\Delta t, r) = -0.5 \frac{141.2qB\mu}{kh} \mathrm{E}i\left(-\frac{\phi\mu c_t r^2}{0.001056k\Delta t}\right) \tag{5.20}$$

For small x, $\mathrm{E}i(-x) = -\ln(\gamma x)$, the exponential integral can be approximated by a log(with $\gamma = 1.78$,Euler's constant).

$$\Delta p(\Delta t, r) = \frac{162.6qB\mu}{kh}\left(\log\frac{0.000264k\Delta t}{\phi\mu c_t r^2} + 0.809\right) \tag{5.21}$$

(for the semi-log straight line Equation 5.21 the radial distance is set at $r = r_w$)

The radius of investigation r_i tentatively describes the distance that the pressure transient has moved into the formation.

$$r_i = 0.029\sqrt{k\Delta t / \phi\mu c_t} \tag{5.22}$$

For interference response analysis:

$$k_{\text{int }er} = \frac{\phi\mu c_t L^2}{(0.029)^2 \Delta t_{delay}} \tag{5.23}$$

In which, $k_{\text{int }er}$ is the inter-well average permeability, while L is the inter-well distance. Δt_{delay} is the delay time, which represents the time of pressure transfer from one well to another.

Radial flow regime

During the radial flow regime in reservoirs with homogeneous behavior, the pressure changes with the logarithm of the elapsed time from when the well is opened. A plot of the bottom home pressure versus the logarithm of time follows a straight line when all wellbore storage traditional effects are finished. The slope m of semi-log straight line is used to estimate the reservoir permeability thickness product kh, and the skin coefficient S is evaluated from the location of the straight line along the y-axis.

$$p_i - p_{wf} = \frac{162.6qB\mu}{kh}\left(\log\Delta t + \log\frac{k}{\phi\mu c_t {r_w}^2} - 3.23 + 0.87S\right) \tag{5.24}$$

Traditionally, the semi-log straight-line location is characterized by the straight-line pressure at 1 hour (Δp_{1hr})

$$kh = 162.6\frac{Bq\mu}{m} \tag{5.25}$$

$$S = 1.151\left(\frac{\Delta p_{1hr}}{m} - \log\frac{k}{\phi\mu c_t r_w^2} + 3.23\right) \tag{5.26}$$

For interference analysis:

$$p_{u12} = \frac{162.6B\mu}{k_{\text{int }er}h}\left(\log\Delta t + \log\frac{k_{\text{int }er}}{\phi\mu c_t L^2} - 3.23 + 0.87S\right) \tag{5.27}$$

$$k_{\text{int }er} = 162.6\frac{B\mu}{m_{\text{int }er}h} \tag{5.28}$$

Where, $m_{\text{int }er}$ is the slope of semi-log straight line of p_{u12}.

Pseudo steady state regime (closed reservoir)

During drawdown, the Pseudo Steady State regime is analyzed with a plot of the pressure versus elapsed time Δt on a linear scale. At late time, the straight line of slope m^* is used to estimate the reservoir pore volume ϕhA.

$$\Delta p = 0.234\frac{qB}{\phi c_t hA}\Delta t + 162.6\frac{qB\mu}{kh}\left(\log\frac{A}{r_w^2} - \log(C_A) + 0.351 + 0.87S\right) \tag{5.29}$$

$$\phi hA = 0.234\frac{qB}{c_t m^*} \tag{5.30}$$

When kh and S are known from semi-log analysis of the early time response, the shape factor C_A can be estimated from time zero intercept Δp^*_{int} of the pseudo-steady state straight line with Equation 5.29 as follows:

$$C_A = 2.2458\ e^{2.303\left[\left(p_i - p^*_{\text{int}}\right)/m - \log\left(A/r_w^2\right) - 0.87\ S\right]} \tag{5.31}$$

or

$$C_A = 5.456\ e^{-\left[2.303\ \left(p_i - p^*_{\text{int}}\right)/m\right]} \tag{5.32}$$

For interference analysis:

$$p_{u12} = 0.234\frac{B}{\phi c_t hA}\Delta t + 162.6\frac{B\mu}{k_{\text{int}er}h}\left(\log\frac{A}{L^2} - \log(C_A) + 0.351 + 0.87S\right) \tag{5.33}$$

$$\phi hA = 0.234\frac{qB}{c_t m^*_{\text{int}er}} \tag{5.34}$$

Where, m^* is the straight line of slope of p_{u12}.

5.4.2 Deconvolution Products and Corresponding Physical Expressions

The developed two-well deconvolution algorithm is based on homogeneous reservoirs. The deconvolution products are h_{11} and h_{12}.

h_{11} is the primary derivative of p_{u11}, while p_{u11} is the pressure response at Well 1 due to the unit-rate production of Well 1 itself; It is the remains of the pressure drop at Well 1 through two-well deconvolution processing. h_{12} is the primary derivative of p_{u12}, while p_{u12} is the pressure response at Well 1 due to the unit-rate production of Well 2.

It is the extraction from the pressure drop at Well 1 through two-well deconvolution processing.

Infinite reservoirs

h_{11} shows a -1 slope curve, while h_{12} shows a "hump" followed by a -1 slope curve. The -1 slope curves from h_{11} and h_{12} will overlap at last. The time at the top of the hump reflects the inter-well distance (L). Namely, the bigger the top time is the longer the inter-well distance will be. It is shown in **Figure 5.5**, where -1 slope represents the radial flow regime.

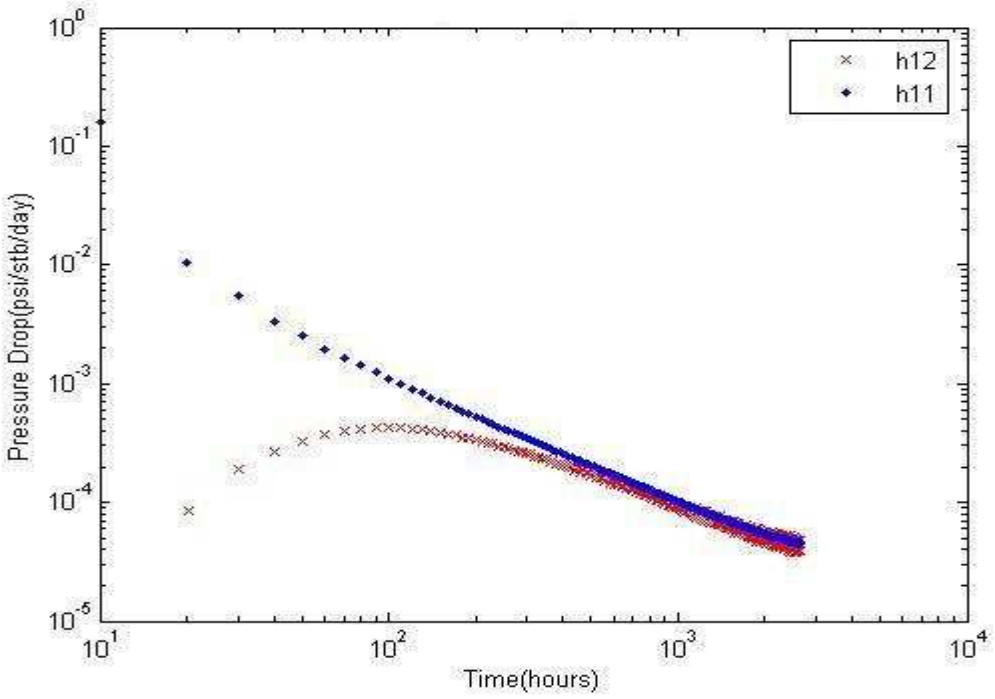

Figure 5. 5 h_{11} and h_{12} in infinite reservoir conditions, on log-log plot

Closed boundary reservoirs

h_{11} shows a -1 slope curve followed by a zero slope line, while h_{12} shows a "hump" followed by a -1 slope curve and then a zero slope line. Generally, h_{11} reflects the real flow behavior of Well 1 itself, while h_{12} reflects the distribution of the interference from Well 2. It is shown in **Figure 5.6**, where -1 slope represents the radial flow regime, while the zero-slope period represents the pseudo steady state regime due to

the outer boundary.

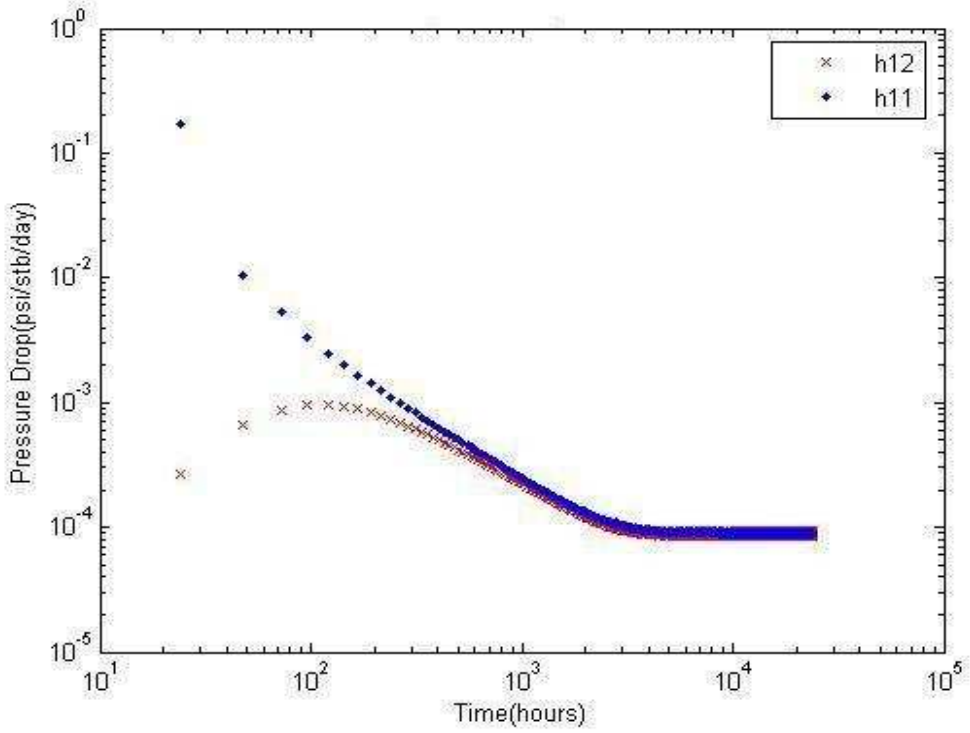

Figure 5. 6 h_{11} and h_{12} in closed boundary reservoir conditions, on log-log plot

If there are two vertical wells in a closed boundary reservoir, changing the values of inter-well permeability and inter-well distance respectively to three values, namely small, medium and large, will generate different h_{12} curves, as shown in **Figure 5.7** and **Figure 5.8**.

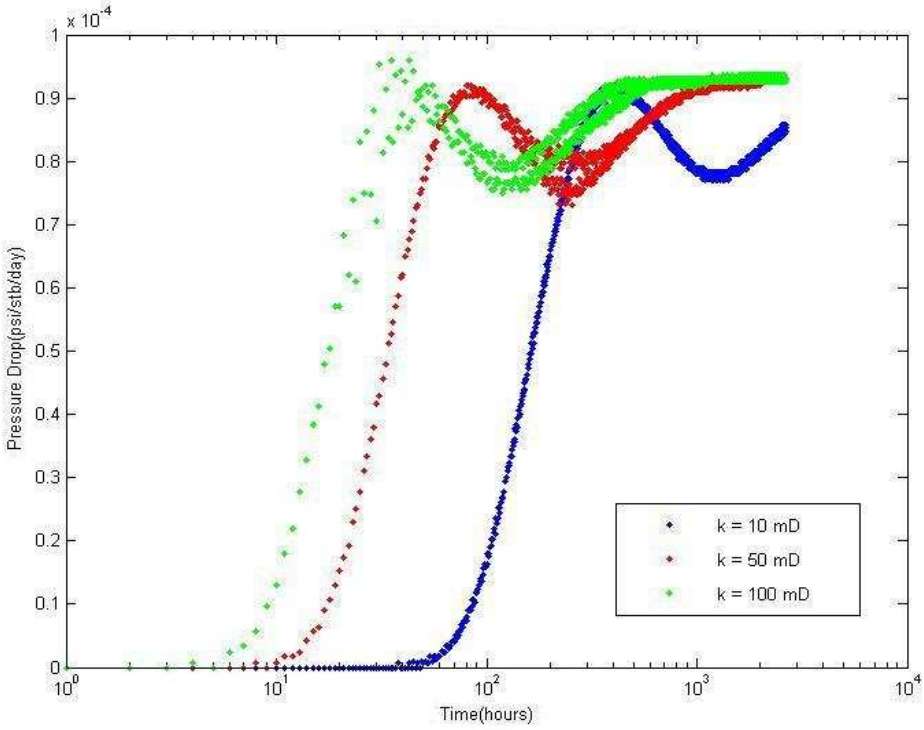

Figure 5. 7 h_{12} with different inter-well permeability on semi-log plot

For the case with different inter-well permeability, as stated above, the extracted interference pressure has three time regions. The first region is from the beginning of Well 1 to the interference (from Well 2 to Well 1) turning up on this extracted interference pressure. While the second region starts from the interference happening to the interference becoming stable. And the third region is the last one, which represents the interference from one well to another becoming stable and keep at a constant value.

The shape of h_{12} from two-well deconvolution stays the same except laterally shifting. The different time delay corresponding to the top of the "hump" represents different inter-well permeability, which describes the progress of pressure diffusion from one well to the other.

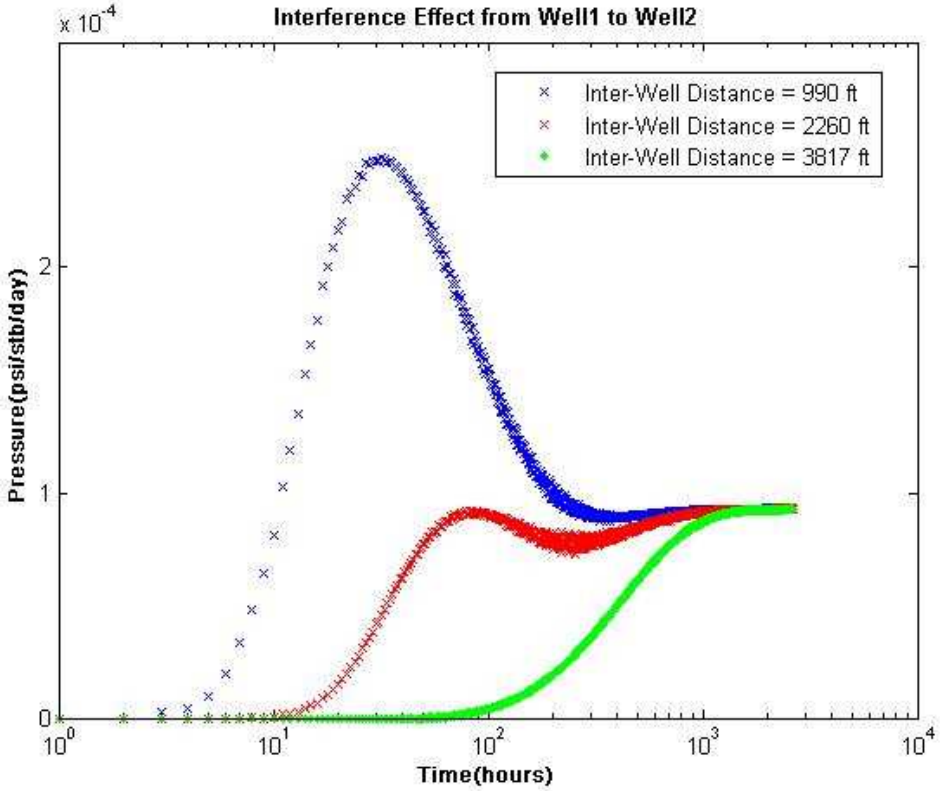

Figure 5. 8 h_{12} with different inter-well distance on semi-log plot

For the case with different inter-well distance, small value case shows a clear hump, which represents the interference distribution time from one well to the other. And a minus slope, which means after the interference reached the other well, the active well itself is producing in radial flow conditions. While, medium value case shows a time delay hump too, but it does not show an obvious minus slope period, because the inter-well distance is close to the distance between the well to the boundary. Once the interference from the well reaches the other one, it reaches the boundary, so h_{12} does not show infinitely acting behavior. In large value case, there is no time delay hump and no minus slope period due to the long inter-well distance. Because before the interference reached the observation well, the pressure distribution from the active well has reached the boundary. Three cases show a zero-slope period, which start at different time but completely overlap at last to a constant value, which represents the three cases have the same drainage area and reservoir volume.

5.5 Synthetic Case Studies

Case 1

This synthetic case is designed to validate applicability of our multi-well deconvolution algorithms for interference processing from PDG. A two-well synthetic model, shown in **Figure 5.9**, is produced. This reservoir model is a fully penetrating model with two vertical wells, located in a uniform formation, bounded on all sides by no-flow boundaries. The distance between two wells is 2260ft. Other parameters are listed in **Table 5.1**.

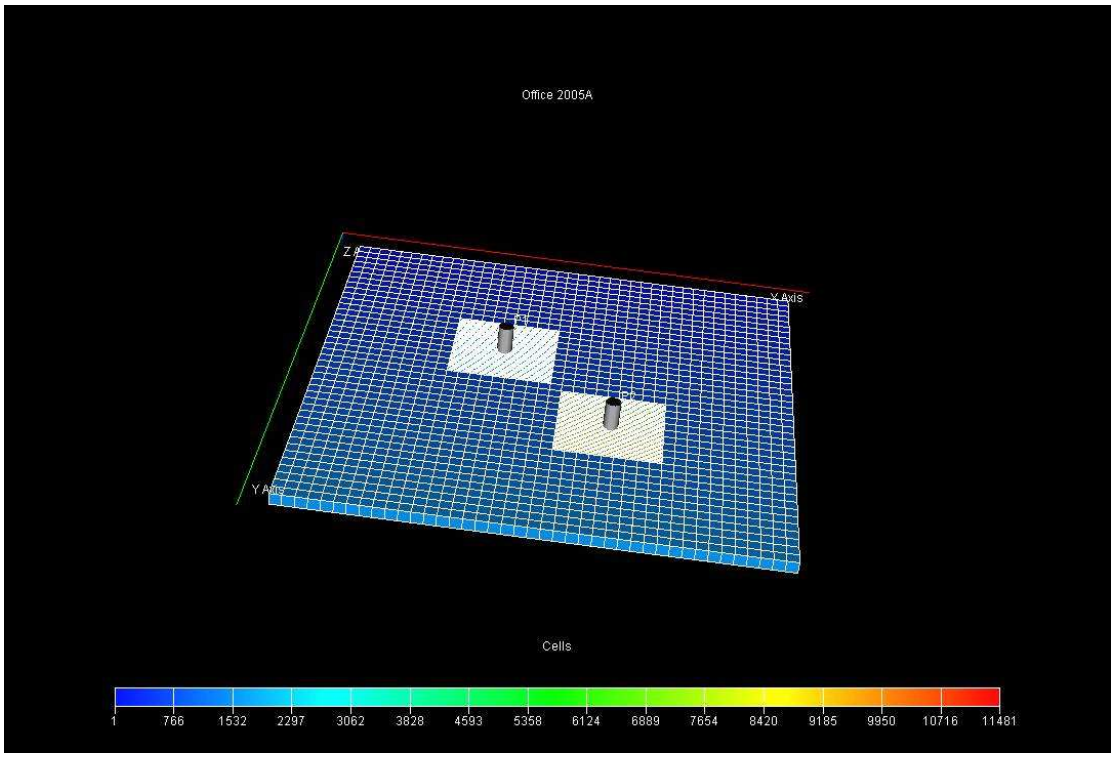

Figure 5. 9 Two-Well Homogeneous Reservoir Model

Initial pressure, p_i	= 3014. 2psia
Porosity, ϕ	= 0.3
Permeability, k	= 50 mD
Thickness, h	= 100 ft
Oil formation volume factor, B_o	= 1.2rb/STB
Viscosity, μ	= 1.2 cp
Total compressibility, c_t	=6e-6 1/psia
Well radius, r_w	= 0.3 ft
Reservoir length, R	= 4100 ft
Reservoir width, R	= 4100 ft

Table 5. 1 Reservoir and Fluid Properties for Homogeneous Model

The inter-well distance of the reservoir model is changed three times to group A, B, and C, in which the inter-well distance is 990ft, 2260ft and 3817ft respectively. As shown in **Figure 5.10**. The flow history of these three cases is the same: Well 1 produces and Well 2 is for observation. Multi-well deconvolution algorithm is implemented on the pressure and rate data of one well with interference from another well.

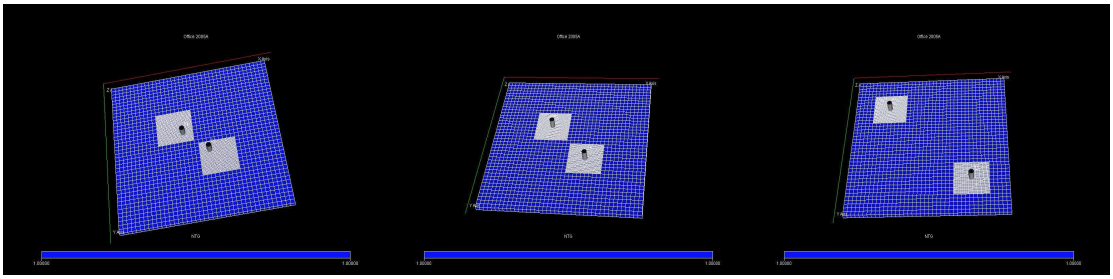

Figure 5. 10 Three closed reservoir models with different inter-well distances

For different inter-well distance test, the interference pressure from Well 2 to Well 1 is separated and the interference system changing with time is shown in **Figure 5.11**. This extracted interference pressure has three time regions. The first region is from the beginning of Well 1 to the interference (from Well 2 to Well 1) turning up on this

extracted interference pressure. While the second region starts from the interference happening to the interference becoming stable. And the third region is the last one, which represents the interference from one well to another becoming stable and keep at a constant value.

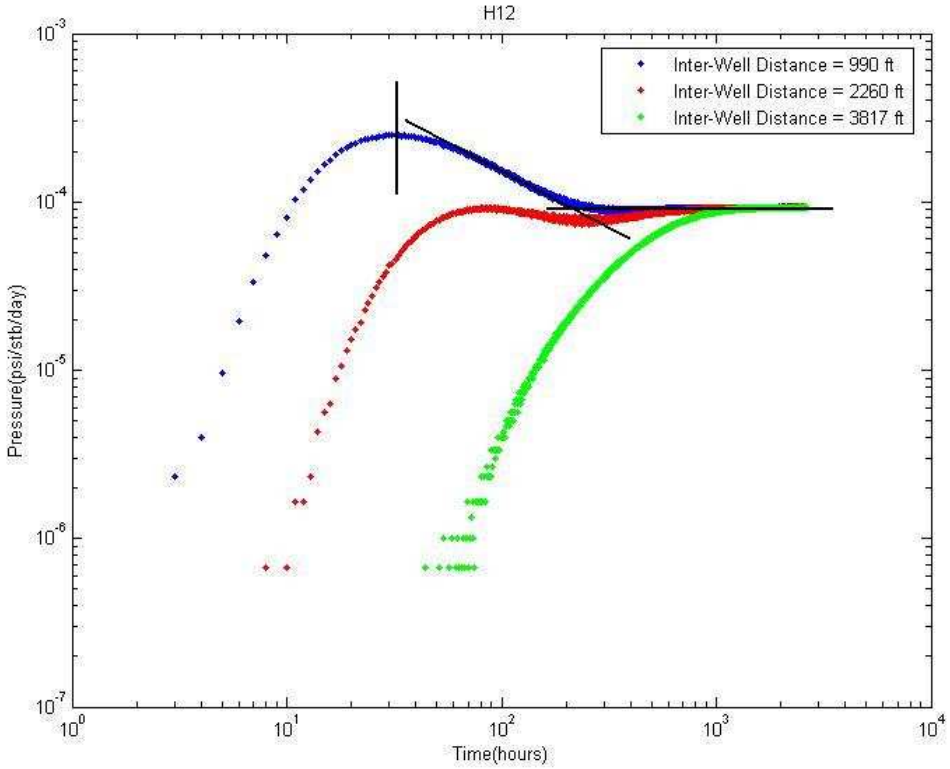

Figure 5. 11 Interference pressure responses from well 1 to well 2 for three cases

The two-well deconvolution product, h_{12}, is described as follows.

Hump period: Case A shows a clear hump, which means the interference distribution time from well 1 to well 2. Case B shows a time delay hump too, but not very clear. In Case C, there is no time delay hump.

-1 slope period: Case A shows a clear -1 slope, which means after the interference reached well 2, well 1 is producing in radial flow conditions. Case B does not show an obvious -1 slope period, because the well1-to-well2 distance is close to well1-to-boundary distance. Once the interference from well1 reached well 2, well1 reached the boundary, so h12 does not show infinitely acting behavior of well1. In Case C, there is no -1 slope period at all due to the long inter-well distance.

Zero slope period: Three cases show zero slope period, which start at different time but completely overlap at last. Case C has only shown zero slope period, because before the interference reached well 2, the pressure distribution from well 1 has reached the boundary.

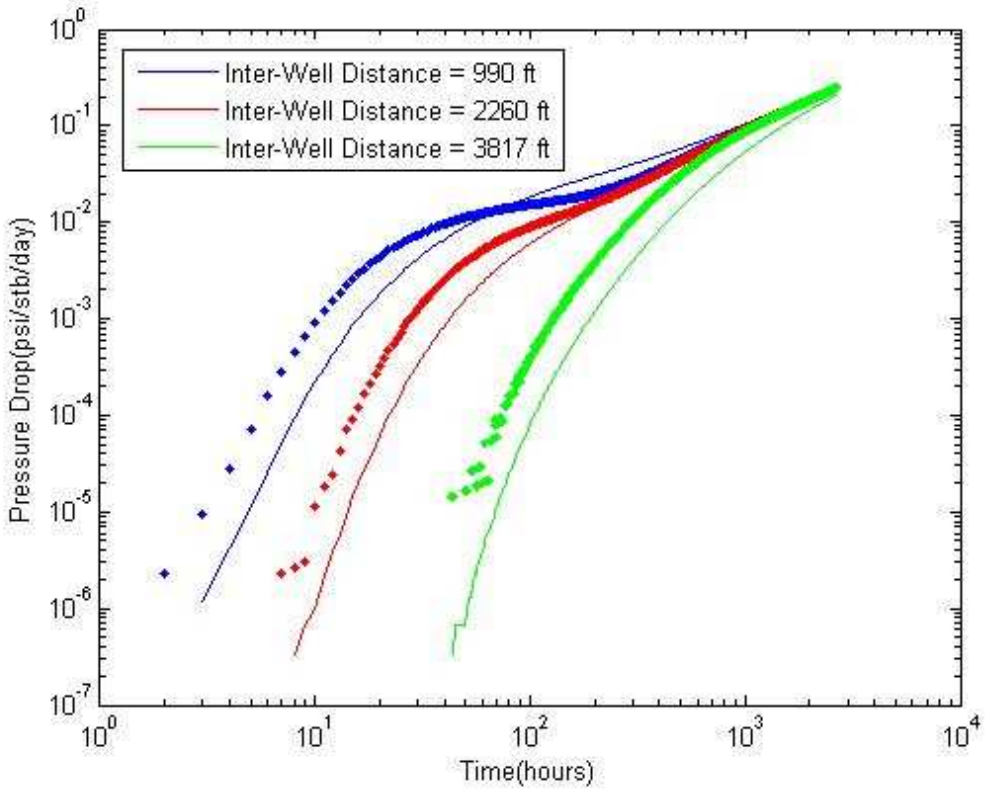

Figure 5. 12 Log-log diagnostic plot of interference response for different inter-well distance

Then this interference pressure is cumulated to get the interference pressure drop for the whole production period, shown on log-log in **Figure 5.12**. The two curves (pressure and pressure derivative) intersect at different time as a result of different inter-well distance. The derivative of interference response is extracted in **Figure 5.13**.

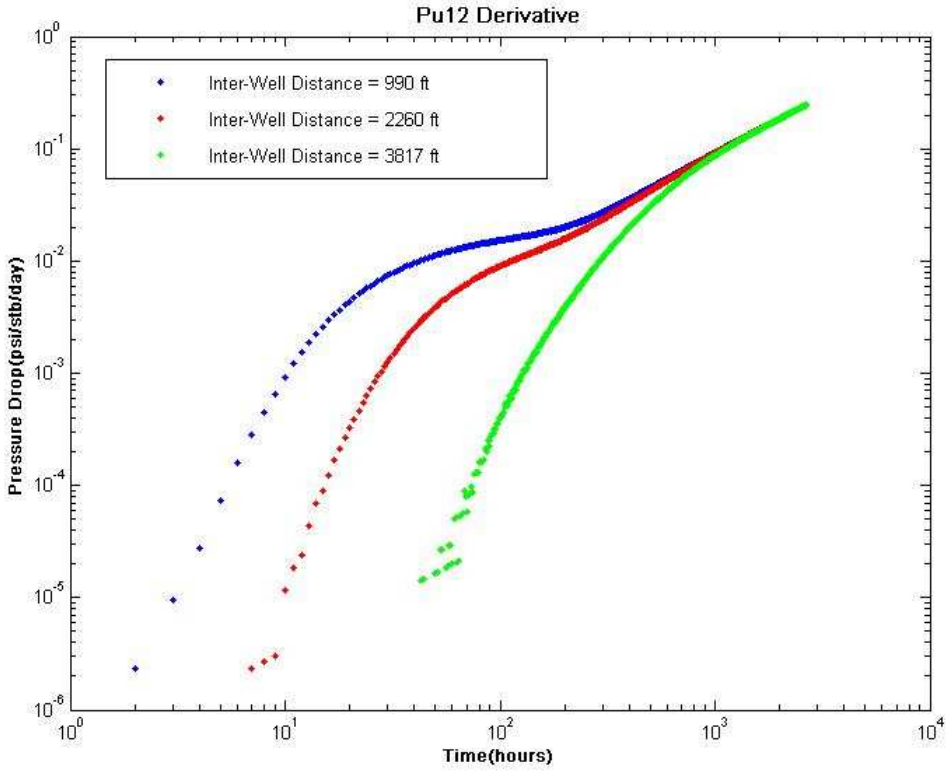

Figure 5. 13 Log-log plot of the pressure derivative of interference response for different inter-well distance

This case validates the applicability of our multi-well deconvolution algorithms for interference processing. The deconvolution program works well and the extracted interference response fairly exhibits through the deconvolution processing.

Case 2

For the multi-well interference study, a two-well synthetic model, shown in **Figure 5.14**, is produced. This reservoir model is a fully penetrating model with two vertical wells, located in a uniform formation, bounded on all sides by no-flow boundaries. The length of foursquare boundary is 20500ft, while the inter-well distance is 2121ft. Other parameters are listed in **Table 5.2**.

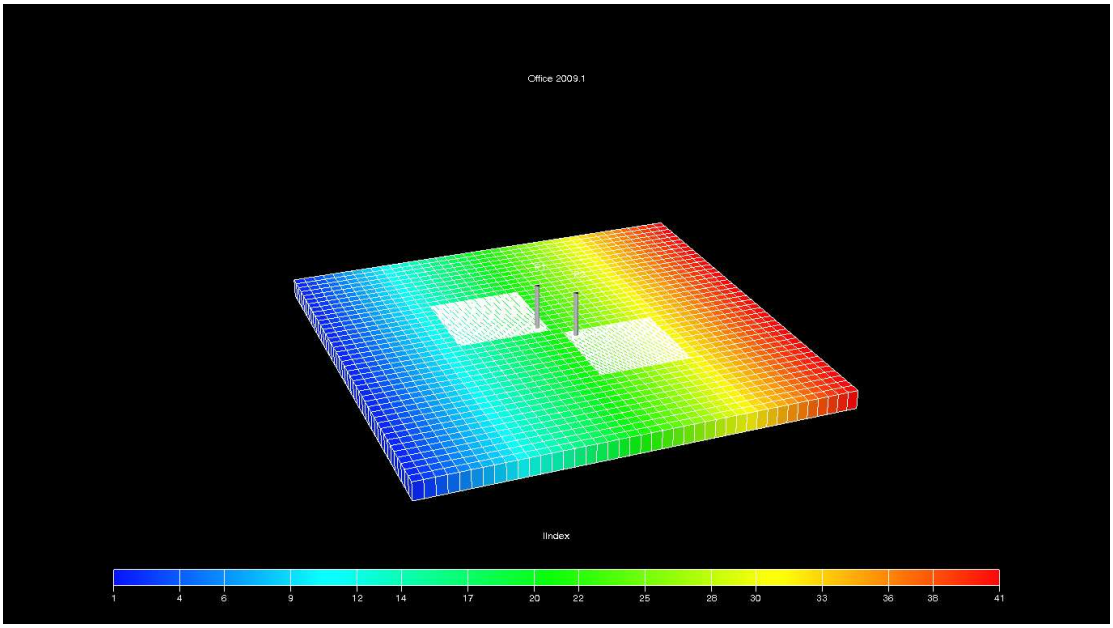

Figure 5. 14 Two-well reservoir model

Initial pressure, p_i	= 3014.2 psia
Porosity, ϕ	= 0.3
Permeability, k	= 50 mD
Thickness, H	= 100 ft
Oil formation volume factor, B_o	= 1.2rb/STB
Viscosity, μ	= 1.2 cp
Total compressibility, c_t	$=6e^{-6}$ 1/psia
Well radius, r_w	= 0.3 ft

Table 5. 2 Reservoir and fluid properties for the synthetic model

A synthetic case is designed for extracting the interference pressure response (p_{u12}) and its primary derivative (h_{12}) from self pressure response of the well with multi-well deconvolution. In this case, Well 1 and Well 2 are put on production at the same time, including three short buildups and three drawdown periods for Well 1, and two short

buildups and three drawdown periods for Well 2. **Figure 5.15** shows the simulated production history of the two wells.

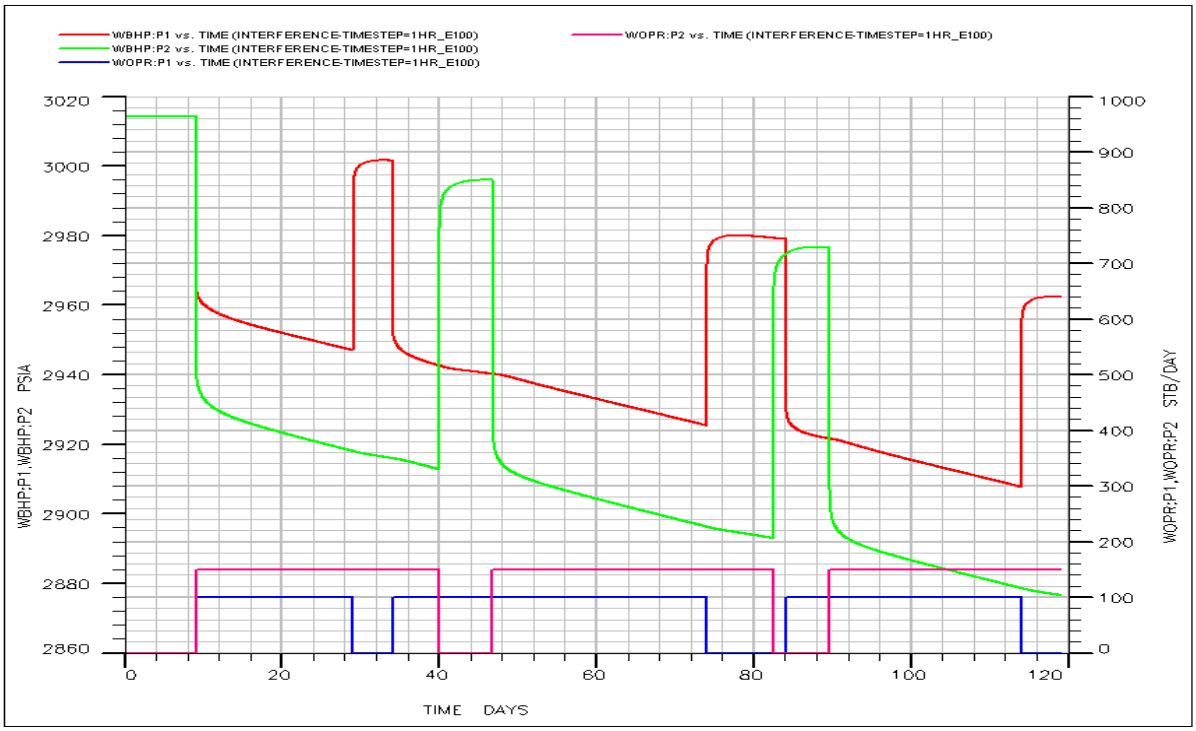

Figure 5. 15 Simulated pressure and flow rate history for two-well transient pressure analysis, in which Well 1 and Well 2 are put on production at the same time, including three short buildups and three drawdown periods for Well 1, and two short buildups and three drawdown periods for Well 2.

Multi-well deconvolution algorithm is implemented on the pressure and rate data from these two wells. The interference pressure response (p_{u12}) from Well 1 to Well 2 is extracted with our developed algorithm. Besides, the self pressure response (p_{u11}) of Well 1 can be obtained simultaneously.

The primary derivatives (h_{11} and h_{12}) are put on semi-log scale for comparison, shown in **Figure 5.16**. It can be clearly found that primary derivative of self pressure response declines with time monotonously. While the primary derivative of interference pressure

response shows a time delay hump and declines with time later. These two curves overlap at last.

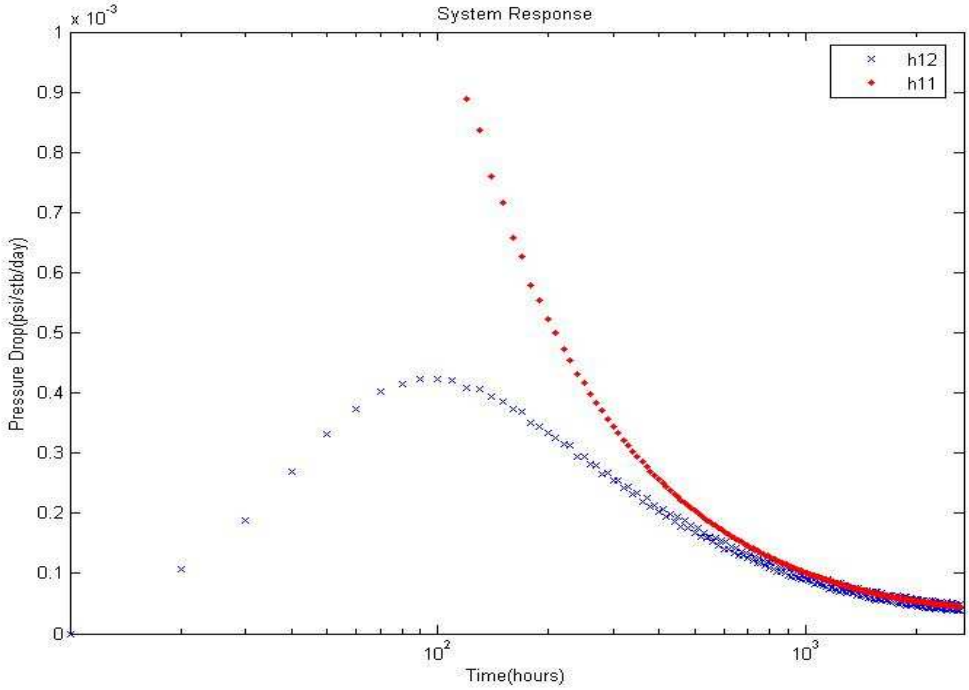

Figure 5. 16 Comparison of primary pressure derivatives of self pressure response and interference pressure response on semi-log plot

After the multi-well deconvolution processing, the extracted interference pressure response (p_{u12}) and the remaining self pressure response (p_{u11}) can be used for transient analysis. The self pressure response and interference response with their corresponding logarithmic derivatives are put on log-log scale together, as shown in **Figure 5.17**. The logarithmic derivative of self pressure response shows infinitely acting behavior earlier than that of interference pressure response does due to the time delay problem. Well 1 keeps flowing in radial flow condition during the designed production period, since there is not any boundary behavior shown on self response or interference response (not reached yet).

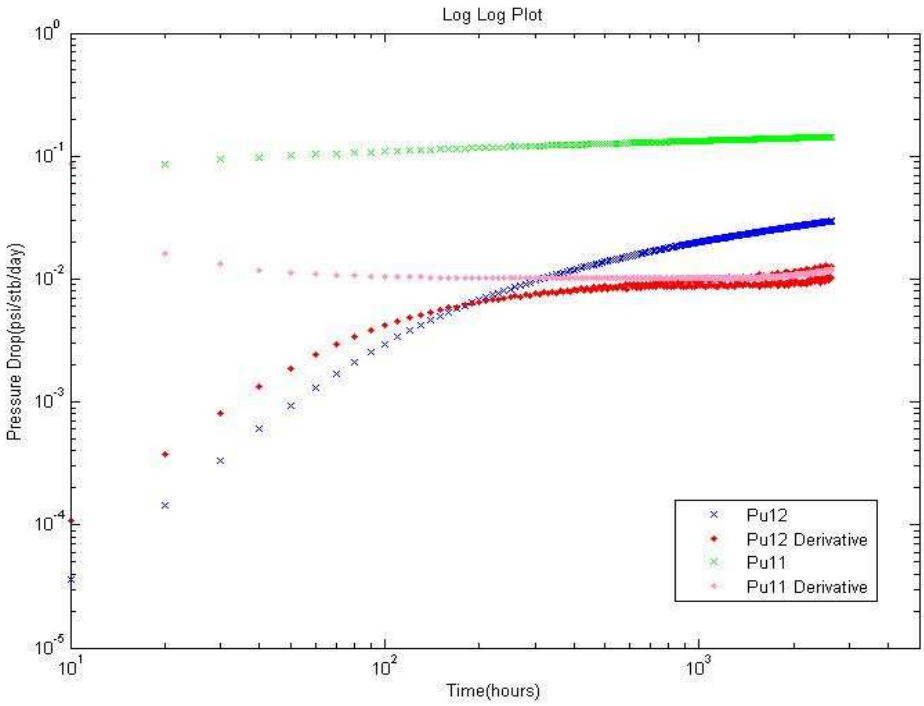

Figure 5. 17 Self pressure response (p_{u11}) and interference pressure response (p_{u12}) with their corresponding logarithmic derivatives on log-log plot

If the two wells produce a longer time to reach the reservoir boundary, the primary derivatives (h_{11} and h_{12}) extracted with the developed deconvolution algorithm are shown in **Figure 5.18**, where two curves overlap and keep at a constant value at last. **Figure 5.19** shows the self pressure response and interference response with their corresponding logarithmic derivatives on log-log plot. Obviously, two derivatives, both exhibiting a unit slope at late time, represent the wells in pseudo steady state flow condition.

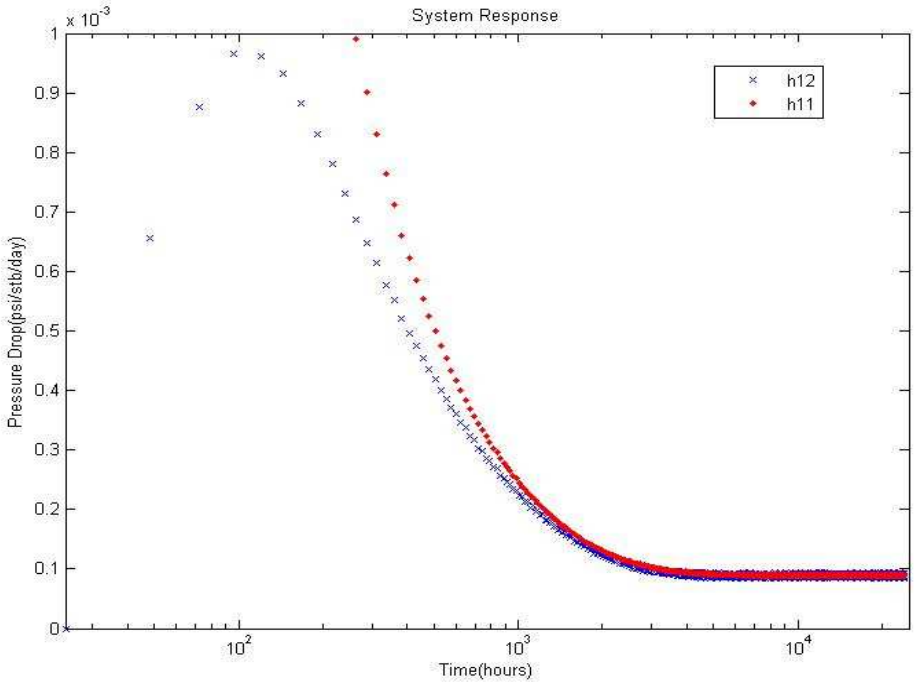

Figure 5. 18 Comparison of primary pressure derivatives of self pressure response and interference pressure response on semi-log plot

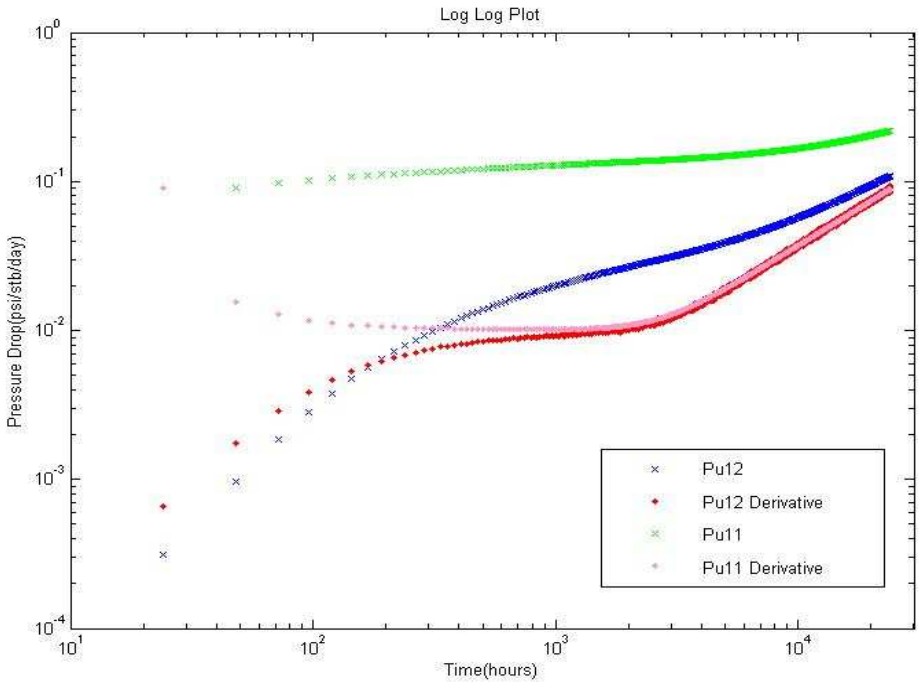

Figure 5. 19 Self pressure response (p_{u11}) and interference pressure response (p_{u12}) with their corresponding logarithmic derivatives on log-log plot

All the agreements above prove that the primary pressure derivatives from multi-well deconvolution can be used for the diagnostic of interference effect. The flow regimes diagnosed by primary pressure derivative are consistent with those from traditional logarithmic derivative diagnostic.

5.6 Chapter Conclusions

According to this study, several conclusions can be derived, as follows:

The computing procedure of the developed two-well deconvolution algorithm is outlined. With this algorithm, the inter-well interference effect in long-term PDG transient pressure data can be separated and variable-rate problem can be solved at the same time.

The interference pressure response (p_{u12}) in two-well reservoir systems was extracted using the developed deconvolution algorithm.

The analytical inter-well interference theory and theoretical derivation of deconvolution products have been completed, which proved that the primary interference derivative (h_{12}) is consistent with that from traditional interference transient theory.

Analytical and simulation cases have been produced for comparison. The results from analytical, simulation and deconvolution solutions agree with each other, which prove that the developed two-well deconvolution algorithm works well.

Deconvolution-based interference analysis theory is proposed in detail. This deconvolution-based analysis procedure has improved the traditional multiple well tests.

Numerical well testing synthetic studies have been performed to demonstrate the procedure of this deconvolution-based interference pressure response analysis. The results proved that this deconvolution-based analysis method worked well in homogeneous reservoirs with two well flowing at single phase, multiple rates. And this new method improved the traditional multi-well interference analysis technique.

Chapter 6
Field Applications of Deconvolution-based Transient Analysis

6.1 Introduction

The deconvolution analysis technique evolved with my deconvolution algorithms developed before has become a useful tool in pressure transient analysis. However, this deconvolution algorithm is limited to the pressure and rate data that originate from single-phase flowing systems. It cannot be used with the data that are acquired during the multi-phase flow conditions.

In this chapter, a new idea for oil-gas two-phase deconvolution is presented with several synthetic cases. The deconvolution algorithm has been modified for this study.

Moreover, previously the developed single-well deconvolution is just used for improving pressure transient analysis and rate transient analysis. In this chapter, the deconvolution results will be applied to give a qualitative diagnostic on single-well nonlinearity due to the interference from other wells and boundary identifications.

Synthetic cases are studied and results are presented to prove the practical applicability

of the developed single-well deconvolution.

6.2 Single-Well and Multi-Well Deconvolution Problems

6.2.1 Single-Well Deconvolution Problem

In reservoir system, the equation of deconvolution is given by Duhaml's integral or principle of superposition, which is a function of time, where the pressure drop across the reservoir is the convolution product of rate and reservoir response as shown below:

$$\Delta p(t) = p_0 - p(t) = \int_0^t q(\tau) g(t-\tau) d\tau \tag{6.1}$$

Where, $q(t)$ and $p(t)$ are the measured flow rate and pressure at any place in the wellbore up to the wellhead, and p_o is the reservoir initial pressure. In equation (6.1), g is referred to as the impulse response of the reservoir system.

Therefore, in order to estimate the reservoir response, the inversion of this convolution integral and this mathematical problem is so-called deconvolution. There are two types of deconvolution, which details are explained below.

Pressure-rate deconvolution

In pressure-rate deconvolution, the unit constant-rate transient pressure response of the reservoir system can be reconstructed based on the following convolution integral:

$$p(t) = p_0 - \int_0^t q(t-\tau) \frac{dp_{ur}(\tau)}{dt} d\tau \tag{6.2}$$

Where, $q(t)$ and $p(t)$ are the measured flow rate and bottom-hole pressure. p_o is the initial reservoir pressure and p_{ur} is the unit-rate pressure response.

Rate-pressure deconvolution

In rate-pressure deconvolution, the unit constant-pressure transient rate response of the reservoir system can be reconstructed based on the following convolution integral:

$$q(t)=\int_0^t q_{up}(t-\tau)\frac{d\Delta p(\tau)}{dt}d\tau \tag{6.3}$$

Where, q_{up} represents the transient rate response of the reservoir system if the well was produced at a unit constant-pressure condition.

6.2.2 Multi-Well Deconvolution Problem

We assume that there are n active wells in a reservoir and these wells are in good connectivity with each other. We use $i=1,2,...,n$ to denote each of these wells. The total bottom-hole pressure drop of well i can be given as this function below:

$$\Delta P_i=\Delta P_{ii}+\sum_{j=1}^{n}\Delta P_{ij} \tag{6.4}$$

Where, ΔP_i represents the total pressure drop at the down-hole of well i . ΔP_{ii} represents the pressure drop at the down-hole of well i due to the self-production of well i and ΔP_{ij} represents the pressure drop at the down-hole of well i due to the production of well j ($i\neq j$). It means that the down-hole pressure measured in one well benefits not only from its self-production but also from the production of other active wells in the same reservoir. And the relationship follows superposition principle.

Multi-Well Pressure-Rate Superposition Function:

$$p_i(t)=p_0-\int_0^t q_i(t-\tau)\frac{dp_{uii}(\tau)}{dt}d\tau-\sum_{j=1}^{n}\int_0^t q_j(t-\tau)\frac{dp_{uij}(\tau)}{dt}d\tau \tag{6.5}$$

p_{uii} represents the pressure response at the down-hole of well i due to the production itself, while p_{uij} represents the interference response, namely the pressure response at the down-hole of well i due to the unit-rate production of well j .Moreover, p_{uij} is a superposition product, which equals to cumulative interference system response:

$$p_{uij}=\sum H_{ij} \tag{6.6}$$

where, H_{ij} represents the interference system, which is changing with time.

In this convolution integral, it is assumed that $p_{uij} = p_{uji}$ and then the number of response functions is $n(n+1)/2$. The multi-well deconvolution is to get the response functions p_{uii} and p_{uij}.

Multi-Well Rate-Pressure Superposition Function:

$$q_i(t) = \int_0^t q_{upi}(t-\tau)\frac{d\Delta p_i(\tau)}{dt}d\tau \tag{6.7}$$

$$\Delta p_i(t) = p_i - p_i(t) - \sum_{j=1}^{n}\int_0^t q_j(\tau)\frac{dp_{uij}(t-\tau)}{dt}d\tau \tag{6.8}$$

When there are two active wells in the reservoir ($n=2$), the deconvolution Function can be expressed as follows：

Pressure-Rate Deconvolution:

$$p_1(t) = p_0 - \int_0^t q_1(t-\tau)\frac{dp_{u11}(\tau)}{dt}d\tau - \int_0^t q_2(t-\tau)\frac{dp_{u12}(\tau)}{dt}d\tau \tag{6.9}$$

$$p_2(t) = p_0 - \int_0^t q_2(t-\tau)\frac{dp_{u22}(\tau)}{dt}d\tau - \int_0^t q_1(t-\tau)\frac{dp_{u12}(\tau)}{dt}d\tau \tag{6.10}$$

Rate-Pressure Deconvolution:

$$q_1(t) = \int_0^t q_{up1}(t-\tau)\frac{d\Delta p_1(\tau)}{dt}d\tau \tag{6.11}$$

$$\Delta p_1(t) = p_i - p_1(t) - \int_0^t q_2(\tau)\frac{dp_{u12}(t-\tau)}{dt}d\tau \tag{6.12}$$

$$q_2(t) = \int_0^t q_{up2}(t-\tau)\frac{d\Delta p_2(\tau)}{dt}d\tau \tag{6.13}$$

$$\Delta p_2(t) = p_i - p_2(t) - \int_0^t q_1(\tau)\frac{dp_{u21}(t-\tau)}{dt}d\tau \tag{6.14}$$

6.3 Application for Oil-Gas Reservoir Systems

6.3.1Multi-Phase Deconvolution Problem

The single-phase deconvolution model mentioned above can only deal with pressure and rate data from a well under the single phase flowing conditions. However, once the

bottom-hole pressure of the well below the reservoir bubble point pressure, the multi-phase flow cannot be avoided. Processing this data through single-phase deconvolution algorithm will not produce a physically meaningful response function. Here, we provide a method where the pressure and rate data, which are higher than those at bubble point, will be separated from the whole dataset. As shown in **Figure 6.1**, the green curve is generated bottom-hole pressure while the horizontal blue line is reservoir bubble point pressure. The pressure data, which are higher than those at bubble point, are separated from the whole dataset, shown as the red part in this figure. Then these separated single-phase data will be used for deconvolution processing. Finally the deconvolution results will be used for analysis of reservoir characteristics and formation information.

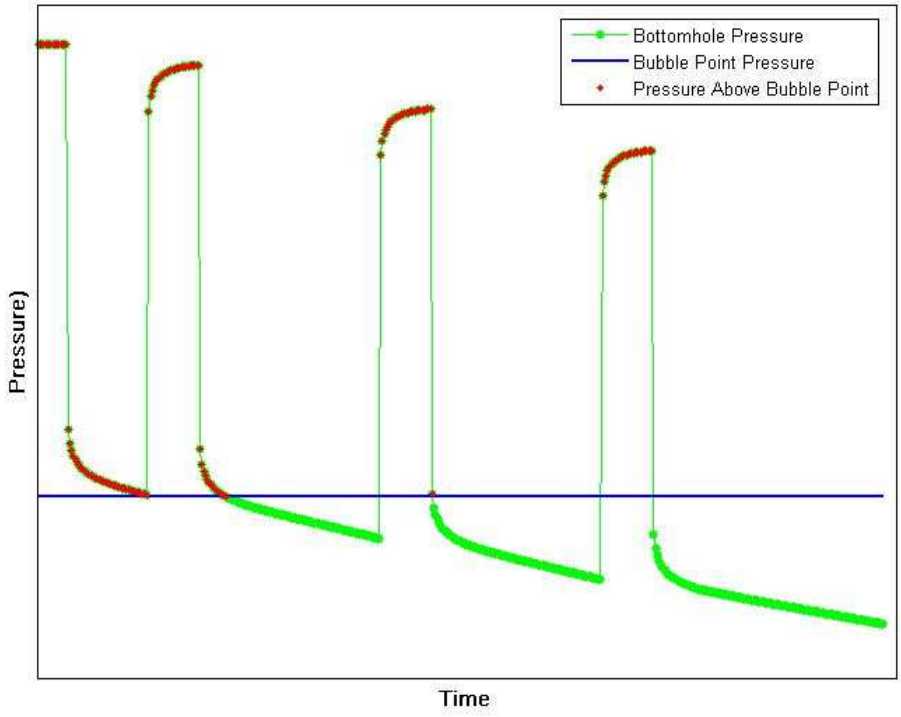

Figure 6. 1 Schematic Diagram of the Multi-phase Deconvolution

6.3.2 Synthetic Case Studies

In order to test the capability of the developed deconvolution algorithm in handling with multi-phase flowing data, several sets of synthetic pressure and rate data are produced. A dissolved gas drive reservoir model is built for this study, shown in **Figure 6.2**.

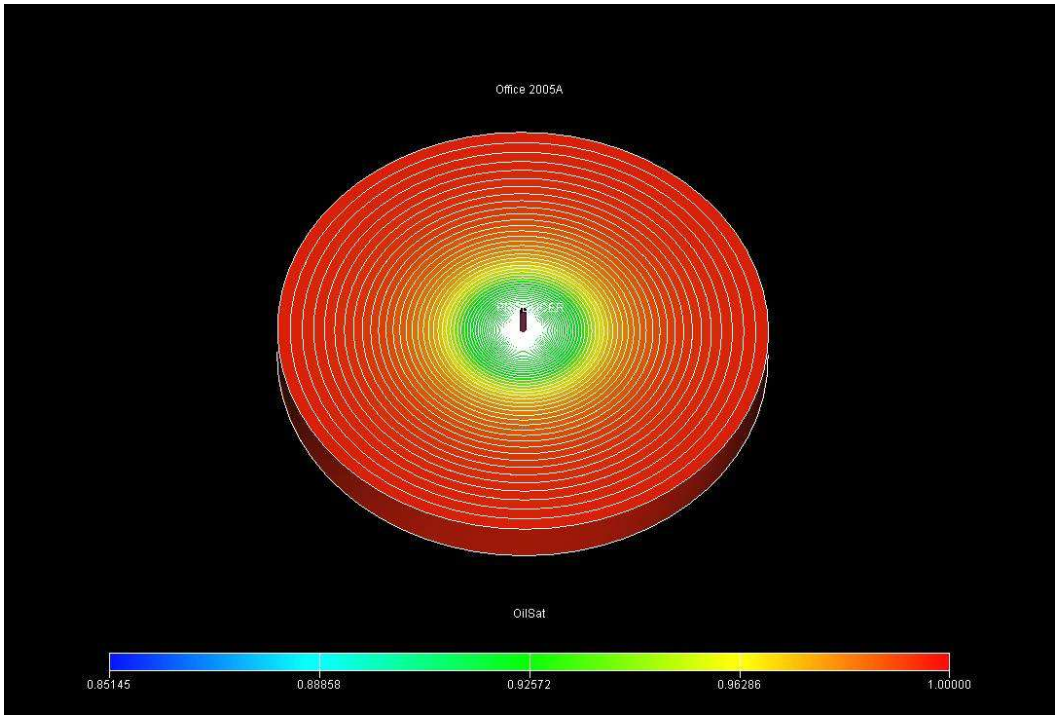

Figure 6. 2 Multi-phase Reservoir Model

The well/reservoir model used for case A,B and C is a fully penetrating single vertical well, located in a uniform formation, bounded on all sides by no-flow boundaries. Other parameters are listed in **Table 6.1** to **Table 6.4.** Results from these cases are interpreted below.

Initial reservoir pressure, p_i	= 3027.8 psia
Porosity, ϕ	= 0.3
Permeability, k	= 50 md
Thickness, h	= 20 ft
Total compressibility, c_t	=9.41 e-5 1/psia
Well radius, r_w	= 0.1 ft
Reservoir radius, R	= 4000 ft

Table 6. 1 Reservoir and Fluid Properties for Multi-phase Model

Press(psia)	FVF (rb /Mscf)	Visc (cp)
15	235	0.008
500	6.711	0.0109
1000	3.145	0.0139
1500	1.987	0.0168
2000	1.431	0.0197
2500	1.117	0.0226
3000	0.923	0.0256
3500	0.798	0.0285
4000	0.716	0.0314
4500	0.663	0.0344
5000	0.63	0.0373
5500	0.612	0.0402
5600	0.609	0.0408
6000	0.599	0.0431
6500	0.596	0.046

Table 6. 2 Dry Gas PVT Properties for Multi-phase Model

Rs (Mscf /stb)	Pbub (psia)	FVF (rb /stb)	Visc (cp)
0.2	600	1.185	0.6
0.4	1400	1.285	0.6
0.622	2200	1.395	0.6
0.686	2420	1.43	0.6
0.746	2650	1.46	0.6
0.804	2830	1.485	0.6
0.9	3130	1.53	0.6
1.05	3590	1.6	0.6
1.358	4430	1.75	0.6

1.882	5600	2.02	0.6
2.285	6500	2.23	0.6

Table 6. 3 Live Oil PVT Properties for Multi-phase Model

Sg	Krg	Kro	Pc (psia)
0	0	1	0
0.1	0	0.78	0
0.15	0.001	0.59	0
0.2	0.002	0.42	0
0.25	0.004	0.29	0
0.3	0.007	0.183	0
0.35	0.009	0.11	0
0.4	0.018	0.036	0
0.45	0.025	0.008	0
0.5	0.04	0.003	0
0.55	0.073	0.0001	0
0.6	0.18	0	0

Table 6. 4 Gas/Oil Saturation Functions for Multi-phase Model

Table 6.4 represents the gas relative permeability, oil relative permeability and oil-gas capillary pressure as functions of the gas saturation (Column 1). The effect of oil-gas capillary pressure is not taken into account in this study. So I put a constant value as the corresponding oil-gas capillary pressure (Column 4) for simulation cases as follows.

Case A is designed for base case. **Figure 6.3** shows its production sequence, which includes three pressure drawdown periods and two pressure buildups. The blue horizontal zero line in this figure indicates that there is no free gas producing during the whole flowing period. So the pressure and oil rate data in this case belong to single-phase. We process this single-phase data using our deconvolution program and

get the smoothly curve, constant-rate pressure response of the reservoir, shown on the right side.

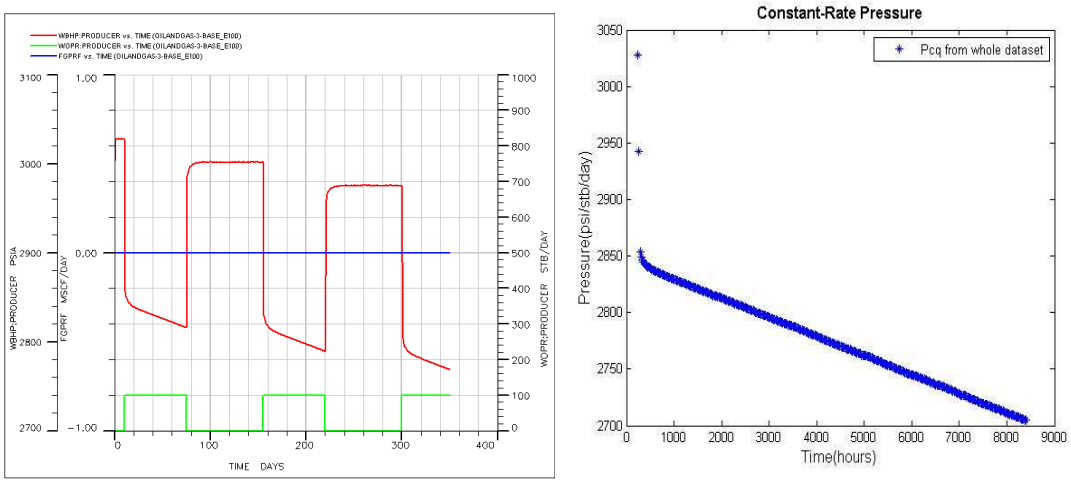

Figure 6. 3 Simulated Production History and Deconvolution Result of Pressure and Oil Rate Data (Base Case-Without Free Gas)

Case B is designed for comparison. **Figure 6.4** shows its production history, which includes several pressure drawdown and buildup periods. At later time, the bottom-hole pressure of this well is below the bubble point pressure of the reservoir during the last two drawdown periods and free gas turns up, as shown on the blue curve of the figure. The pressure and oil rate data, which are higher than those at bubble point are separated and collected from the whole dataset. And then they can be used for single-phase deconvolution processing. The deconvolution results of the whole two-phase dataset and separated single-phase dataset have been shown on the right side. The blue curve is two-phase deconvolution result, while the red curve shows the separated single-phase deconvolution result.

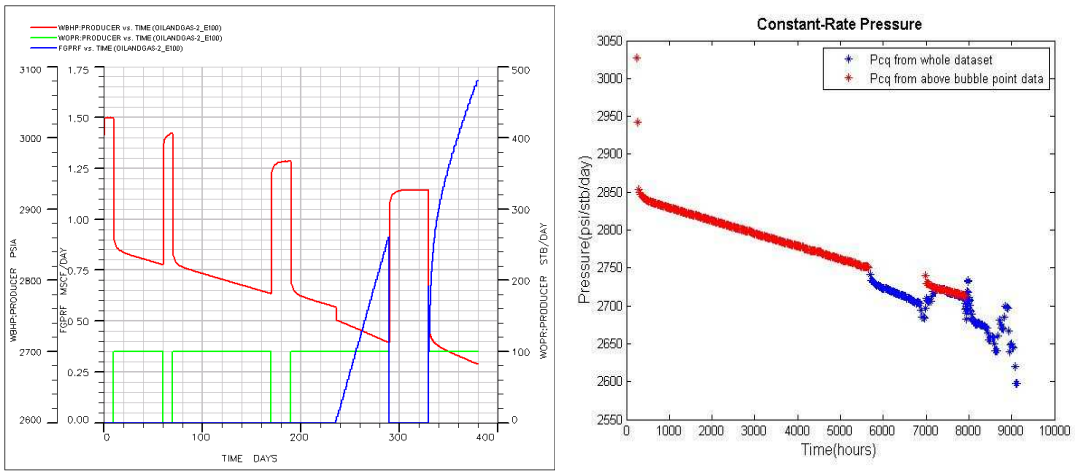

Figure 6. 4 Simulated Production History and Comparison of Deconvolution Results on Whole Data and Separated Data (Case B-With Free Gas)

Case C is another comparison case. **Figure 6.5** shows its multiple rate production history, which includes three pressure drawdown and buildup periods respectively. At the beginning, this well produces under a high rate flowing condition, which leads the bottom-hole pressure of this well declines deeply and becomes below the bubble point pressure at later time of the first drawdown period. And then through shut-in well and flow-rate schedule change, the bottom-hole pressure of this well recovers to be higher than bubble point pressure. With the well producing, the bottom-hole pressure of this well cannot keep higher that that at bubble point. So it turns to produce free gas at the last pressure drawdown period, as shown on the blue curve of the figure. The pressure and oil rate data, which are higher than those at bubble point during the whole flowing periods are separated and collected. And then they can be used for single-phase deconvolution processing. The deconvolution results of the whole two-phase dataset and separated single-phase dataset have been shown on the right side. The blue curve is two-phase deconvolution result, while the red curve shows the separated single-phase deconvolution result.

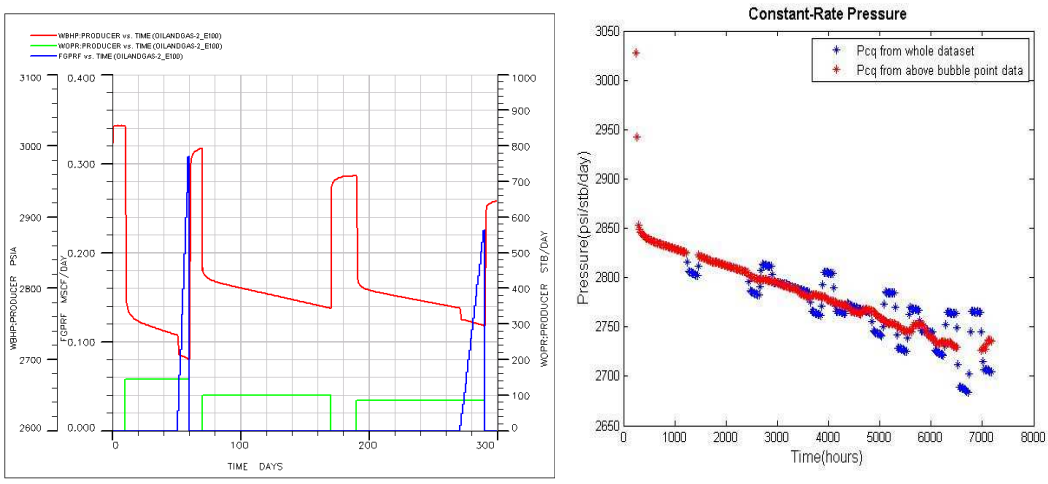

Figure 6. 5 Simulated Production History and Comparison of Deconvolution Results on Whole Data and Separated Data (Case C-With Free Gas)

Finally, the comparison of deconvolution results from two multi-phase cases and the base single-phase case has shown on **Figure 6.6**. The trends of three curves are identical, which indicates that the behavior of deconvolved data can represent the true reservoir response under the constant flowing conditions.

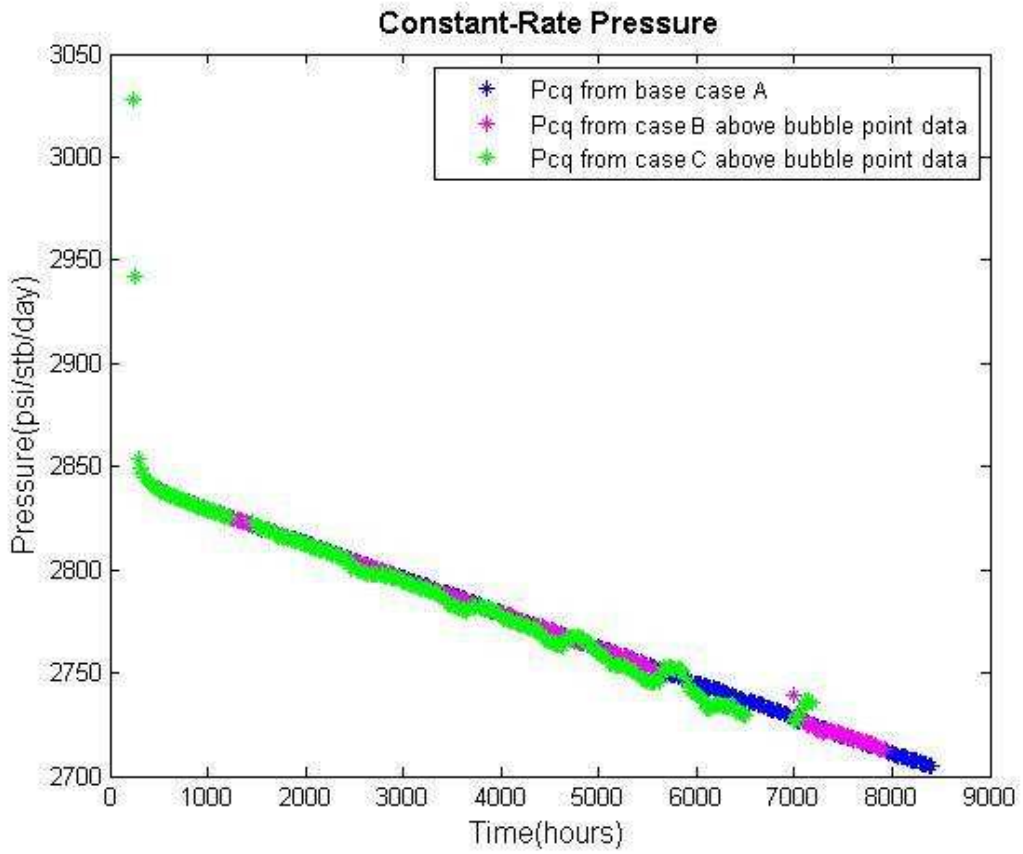

Figure 6. 6 Comparison of Deconvolution Results from Two Multi-phase Cases and the Base Single-phase Case

6.4 Application for Interference Diagnostics

6.4.1 Theory of Interference Diagnostics

For system identification, deconvolved rate is compared with the empirical Arps decline models (exponential, hyperbolic or harmonic) of the system under depletion as a base. Any derivation from the Arps decline may indicate nonlinearities about the system. Such nonlinearities include changing storage, skin effects, interference between wells, multiphase flow effects, etc. Recall that Arps rate-time equation is given by

$$q(t) = \frac{q_i}{[1 + bD_i t]^{1/b}} \tag{6.15}$$

For $b = 0$, we can obtain the exponential decline equation from equation above,

$$q(t) = q_i \exp(-D_i t) \tag{6.16}$$

and for $b = 1$,referred to as harmonic decline, we have

$$q(t) = \frac{q_i}{[1 + D_i t]} \tag{6.17}$$

A unit solution ($D_i = 1$) of equation (6.15) was developed for values of b between 0 and 1 in 0.1 increments. The results are plotted as a set of log-log type curves (**Figure 6.7**) in terms of a decline curve dimensionless rate,

$$q_{Dd} = \frac{q(t)}{q_i} \tag{6.18}$$

and a decline curve dimensionless time,

$$t_{Dd} = D_i t \tag{6.19}$$

From **Figure 6.7** we see that when all the basic decline curves and normal ranges of b are displayed on a single graph, all curves coincide and become indistinguishable at $t_{Dd} \cong 0.3$. Any data existing before a t_{Dd} of 0.3 will appear to be an exponential decline regardless of the true value of b and thus plot as a straight line on semi-log paper.

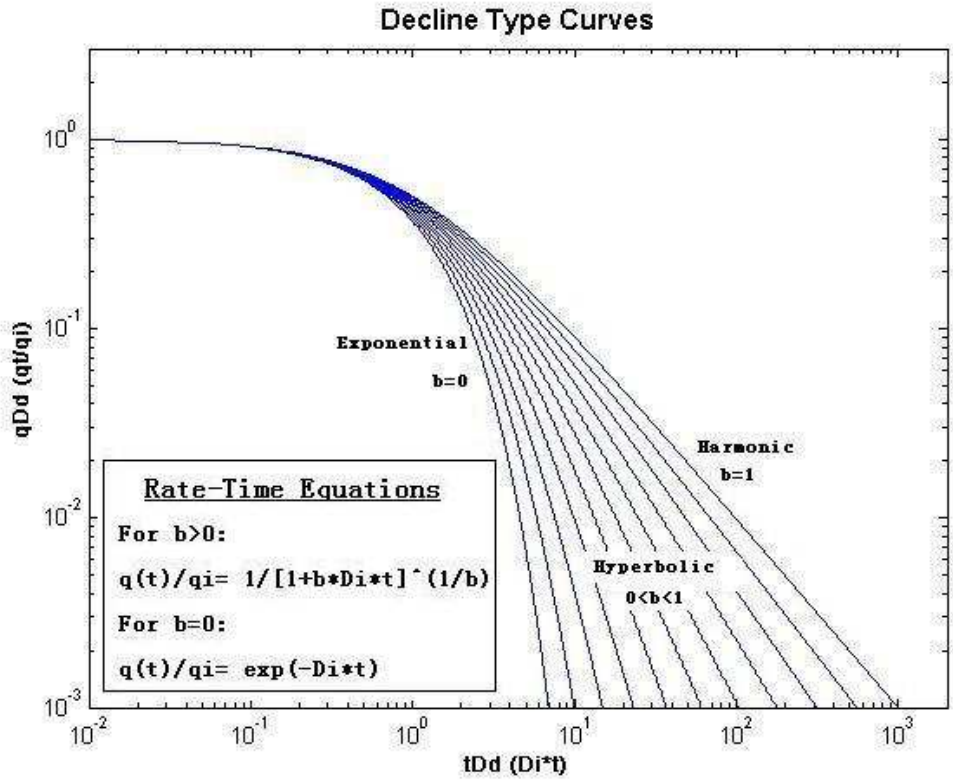

Figure 6. 7 Type curves for Arps empirical rate-time decline equations, unit

solution ($D_i = 1$).

The values of b have been derivated for different reservoir drive or recovery mechanisms. For homogeneous single-layer systems with single-phase liquid (highly undersaturated oil wells), the value of b is zero, exponential:

$$q(t) = q_i \exp(-D_i t) \tag{6.20}$$

which can also be expressed as

$$\log q(t) = \log q_i - \frac{D_i}{2.303} t \tag{6.21}$$

This diagnostic procedure above is conceptually similar to using unit-rate pressure response generated from pressure-rate deconvolution. Once deconvolved pressure is compared with numerical solution for the constant-rate production without any change or interference as a base, deconvolved pressure responses generated from different skin factor data shows a set of parallel curves oppose the base curve, while those from data due to different interference from other well production shows a set of derivations in terms of different pressure drops.

6.4.2 Work Flow of Interference Processing and Analysis

After the diagnostic procedure, it is necessary to process the interference data. The procedure is firstly to extract the interference effect from the total pressure response.

After the processing procedure above, traditional transient-pressure and transient-rate analysis methods for constant-rate or constant-pressure solutions are available. All the produces are included in the workflow, as follows:

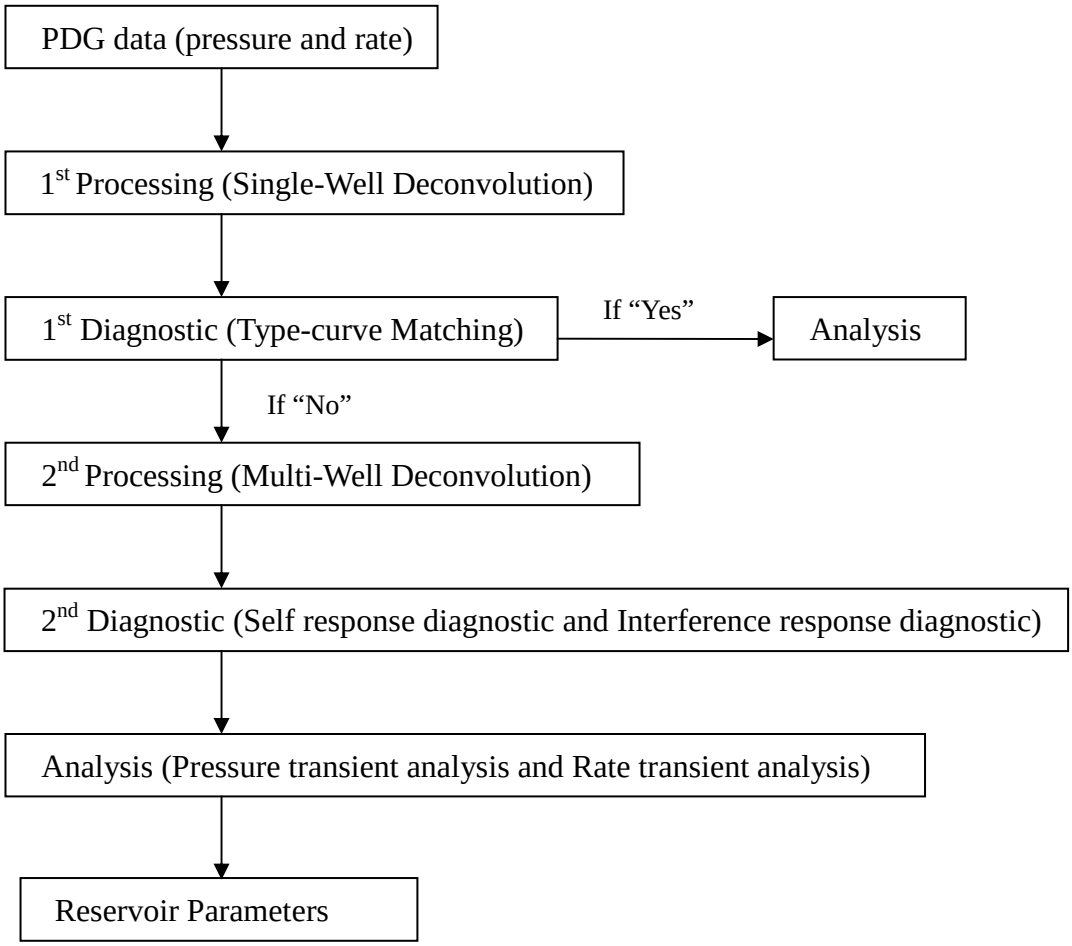

Figure 6. 8 Work Flow of Interference Processing and Analysis

6.4.3 Synthetic Case Studies

In order to validate the multi-well deconvolution algorithm, a two-well synthetic model, shown in **Figure 6.9**, is produced. This reservoir model is a fully penetrating model with two vertical wells, located in a uniform formation, bounded on all sides by no-flow boundaries. The distance between two wells is 2260ft. Other parameters are listed in **Table 6.5**.

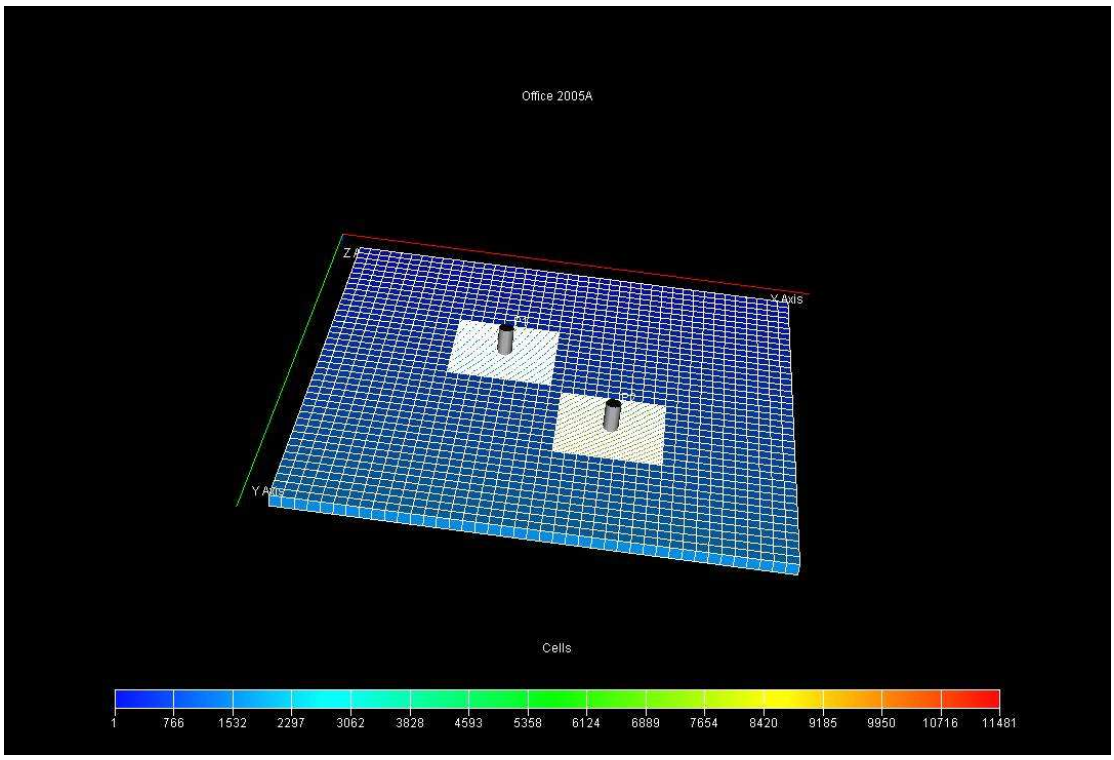

Figure 6. 9 Two-Well Reservoir Model

Initial pressure, p_i	= 3014.2psia
Porosity, ϕ	= 0.3
Permeability, k	= 50 mD
Thickness, H	= 100 ft
Oil formation volume factor, B_o	= 1.2rb/STB
Viscosity, μ	= 1.2 cp
Total compressibility, c_t	$=6e^{-6}$ 1/psia
Well radius, r_w	= 0.3 ft
Reservoir length, R	= 4100 ft
Reservoir width, R	= 4100 ft

Table 6. 5 Reservoir and Fluid Properties for Synthetic Model

The synthetic case is designed to validate applicability of our deconvolution algorithms (single-well deconvolution and multi-well deconvolution) in (1) interference

diagnostics, (2) interference data processing and (3) interference data analysis (after processing). Results from these cases are interpreted below.

To test the performance of multi-well deconvolution on interference diagnostics, one base case is produced, in which only Well 1 produce, including three short buildups and three drawdown periods without any interference and the skin factor for the whole flowing period keeps at 5. The total time period of the data is 2640 hours. **Figure 6.10** shows the simulated pressure and flowing rate history. Another case is that Well 1 is put on production first, same flowing schedule as base case, and then the Well 2 starts to produces 600 hours later. **Figure 6.11** shows the simulated production history. The third case is like base case, which only has Well 1 producing, and same flowing schedule like before. However, the skin factor of the system changes at 600 hours production later from 5 to 2. The flowing history is shown in **Figure 6.12**.

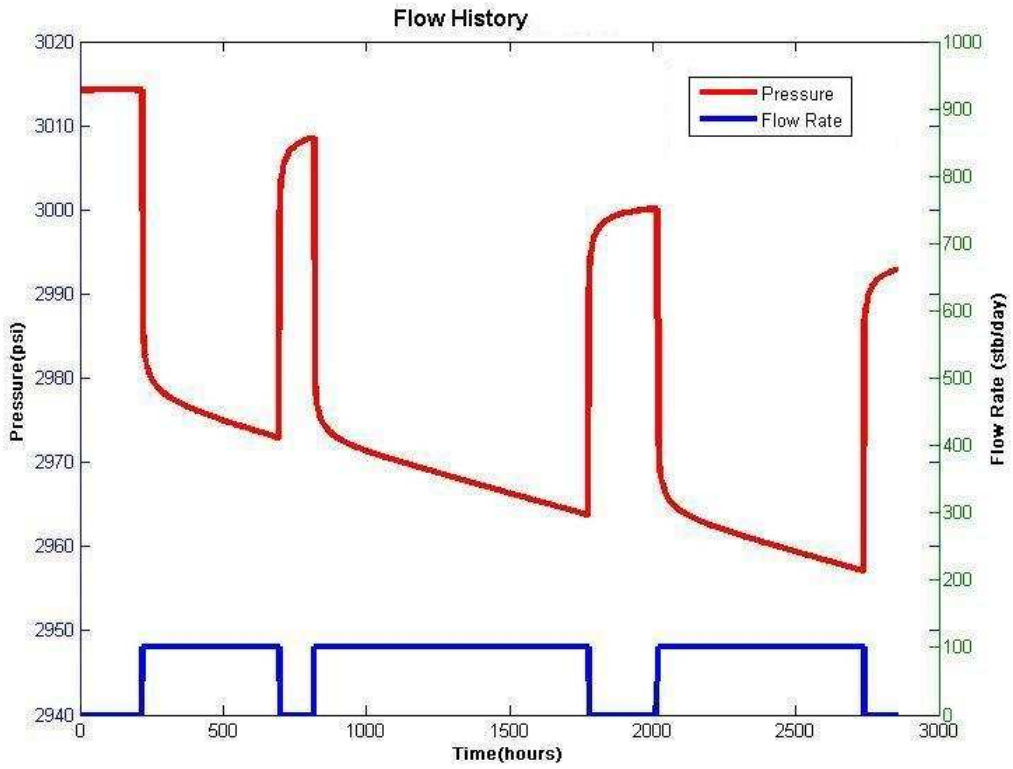

Figure 6. 10 This figure shows a simulated production history of Well 1(single-well production), which includes three pressure draw downs and three short buildups. The blue line represents flowing rate while the red line represents the corresponding pressure response.

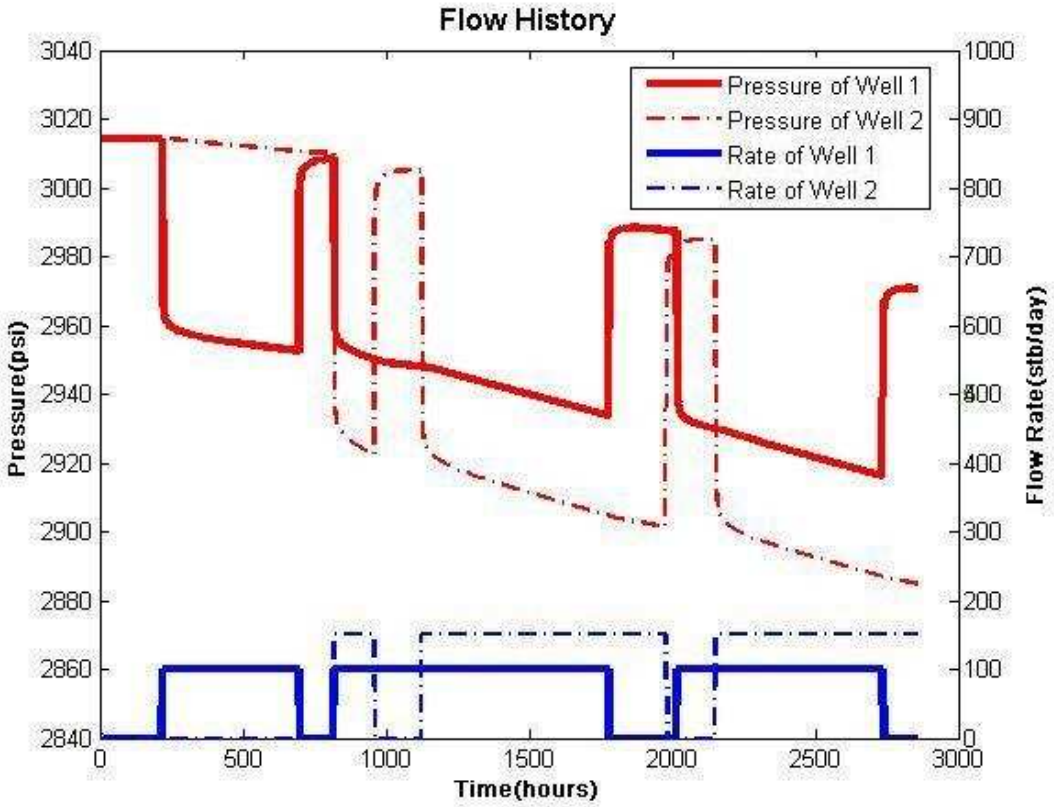

Figure 6. 11 This figure shows a simulated two-well production history, which includes several pressure draw downs and buildups. The solid lines present the pressure and flow rate of Well 1. The dotted lines are for Well 2.

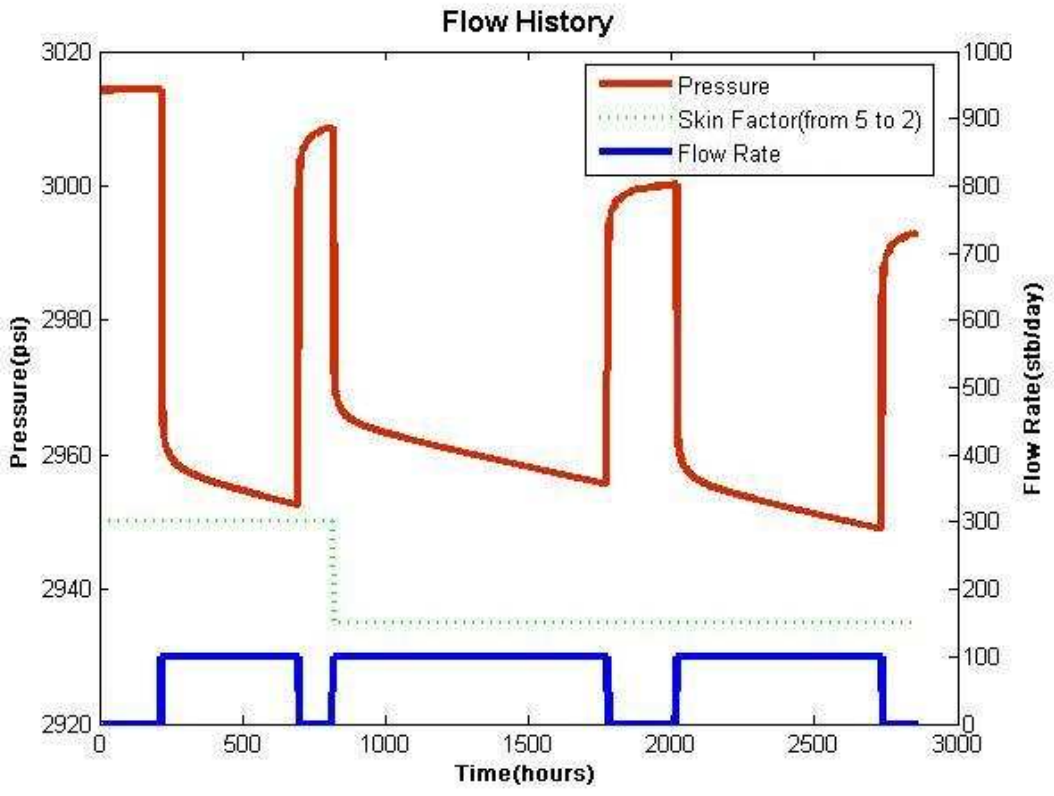

Figure 6. 12 This figure shows a simulated production history of Well 1(single-well production), which includes three pressure draw downs and three short buildups. The blue line represents flowing rate while the red line represents the corresponding pressure response. The skin factor of the well changes at 600 hours production later from 5 to 2.

For diagnostic of interference happening**,** single-well pressure-rate deconvolution is implemented on the whole period of the test data from Well 1 for three cases above. The results, three unit-rate pressures have shown in **Figure 6.13**, in which deconvolved pressure from interference data and skin changed data match the simulated pressure well at the beginning and then they separated at the point when Well 2 begins to produce (skin change point at the same time).

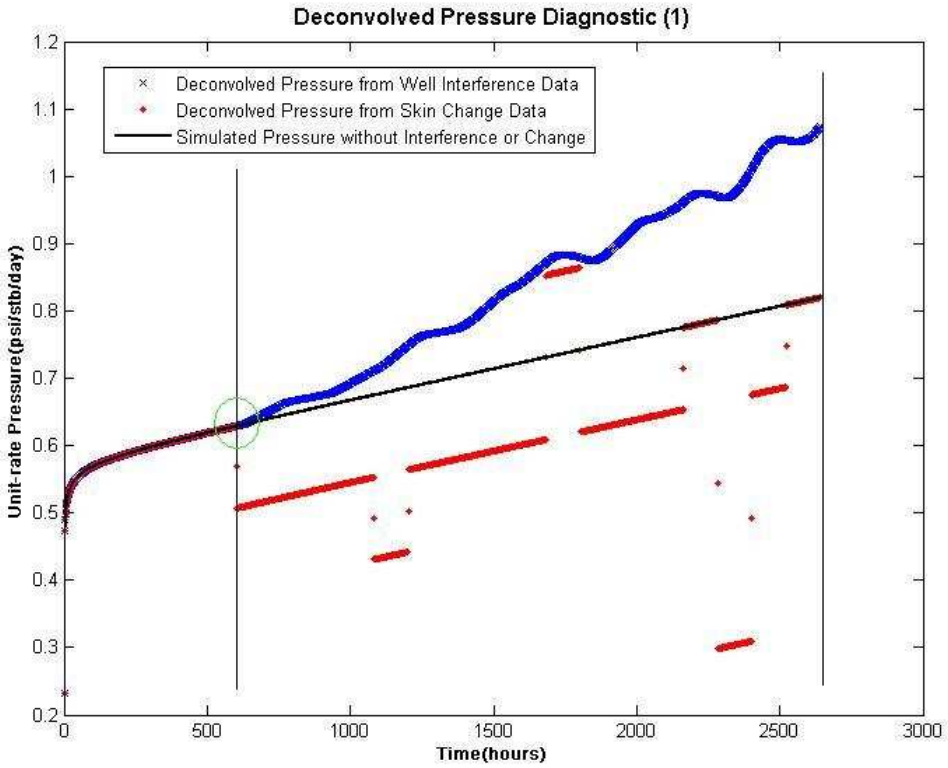

Figure 6. 13 This figure shows the transient-pressure diagnostic of interference happening on Cartesian plot. The blue line is the deconvolved pressure from interference data and the red line is the deconvolved pressure from skin change data. These two deconvolution curves are compared with the black line, simulated pressure without any interference or change.

For further diagnostic, second deconvolution is implemented on the Well 1 data after the separated point and the results verify that the second deconvolved pressure from skin changed data parallels the base curve, while the second deconvolved pressure from interference data is separated from the base curve due to added pressure drop of Well 2 production. The results have shown in **Figure 6.14**.

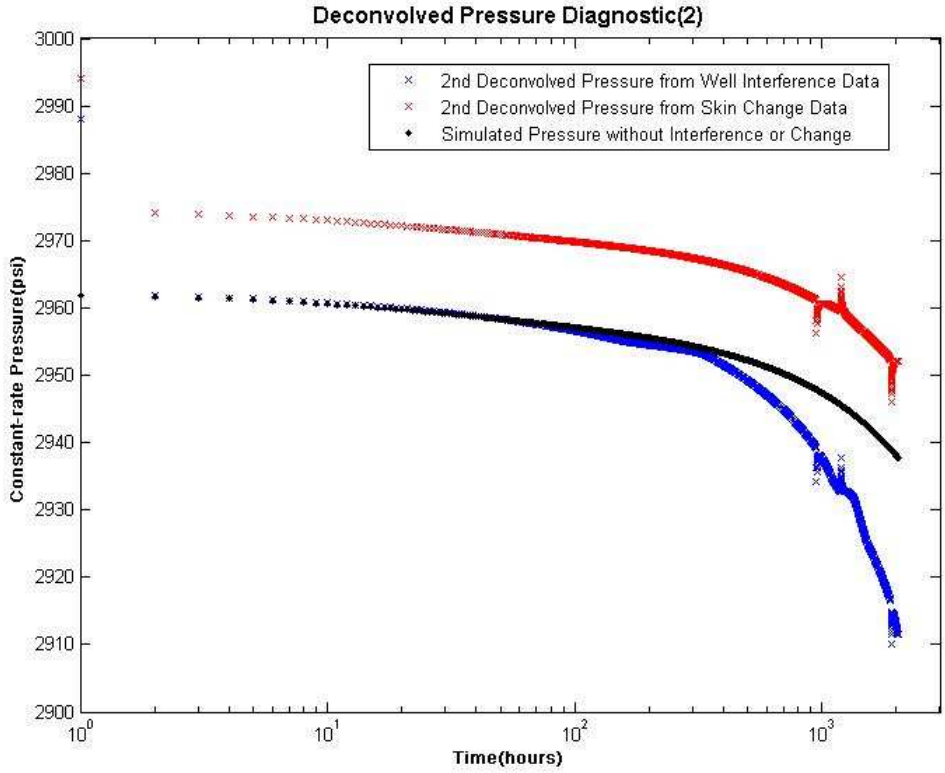

Figure 6. 14 This figure shows the second deconvolved transient-pressure diagnostic on semi-log plot. The blue line is the deconvolved pressure from interference data and the red line is the deconvolved pressure from skin change data. These two deconvolution curves are compared with the black line, simulated pressure without any interference or change.

Like transient-pressure diagnostic procedure above, single-well rate-pressure deconvolution is implemented on the whole period of the test data from Well 1 for system identification using transient rate. The result as the unit- pressure rate is compared with the Arp's decline model as a base. Any derivation from the Arp's

decline may indicate nonlinearities about the system. **Figure 6.15** shows the Cartesian plot, in which deconvolved rate from interference data and skin changed data match the simulated rate well at the beginning and then they separated at the point when Well 2 begins to produce (skin change point at the same time). **Figure 6.16** shows obviously that on log-log plot the deconvolved unit-pressure rate line separates from the simulated unit-pressure rate and drops quickly.

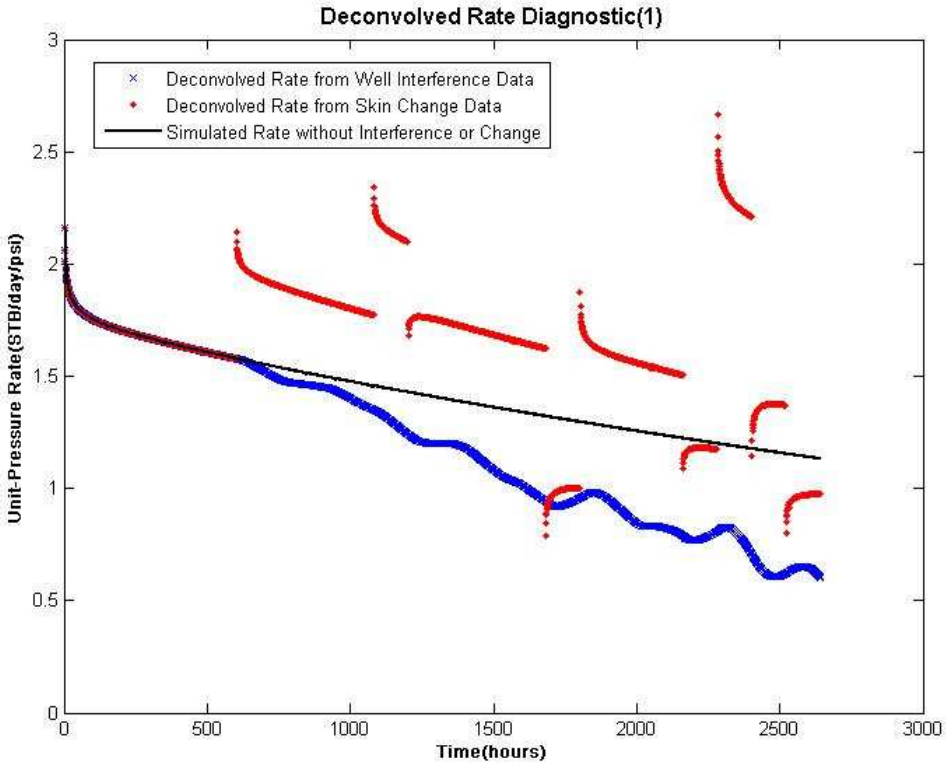

Figure 6. 15 This figure shows the transient-rate diagnostic of interference happening on Cartesian plot. The blue line is the deconvolved rate from interference data and the red line is the deconvolved rate from skin change data. These two deconvolution curves are compared with the black line, simulated unit-pressure rate without any interference or change.

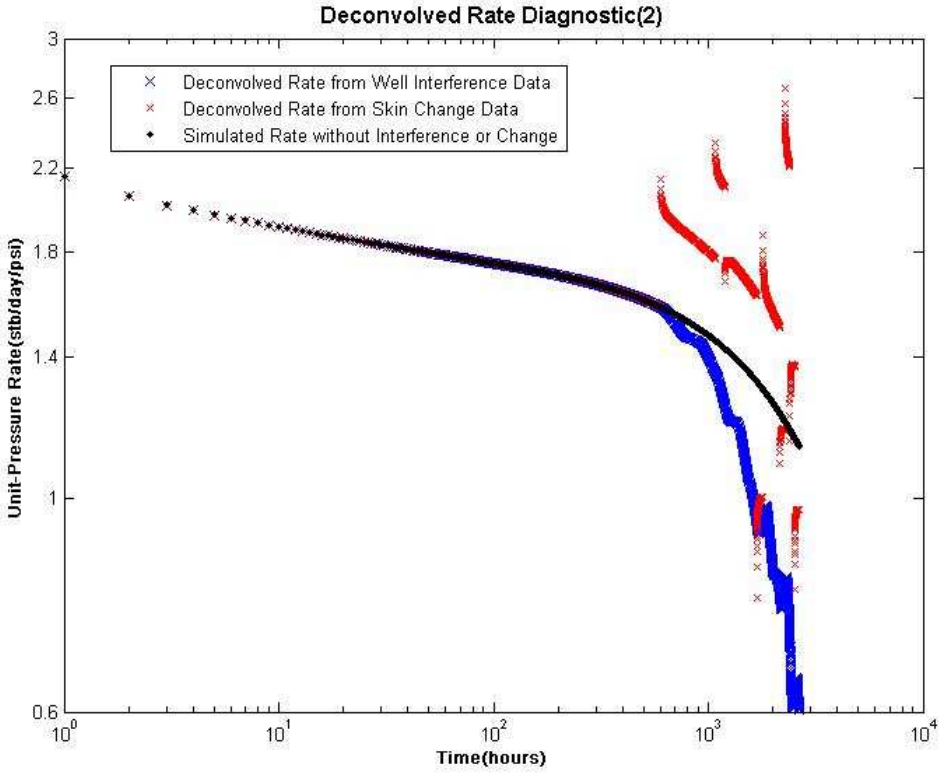

Figure 6. 16 This figure shows the transient-rate diagnostic on log-log plot. The blue line is the deconvolved rate from interference data and the red line is the deconvolved rate from skin change data. These two deconvolution curves are compared with the black line, simulated pressure without any interference or change. At the beginning deconvolved rate matches the simulated rate (Arp's decline model) well and then they separated at the point when Well 2 begins to produce (or skin factor changes). It proves that any derivation from the Arp's decline may indicate nonlinearities about the system.

After the diagnostic, multi-well deconvolution algorithm is implemented on the pressure and rate data of Well 1 during the time before Well 2 produces. The interference pressure effect from Well 2 to Well 1 is separated and interference system changing with time is shown in **Figure 6.17**. Then this interference effect curve is cumulated to the whole production period, shown in **Figure 6.18**. This interference curve for whole dataset can be used to obtain the equivalent constant-rate pressure response and constant-pressure rate response without interference.

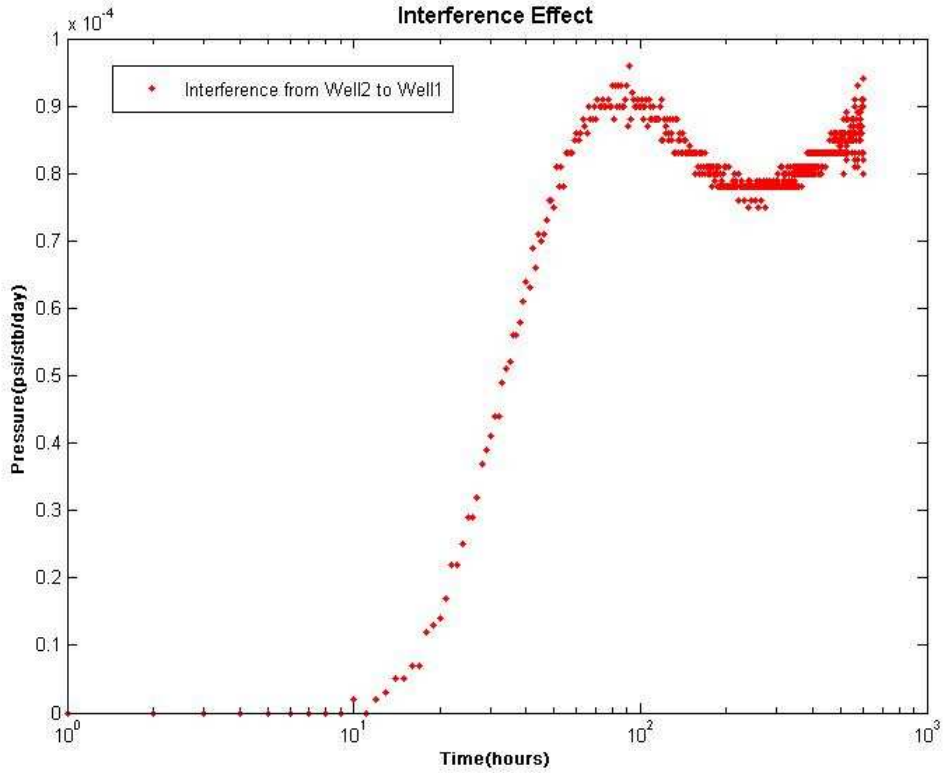

Figure 6. 17 This figure shows the interference system changing with time from Well 2 to Well 1, which is separated by multi-well deconvolution.

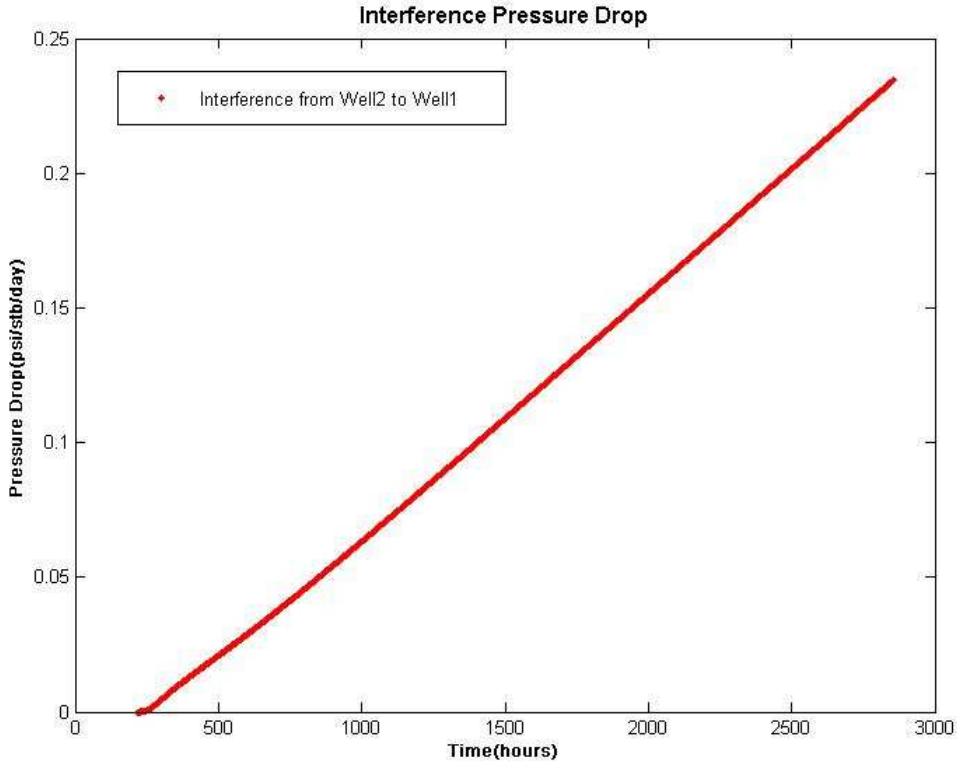

Figure 6. 18 This figure shows the cumulative interference response and its extension on Cartesian plot.

Then pressure-rate and rate-pressure deconvolution programs are both implemented on the well 1 data using the separated interference curve above. The deconvolved constant-rate pressure and constant-pressure rate respond true trends and smooth curves. **Figure 6.19** separately shows the two deconvolved pressure responses: the big differences between using single-well deconvolution (not using the separated interference pressure curve) and multi-well deconvolution algorithms (using the separated interference pressure curve). **Figure 6.20** shows the two deconvolved rate responses.

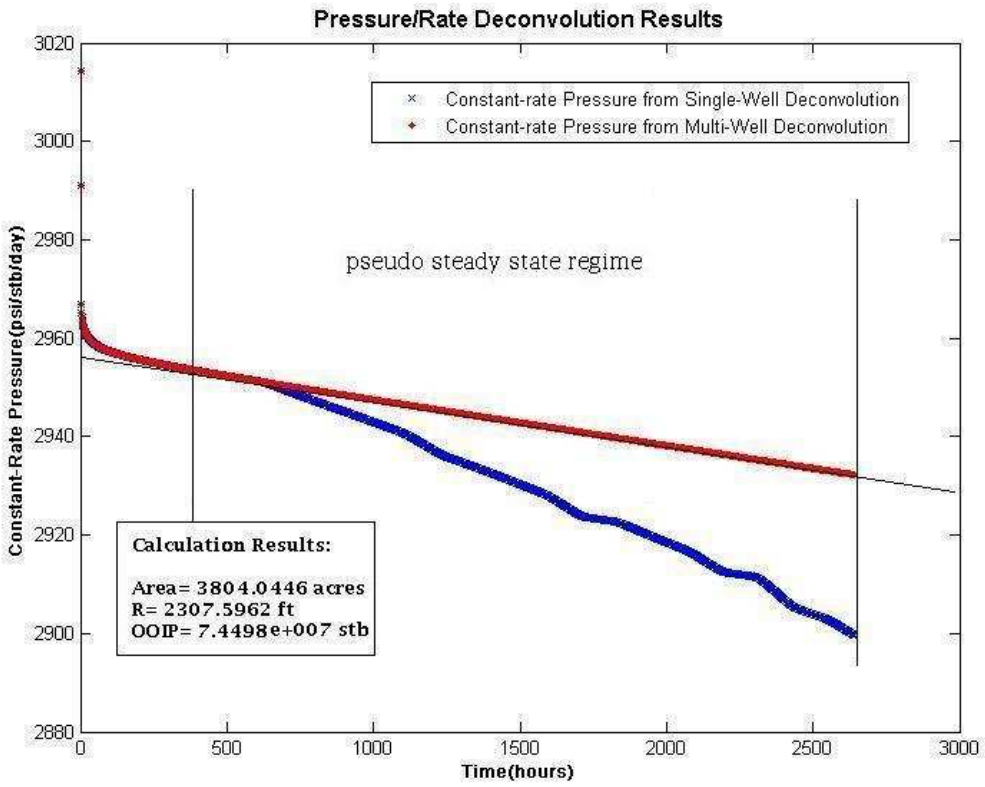

Figure 6. 19 This figure shows the big difference of deconvolved constant-rate pressure between using single-well deconvolution algorithm and multi-well deconvolution algorithm. The red smooth curve is generated by multi-well deconvolution, while the blue line is from single-well deconvolution processing.

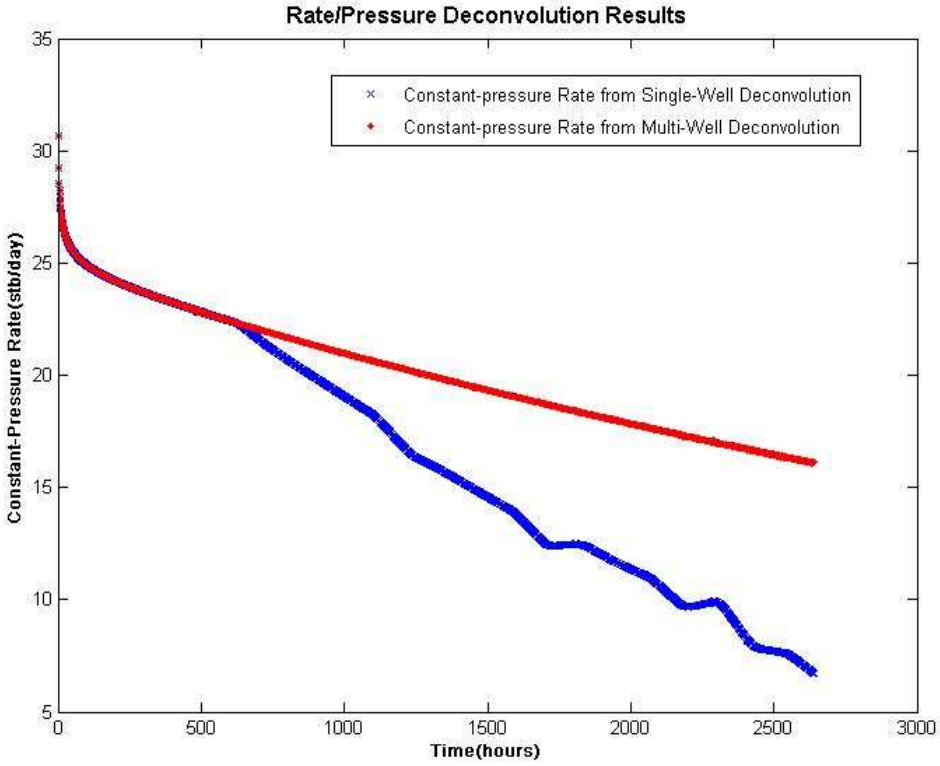

Figure 6. 20 This figure shows the big difference of deconvolved constant-pressure rate between using single-well deconvolution algorithm and multi-well deconvolution algorithm. The red smooth curve is generated by multi-well deconvolution, while the blue line is from single-well deconvolution processing.

Then this interference pressure is cumulated to get the interference pressure drop for the whole production period, shown on log-log in **Figure 6.21**. The interference response starts to be identified after 6 hours; the intersection of the pressure and derivative curves is seen at 200hours. No semi-log radial flow behavior to be identified before the derivative going upwards and the pseudo-steady state flowing condition is reached only at 400 hours. The pressure and derivative of interference response are extracted in **Figure 6.22.** The self pressure response curve extends over more than three log-cycles, and the semi-log approximation is reached after 20 hours. The pseudo-steady state flowing condition of Well 1 itself is reached at about 400 hours. **Figure 6.23** shows the Cartesian analysis plot of extracted interference response compared with self response and obtains relevant reservoir parameters.

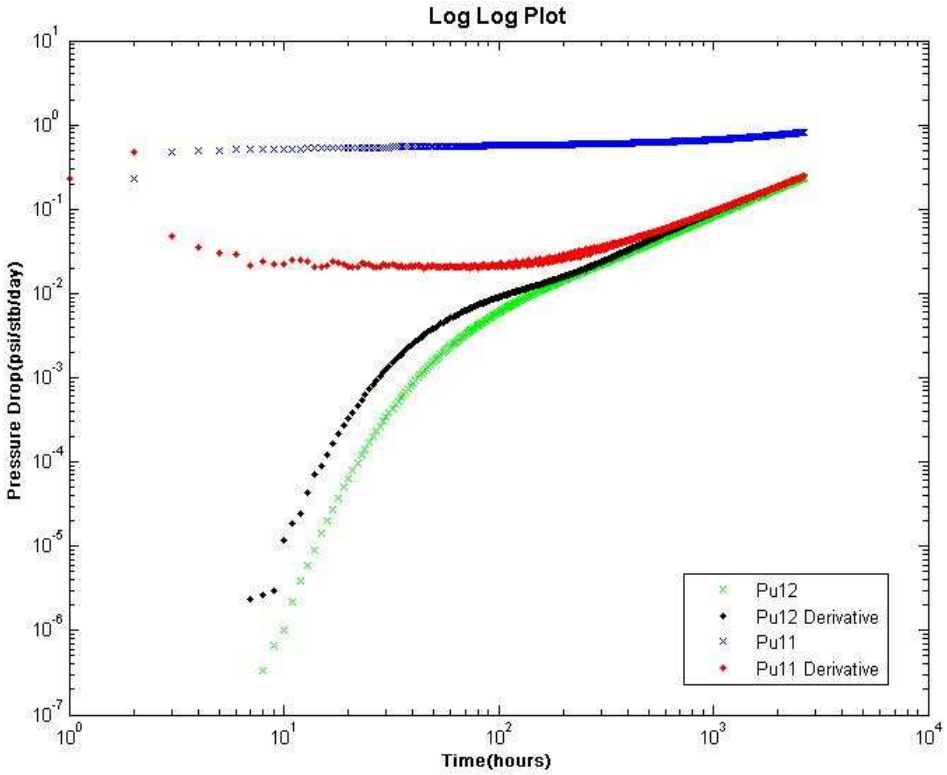

Figure 6. 21 Drawdown response of two wells on log-log plot

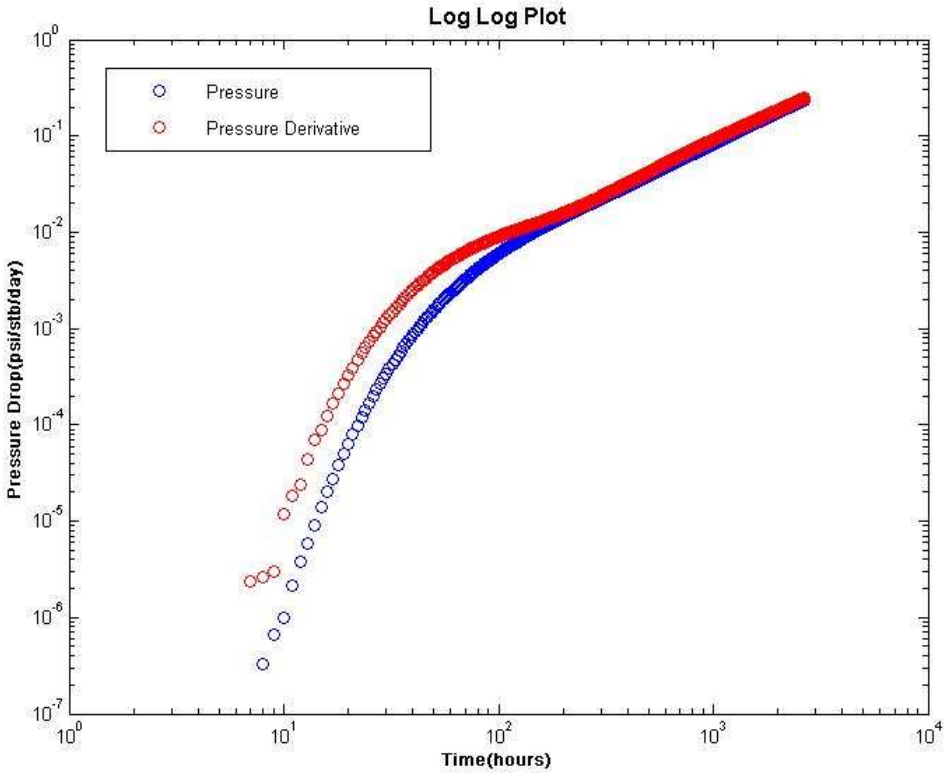

Figure 6. 22 Log-log diagnostic plot of interference response

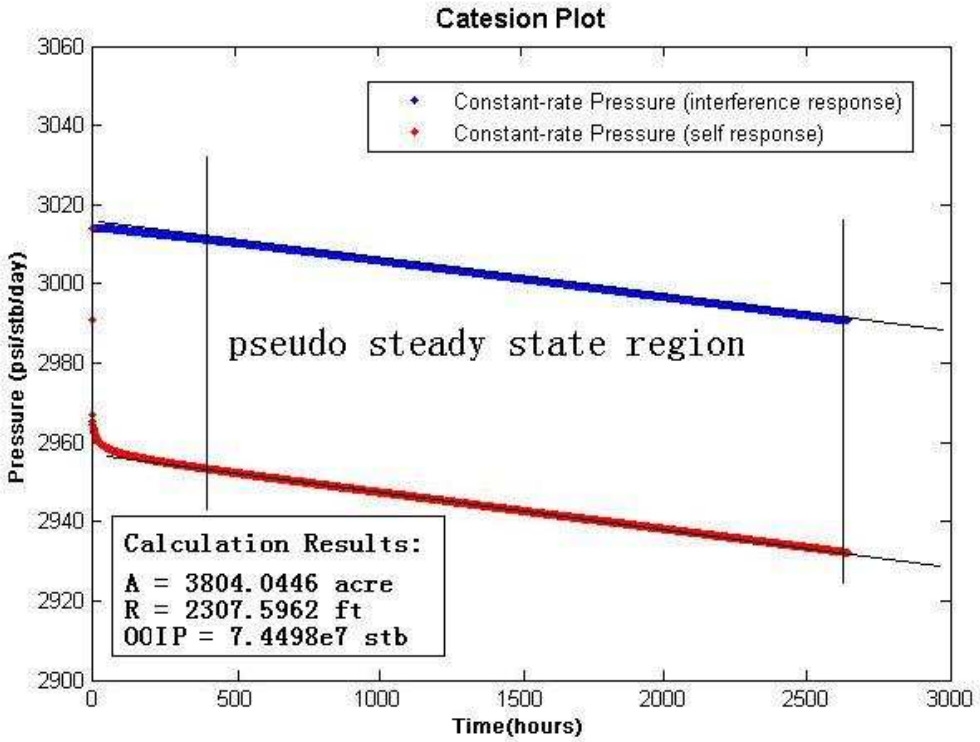

Figure 6. 23 Cartesian plot of interference response and self response

Following the procedure above, the processed interference data by multi-well deconvolution are used for traditional transient pressure analysis and transient rate analysis. From the log-log diagnostic plot of deconvolved unit-pressure rate response shown in **Figure 6.24**, it is obvious that pseudo-steady state flowing condition was reached at a time of about 400 hours.

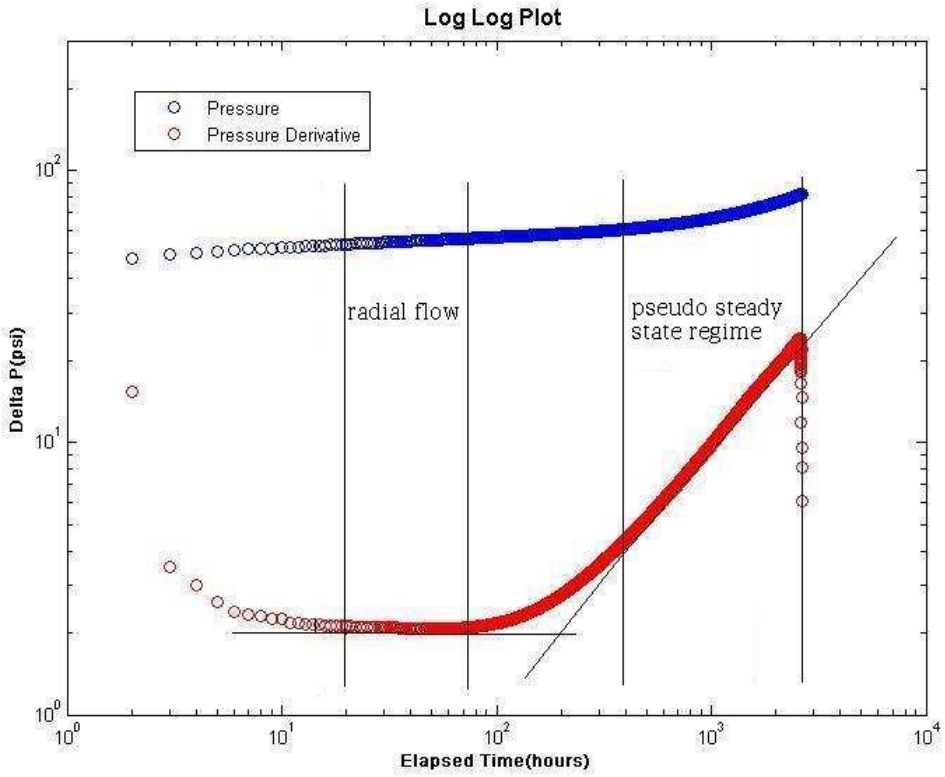

Figure 6. 24 This figure shows the comparison of deconvolved constant-rate pressure on log-log diagnostic plot. The blue line shows deconvolved transient pressure, while the red line is associated derivatives. The flow moves into pseudo steady state flowing period at about 400 hours.

Figure 6.25 shows the semi-log analysis plot p_{cq} vs. $\log(t)$ and obtains the reservoir parameters. **Figure 6.26** shows the semi-log plot $\log(q_{cp})$ vs. t .and verifies that late-time response exhibits a well-defined straight line indicating exponential decline. The decline curve parameters are estimated by non-linear regression for times greater than 400 hours, as the log-log diagnostic plot of unit-pressure rate responses (**Figure 6.24**) clearly determines that it has reached pseudo-steady state at 400 hours. Finally, traditional Arp's decline curve model and the decline curve parameters, b , D_i and q_i , are obtained by non-linear fitting for production forecast.

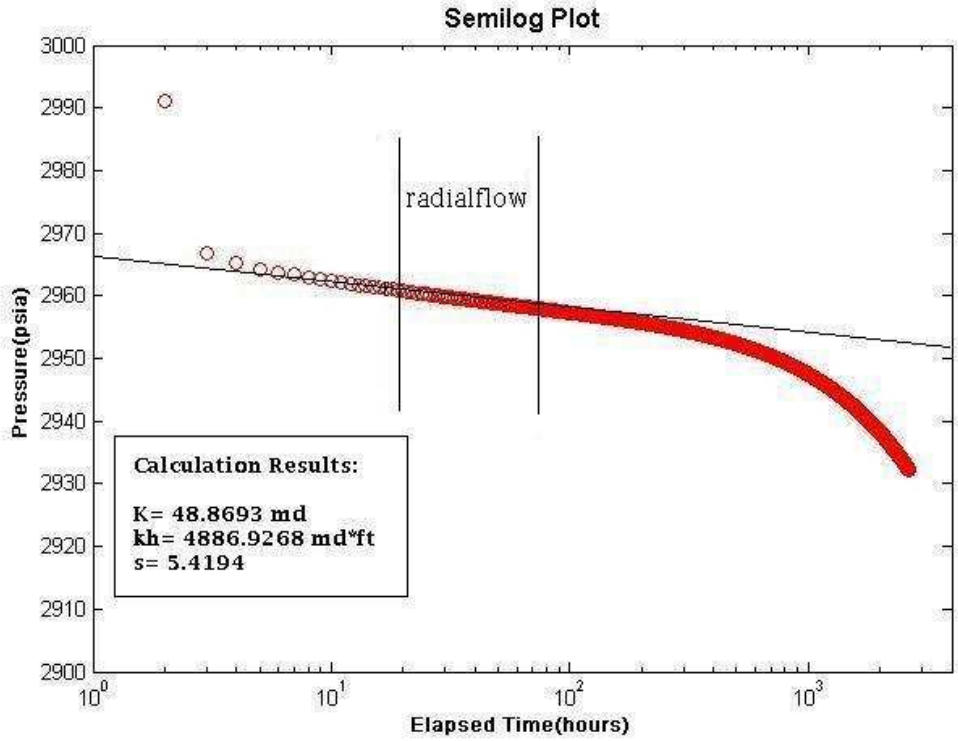

Figure 6. 25 This figure shows the semi-log transient-pressure analysis and estimated parameters are obtained.

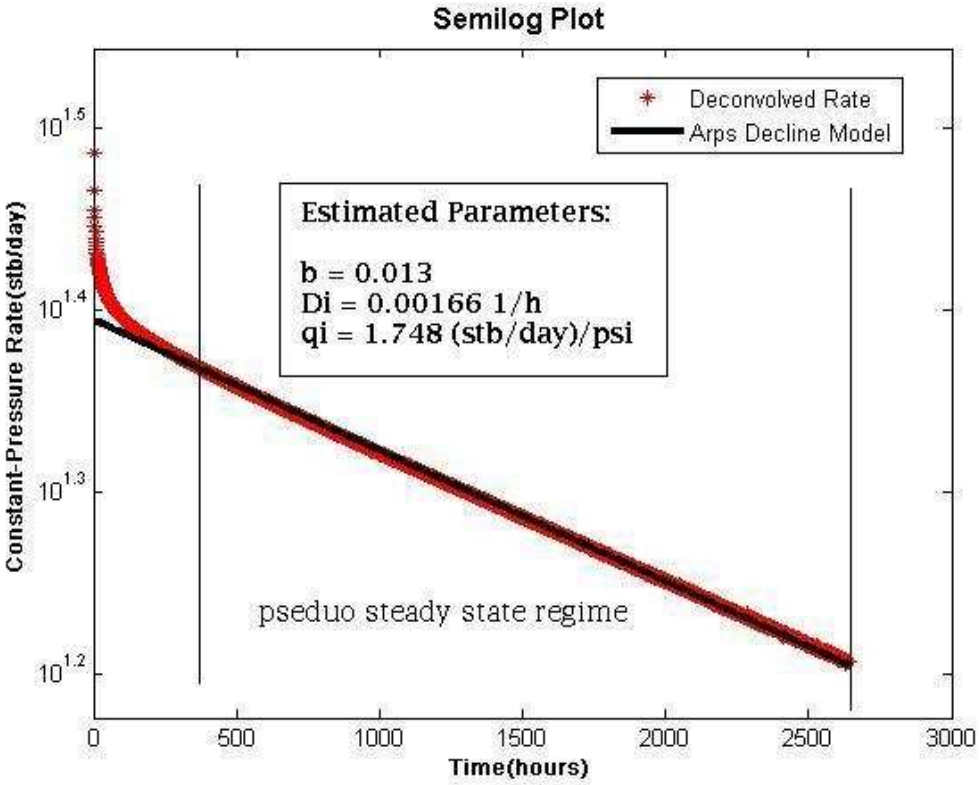

Figure 6. 26 This figure shows the non-linear regression analysis of transient-rate. The red line is the deconvolved unit-pressure rate response, while the black line is the

nonlinear regression curve based on Arp's decline model from 400 hours. The best fit values are derived from regression curve fitting.

The reservoir parameters estimated from the deconvolution-based transient rate analysis and deconvolution-based transient pressure analysis are shown together in **Table 6.6**. This reveals that the results from traditional well testing analysis are consistent with those from decline-curve analysis. The results derived from different approaches can support each other in practical case.

	Deconvolution -based Pressure-Transient Analysis	Deconvolution -based Rate-Transient Analysis	Calculation	True Model
k(md)	48.8693	47.4006	49.4631	50
s	5.4194	*	5.6341	5
A(acre)	384.0446	384.4594	385.3213	386.7452
R (ft)	2307.5962	2312.6757	2311.4287	2313.1773
OOIP(STB)	7.4498e7	7.4564e7	7.4740e7	*

Table 6. 6 Comparison of the parameters estimated by deconvolution and calculation with true model parameters

6.5 Application for Reservoir Boundary Identification

6.5.1 Problem Statement of Current PTA Techniques

Well test data as one of the key dynamic sources is used to characterize the well and reservoir parameters, such as well deliverability, skin factor, permeability, various reservoir heterogeneities, boundaries and reservoir connectivity. All these parameters are interpreted on the basis of constant rate drawdown theories. However, due to the operation limitation in practice, it hardly maintains the flow rate constant. As a result, the current pressure transient analysis techniques are mainly based on the analysis of individual flow periods, usually the longest build-up or drawdown period in the test.

However, the whole test sequence, i.e. PDG dataset, usually comprising several cycles of flow and shut-in periods such as the one showed in **Figure 1.1**. It covers a much longer duration and contains more reservoir information than that of the longest build-up or drawdown period does.

The current pressure drawdown analysis technique has drawbacks, such as it gives a limited reservoir volume, reveals limited reservoir information and sometimes provides an incorrect diagnosis of the reservoir model.

Deconvolution technique, as illustrated in previous chapters, can transform variable-rate pressure into equivalent constant rate pressure response over duration equal to the entire test time. So it can enable the whole duration of the PDG data to be analysed, rather than on just a single flow period, thereby overcoming the drawbacks of the traditional pressure drawdown or build-up analysis mentioned above.

In the following section, a synthetic case will be presented to prove that my developed deconvolution technique can give additional reservoir diagnostics, hence improving reservoir characterisation.

6.5.2 Synthetic Case Study

Synthetic Model

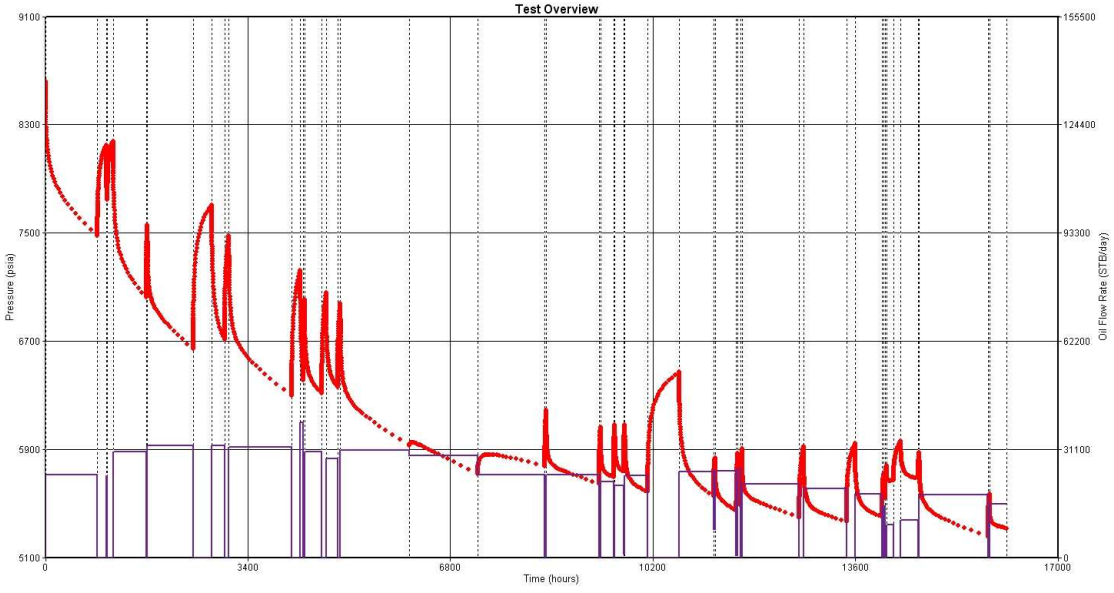

Figure 6. 27 Flow History of the Well

Figure 6.27 shows the whole flowing history for the well. This data has been synthetically generated from a fractured well model. The data is close to a PDG field example. All the parameters are listed in Tables as follows:

Fluid type	Single-phase Oil
Well orientation	Vertical
Number of wells	1
Number of layers	1

Table 6. 7 Reservoir Description

Formation thickness (ft)	100.0000
Average formation porosity	0.2800
Total system compressibility (psi-1)	1.3874e-5
Layer pressure (psia)	8623.000000

Table 6. 8 Layer Parameters Data (Layer 1)

Well radius (ft)	0.3500
Wellbore storage coefficient (bbl/psi)	0.0000

Table 6. 9 Well Parameters Data

Oil formation volume factor (RB/STB)	1.166
Oil viscosity (cp)	3.169

Table 6. 10 Fluid Parameters Data

Layer 1 Boundary Type	Parallel faults
L1 Boundary	No-flow
L3 Boundary	No-flow
L1 (ft)	2310.823366
L2 (ft)	0.000000

L3 (ft)	2366.513779
L4 (ft)	0.000000

Table 6. 11 Boundary Geometry

Layer 1 Model Type	Vertical fracture - infinite conductivity
Permeability (md)	351.6970
Fracture face skin	6.4003e-4
Fracture half-length (ft)	492.659326

Table 6. 12 Model Parameters

The last pressure drawdown (PDD) period of this sequence on log-log plot is shown in **Figure 6.28**, in which just one linear flow, i.e. fracture linear flow, can be investigated.

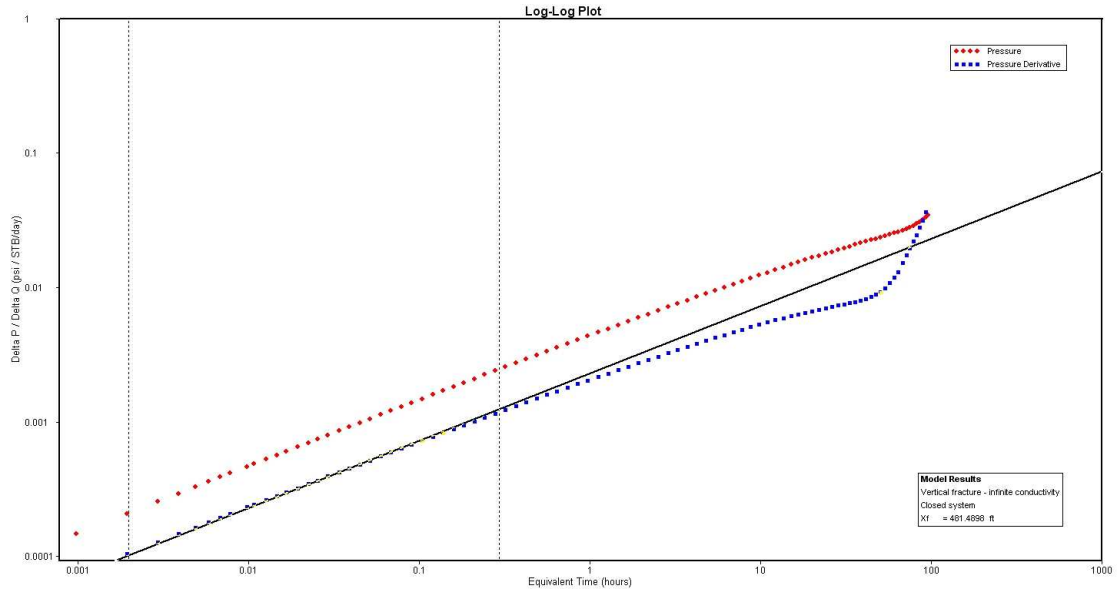

Figure 6. 28 Last DD just show the first linear flow (Fracture linear flow)

Figure 6.29 displays the first pressure drawdown (PDD) period on log-log plot, in which the first pressure drawdown (as well as the longest DD) shows one linear flow at the beginning, followed by a late pseudo-radial flow. The first linear flow here represents the fracture linear flow. The second linear flow, i.e. reservoir linear flow, is relatively short since the limited duration of this drawdown. So the reservoir boundary type is either parallel faults or intersectional faults. The boundary models theory of well testing gives that if there is a flat slope line followed by the half slope line, which

represents the reservoir linear flow, the reservoir boundary should be intersectional faults. Otherwise, it will be parallel faults. **Figure 6.30** and **Figure 6.31** show the first pressure drawdown (PDD) period on radial flow plot and linear flow plot, respectively.

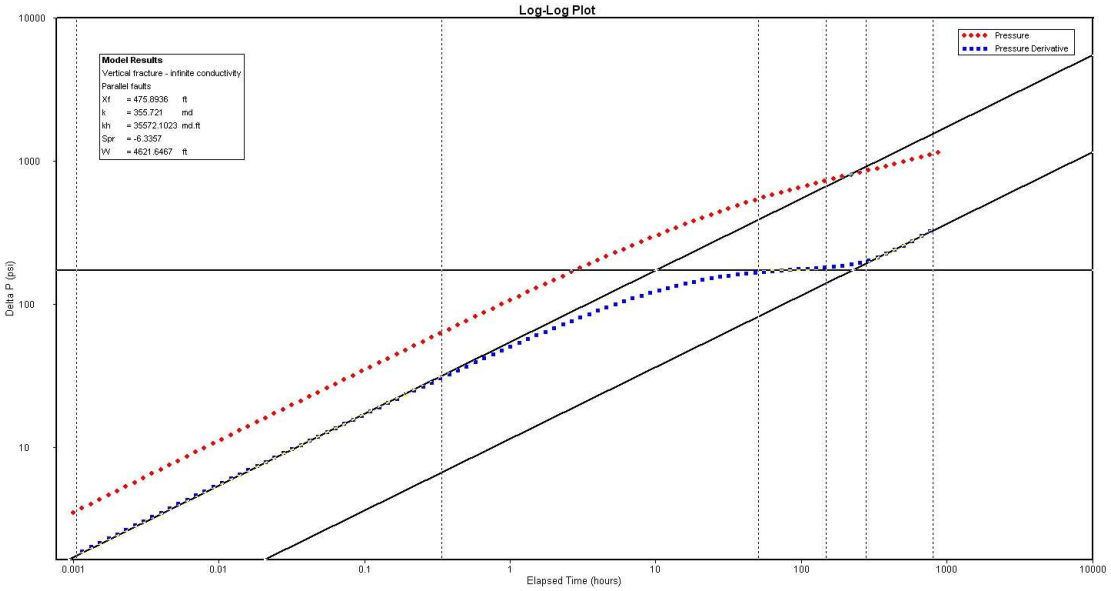

Figure 6. 29 First DD on log-log plot

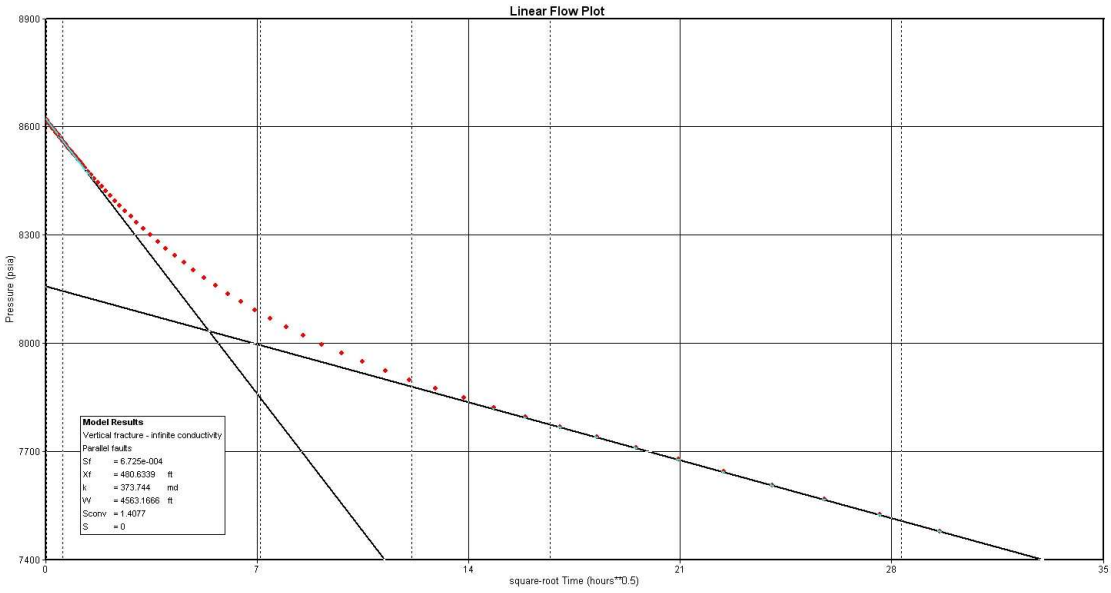

Figure 6. 30 First DD on Linear Flow Plot

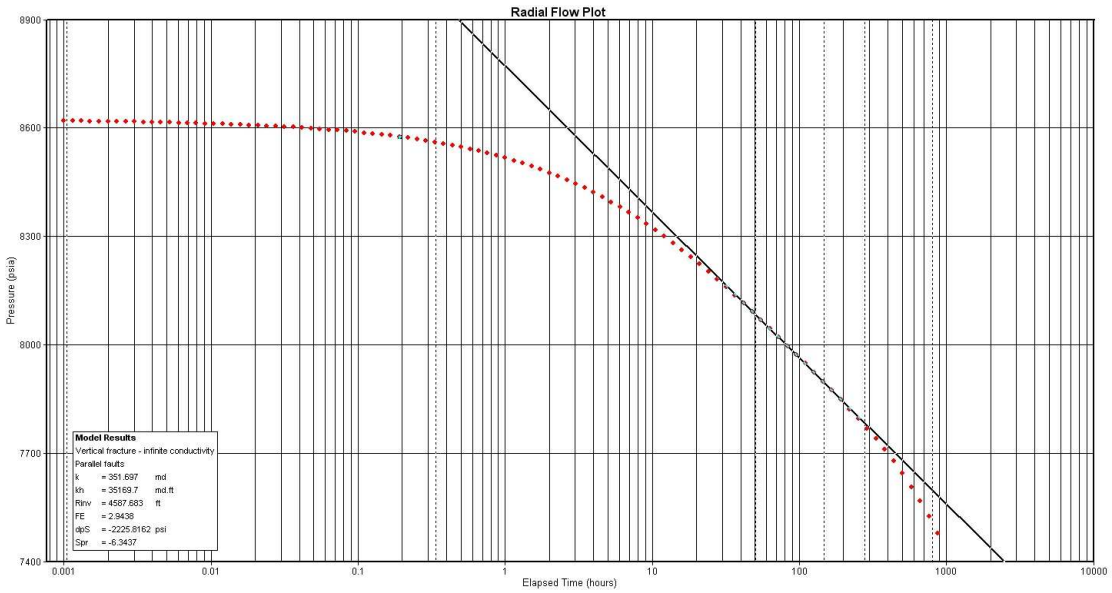

Figure 6. 31 First DD on Radial Flow Plot

In this case, apparently, the analysis of individual flow periods, i.e. analyzing the longest drawdown above, cannot determine the reservoir boundary type.

Pressure-rate deconvolution is then implemented for the whole test period. The result is shown in **Figure 6.32**, which is the constant-rate pressure response with a fixed value of flow rate.

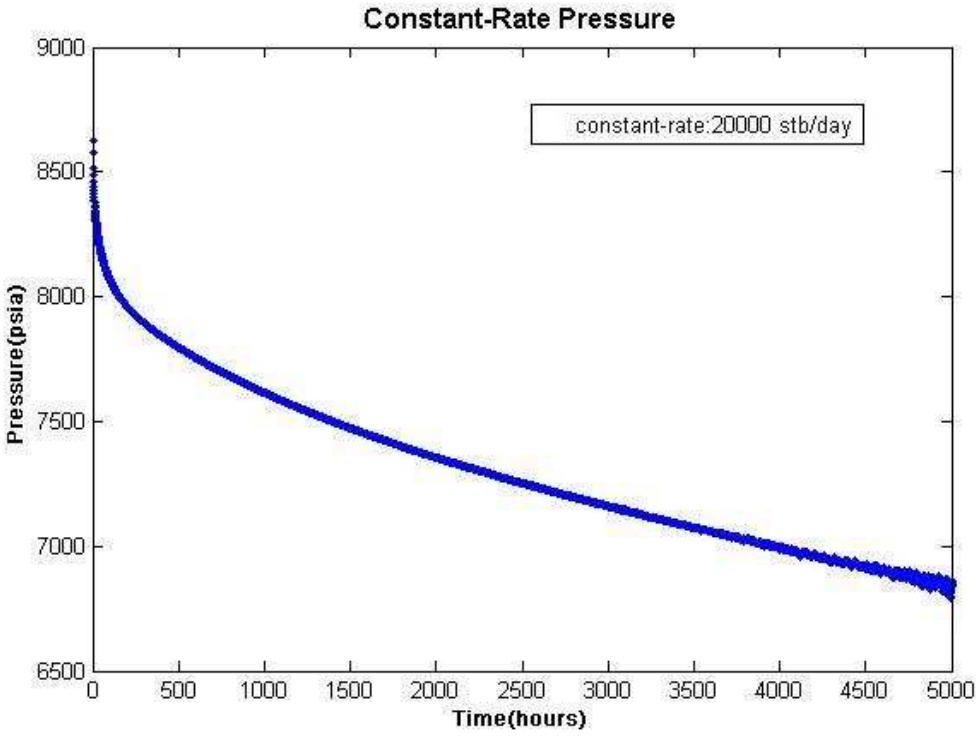

Figure 6. 32 Deconvolved DD on Cartesian plot

Figure 6.33 shows the deconvolved pressure and its derivative on log-log plot. It clearly the second linear flow, i.e. reservoir linear flow, since there is no flat slope line followed by the half slope line. So the reservoir boundary type can be identified as parallel faults.

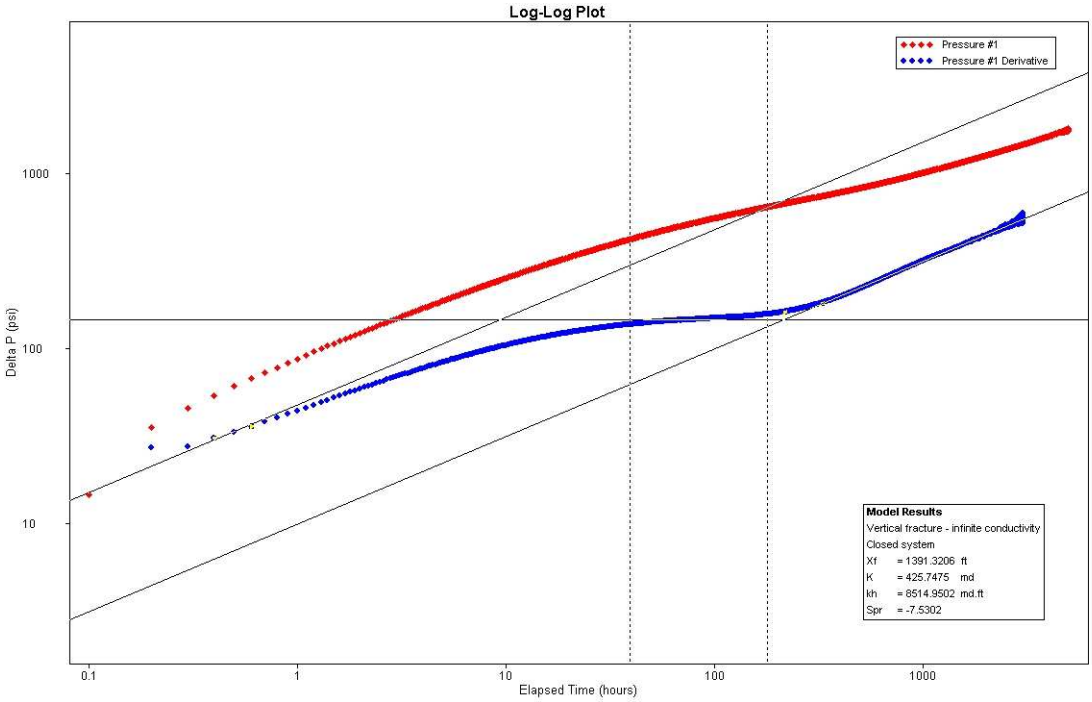

Figure 6. 33 Deconvolved DD on log-log plot

Thereafter deconvolution-based pressure transient analysis can be used to calculate the reservoir parameters. Results in this case have shown in **Table 6.13**.

	Deconvolution-based Analysis Results
Permeability (md)	351.6970
Permeability-thickness (md.ft)	3.5170e4
Pseudo-radial skin factor	-6.343717
Fracture face skin	6.3279e-4
Fracture half-length (ft)	495.469748
Channel width (ft)	4704.019464

Table 6. 13 Reservoir parameters estimated by deconvolution-based pressure transient analysis

6.6 Chapter Conclusions

In this chapter, single-well deconvolution has been applied to oil-gas reservoir system, reservoir boundary identification and interference diagnostics. Previous deconvolution algorithm has been modified for this application. In summary, deconvolution makes contribution in multi-phase and multi-well reservoir conditions in terms of:

For multi-phase problem, deconvolving single-phase part of the oil-gas two-phase data under the condition, which are higher than that at bubble point, is proved viable. It has been indicated that the behavior of deconvolved data can represent the true reservoir response under the constant flowing conditions.

For interference diagnostics, single-well deconvolution can transfer the transient pressure as a result of variable rate into an equivalent unit-rate transient pressure. It also can convert a series of transient pressure, due to variable or step rate history into an equivalent unit-pressure transient rate. Once such responses (unit-rate pressure and unit-pressure rate) are generated, they can be used to identify the reservoir model and diagnose the interference happening.

For interference processing, multi-well deconvolution can be used to extract the interference information from long-term real-time PDG data and then generate equivalent constant-rate pressure and constant-pressure rate response. The processed data can be used for regular analysis.

For interference analysis, deconvolution-based pressure and rate transient rate theory is implemented on the deconvolved pressure and rate data. The results of two deconvolution-based analysis show good match, which prove that this is a reliable technique in multi-well reservoir conditions.

Chapter 7
Conclusions and Future Guidelines

The chapter firstly presents a summary and conclusions of the work in this thesis. It then recommends areas for further research. In brief, this thesis presented a new multi-well deconvolution method, which is suitable for processing and analysis of transient pressure data from permanent down-hole gauges. The original objectives of this thesis described in Chapter 1 have been achieved.

7.1 Summary and Conclusions

From this thesis, the main understandings and findings are as follows:

Variable Pressure/Rate Problem in PDG Data

Traditionally reservoir properties such as permeability and outer boundary conditions can be derived by analyzing transient data obtained from the measurement gauge in the well bore. There are two types of transient data:

- (1) Constant rate transient pressure, which is due to fixed flowing rate, so the well bottom hole flowing pressure, is a function of time;

- (2) Constant pressure transient rate created by setting the bottom hole flowing pressure as constant, so the flowing rate is a function of time, i.e. transient rate.

Transient data in case (1) can be analyzed using method developed for transient well testing, while in case (2), the traditional decline curve analysis method will be used. Both these cases will yield information about the tested reservoir such as model and associated parameters.

However, in practice the conditions described in cases (1) and (2) are hard to maintain, so the transient data obtained from PDG will either be variable rate transient pressure or variable bottom-hole pressure transient rate. Therefore, the transient well testing or decline curve analysis methods cannot be applied directly before having the specified conditions met the criteria.

Interference Problem in PDG Data

Interference effect between wells is very common in transient pressure data from permanent down-hole gauges. As soon as the recorded pressure interfered by the pressure disturbance from other wells nearby, the PDG pressure becomes the product of two components, i.e. self response due to the well production and interference response from neighboring wells.

This combined pressure data recorded by the PDG cannot be well analyzed by traditional well testing methods. There are two approaches handling this type of data.

- One is numerical well testing designed for solving well testing problems in a nonlinear reservoir system;

- Another is to pre-process the data by decomposing the total pressure response into linear reservoir response and the component that causes the nonlinearity of the response, i.e. interference effect. Thereafter, the extracted interference data can be analysed as interference test, and the remaining data can be analysed by traditional well testing methods.

In this thesis, a newly developed multi-well deconvolution algorithm specially designed for analyzing long-term transient pressure with interference. The procedure is firstly to extract the interference from the total pressure response. Then, the analysis of the decomposed data can be made using the available traditional well testing methods.

The main conclusions of developing deconvolution algorithm, applying deconvolution techniques for processing and analysis of PDG transient pressure, dealing with noise, pressure/rate variations and multi-well interference effects can be summarized in the following points:

1, A new pressure-rate deconvolution algorithm is developed to deal with the flow rate variations and noise problem in single-well PDG data. The constant-rate pressure response of a single-well reservoir system was calculated using the developed pressure-rate algorithm. This deconvolved pressure can be used for reservoir system identification and parameter estimation.

2, A new rate-pressure deconvolution algorithm in time-domain is developed to deal with the flowing pressure variations and noise problem in single-well PDG data. The constant-pressure rate response of a single-well reservoir system was calculated using the developed rate-pressure algorithm. This deconvolved rate was found to be successful in the following situations:

- Diagnostics for reservoir nonlinearity
- Reservoir model identification
- Reservoir recoverable reserve estimation and production forecast.

3, A new multi-well deconvolution algorithm has been developed for analyzing long-term PDG transient pressure with interference and multi-rate superposition effects. With added nonlinear least-squares optimization, this algorithm can solve noisy data problem and improve the precision in calculation. With this algorithm, the inter-well interference effect in PDG transient pressure data can be extracted and variable-rate problem can be solved at the same time. The primary pressure derivatives of multi-well

deconvoloved self pressure and interference pressure can be used for flow regime diagnostics.

4, Deconvolution algorithm has been modified for multi-phase deconvolution study. A new idea for multi-phase deconvolution, i.e. deconvolving single-phase part of the oil-gas two-phase data under the condition, which are higher than that at bubble point, is proved viable. It has been indicated that the behavior of deconvolved data can represent the true reservoir response under the constant flowing conditions.

5, A comprehensive of case studies showed that the single-well deconvolution algorithm works well in the following situations:

- Single-phase flow
- Homogeneous reservoirs
- Single-well conditions
- Variable pressure/rate flowing situations

And the corresponding deconvolution-based analysis found to be successful in the following aspects:

- Analysis BU and DD together
- Give extended investigation/reservoir volume
- Interference diagnostics
- Reservoir boundary identification(type curves)

6, A comprehensive of case studies showed that the multi-well deconvolution algorithm works well in the following situations:

- Single-phase flow
- Homogeneous reservoirs
- Multi-well conditions
- Variable pressure / rate flowing situations

And the corresponding deconvolution-based analysis was found to be successful in the

following aspects:

- Analysis BU and DD together
- Give extended investigation/reservoir volume
- Interference extraction
- Reservoir boundary identification (primary pressure derivative)

7, For reservoir description and production forecasting from single-well PDG pressure and flow rate data, a double-checked practice method was proposed:

Data Processing

- Pressure-rate deconvolution
- Rate-pressure deconvolution

Data Analysis

- Deconvolution-based pressure transient analysis
- Deconvolution-based rate transient analysis

The procedures include firstly, the processing of the variable pressure and rate data with two single-well deconvolution algorithms respectively. Once the deconvolved pressure/rate, where deconvolved pressure is for pressure transient analysis and deconvolved rate is for rate transient analysis, is obtained, these deconvolution-based analysis methods can be used for reservoir system identification and parameter estimation at the same time. As the theory for both methods are the same, the results from transient-pressure analysis and transient-rate analysis can support each other to ensure the result is more reliable.

8, For applying deconvolution technique to PDG data in multi-well reservoir conditions, a three-step methodology was proposed:

- Interference Diagnostics
- Interference Extraction
- Interference Analysis

The procedures include firstly, the diagnostic of the reservoir system response for the nonlinearity. As soon as the reason causing this nonlinearity due to interference is found, the following step is to extract the interference from the total pressure response. Then, the analysis of the decomposed data can be made using the available traditional well testing methods.

Interference diagnostics

Single-well deconvolution can transfer the transient pressure as a result of variable rate into an equivalent unit-rate transient pressure. It also can convert a series of transient pressure, due to variable or step rate history into an equivalent unit-pressure transient rate. Once such responses (unit-rate pressure and unit-pressure rate) are generated, they can be used to identify the reservoir model and diagnose the interference happening.

Interference processing (extraction)

Multi-well deconvolution can be used to separate interference information from long-term real-time PDG data and then generate equivalent constant-rate pressure and constant-pressure rate data. The processed data can be used for regular analysis.

Interference analysis

Transient pressure analysis and transient rate analysis are implemented on the deconvolved pressure and rate data. The results of two deconvolution-based analysis show good match, which prove that deconvolution is a reliable technique multi-well reservoir conditions.

7.2 Future Research Directions

As shown in this thesis, the new multi-well deconvolution algorithm and corresponding deconvolution-based analysis method has a good capability for processing and analysis of transient pressure data from permanent down-hole gauges. With this method, long-term, noisy, variable-rate superposition and multi-well

interference issues involved in PDG transient pressure can be solved well. However, it should be noted that the multi-well deconvolution method are not omnipotent and cannot be routinely applied to some certain areas. For the sake of future research guidance, it may be useful to understand the application restrictions of the multi-well deconvolution method so that this technique can be further developed. In future, more relevant research may be suggested as follows:

Firstly, the importance of pressure-rate deconvolution technique is not just for the pressure transient analysis to estimate reservoir parameters and indentify reservoir model, it can also used for diagnostics.

During the life of the well, PDG pressure data and flow rate measurements are affected by several dynamic factors including changes in reservoir pressure, skin, permeability and reservoir drive mechanism. A major challenge facing the oil industry is how to diagnose production problems and these effects to know whether a change in measured downhole pressure and rate data is caused by depletion, changes in skin, permeability or drive mechanism.

Since the basic assumption of all deconvolution techniques is the consistency of measured pressure and rate data with the linear Duhamel’s model, which is based on the principle of superposition. The linearity of the system suggests only one well creating pressure perturbation to initially equalized region and static character of the parameters of reservoir and well. In other words, initial equilibrium state must be satisfied during the deconvolution procedure.

Therefore, by automatically deconvolving pressure data over variable time ranges, distortion in the deconvolved pressure derivatives should appear if any above-mentioned reservoir pressure, parameters or drive mechanism changes in well-reservoir behavior occurs. That would act as an alarm signal and suggest the need for closer examination of the data by time-lapsed well test analysis in order to indentify the causes of the changes and develop solutions as required before potential damage

develops and becomes irreversible.

Similarly, the importance of rate-pressure deconvolution technique is not just for the rate transient analysis to estimate the reservoir recoverable reserve and predict the production. This is conceptually similar to the diagnostic procedure for the interpretation of unit-pressure response generated from pressure-rate deconvolution discussed above. Once unit-pressure rate response is generated from the single-well rate-pressure deconvolution, additional diagnostics can be performed to identify the appropriate model exhibited by the data, yet consistent with the available geological model. Although it is somewhat qualitative, this derivation gives a measure of fluid and rock nonlinearity and heterogeneity, as well as unknown boundary effects. Therefore, deconvolved rate response will provide clues for obtaining an accurate model.

In this respect, it is worthwhile to investigate more diagnostic areas based on current deconvolution technique, e.g. further applying deconvolution technique to diagnose the reservoir nonlinearity, depletion, skin, permeability changes, drive mechanism effects and a series of above-mentioned production problems using the PDG pressure data and flow rate measurements.

Secondly, the basic assumption of the developed deconvolution method is for homogeneous reservoirs. And in this thesis, all the cases for investigation of two-well interference are restricted by the well location, namely, the location of two wells is completely symmetrical. In this respect, the equivalent interference pressure responses ($p_{u12} = p_{u21}$) can be assumable. While if the two active wells are located on unsymmetrical places in a reservoir, which is not infinite, the well interference response from well 1 to well 2 may be not equal to that from well 2 to well 1 due to different boundary effects. Future research will be carried out to build different reservoir models with kinds of unsymmetrical boundaries and wells, in order to investigate the symmetry of the interference pressure responses.

Thirdly, the interference problem, as one of critical factor for deconvolution, which made this technique cannot be routinely utilized in practice, has been solved with the developed multi-well deconvolution method. Another requirement for linearity of the system is the single-phase flow only that puts the limitation on the bottom-hole pressure be higher than that at the bubble point. Once multi-phase flow exists, deconvolution cannot work. In this thesis, the developed multi-well deconvolution is based on single-phase pressure solutions; the multi-phase flow effect is not captured. (although the influence of multi-phase problem has been considered and current deconvolution algorithm has been modified to deal with the oil-gas two-phase deconvolution problem). So it is worthwhile to investigate some general form of deconvolution algorithm by including the multi-phase flow term to improve the applicability of deconvolution techniques.

Finally, the developed multi-well deconvolution algorithm and corresponding deconvolution-based analysis method can be applied to not only the PDG data and traditional well test data, but also the data from multi-well interference tests, interval pressure transient tests, mini DST and vertical interference tests. Future research will further carry on how to use the continuous measurement from permanent downhole gauges to improve reservoir description and forecast performance. A stronger link should be made between real-time downhole data and assistant history matching of numerical models, which aims at enhancing reservoir management.

References

[1] R. Chedid and F. Colmenares**:** "Designing a New Plan for the Redevelopment of a Mature Oil Field by Using Various Technologies**,"** paper SPE76777 presented at the 2002 Western Regional/AAPG Pacific Section Joint Meeting, 20-22 May, Anchorage, Alaska.

[2] Brian Carr, Pradeep S. Kumar, and Qasem Dashti: "A Unique Method for Predicting Long-Term Performance of a Mature Supergiant Kuwait Oil Field Using Complex Simulation Modeling, Simple Analogies, and Classical Analyses," paper SPE 87252 presented at the 9th Abu Dhabi International Petroleum Exhibition and Conference, 13-15 October, 2000, Abu Dhabi, United Arab Emirates.

[3] F.A. Mahroos.: "Future Challenges for Producing Middle East Oilfields during Maturation Stage," paper SPE 93708 presented at the SPE Middle East Oil and Gas Show and Conference, Mar 12 - 15, 2005, Kingdom of Bahrain.

[4] L. Xiaoguang, Z. Xuewen B. Sincock, and F. Mayanullah: "Integrated Approach for Improving Development of a Mature Field," paper SPE 92895 presented at the 2005 SPE Asia Pacific Oil and Gas Conference and Exhibition, 5-7 April, Jakarta, Indonesia.

[5] M.S. Guimarães, D.J. Schiozer and C. Maschio.: "Use of Streamlines and Quality Map in the Optimization of Production Strategy of Mature Oil Fields," paper SPE

94746 presented at the SPE Latin American and Caribbean Petroleum Engineering Conference, 20-23 June, Rio de Janeiro, Brazil.

[6] M.A. Naguib, E. Shahin, J. Seeby, and J. Moore: “Integration Tools to Streamline Reservoir Management and Field Development Workflows for Mature Fields in South Oman,” Paper SPE93697 presented at the SPE Middle East Oil and Gas Show and Conference, Mar 12 - 15, 2005, Kingdom of Bahrain.

[7] J.L. Ziritt: “Mature vs. Unknown, Where Are We Really? - An Ecuadorian Field Case,” paper SPE 97636 presented at SPE Latin American and Caribbean Petroleum Engineering Conference, 20-23 June, Rio de Janeiro, Brazil.

[8] R. Bischoff and R. Bejaoui: “Integrated Modeling of the Mature Ashtart Field, Tunisia,” paper SPE 94007 presented at the 2005 SPE Europec/EAGE Annual Conference, 13-16 June, Madrid, Spain.

[9] L. Ormerod et al.: “Real-Time Field Surveillance and Well Services Management in a Large Mature Onshore Field: Case Study,” paper SPE 99949 presented at the 2006 Intelligent Energy Conference and Exhibition, 11-13 April, Amsterdam, The Netherlands.

[10] T. Babadagli: “Mature Field Development - A Review,” paper SPE 93884 presented at the 2005 SPE Europec/EAGE Annual Conference, 13-16 June, Madrid, Spain.

[11] W.S. Meddaugh : “Reservoir Modeling for Mature Fields—Impact of Work Flow and Upscaling on Fluid-Flow Response,” paper SPE 99833 presented at the 2006 SPE Europec/EAGE Annual Conference and Exhibition, 12-15 June, Vienna, Austria.

[12] T. Bui, M. Bandal, N. Hutamin, and A. Gajraj: “Material Balance Analysis in Complex Mature Reservoirs - Experience in Samarang Field, Malaysia,” paper SPE 101138 presented at the 2006 SPE Asia Pacific Oil & Gas Conference and Exhibition, 11-13 September, Adelaide, Australia.

[13] M. Claverie, N.A. Malek and K.F. Goh: “Practical Steps for Successful Identification and Production of Remaining Hydrocarbons Reserves in a Mature Field - Case study From Tinggi, Malaysia,” paper SPE 101140 presented at the SPE Asia Pacific Oil & Gas Conference and Exhibition, 11-13 September, Adelaide, Australia.

［14] Wenling Liu, Dakuang Han, Jingrong Wang, Shuiqing Hu, and Jigen Ye: “Techniques of Predicting Remaining Oil in a Mature Oil Field with High Water Cut—Case Study,” paper SPE 104437 presented at the International Oil & Gas Conference and Exhibition in China, 5-7 December, Beijing, China.

[15] Arps, J. J.: “Analysis of Decline Curves,” Trans. AIME (1945)160, 228-247.

[16] Arps, J.J.: “Estimation of Primary Oil Reserves,” Trans., AIME (1956) 207,182-91.

[17] Slider, H. C.: “A Simplified Method of Hyperbolic Decline Curve Analysis,” JPT (March 1968) 235-236.

[18] Agarwal, R.G, Gardner, D.C, Kleinsteiber, S.W, and Fussell, D.D.: "Analyzing Well Production Data Using Combined Type Curve and Decline Curve Concepts," paper SPE 49222 presented at the 1998 SPE Annual Technical Conference and Exhibition, New Orleans, 27-30 September.

[19] Blasingame, T.A., Johnston, J.L., Lee, W. J.: "Type-Curve Analysis Using the Pressure Integral Method," paper SPE 18799 presented at the SPE California Regional Meeting held in Bakersfield, April 5-7, 1989.

[20] Blasingame, T.A. and Rushing, J.A.: "A Production-Based Method for Direct Estimation of Gas-in-Place and Reserves," paper SPE 98042 presented at the 2005 SPE Eastern Regional Meeting held in Morgantown, W.V., 14-16 September 2005.

[21] Gentry, R. W.: “Decline-Curve Analysis,” JPT (Jan. 1972) 38-41.

[22] Doublet, L.E., Pande, P.K., McCollum, T.J., and Blasingame, T.A.: "Decline Curve Analysis Using Type Curves Analysis of Oil Well Production Data Using Material Balance Time: Application to Field Cases," paper SPE 28688 presented at the 1994 Petroleum Conference and Exhibition of Mexico held in Veracruz, Mexico,10-13 October.

[23] Agarwal, R.G., Gardner, D.C., Kleinsteiber, SW., and Fussell， D.D.: "Analyzing Well Production Data Using Combined-Type-Curve and Decline-Curve Analysis Concepts," SPEREE (Oct. 1999)478-486.

[24] Fetkovich, M. J.: “Decline Curve Using Type Curves,” JPT (June 1980), 1065-77.

[25] Carter, R. D.: “Type Curves for Finite Radial and Linear Gas Flow Systems: Constant Terminal Pressure Case,” SPEJ (Oct. 1985), 719-728.

[26] Blasingame, T .A. and Lee, W J.: “Variable-Rate Reservoir Limits Testing,” paper SPE15028 presented at the 1986 SPE Permian Basin Oil & Gas Recovery Conference, Midland, TX, March 13-14.

[27] Fetkovich, M.J. et al.: “Decline Curve Analysis Using Type Curves – Case Histories SPEFE (Dec. 1987) 637-656.

[28] Blasingame, T.A., McCray, T.C. and Lee, W.J.: “Decline Curve Analysis for Variable Pressure Drop/Variable Flowrate Symposium, paper SPE21513 presented at the 1991 SPE Gas Technology Symposium, Houston, TX, January 23-24.

[29] Palacio. J. C. and Blasingame. T, A.: “Decline-Curve Analysis Using Type Curves - Analysis of Gas Well Production Data,” paper SPE 25909 presented at the 1993 Joint Rocky Mountain Regional and Low Permeability Reservoirs Symposium, Denver, CO, April 26-28, 1993.

[30] Fetkovich, M.J., Fetkovich, E.J., and Fetkovich, M.D.: "Useful Concepts for Decline-Curve Forecasting, Reserve Estimation, and Analysis," SPEPE (February 1996) 13.

[31] Fetkovitch, M.J., Vienot, M.E., Johnson, R.D., and Bowman, B.A.:" Case Study of a Low-Permeability Volatile Oil Field Using Individual Well Advanced Decline Curve Analysis," paper SPE 14237 presented at the 1985 Annual Technical Conference and Exhibition, Las Vegas, NV, 22-25 Sept.

[32] Fetkovich, E. J.: “Advanced Decline Curve Analysis Identifies Fracture Stimulation Potential” SPE38903 Annual Technical Conference and Exhibition, 5-8 October1997，San Antonio, Texas.

[33] Noel D. Rietman: “Determining Permeability, Skin Effect and Drainage Area from the Inverted Decline Curve (IDC)”, SPE 29464 Production Operations Symposium, 2-4 April1995, Oklahoma City, Oklahoma.

[34] Cox, D.O., Kuuskraa, V.A., Hansen, J.T.: “Advanced Type Curve Analysis for Low Permeability Gas Reservoirs”SPE35595 Gas Technology Symposium, 28 April-1 May1996, Calgary, Alberta, Canada.

‘

[35] Wenxia, Zhang and Grader, A.S.: “Analysis of Rate Decline Derivatives”, SPE29180 Eastern Regional Meeting, 8-10 November1994, Charleston, West Virginia.

[36] Huffman, C.H. and Thompson, R.S.: “Probability Ranges for Reserve Estimates from Decline Curve Analysis,” paper SPE 28333 presented at SPE Annual Technical Conference and Exhibition, 25-28 September 1994, New Orleans, Louisiana.

[37] Trond Unneland, Yves Manin and Fikri Kuchuk : “Permanent Gauge Pressure and Rate Measurements for Reservoir Description and Well Monitoring: Field Cases,” paper SPE 38658 presented at Journal SPE Reservoir Evaluation & Engineering , Issue

Volume 1, Number 3, June 1998,pages224-230.

[38]D.M.Anderson.et al.:“ Production Data Analysis--Challenges, Pitfalls, Diagnostics,” paper SPE 102048 presented at SPE Annual Technical Conference and Exhibition, 24-27 September 2006, San Antonio, Texas, USA.

[39] S.D. Mohaghegh, R. Gaskari, and J. Jalali: “A New Method for Production Data Analysis To Identify New Opportunities in Mature Fields: Methodology and Application,” paper SPE 98010 presented at SPE Eastern Regional Meeting, 14-16 September 2005, Morgantown, West Virginia.

[40] R. Gaskari, S.D. Mohaghegh, and J. Jalali: “An Integrated Technique for Production Data Analysis with Application to Mature Fields,” paper SPE 100562 presented at SPE Gas Technology Symposium, 15-17 May 2006, Calgary, Alberta, Canada.

[41] J. Jalali, SPE, S.D. Mohaghegh and R. Gaskari: “Identifying Infill Locations and Underperformer Wells in Mature Fields Using Monthly Production Rate Data, Carthage Field, Cotton Valley Formation, Texas,” paper SPE 104550 presented at SPE Eastern Regional Meeting, 11-13 October 2006, Canton, Ohio, USA.

[42] Jericho L.P. Reyes, Kewen Li, Roland N. Horne: “Application of a New Mechanistic Decline Curve Method to Kern County Oil Fields,” paper SPE 90212 presented at SPE Annual Technical Conference and Exhibition, 26-29 September 2004, Houston, Texas.

[43] C.S. Kabir and B. Izgec: “Diagnosis of Reservoir Behavior from Measured Pressure/Rate Data,” paper SPE 100384 presented at SPE Gas Technology Symposium, 15-17 May 2006, Calgary, Alberta, Canada.

[44] Y.Cheng. et al: “Practical Application of Probabilistic Approach To Estimate Reserves Using Production Decline Data,” paper SPE 95974 presented at SPE Annual Technical Conference and Exhibition, 9-12 October 2005, Dallas, Texas.

[45] K. Li and R.N. Horne: “Verification of Decline Curve Analysis Models for Production Prediction,” paper SPE 93878 presented at SPE Western Regional Meeting, Mar 30 - Apr 01, 2005, Irvine, California.

[46] R. Camacho-Velazquez, G. Fuentes-Cruz and M. Vasquez-Cruz: “Decline Curve Analysis of Fractured Reservoirs with Fractal Geometry” SPE104009 First International Oil Conference and Exhibition in Mexico, 31August-2 September2006, Cancun, Mexico.

[47] F.J. Kuchuk et al.: “Decline Curves from Deconvolution of Pressure and Flow-Rate Measurements for Production Optimization and Prediction,” paper SPE 96002 presented at SPE Annual Technical Conference and Exhibition, 9-12 October 2005, Dallas, Texas.

[48] von Schroeter, T., Hollaender, F., and Gringarten, A.C.: "Analysis of Well Test Data From Downhole Permanent Downhole Gauges by Deconvolution," paper SPE 77688 presented at the 2002 SPE Annual Technical Conference and Exhibition, San Antonio, Texas, 29 September -2 October.

[49] von Schroeter, T., Hollaender, F., and Gringarten, A.C.: "Deconvolution of Well Test Data as a Nonlinear Total Least Squares Problem," SPEJ (December 2004) 375-390.

[50] Levitan, M.M.: "Practical Application of Pressure/Rate Deconvolution to Analysis of Real Well Tests," SPEREE (April 2005) 113.

[51] Levitan, M.M., Crawford, G.E., and Hardwick, A., "Practical Considerations for Pressure-Rate Deconvolution of Well-Test Data," SPEJ (March 2006) 35.

[52] Ilk, D., Valko, P.P., and Blasinga me, T.A.: "Deconvolution of Variable-Rate Reservoir Performance Data Using B-Splines," paper SPE 95571 presented at the 2005 SPE Annual Technical Conference and Exhibition, Dallas, TX, 9-12 October.

[53] Ilk, D., Anderson, D.M., Valko, P.P., and Blasingame, T.A.:" Analysis of Gas Well Reservoir Performance Data Using B-Spline Deconvolution," paper SPE 100573 presented at the 2006 SPE Gas Technology Symposium, Calgary, Alberta, Canada, 15-17 May.

[54] Jargon J.R. and van Pollen, H.K.: “Unit Response Function From Varying Rate Data,” JPT (August 1965) 965; Trans., AIME , 234.

[55] Kuchuk F.J., Carter R.G., Ayestaran L.: Deconvolution of Wellbore Pressure and Flow Rate, SPEFE, 53, March 1990.

[56] Thompson L.G., Reynolds A.C.: Analysis of Variable-Rate Well Test Pressure Data Using Duhamel’s Principle, SPEFE, 453, October 1986.

[57] Baygun B., Kuchuk F.J., Arikan O.: Deconvolution under Normalized Autocorrelation Constraints, SPEJ 246, September 1997.

[58] Bourgeois M.J., Horne R.N.: Well-Test Model Recognition with Laplace Space, SPEFE, 17, March 1993.

[59] Cinar M.,Ilk, D., Valko, P.P., and Blasingame, T.A.: "A comparative Study of recent Robust Deconvolution Algorithms for Well-Test and Production-data Analysis," paper SPE 102575 presented at the 2006 SPE Annual Technical Conference and Exhibition, San Antonio, Texas, 24-27 September.

[60] Yueming.Cheng. “Fast-Fourier-Transform-Based Deconvolution for Interpretation

of Pressure-Transient-Test Data Dominated by Wellbore Storage”, paper SPE 84471 presented at the 2003 SPE Annual Technical Conference and Exhibition, Denver, Colorado, Oct 5-8.

[61] Kuchuk, F.J. and Ayestaran: “Analysis of Simultaneously Measured Pressure and Sandface Flow Rate in Transient Well Testing”, JPT (Feb.1985)323.

[62] Roumboutsos, A. and Stewart, G..: "A Direct Deconvolution or Convolution Algorithm for Well-Test Analysis," paper SPE 18157 presented at the SPE Annual Technical Conference and Exhibition, Houston, Texas. (October, 1988).

[63] Athinichanagorn, Suwat: “Development of an interpretation methodology for long-term data from permanent downhole gauges”, PhD thesis, Standford University, Department of Petroleum Engineering, 1999.

[64] Hollaender, F., Schoreter, T., and Gringarten, A.C.: "Deconvolution of well test data as a nonlinear total least squares problem," paper SPE 71574 presented at the SPE Annual Technical Conference and Exhibition, New Orleans, Lousiana. (October, 2001).

[65] Levitan, M.M., Crawford, G.E., and Hardwick, A.: "Practical considerations of pressure-rate deconvolution of well test," paper SPE 90680 presented at the SPE Annual Technical Conference and Exhibition, Houston, Texas. (September, 2004).

[66] Iseger, P.D.: "Numerical Transform Inversion Using Gaussian Quadrature," probability in the Engineering and Informational Sciences 20:1-44, 2006.

[67] Levitan, M.M.: "Deconvolution of Multiwell Test Data," paper SPE 102484 presented at the 2006 SPE Annual Technical Conference and Exhibition, San Antonio, Texas, 24-27 September.

[68] Al-Ajmi, N., Ahmadi, M., Ozkan, E., and Kazemi, H.: "Numerical Inversion of

Laplace Transforms in the Solution of Transient Flow Problems with Discontinuities," paper SPE 116255 presented at the SPE Annual Technical Conference and Exhibition, Denver, CO. (September, 2008).

[69] Pimonov, E., Ayan, C., Onur, M., and Kuchuk, E.J.: "New Pressure/Rate Deconvolution Algorithm to Analyze Wireline Formation Tester and Well-Test Data," paper SPE 123982 presented at the 2009 SPE Annual Technical Conference and Exhibition, New Orleans, 4-7 October.

[70] KuiFu. Du “Use of Advanced Pressure Transient Analysis Techniques to Improving for Drainage Area Calculations and Reservoir Characterizations: Field Case Studies”, paper SPE 109053 presented at Offshore Europe 2007, Aberdeen , UK, 4-7 September.

[71] S.J.C.H.M. van Gisbergen and A.A.H. Vandeweijer: “Reliability Analysis of Permanent Downhole Monitoring Systems,” paper SPE 57057 presented at Journal SPE Drilling & Completion Issue Volume 16, Number 1, March 2001, Pages 60-63.

[72] H.M. Frota and W. Destro: “ Reliability Evolution of Permanent Downhole Gauges for Campos Basin Subsea Wells: A 10-Year Case Study,” paper SPE102700 presented at the 2006 SPE Annual Technical Conference and Exhibition, 24-27 September, San Antonio, Texas, USA.

[73] Suwat Athichanagorn, Roland N. Horne and Jitendra Kikani: “Processing and Interpretation of Long-term Data from Permanent Downhole Pressure Gauges,” paper SPE 56419presented at the 1999 SPE Annual Technical Conference and Exhibition, 3-6 October, Houston, Texas.

[74] Marcia Ida de Oliveira Silva, and Edson Tsuneo Kato: “Reservoir Management Optimization Using Permanent Downhole Gauge Data,” paper SPE 90973 presented at the SPE Annual Technical Conference and Exhibition, 26-29 September 2004, Houston, Texas.

[75] D.M. Chorneyko: “ Real-Time Reservoir Surveillance Utilizing Permanent Downhole Pressures - An Operator's Experience,” paper SPE 103213 presented at the 2006 SPE Annual Technical Conference and Exhibition, 24-27 September, San Antonio, Texas, USA.

[76] M. McCracken and D. Chorneyko: “Rate Allocation Using Permanent Downhole Pressures,” paper SPE 103222 presented at the 2006 SPE Annual Technical Conference and Exhibition, 24-27 September, San Antonio, Texas, USA.

[77] Liang-Biao, Ouyang and Ramzy Sawiris : “Production and Injection Profiling: A Novel Application of Permanent Downhole Pressure Gauges,” paper SPE 84399 presented at the SPE Annual Technical Conference and Exhibition, 5-8 October 2003, Denver, Colorado.

[78] Tibold, M.P., ExxonMobil Exploration Company, Simonian, S., Schlumberger-Riboud Product Centre, Chawla, M., Kuwait Oil Company, Akbar, M., Kuwait Oil Company,“Well Testing with a Permanent Monitoring System”, SPE 63079, 2000.

[79] Queipo，N.V., SPE, Verde, A., SPE, Goicochea, J., Romero, D., Applied Computing Institute, University of Zulia, Venezuela; Zambrano, A., and Bracho, A., PDVSA Exploration and Production,“ Applications of Permanent Downhole Pressure, Temperature, and Flow Rate Measurements for Reservoir Description and Production Optimization: a Taxonomy, Processes, and Benefits”, SPE 77897, 2002.

[80] Gringarten, A.C., Imperial College London, SPE, Schroeter, Thomas von, Imperial College London, Rolfsvaag, T., ConocoPhillips, SPE, and Bruner , J., ConocoPhillips, SPE,“ Use of Downhole Permanent Pressure Gauge Data to Diagnose Production Problems in a North Sea Horizontal Well”, SPE 84470, 2003.

[81] Ouyang, Liang-Biao., and Kikani, J., SPE, ChevronTexaco Exploration & Production Technology Co.,“ Improving Permanent Downhole Gauge (PDG) Data

Processing via Wavelet Analysis”, SPE 78290, 2002.

[82] Kama, M.M.: "Interference and Pulse Testing—A Review," JPT (December 1983), 2257-2270.

[83] Dominique Bourdarot: “Well Test Analysis: The Use of Advanced Interpretation Models” Handbook of Petroleum Exploration and Production 3, 2002, 273-301.

[84] Onur, M., Serra, K.V., and Reynolds, A.C.: "Analysis of Pressure Buildup Data Obtained at a Well located in a Multiwell System," paper SPE 18123 presented at the 1988 SPE Annual Technical Conference and Exhibition, Houston, Oct. 2-5.

[85] Onur, M.: “New Well Testing Applications of the Pressure Derivative,” PhD dissertation, U. of Tulsa, OK (June 1989).

[86] Onur, M., Serra, K.V., and Reynolds, A.C.: "Analysis of Pressure Buildup Data Obtained at a Well located in a Multiwell System," SPEFE (March 1991) 101-110.

[87]Marhaendrajana, T. and Blasingame, T.A.: "Rigorous and Semi- Rigorous Approaches for the Evaluation of Average Reservoir Pressure from Pressure Transient Tests," paper SPE 38725 presented at the 1997 SPE Annual Technical Conference and Exhibition, San Antonio, TX, 5-8 October 1997.

[88] Marhaendrajana, T., Kaczorowski, N. J., and Blasingame, T. A.: "Analysis and interpretation of well test performance at Arun Field, Indonesia," paper SPE 56487 presented at the 1999 SPE Annual Technical Conference and Exhibition, Houston, TX, Oct. 3-7.

[89] Economies, M.J., and Ogbe, D.O., U. of Alaska.,“Single-Well and Multiwell Pressure Interference Analysis,”SPE 13665, 1985.

[90] Leaver, J.D., Grader, A. and Ramey, H.J., Stanford U.J.,“Multiple-Well Interference Testing in the Ohaaki Georhermal Field,”SPE 15122, 1988.

[91] Onur, M., Serra ,K.V., and Reynolds ,A.C., U. of Tulsa.,“ Analysis of Pressure-Buildup Data From a Well in a Multiwell System,”SPE 18123, 1991.

[92] Britt, L.K., Jones, J.R., Pardinl, R.E., and Plum, G.L., Amoco Production Co.,“Reservoir Description by Interference Testing of the Clayton Field,”SPE 19846, 1991.

[93] Hallford, D.L., GeoQuest, Hegeman, P.S., Schlumberger.,“ A Field Application of Multiple-well Testing for Reservoir Characterization,” SPE 30575, 1995.

[94] Erwin ,M.D., Phillips Alaska,Inc, Sander,L.Allen.s., Anadarko Petroleum Corp., Redman ,R.Scott., Phillips Alaska,Inc.,“ multiwell Interference Test in the Colville River Field, Alaska,”SPE 77453, 2002.

[95] Marhaendrajana, T., Ariadji, T., and Permadi, A.K., Institute Teknologi Bandung.,“Performance Prediction of a Well under Multiphase Flow Conditions,” SPE 80534, 2003.

[96] Perrine,R.L.,“Analysis of Pressure Buildup Curves”, Drill&Prod. Prac., API,Dallas(1956)482-509.

[97] Horne, R.N., Modern Well Test Analysis.

[98] Lee, J., Rollins, J.B., and Spivey, J.P., Pressure Transient Testing.

[99] Lee, W.J., and Spivey, J.P., SPE, S.A.Holditch & Associates , Inc., “Numerical and analytical well test analysis: a case history”, SPE 50946,1998.

[100] Jackson, R.R., SPE, and Banerjee.R., SPE, Schlumberger, “Advances in multiplayer reservoir testing and analysis using numerical well testing and reservoir simulation”, SPE 62917, 2000.

[101] Kamal, M.M., Pan.Y. and Landa, J.L., Chevron Corp., and Thomas, O.O., Stanford U, “Numerical well testing –A method to use transient testing results in reservoir simulation”, SPE 95905, 2005.

[102] Weiland, J., Shell Exploration&Production; Azari.M., SPE, Suparman, “Case History Review of the Applocation of Pressure Transient Testing and Production Logging in Monitoring the Performance of the Mars Deepwater Gulf of Mexico Field”, SPE 115591, 2008.

[103] Landa, J.L., SPE, and Horne, R.N., SPE, Stanford U., Kamal, M.M., SPE and Jenkins, C.D., SPE, Arco Exploration and Production Technology, “Reservoir Characterization Constrained to Well-Test Data: A Field Example”, SPE 65429, 2000.

[104] Nnadi.M., SPE, Laser Engineering and Resources Consultants Ltd., Port Harcourt; Onyekonwu.M., SPE, University of Port Harcourt., “Numerical Welltest Analysis”, SPE 88876, 2004.

[105] Freddy, H.E., Universidad Surcolombiana, Juan Miguel Navarrete, Hydrocarbon services Ltd., Hernan Dario Losada, Hydrocarbon Services Ltd., “Evaluation of Pressure Derivative Algorithms for Well-Test Analysis”, SPE 86936, 2004.

[106] Zakirov, S.N., Indrupskiy, I.M., Zakirov, E.S., SPE, Anikeev,D.P., Tarasov, A.I., and Bradulina, O.V., Inst. of the Russian Academy of Sciences,“New Approaches in well Testing”, SPE 100136, 2006.